ZooKeys 923: 1–14 (2020)
doi: 10.3897/zookeys.923.26018
http://zookeys.pensoft.net

RESEARCH ARTICLE

A peer-reviewed open-access journal
ZooKeys
Launched to accelerate biodiversity research

Sphaerillo boninensis Nunomura, 1990 (Crustacea, Isopoda, Oniscidea) is a junior synonym of a pantropical species, *Venezillo parvus* (Budde-Lund, 1885)

Shigenori Karasawa[1]

1 *Department of Life and Environmental Agricultural Sciences, Faculty of Agriculture, Tottori University, 4-101 Koyama-machi Minami, Tottori 680-8553, Japan*

Corresponding author: Shigenori Karasawa (dojyoudoubutu@gmail.com)

Academic editor: S. Taiti | Received 20 April 2018 | Accepted 14 February 2020 | Published 1 April 2020

http://zoobank.org/B574D460-C84B-4D01-BD10-B4AB2D1C0C85

Citation: Karasawa S (2020) *Sphaerillo boninensis* Nunomura, 1990 (Crustacea, Isopoda, Oniscidea) is a junior synonym of a pantropical species, *Venezillo parvus* (Budde-Lund, 1885). ZooKeys 923: 1–14. https://doi.org/10.3897/zookeys.923.26018

Abstract

Re-examination of the holotype and paratype of *Sphaerillo boninensis* Nunomura, 1990 from Chichijima Island of the Ogasawara archipelago, which is registered as a UNESCO World Heritage Site, indicates that this species is a junior synonym of a pantropical species, *Venezillo parvus* (Budde-Lund, 1885).

Keywords

Armadillidae, Chichijima Island, Ogasawara archipelago, terrestrial isopods, UNESCO World Heritage Site

Introduction

Sphaerillo boninensis Nunomura, 1990, described from specimens collected on Chichijima Island, Ogasawara archipelago, is a small terrestrial isopod formerly considered endemic to this archipelago, a UNESCO World Heritage site approximately 1,000 km from the mainland of Japan. However, there are questions around the taxonomy of this species. The genus that this species has been attributed to has changed many times (see

the taxonomic account; Nunomura 1990, 1999a, 2011), and the species is included in the genus *Spherillo* in the current taxonomic treatment (Nunomura 2015). In addition, Saito (1993) recorded specimens collected from Chichijima Island and identified as the pantropical species *Venezillo parvus* (Budde-Lund, 1885) by Drs Ferrara and Taiti, but this species has been overlooked in reviews of Japanese terrestrial isopod species (Nunomura 1999a, b, 2015; Saito et al. 2000).

Venezillo parvus, originally and imperfectly described as *Armadillo parvus* by Budde-Lund (1885), was subsequently transferred to the genus *Venezillo* Verhoeff, 1928 (Green et al. 1990; Taiti and Ferrara 1991a). Today *Venezillo* accommodates more than 140 recognized species (Boyko et al. 2008). More comprehensive, subsequent descriptions of *V. parvus* provided more useful taxonomic characteristics than those present in the original description, i.e., in Schultz (1963) as *V. evergladensis* Schultz, 1963, a species now considered to be a junior synonym of *V. parvus*, Ferrara & Taiti, 1983 as *Sphaerillo* (?) *parvus* (Budde-Lund, 1885), Schmidt (2003) and Gregory (2014) as *V. parvus*. Figures provided by Schmidt (2003) depicted the basis of the male pereopod 7 as bearing dense setae on the anterior corner of the ventral side, a characteristic present also on the male pereopod 7 of *S. boninensis* (Nunomura 1990, fig. 146I). Additionally, the oblique lobe on the ventral surface of pereonite 2 reported for *S. boninensis* by Nunomura (1990, fig. 146B) is a diagnostic feature of the genus *Venezillo* (Verhoeff 1928; Vandel 1952). These similarities indicated that *S. boninensis* was referable to *Venezillo* and a close relationship between *S. boninensis* and *V. parvus* might exist.

Terrestrial isopods are now scarce in the southern part of Hahajima Island, Ogasawara archipelago, in an area invaded by the land nemertean *Geonemertes pelaensis* Semper, 1863 (Shinobe et al. 2017). This terrestrial predator poses a threat to native biodiversity in this region. Resolving the systematic status of *S. boninensis*, or at least specimens referred to it, from this area would improve our understanding of actual versus perceived threats to endemic faunas of this region, and ultimately, the conservation and management of species throughout this archipelago.

The aim of this study was to resolve relationships between *S. boninensis* and *V. parvus*. This is achieved through re-examination and redescription of appropriate type material of the former.

Materials and methods

Sample collection

Type material was loaned from the Toyama Science Museum (collection acronym TOYA). As the previously dissected male holotype and paratype of *S. boninensis* were in poor condition, a description of the whole body, cephalon, antenna 1, and pleopod 5 of the female paratype was necessary. Additionally, as the male pereopods 1 and 7 are broken in male holotype, they can be only partly described. Male pereopod 2 was not found in the holotype and paratype.

Morphology observation

Antennae 1 and 2, mandible, maxillae 1 and 2, maxilliped, pleopods, and pereopods were placed in Hoyer's mounting medium (Krantz and Walter 2009) on slides, covered with a coverslip, and drawn under a microscope (magnification of 40–400 ×; Eclipse E400, NIKON Corp.). The whole body, cephalon, and epimera of pereonites 1–7 were examined using a Nikon SMZ1500 microscope (magnification of 7.5–112.5 ×).

Results

Taxonomic account
Genus *Venezillo* Verhoeff, 1928

Venezillo parvus (Budde-Lund, 1885)

Armadillo parvus Budde-Lund, 1885: 25–26; Dollfus 1893: 187; Verhoeff 1946: 4; Jeppesen 2000: 254.

Spherillo parvus: Budde-Lund 1904: 91; Budde-Lund 1908: 270–271, taf 12, figs 30–37; Budde-Lund 1912: 371; Barnard 1964: 53.

Venezillo evergladensis Schultz, 1963: 209–213, figs 1–26; Schultz 1972: 1–4, figs 4–6; Schultz 1975: 186; Johnson 1976: 157, fig. 1; Johnson 1977: 603; Johnson 1978: 140; Johnson 1980: 124; Johnson 1981: 351, fig. 1; Johnson 1982: 225; Johnson 1983: 209; Johnson 1984: 465; Johnson 1985a: 403; Johnson 1985b: 216; Keeney 1990: 1–2, figs 1, 2.

Sphaerillo parvus: Ferrara and Taiti 1979: 182.

Sphaerillo (?) *parvus*: Ferrara and Taiti 1981: 196; Ferrara and Taiti 1983: 70–71, figs 131–136; Taiti and Ferrara 1983: 220–222.

Sphaerillo boninensis Nunomura, 1990: 19–21, fig. 146. Syn. nov.

Venezillo parvus: Green et al. 1990: 431, 433; Taiti and Ferrara 1991a: 220; Taiti and Ferrara 1991b: 915; Kwon and Taiti 1993: 77; Kwon 1995: 533; Taiti and Howarth 1996: 68; Taiti et al. 1998: 300; Leistikow and Wägele 1999: 49; Taiti 1999: 38; Jass and Klausmeier 2000: 781; Stoyenoff 2001: tab. 2; Green et al. 2002: 301; Zimmer et al. 2002: 597; Buck et al. 2003: 106; Kelly and Samways 2003: app 1; Schmidt 2003: 107, figs 122–128; Soesbergen 2003: 97, figs 1, 2, tab. 1; Schmalfuss 2004: 291; Zimmer et al. 2004: 754, figs 1–3, 5–12; Dias et al. 2005: tab. 3; McLaughlin et al. 2005: 198; Poore 2005: 11; Berg et al. 2008: 61; Gregory 2009a: 7; Gregory 2009b: 1; Barber 2010: 73; Cochard et al. 2010: tab. 7.1.1; Senterre et al. 2011: app 2; Murphy et al. 2012: 3; Arab and Wimp 2013: 333; Treplin et al. 2013: 84; Wimp et al. 2013: 507, fig. 1; Angelini and Silliman 2014: 188; Gregory 2014: 21–23, fig. 11, tab. 3; Humphreys 2014: tab. 2; Lemaire and Gerriet 2014: 43–44; Taiti and Wynne 2015: 44; Taiti 2018: 88;

Vittori and Štrus 2017: 396; De los Rios-Escalante et al. 2018: 50, tab. 1; Pérez-Schultheiss et al. 2018: 8.

Venezillo boninensis: Nunomura 1999a: 89; Nunomura 1999b: 598, 614, 624; Saito et al. 2000: 94. Syn. nov.

Spherillo boninensis: Nunomura 2011: 71; Nunomura 2015: 1032, 1050, 1063; Shinobe et al. 2017: 3. Syn. nov.

Material examined. *Sphaerillo boninensis*: Holotype, TOYA-Cr-8953, male, dissected, forest of *Casuaria equisetifolia*, Suzaki, Chichijima Island, Tokyo Metropolis, Japan, 1 July 1977, Jun-Ichi Aoki leg; paratype, TOYA-Cr-8955, male, dissected, forest of *Casuaria equisetifolia*, Suzaki, Chichijima Island, Tokyo Metropolis, Japan, 1 July 1977, Jun-Ichi Aoki leg; paratype, TOYA-Cr-8961, female, dissected, forest of *Casuaria equisetifolia*, Suzaki, Chichijima Island, Tokyo Metropolis, Japan, 1 July 1977, Jun-Ichi Aoki leg.

Redescription of *Sphaerillo boninensis* Nunomura, 1990

Body color yellowish in alcohol. Pereonites 1–7 with single nodulus lateralis per side, all similarly distanced from lateral margin (Fig. 1A). Pereonite 1 with lateral margin not grooved; schisma deep, with rounded inner and outer lobes, outer lobe protruding posteriorly compared to inner lobe (Fig. 1A, B). Pereonite 2 with an oblique lobe on ventral surface (Fig. 1C). Pereonite 3 without ventral lobe (Fig. 1D). Pereonites 4–7 with a small lobe on ventral surface (Fig. 1D–H). Eyes (of female paratype) with ten ommatidia (Fig. 1I, J). Upper middle edge of cephalon convex; frontal shield separated from vertex, trapezoidal in frontal view (Fig. 1I, J). Flagellum of second antenna with two articles (Fig. 1K). First antenna of three articles; apical article with numerous aesthetascs (Fig. 1L). Right mandible with two plumose setae between lacinia mobilis and molar penicil; lacinia mobilis of left mandible larger than right mandible; molar penicil unbranched; left mandible with three plumose setae between hairy lobe and molar penicil (Fig. 2A, B). First maxilla outer endite with ten simple teeth; inner endite with two stout plumose penicils (Fig. 2C, D). Second maxilla apically bilobate, covered with short setae (Fig. 2E). Endite of maxilliped rectangular, bearing three spines on distal margin; maxilliped palp with basal article bearing two long setae, distal article with apical tuft of small setae (Fig. 2F). Male pereopod 1 with antennal brush on carpus; propodus with numerous short setae on basal half of inner margin; carpus with five long stout setae on inner margin; apical point of outer margin of merus with two tapering setae, inner margin with three branched setae (Fig. 3A). Male pereopods 3–6 unremarkable (Fig. 3B–E). Basis of male pereopod 7 with dense setae on apical corner of inner margin (Fig. 3F). All pleopod exopodites with monospiracular covered lungs (Fig. 4). Male pleopod 1 with straight endopodite, with apical part bent outward with long setae; inner margin with row of small setae; outer margin with at least three tooth-like setae (Fig. 4A); exopodite triangular, with small setae on inner margin (Fig. 4B). Male pleopod 2 endopodite slender (apical part

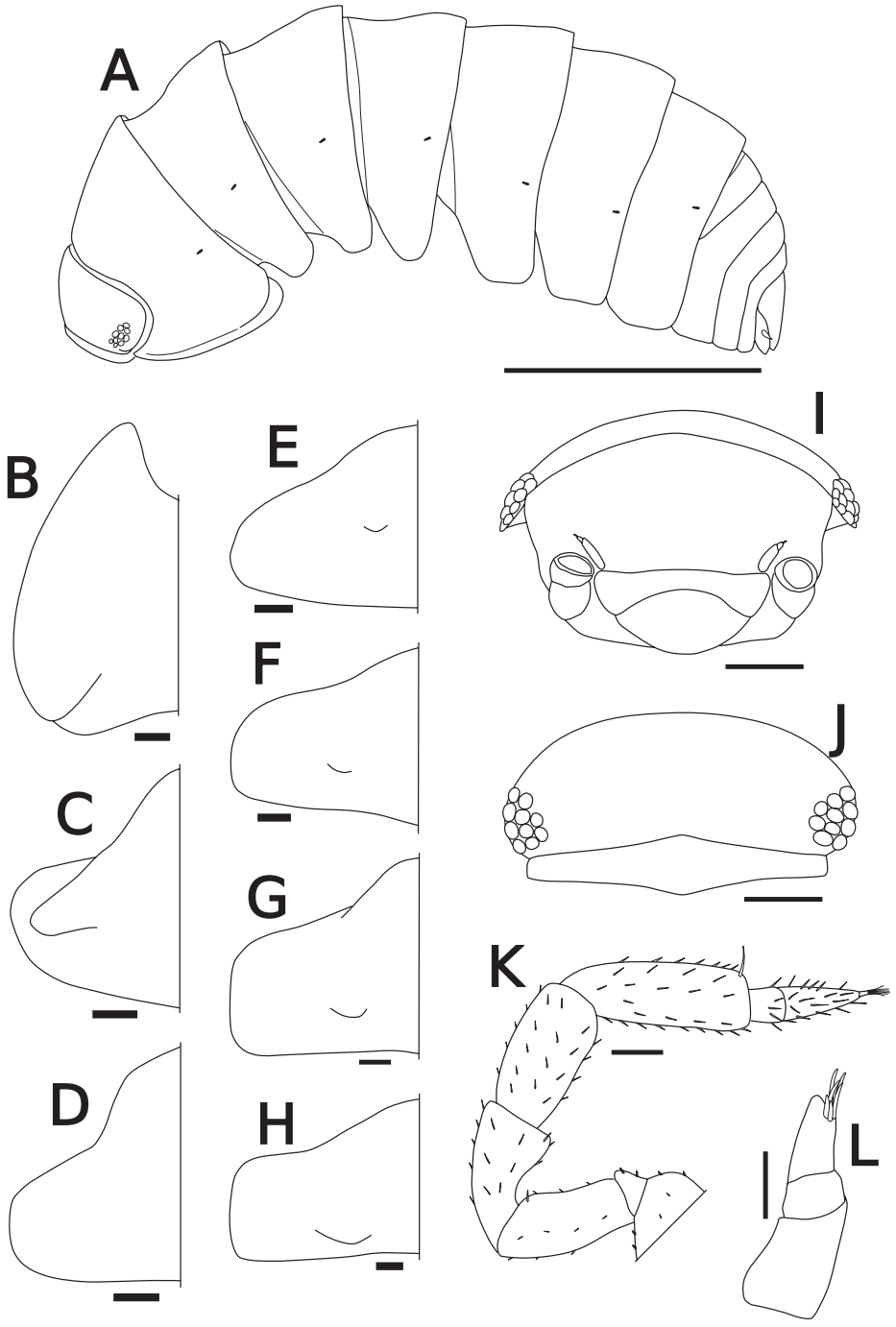

Figure 1. *Sphaerillo boninensis* **A** whole body, lateral view, paratype (female) **B–H** epimeron of pleonites 1–7, ventral view, holotype (male) **I** cephalon, frontal view, paratype (female) **J** cephalon, dorsal view, paratype (female) **K** second antenna, holotype (male) **L** first antenna, paratype (female). Scale bars: 1.5 mm (**A**); 100 μm (**B–H, K**); 300 μm (**I, J**); 50 μm (**L**).

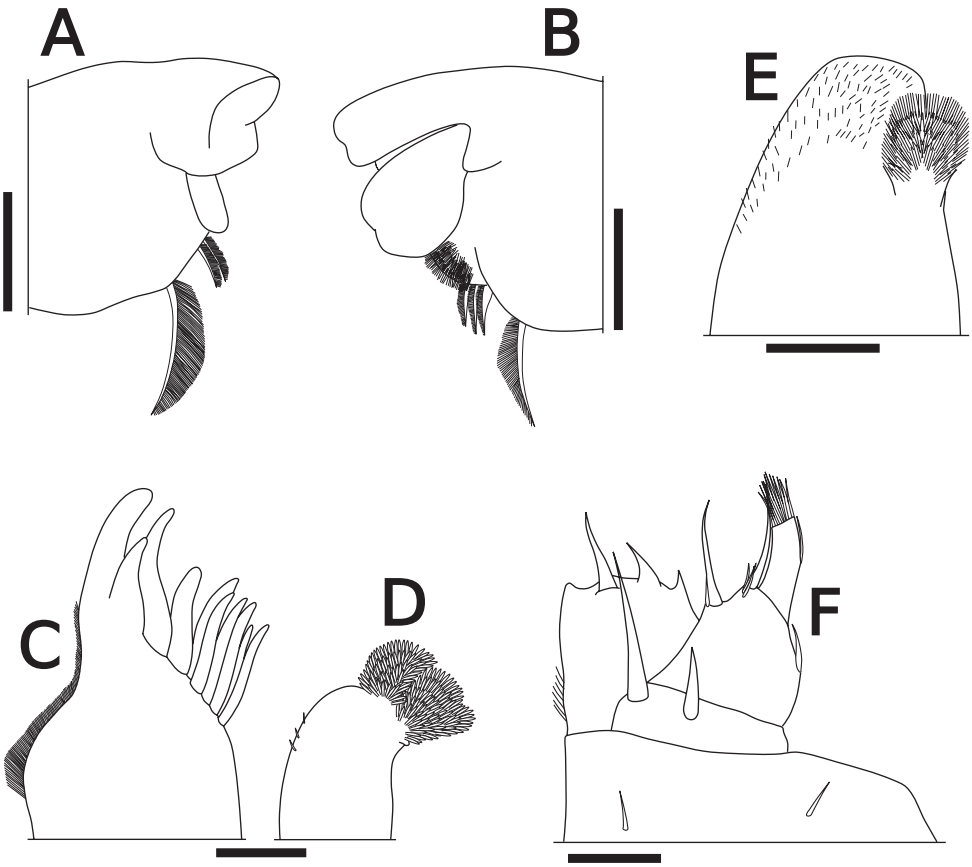

Figure 2. *Sphaerillo boninensis* **A** right mandible, holotype (male) **B** left mandible, holotype (male) **C** outer endite of first maxilla, holotype (male) **D** inner endite of first maxilla, holotype (male) **E** second maxilla, holotype (male) **F** maxilliped, holotype (male). Scale bars: 100 μm (**A, B**); 50 μm (**C–F**).

broken); exopodite triangular, with distal half elongated (Fig. 4C). Male pleopod 3 exopodite with triangular part on posterior inner corner (Fig. 4D). Male pleopod 4 exopodite parallelogram-shaped (Fig. 4E). Female pleopod 5 parallelogram-shaped, with fine setae of variable length along inner margin (Fig. 4F). Pleotelson hour-glass-shaped, distal part narrower than basal part (Fig. 5A). Uropodal protopod trapezoidal, with exopodite inserted on dorsal surface of protopod; endopodite about twice as long as exopodite (Fig. 5B).

Discussion

The genus *Venezillo* is characterized among other characters by a narrow lobe located obliquely or horizontally on the ventral surface of the pereon epimeron 2 (Verhoeff

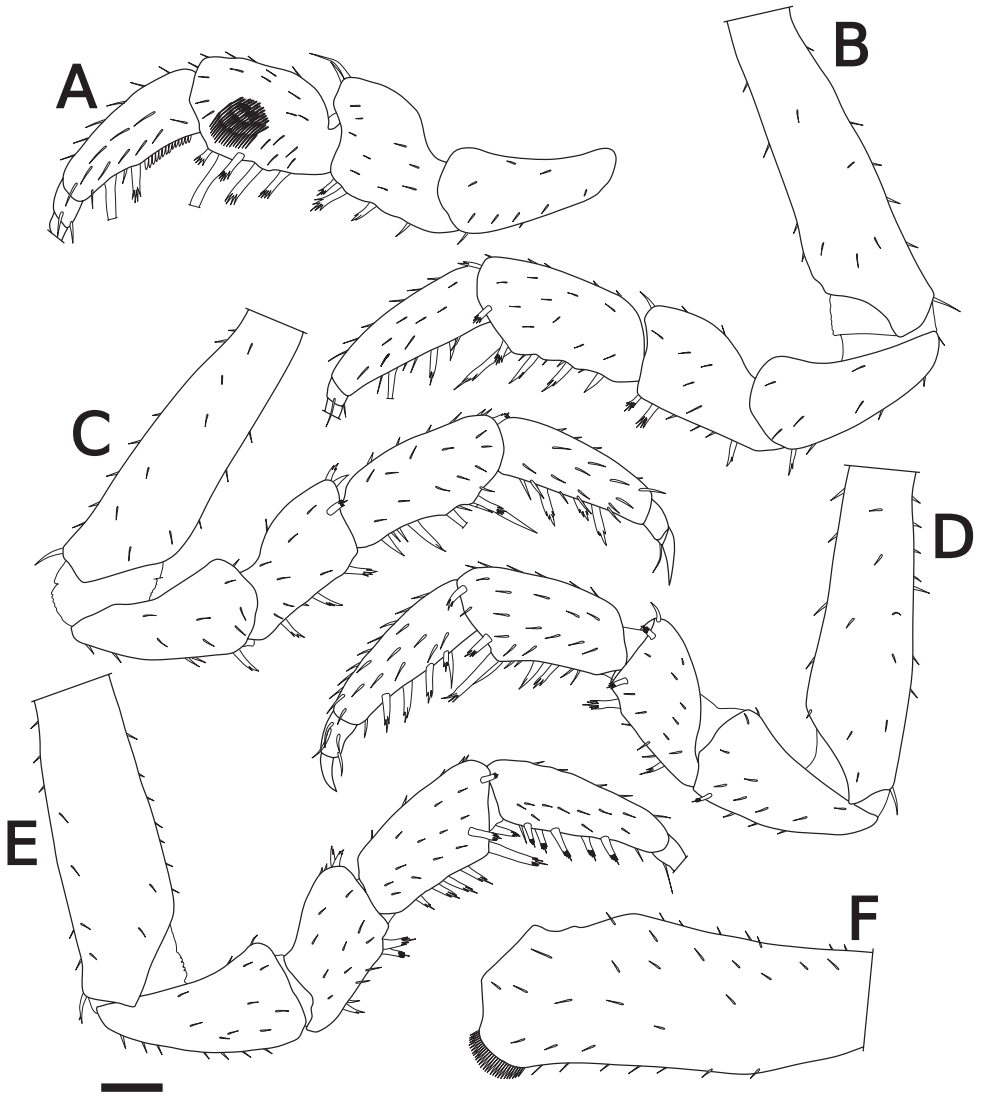

Figure 3. *Sphaerillo boninensis* **A** pereopod 1, holotype (male) **B–E** pereopods 3–6, holotype (male) **F** basis of pereopod 7, holotype (male). Scale bar: 100 μm.

1928; Vandel 1952). The holotype of *S. boninensis* has an oblique lobe on the ventral surface of the epimeron 2, for which reason it is more appropriately assigned to the genus *Venezillo*. In addition, in all other morphological characteristics, type materials of *S. boninensis* are consistent in morphology with those of *V. parvus* as redescribed by Schmidt (2003): the apical corner of the basis of the male pereopod 7 bears dense short setae (Fig. 3F), the endopodite of the male pleopod 1 has long setae at the tip and scale-like setae on the inner margin (Fig. 4A), and the exopodite of the male pleopod 1

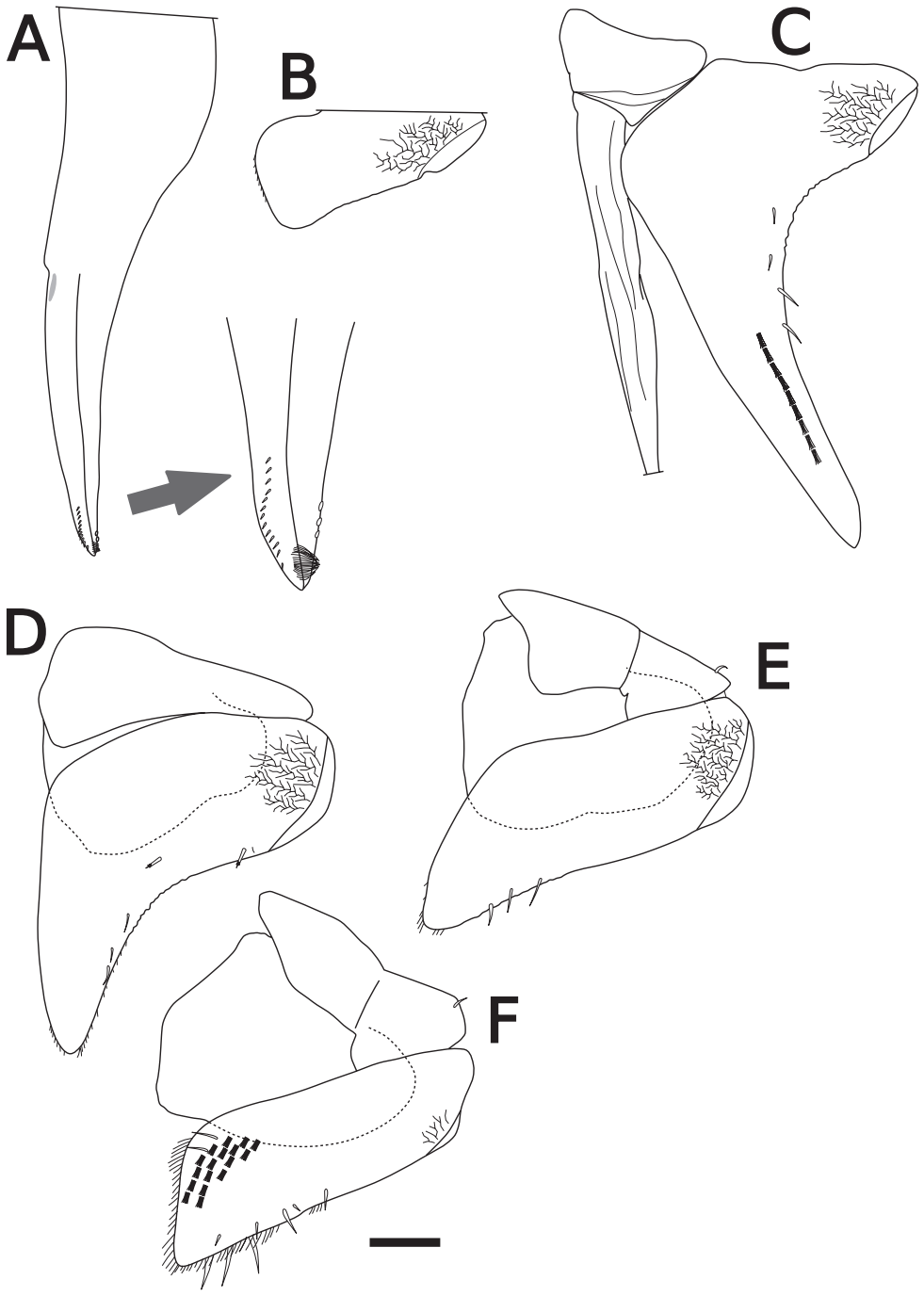

Figure 4. *Sphaerillo boninensis* **A** endopodite of pleopod 1, holotype (male) **B** exopodite of pleopod 1, holotype (male) **C–E** pleopods 2–4, holotype (male) **F** pleopod 5, paratype (female). Scale bar: 100 μm.

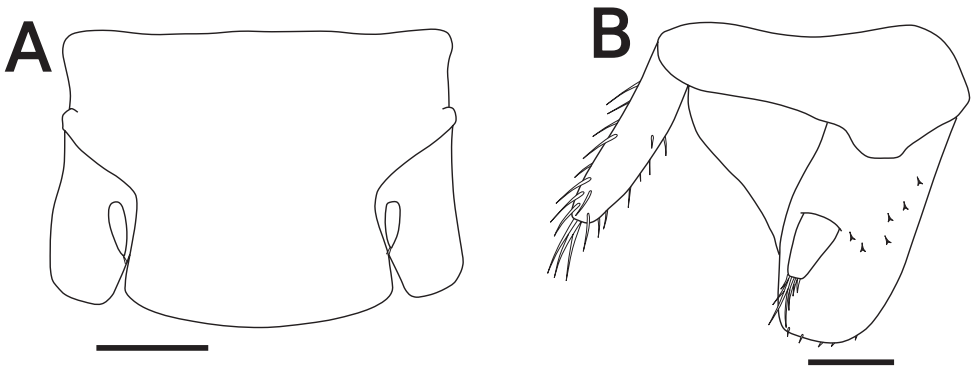

Figure 5. *Sphaerillo boninensis* **A** pleotelson, holotype (male) **B** uropod, holotype (male). Scale bars: 200 μm (**A**); 100 μm (**B**).

is triangular (Fig. 4B). For these reasons, I regard *S. boninensis* to be a junior synonym of *V. parvus*, a species widely distributed in the tropical belt.

While *S. boninensis* was considered endemic to the Ogasawara archipelago, and potentially threatened by an invasive nemertean predator (Shinobe et al. 2017), the pantropical *V. parvus*, due to its widespread distribution and invasive tendency, is not considered to be threatened at species level.

Acknowledgements

I would like to thank Dr Tomofumi Iwata (Toyama Science Museum) and Mr Noboru Nunomura (Kanazawa University, Institute of Nature and Environmental Technology) for loaning type materials of *Sphaerillo boninensis*. This work was supported by a Grant-in-Aid for Young Scientists (B) Grant Number 26830145.

References

Angelini C, Silliman BR (2014) Secondary foundation species as drivers of trophic and functional diversity: evidence from a tree-epiphyte system. Ecology 95: 185–196. https://doi.org/10.1890/13-0496.1

Arab A, Wimp GM (2013) Plant production and alternate prey channels impact the abundance of top predators. Oecologia 173: 331–341. https://doi.org/10.1007/s00442-013-2618-7

Barber T, Gregory S, Lee P (2010) Reports on the 2009 BMIG spring meeting in Cornwall. Bulletin of the British Myriapod Isopod Group 24: 65–74.

Barnard KH (1964) The terrestrial Isopoda and Amphipoda of the Mascarene Islands. Bulletin of the Mauritius Institute 6: 49–60.

Berg MP, Soesbergen M, Tempelman D, Wijnhoven H (2008) Verspreidingsatlas Nederlandse landpissebedden, Duizendpoten en Miljoenpoten (Isopoda, Chilopoda, Diplopoda). EIS-Nederland, Leiden Vrije Universiteit-Afdeling Dierecologie, Amsterdam, 194 pp.

Boyko CB, Bruce NL, Hadfield KA, Merrin KL, Ota Y, Poore GCB, Taiti S, Schotte M, Wilson GDF (2008) World Marine, Freshwater and Terrestrial Isopod Crustaceans database. *Venezillo* Verhoeff, 1928. Accessed through: World Register of Marine Species. http://www.marinespecies.org/aphia.php?p=taxdetails&id=249464 on 2019-03-15

Buck TL, Breed GA, Pennings SC, Chase ME, Zimmer M, Carefoot TH (2003) Diet choice in an omnivorous salt-marsh crab: different food types, body size, and habitat complexity. Journal of Experimental Marine Biology and Ecology 292: 103–116. https://doi.org/10.1016/S0022-0981(03)00146-1

Budde-Lund G (1885) Crustacea Isopoda Terrestria, per Familias et Genera et Species Descripta. Hauniæ, Copenhagen, 319 pp. https://doi.org/10.5962/bhl.title.109769

Budde-Lund G (1904) Revision of Crustacea Isopoda Terrestria, with Additions and Illustrations. pt. 1. *Eubelum*, pt. 2 Spherilloninae, pt. 3 *Armadillo*. H. Hagerup, Copenhagen. https://doi.org/10.5962/bhl.title.9883

Budde-Lund G (1908) Isopoda von Madagaskar und Ostafrika. Mit diagnosen verwandter arten. Reise in Ostafrika in den Jahren 1903-1905, Wissenschaftliche Ergebnisse 2: 265–308. https://doi.org/10.5962/bhl.title.12989

Budde-Lund G (1912) Terrestrial Isopoda, Particularly Considered in Relation to the Distribution of the Southern Indopacific Species. Transactions of the Linnean Society of London, 2nd Series, Zoology. https://doi.org/10.1111/j.1096-3642.1912.tb00107.x

Cochard PO, Vilisics F, Sechet E (2010) Alien terrestrial crustaceans (Isopods and Amphipods). Chapter 7.1. In: Roques A, Kenis M, Lees D, Lopez-Vaamonde C, Rabitsch W, Rasplus J-Y, Roy D (Eds) Alien terrestrial arthropods of Europe. BioRisk 4: 81–96. https://doi.org/10.3897/biorisk.4.54

De los Rios-Escalante P, Arancibia EI, Pérez-Schultheiss J (2018) A checklist of non-marine crustaceans from Chilean oceanic islands. Proceedings of the Biological Society of Washington 131: 47–52. https://doi.org/10.2988/17-00007

Dias N, Sprung M, Hassall M (2005) The abundance and life histories of terrestrial isopods in a salt marsh of the Ria Formosa lagoon system, southern Portugal. Marine Biology 147: 1343–1352. https://doi.org/10.1007/s00227-005-0033-2

Dollfus A (1893) Voyage de M. Charles Alluaud aux Iles Séchelles. Crustacés isopodes terrestres. Bulletin de la Société Zoologique de France 18: 186–190.

Ferrara F, Taiti S (1979) A check-list of terrestrial isopods from Africa (south of the Sahara). Monitore Zoologico Italiano (Nuova Serie) Supplemento 12: 89–215. https://doi.org/10.1080/03749444.1979.10736595

Ferrara F, Taiti S (1981) Terrestrial isopods from Ascension Islands. Monitore Zoologico Italiano (Nuova Serie) Supplemento 14: 189–198. https://doi.org/10.1080/03749444.1981.10736621

Ferrara F, Taiti S (1983) Isopodi terrestri: contributions à l'étude de la faune terrestre des îles granitiques de l'archipel des Séchelles (Mission P.L.G. Benoit, J.J. Van Mol 1972). Annales Du Musée Royal De l'Afrique Centrale, Série 8vo, Sciences Zoologiques 240: 1–92.

Green AJA, Ferrara F, Taiti S (1990) Terrestrial isopoda from the Krakatau islands, south Sumatra and west Java. Memoirs of the Museum of Victoria 50: 417–436. https://doi.org/10.24199/j.mmv.1990.50.13

Green AJA, Lew Ton HM, Poore GCB (2002) Suborder: Oniscidea Latreille, 1802. In: Poore GCB (Ed.) Zoological Catalogue of Australia 19.2A: Crustacea: Malacostraca: Syncarida, Peracarida, Isopoda, Tanaidacea, Mictacea, Thermosbaenacea, Spelaeogriphacea. CSIRO Publishing, Melbourne, 279–344.

Gregory S (2009a) Woodlice and Waterlice (Isopoda: Oniscidea & Asellota) in Britain and Ireland. FSC Publications, Shrewsbury, 175 pp.

Gregory S (2009b) A tropical woodlouse new to Britain. British Myriapod and Isopod Group Newsletter 18: 1–2.

Gregory S (2014) Woodlice (Isopoda: Oniscidea) from the Eden Project, Cornwall, with descriptions of new and poorly known British species. Bulletin of the British Myriapod Isopod Group 27: 3–27.

Humphreys WF (2014) Subterranean fauna of Christmas Island: habitats and salient features. Raffles Bulletin of Zoology Supplement 30: 29–44.

Jass J, Klausmeier B (2000) Endemics and immigrants: North American terrestrial isopods (Isopoda, Oniscidea) north of Mexico. Crustaceana 73: 771–799. https://doi.org/10.1163/156854000504804

Jeppesen PC (2000) Catalogue of terrestrial isopod taxa and type material described by Gustav Budde-Lund (Crustacea: Isopoda). Steenstrupia 25: 221–265.

Johnson C (1976) Genetics of red body polymorphism in the isopod, *Venezillo evergladensis*. Journal of Heredity 67: 157–160. https://doi.org/10.1093/oxfordjournals.jhered.a108693

Johnson C (1977) Evolution of sex ratios in the isopod, *Venezillo evergladensis*. Evolution 31: 603–610. https://doi.org/10.1111/j.1558-5646.1977.tb01049.x

Johnson C (1978) A note on codominance in the terrestrial isopod, *Venezillo evergladensis*. Journal of Heredity 69: 1–140. https://doi.org/10.1093/oxfordjournals.jhered.a108902

Johnson C (1980) Genetics of albinism in the isopod. Journal of Heredity 71: 124–126. https://doi.org/10.1093/oxfordjournals.jhered.a109323

Johnson C (1981) Genetics of mottling in the terrestrial isopod. Journal of Heredity 72: 351–352. https://doi.org/10.1093/oxfordjournals.jhered.a109521

Johnson C (1982) Multiple insemination and sperm storage in the isopod, *Venezillo evergladensis* Schultz, 1963. Crustaceana 42: 225–232. https://doi.org/10.1163/156854082X00920

Johnson C (1983) Eye color genetics and allelism of r-locus factors in the Isopod, *Venezillo evergladensis*. Journal of Heredity 74: 209–210. https://doi.org/10.1093/oxfordjournals.jhered.a109770

Johnson C (1984) Geographic variability in the genetic polymorphism of the isopod, *Venezillo evergladensis*. Journal of Heredity 18: 465–474. https://doi.org/10.1080/00222938400770391

Johnson C (1985a) Selection dynamics in the isopod *Venezillo evergladensis*. Pedobiologia 28: 403–412.

Johnson C (1985b) Mating behavior of the terrestrial isopod, *Venezillo evergladensis* (Oniscoidea, Armadillidae). The American Midland Naturalis 114: 216–224. https://doi.org/10.2307/2425597

Kelly JA, Samways MJ (2003) Diversity and conservation of forest-floor arthropods on a small Seychelles island. Biodiversity and Conservation 12: 1793–1813. https://doi.org/10.1023/A:1024161722449

Keeney GD (1990) Some exotic terrestrial isopods (Oniscoidea) from the Columbus Zoo Exploration Center, Powell, Ohio: two new state records. Ohio Journal of Science 90: 133–134. http://hdl.handle.net/1811/23407

Krantz W, Walter E (2009) A Manual of Acarology (3rd ed). Texas Tech University Press, Texas, 807 pp.

Kwon DH (1995) Terrestrial Isopoda (Crustacea) from Cheju Island, Korea. The Korean Journal Systematic Zoology 11: 509–538.

Kwon DH, Taiti S (1993) Terrestrial Isopoda (Crustacea) from southern China, Macau and Hong Kong. Stuutgarter Beitr Naturk (Serie a) 490: 1–83. https://www.biodiversitylibrary.org/page/33439218#page/79/mode/1up

Leistikow A, Wägele JW (1999) Checklist of the terrestrial isopods of the new world (Crustacea, Isopoda, Oniscidea). Revista Brasileira de Zoologia 16: 1–72. https://doi.org/10.1590/S0101-81751999000100001

Lemaire JM, Gerriet O (2014) Les invertébrés (Arthropoda & Mollusca) de la grande serre du Parc Phoenix (Nice, Alpes-Maritimes, France). Riviera Scientifique 98: 39–52.

McLaughlin PA, Camp DK, Angel MV, Bousfi EL, Brunel P, Brusca RC, Cadien D, Cohen AC, Conlan K, Eldredge LG, Felder DL, Goy JW, Haney R, Haan B, Heard RW, Hendrycks EA, Hobbs III HH, Holsinger JR, Kensley B, Laubitz DR, LeCroy SE, Lemaitre R, Maddocks RF, Martin JW, Mikkelsen P, Nelson E, Newman WA, Overstreet RM, Poly WJ, Price WW, Reid JW, Robertson A, Rogers DC, Ross A, Schram FR, Shih CT, Watling L, Wilson GDF, Turgeon DD (2005) Common and scientific names of aquatic invertebrates from the United States and Canada: crustaceans. American Fisheries Society Special Publication 31: 1–533.

Murphy SM, Wimp GM, Lewis D, Denno RF (2012) Nutrient presses and pulses differentially impact plants, herbivores, detritivores and their natural enemies. PLoS ONE 7: e43929. https://doi.org/10.1371/journal.pone.0043929

Nunomura N (1990) Studies on the terrestrial isopod crustaceans in Japan V. Taxonomy of the families Armadillidiidae, Armadillidae and Tylidae, with taxonomic supplements to some other families. Bulletin of the Toyama Science Museum 13: 1–58.

Nunomura N (1999a) Taxonomical revisions on some groups of terrestrial isopods in Japan. Edaphologia 62: 81–91. [In Japanese]

Nunomura N (1999b) Crustacea, Isopoda. In: Aoki J (Ed.) Pictorial Keys to Soil Animals of Japan. Tokai University Press, Tokyo, 569–625. [In Japanese]

Nunomura N (2011) Crustaceans No.2 (Isopoda). Special Publication of the Toyama Science Museum 24: 1–133. [In Japanese]

Nunomura N (2015) Crustacea, Isopoda. In: Aoki J (Ed.) Pictorial Keys to Soil Animals of Japan. Tokai University Press, Kanagawa, 997–1065. [In Japanese]

Pérez-Schultheiss J, Ayala K, Fariña JM, Coccia C (2018) Exotic oniscideans (Crustacea: Isopoda) in coastal salt marshes: first record of the families Halophilosciidae and Platyarthridae in continental Chile. New Zealand Journal of Zoology: 1–11. https://doi.org/10.1080/03014223.2018.1539017

Poore GCB (2005) Supplement to the 2002 catalogue of Australian Crustacea: Malacostraca—Syncarida and Peracarida (Volume 19.2A): 2002–2004. Museum Victoria Science Reports 7: 1–15. https://doi.org/10.24199/j.mvsr.2005.07

Saito S (1993) Terrestrial crustaceans. In: Society of Nature Study of Yanba Dam (Ed.) Nature of Naganohara. Naganohara Town, Gunma, 345–356. [In Japanese]

Saito N, Itani G, Nunomura N (2000) A preliminary check list of isopod crustaceans in Japan. Bulletin of the Toyama Science Museum 23: 11–107. [In Japanese]

Schmalfuss H (2004) World catalog of terrestrial isopods (Isopoda: Oniscidea). http://www.oniscidea-catalog.naturkundemuseum-bw.de

Schmidt C (2003) Contribution to the phylogenetic system of the Crinocheta (Crustacea, Isopoda). Part 2. (Oniscoidea to Armadillidiidae). Mitteilungen aus dem Museum für Naturkunde in Berlin, Zoologische Reihe 79: 3–179. https://doi.org/10.1002/mmnz.20030790102

Schultz GA (1963) *Venezillo evergladensis*, a new species of terrestrial isopod crustacean from Florida. Transactions of the American Microscopical Society 82: 209–213. https://doi.org/10.2307/3223996

Schultz GA (1972) The Armadillidae of Florida (Isopoda, Oniscoidea). Quarterly Journal of the Florida Academy of Sciences 35: 1–4. https://www.jstor.org/stable/24318279

Schultz GA (1975) Terrestrial isopod crustaceans (Oniscoidea) from coastal sites in Geogia. Bulletin of the Georgia Academy of Science 34: 185–194.

Senterre B, Henriette E, Chong-Seng L, Beaver K, Mougal J, Vel T, Gerlach J (2011) Seychelles Key Biodiversity Areas–Output 1: List of species of special concern. Consultancy Report, Ministry of Environment-UNDP-GEF Project, Victoria, 67 pp.

Shinobe S, Uchida S, Mori, H, Okochi I, Chiba S (2017) Declining soil Crustacea in a World Heritage Site caused by land nemertean. Scientific Reports 7: 1–8. https://doi.org/10.1038/s41598-017-12653-4

Soesbergen M (2003) *Venezillo parvus* en *Synarmadillo* spec., twee nieuwe land-pissebedden in Nederland (Crustacea: Isopoda: Armadillidae). Nederlandse Faunistische Mededelingen 18: 97–101.

Stoyenoff JL (2001) Distribution of terrestrial isopods (Crustacea: Isopoda) throughout Michigan: early results. The Great Lakes Entomologist 34: 29–50. https://scholar.valpo.edu/tgle/vol34/iss2/4

Taiti S (1999) Terrestrial isopods from the Midway Islands. Occasional Papers of the Bishop Museum 58: 37–38.

Taiti S (2018) Biology and biogeography of terrestrial isopods (Crustacea, Isopoda, Oniscidea). Atti Accademia Nazionale Italiana di Entomologia 65: 83–90.

Taiti S, Ferrara F (1983) Su alcuni isopodi terrestri della Réunion, di Mauritius e delle Seycelles. Revue Suisse de Zoologie 90: 199–231. ttps://doi.org/10.5962/bhl.part.81973

Taiti S, Ferrara F (1991a) Terrestrial isopods (Crustacea) from the Hawaiian Islands. Bishop Museum Occasional Papers 31: 202–227.

Taiti S, Ferrara F (1991b) Two new species of terrestrial Isopoda (Crustacea, Oniscidea) from Ascension Island. Journal of Natural History 25: 901–916. https://doi.org/10.1080/00222939100770591

Taiti S, Howarth FG (1996) Terrestrial isopods from the Hawaiian Islands (Isopoda: Oniscidea). Bishop Museum Occasional Papers 45: 59–71. http://hbs.bishopmuseum.org/pdf/op45-59-71.pdf

Taiti S, Paoli P, Ferrara F (1998) Morphology, biogeography, and ecology of the family Armadillidae (Crustacea, Oniscidea). Israel Journal of Zoology 44: 291–301. https://www.tandfonline.com/doi/abs/10.1080/00212210.1998.10688952

Taiti S, Wynne JJ (2015) The terrestrial Isopoda (Crustacea, Oniscidea) of Rapa Nui (Easter Island), with descriptions of two new species. In: Taiti S, Hornung E, Štrus J, Bouchon D (Eds) Trends in Terrestrial Isopod Biology. ZooKeys 515: 27–49. https://doi.org/10.3897/zookeys.515.9477

Treplin M, Pennings SC, Zimmer M (2013) Decomposition of leaf litter in a U.S. saltmarsh is driven by dominant species, not species complementarity. Wetlands 33: 83–89. https://doi.org/10.1007/s13157-012-0353-1

Vandel A (1952) Etude des isopodes terrestres récoltés au Vénézuela par le Dr. G. Marcuzzi, suivie de considerations sur le peuplement du Continent de Gondwana. Memoire del Museo Civico di Storia Naturale di Verona 3: 59–203.

Verhoeff KW (1928) Über einige Isopoden der zoologischen Staatssammlung in München. 38. Isopoden-Aufsatz. Zoologischer Anzeiger 76: 113–123.

Verhoeff KW (1946) Über Land-Isopoden der Seychellen und aus Burma. Arkif för Zoologi 37: 1–18.

Vittori M, Štrus J (2017) Male tegumental glands in the cavernicolous woodlouse *Cyphonethes herzegowinensis* (Verhoeff, 1900) (Crustacea: Isopoda: Trichoniscidae). Journal of Crustacean Biology 37: 389–397. https://doi.org/10.1093/jcbiol/rux067

Wimp GM, Murphy SM, Lewis D, Douglas MR, Ambikapathi R, Van-Tull L, Gratton C, Denno RF (2013) Predator hunting mode influences patterns of prey use from grazing and epigeic food webs. Oecologia 171: 505–515. https://doi.org/10.1007/s00442-012-2435-4

Zimmer M, Pennings SC, Buck TL, Carefoot TH (2002) Species-specific patterns of litter processing by terrestrial isopods (Isopoda: Oniscidea) in high intertidal salt marshes and coastal forests. Functional Ecology 16: 596–607. https://doi.org/10.1046/j.1365-2435.2002.00669.x

Zimmer M, Pennings SC, Buck TL, Carefoot TH (2004) Salt marsh litter and detritivores: A closer look at redundancy. Estuaries 27: 753–769. https://doi.org/10.1007/BF02912038

ZooKeys 923: 15–32 (2020)
doi: 10.3897/zookeys.923.48593
http://zookeys.pensoft.net

RESEARCH ARTICLE

A peer-reviewed open-access journal
ZooKeys
Launched to accelerate biodiversity research

Two freshwater shrimp species of the genus *Caridina* (Decapoda, Caridea, Atyidae) from Dawanshan Island, Guangdong, China, with the description of a new species

Qing-Hua Chen[1], Wen-Jian Chen[2], Xiao-Zhuang Zheng[2], Zhao-Liang Guo[2]

1 *South China Institute of Environmental Sciences, Ministry of Ecology and Environment, Guangzhou 510520, Guangdong Province, China* **2** *Department of Animal Science, School of Life Science and Engineering, Foshan University, Foshan 528231, Guangdong Province, China*

Corresponding author: Zhao-Liang Guo (zlguo@fosu.edu.cn)

Academic editor: I.S. Wehrtmann | Received 19 November 2019 | Accepted 7 February 2020 | Published 1 April 2020

http://zoobank.org/138A88CC-DF41-437A-BA1A-CB93E3E36D62

Citation: Chen Q-H, Chen W-J, Zheng X-Z, Guo Z-L (2020) Two freshwater shrimp species of the genus *Caridina* (Decapoda, Caridea, Atyidae) from Dawanshan Island, Guangdong, China, with the description of a new species. ZooKeys 923: 15–32. https://doi.org/10.3897/zookeys.923.48593

Abstract

A faunistic and ecological survey was conducted to document the diversity of freshwater atyid shrimps of Dawanshan Island. Two species of *Caridina* that occur on this island were documented and discussed. One of these, *Caridina tetrazona* **sp. nov.** is described and illustrated as new to science. It can be easily distinguished from its congeners based on a combination of characters, which includes a short rostrum, the shape of the endopod of the male first pleopod, the segmental ratios of antennular peduncle and third maxilliped, the slender scaphocerite, and the absence of a median projection on the posterior margin. Live individuals of the new species display a unique coloration pattern with four dark blue transverse bands on the body, and can be easily recognized in the field. So far, despite considerable surveying efforts made on neighboring islands, this species has only been found from a small stream on Dawanshan Island, which suggests that it may have a very limited range, probably endemic to Dawanshan Island. Molecular characteristics of the mitochondrial cytochrome c oxidase subunit I (COI) demonstrate that this species shows sufficient interspecific divergence from its congeners, including *C. serrata* Stimpson, 1860, which was found in four streams on Dawanshan Island, and has been previously reported on the neighboring islands of Hong Kong, Dong'ao, Wailingding, and Guishan.

Keywords
COI, morphology, rice shrimp, systematics, taxonomy

Introduction

The genus *Caridina* H. Milne Edwards, 1837, comprising 302 species and mainly present in the Indo-Pacific region, is the most diversified genus of the Atyidae (De Grave et al. 2015; De Mazancourt et al. 2018). Collecting evidence-based information is the foundation for addressing urgent global challenges in biodiversity conservation and sustainable management of native species. The critical knowledge gaps in the taxonomy, population and distribution patterns have to be filled before any decisions can be taken on biologically meaningful and effective conservation management. The atyid fauna of Dawanshan Island has not been properly surveyed. In order to better understand the diversity of the freshwater atyid fauna in the Dawanshan Island, an intensive field survey was carried out in June 2017. The results show that there are two species of atyid shrimps, *Caridina tetrazona* sp. nov. and *C. serrata* Stimpson, 1860.

The Wanshan Islands are located in the Pearl River Estuary, Zhuhai, Guangdong Province, southern China. Dawanshan Island (21°55'19.69" – 21°57'21.46"N, 113°42'54.30" – 113°45'06.09"E) covers an area of 8175 km^2, and is situated in the south of the Wanshan Islands. It is about 29 km northwest from Macau, 33 km from Zhuhai City, and 56 km northeast from Hong Kong (Fig. 1).

With an unspoiled natural landscape and an ideal climate, the island is promising for marine ecotourism development. The increasing exploitation of resources for tourism threatens the species that live there. The new species could be potentially seriously threatened and should be regarded as an endangered species.

Material and methods

Study area

Dawanshan Island (21°55'19.69" – 21°57'21.46"N, 113°42'54.30" – 113°45'06.09"E) belongs to the Wanshan Islands. It is a small island, 3.35 km in length, 2.45–3.88 km in width, with a coastline of 14.42 km, and five bays around the island. There are five peaks, with the highest point of Wanshan Peak in the central part of the north, at 432.5 m above sea level. Dawanshan Island has loess sandy soil over a rocky base. There are many cliffs on both sides of the south and west, and huge rocks on both sides of the east and north. The island has a subtropical oceanic monsoon climate, which is warm and humid throughout the year, with an average annual temperature of 22–23 °C, an average annual precipitation of 1800–2000 mm and an average annual relative humidity of 81.0%. Vegetation on Dawanshan Island is of evergreen broad-leaved forest type,

with a forest coverage rate of about 60% (Huang and Wang 2000; Liao et al. 2000; He et al. 2004; Huang et al. 2012). The sampling sites of the current study, covering habitats of streams, pools, agricultural waterways, swamps, and brackish water bays are provided in Figure 1.

Collection

Samples were collected by a hand net with a mesh size of 0.8 mm. All specimens obtained were fixed in 95% ethanol. The ethanol was changed after 24 hours with fresh 75% ethanol. The drawings were made with the aid of a drawing tube mounted on an Olympus BX – 41 compound microscope.

Genetic analyses

The forward and reverse primers of the mitochondrial COI gene in this study were: LCO1490 and HCO2198, respectively (Folmer et al. 1994). The PCR reaction was carried out on a Bio-Rad/T^{100}TM Thermal Cycler instrument with a system of 50 μL, of which 25 μL of 2 × EasyTaq Mix, 20 μL of ddH_2O, 2 μL of each of the forward and reverse primers, and 1 μL of the DNA template. The PCR amplification conditions were: 35 cycles of denaturation at 94 °C for 30 s, annealing at 46 °C for 60 s, extension at 72 °C for 60 s, and a final extension at 72 °C for 5 min. Five μL of the PCR product was subjected to 1.5% agarose gel electrophoresis for detection of the amplified product. After successful detection, sequences were obtained by Applied Biosystems 3730 Analyzer (Applied Biosystems, Foster City, CA, USA), after verification with the complementary strand.

A total of 26 nucleotide sequences were analyzed. Selected species for the molecular analyses were species similar to the morphology and the color of the new species and the *Caridina* species that are known to occur on neighbouring islands. All the sequences were aligned with MAFFT v7.313 software using the auto strategy and normal alignment mode (Katoh and Standley 2013). In order to find the best-fitting model for sequence evolution, ModelFinder (Kalyaanamoorthy et al. 2017) was used. According to Bayes information criterion (ModelFinder default recommendation), the best models for analysis maximum likelihood method (ML) and Bayesian method (BI) are TIM2+F+I+G4 and GTR+F+G4, respectively. ML was performed using IQ-TREE 1.6.12 (Nguyen et al. 2015). Bayesian phylogeny was applied using MrBayes v3.2.6 (Ronquist et al. 2012). Markov chain Monte Carlo analysis was performed with two simultaneous runs starting with random tress to approximate the posterior probabilities of trees. Each run consisted of four chains, with default heating parameters. It lasted for 2 × 10^6 generations for the selected Atyidae and the first 25% of the samples were discarded. Standard deviation of split frequencies (<0.01) was accounted as a convergence index. Genetic distances were calculated using the Kimura 2-parameter model in MEGA 7.0 based on COI (Kumar et al. 2016).

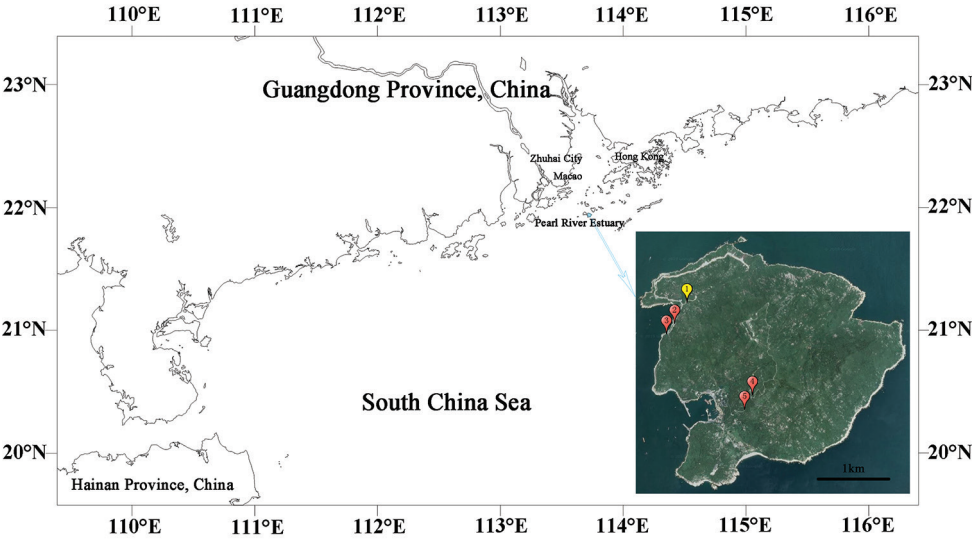

Figure 1. The light blue point shows the location of Dawanshan Island. The inset shows the sample locations. The yellow icon (stn 1) shows the collection site of *Caridina tetrazona* sp. nov., and red icons (stns 2–5) are the collection sites of *C. serrata*.

Table 1. Specimens of the atyids *Caridina* and *Neocaridina* used in the molecular analyses (new sequences), listed by localities, geographical coordinates and GenBank accession numbers.

Species	Locality	Geographical coordinates	Accession no.
C. cantonensis	Wutong Mountain, Shenzhen	22°34'49"N, 114°12'44"E	MN701589
	Wutong Mountain, Shenzhen	22°34'49"N, 114°12'44"E	MN701590
	Baiyun Mountain, Guangzhou	23°10'05"N, 113°17'36"E	MN701591
	Baiyun Mountain, Guangzhou	23°10'05"N, 113°17'36"E	MN701592
C. huananensis	Yingde, Qingyuan	23°54'17"N, 113°15'55"E	MN701607
	Yingde, Qingyuan	23°54'17"N, 113°15'55"E	MN701608
C. lanceifrons	Dongfang, Hainan	18°40'06"N, 109°56'32"E	MN701605
	Dongfang, Hainan	18°40'06"N, 109°56'32"E	MN701606
C. mariae	Nankun Mountain, Huizhou	23°39'32"N, 113°54'19"E	MN701601
	Nankun Mountain, Huizhou	23°39'32"N, 113°54'19"E	MN701602
C. serrata	Dawanshan Island, Zhuhai	21°33'41"N, 113°25'59"E	MN701595
	Dawanshan Island, Zhuhai	21°33'41"N, 113°25'59"E	MN701596
	Dong'ao Island, Zhuhai	22°00'17"N, 113°25'27"E	MN701599
	Dong'ao Island, Zhuhai	22°00'17"N, 113°25'27"E	MN701600
C. tetrazona sp. nov.	Dawanshan Island, Zhuhai	21°33'57"N, 113°25'48"E	MN701593
	Dawanshan Island, Zhuhai	21°33'57"N, 113°25'48"E	MN701594
C. zhujiangensis	Dong'ao Island, Zhuhai	22°00'38"N, 113°25'13"E	MN701603
	Dong'ao Island, Foshan	22°00'38"N, 113°25'13"E	MN701604
N. palmata	Yangshan, Qingyuan	24°25'28"N, 112°36'28"E	MN701609
	Yangshan, Qingyuan	24°25'28"N, 112°36'28"E	MN701610
N. hofendopoda	Sanxia, Yichang	30°49'32"N, 111°00'59"E	MN701611
	Sanxia, Yichang	30°49'32"N, 111°00'59"E	MN701612

Abbreviations

The following abbreviations are used throughout the text: al: altitude; cl: carapace length (measured from the postorbital margin to the posterior margin of the carapace); coll: sample collectors; rl: rostral length (measured from the rostral tip to the postorbital margin); stn: sampling station; tl: total length (measured from the rostral tip to the posterior margin of the telson). All measurements are in millimeters.

Specimens were deposited in the Department of Animal Science, School of Life Science and Engineering, Foshan University (FU).

Systematic accounts

Family Atyidae De Haan, 1849
Subfamily Atyinae De Haan, 1849
Genus *Caridina* H. Milne Edwards, 1837

***Caridina serrata* Stimpson, 1860**
Figs 2B, C, 3B, C

Caridina serrata Stimpson, 1860: 29 [type locality: Hong Kong, China].
Caridina serrata-Ortmann 1894: 406; Bouvier 1905: 76; 1925: 258, fig. 593; Kemp 1918: 289, fig. 12; Cai and Ng 1999: 1605, figs 2, 3; Liang 2004: 173, fig. 83; Chen et al. 2018: 315, figs 2, 3.

Material examined. 13 females, cl 3.5–6.8 mm, 2 ovigerous cl 3.7–5.6 mm, 5 males cl 3.0–5.8 mm, a small pool (21°56'48.6"N, 113°42'55.5"E, al. 5.4 m, stn 2), 27 June 2017, coll. Z. L. Guo, W. J. Chen; 17 females, cl 3.4–6.6 mm, 2 ovigerous females, cl 4.1–5.6 mm, 15 males, cl 2.9–5.5 mm, a small stream (21°56'43.6"N, 113°42'51.4"E, al. 27.2 m, stn 3), 27 June 2017, coll. Z. L. Guo, W. J. Chen; 5 females, cl 3.1–6.9 mm, 3 ovigerous, cl 3.5–5.8 mm, 3 males, cl 3.0–5.2 mm, a small stream (21°56'15.6"N, 113°43'33.4"E, al. 186.6 m, stn 4), 28 June 2017, coll. Z. L. Guo, W. J. Chen; 7 females, cl 3.4–6.9 mm, 4 males, cl 3.5–5.7 mm, a small stream (21°56'02.8"N, 113°43'29.0"E, al. 122.8 m, stn 5), 28 June 2017, coll. Z. L. Guo, W. J. Chen.

Remarks. The present specimens are in agreement with the description and illustrations of Cai and Ng (1999) and Liang (2004). *Caridina serrata* is highly adaptable and prolific, distributed everywhere on the Wanshan Islands, such as Dong'ao Island, Guishan Island, and Wailingding Island (Chen et al. 2018). A close biogeographical connection of the atyid faunas among the Wanshan Islands is evident. This species is also distributed in Hong Kong (Cai and Ng 1999), Chaqiao, and Zhongshan City (Liang 2004).

Figure 2. Habitats of the two shrimp species in this study. **A** Habitat of *Caridina tetrazona* sp. nov. **B, C** habitat of *C. serrata*.

Ecological notes. *Caridina serrata* is commonly found in pools, streams, and artificial ditches on the island. Sometimes, the stream connects with the sea. Sediment at the site comprised sand, pebbles and gravel patches between large boulders. Hill streams are within secondary forests and are covered with aquatic plant (Fig. 2B, C). The water parameters of the streams at the time of collection were: temperature 24–26 °C, pH 5.8–6.5, dissolved ammonia nitrogen 0.20–0.22 mgl^{-1}, and dissolved oxygen 7.8–8.6 mgl^{-1}; the water was clear and flowing. *Caridina serrata* is associated with dead leaves and aquatic plants, but also lives under pebbles and stones. The female carries fewer but large eggs (0.5–0.7 × 0.9–1.0 mm). The larvae go through direct development and hatch into benthic hatchlings that resemble miniature adults.

Coloration. The live shrimp show light-red coloration and are translucent (Fig. 3B, C).

Distribution. Southern China (Hong Kong, Zhuhai City and Zhongshan City of Guangdong Province).

***Caridina tetrazona* sp. nov.**
http://zoobank.org/F3E1596D-A5CE-47B0-8926-19E95DAAC97A
Figs 2A, 3A, 4, 5

Material examined. ***Holotype*:** male (FU, 2017-06-27-01), cl 3.9 mm, tl 14.4 mm, rl 1.3 mm, a stream near Longtangzui Dawanshan Island, Zhuhai City, Guangdong, China (21°56'59.2"N, 113°43'00"E, al. 8 m, stn 1), 9 June 2017. ***Paratypes*:** male (FU, 2017-06-27-02), cl 4.3 mm, 4 males (FU, 2017-06-27-03), cl 3.8–4.3 mm, 33 females, 4 ovigerous (FU, 2017-06-27-04), cl 3.8–5.4 mm, same collection data as for holotype, coll. Z. L. Guo, W. J. Chen.

Comparative material. *Caridina serrata* Stimpson, 1860 (see material under *Caridina serrata*). *Caridina cantonensis* Yu, 1938; 8 males, cl 3.5–6.3 mm, 5 females, 2 ovigerous, cl 4.1–6.3 mm, a stream at Mangzixia, Yingde, Qingyuan City, Guangdong, China (24°3'20"N, 113°19'6"E, al. 20 m), 4 June 2018, coll. Z. L. GUO, W. J. Chen, X. Z. Zheng.

Diagnosis. Rostrum short, straight or slightly sloping downwards, nearly reaching to or slightly reaching beyond end of 1st segment of antennular peduncle, rostral formula 3–8 (usually 5–7) + 4–6/1–2. 1st pereiopod carpus 0.63–0.70 × as long as chela, 1.6–1.7 × as long as high; chela 1.8–2.0 × as long as broad; fingers 0.92–1.1 × as long as palm. 2nd pereiopod carpus 1.1–1.3 × as long as chela, 4.9–5.3 × as long as high; chela 2.7–2.9 × as long as broad; fingers 1.7–1.8 × as long as palm. 3rd pereiopod propodus 3.9–4.5× as long as dactylus, with 8–11 thin spines on the posterior and lateral margins. 5th pereiopod propodus 4.9–5.1 × as long as dactylus, with 8–11 thin spines on the posterior and lateral margins, dactylus terminating in one claw, with 27–31 spinules on flexor margin. Endopod of male 1st pleopod extending to 0.56 × exopod length, wider proximally, subrectangular, 2.5–2.6 × as long as wide, appendix interna well developed, arising from distal 1/3 of endopod, reaching beyond end of

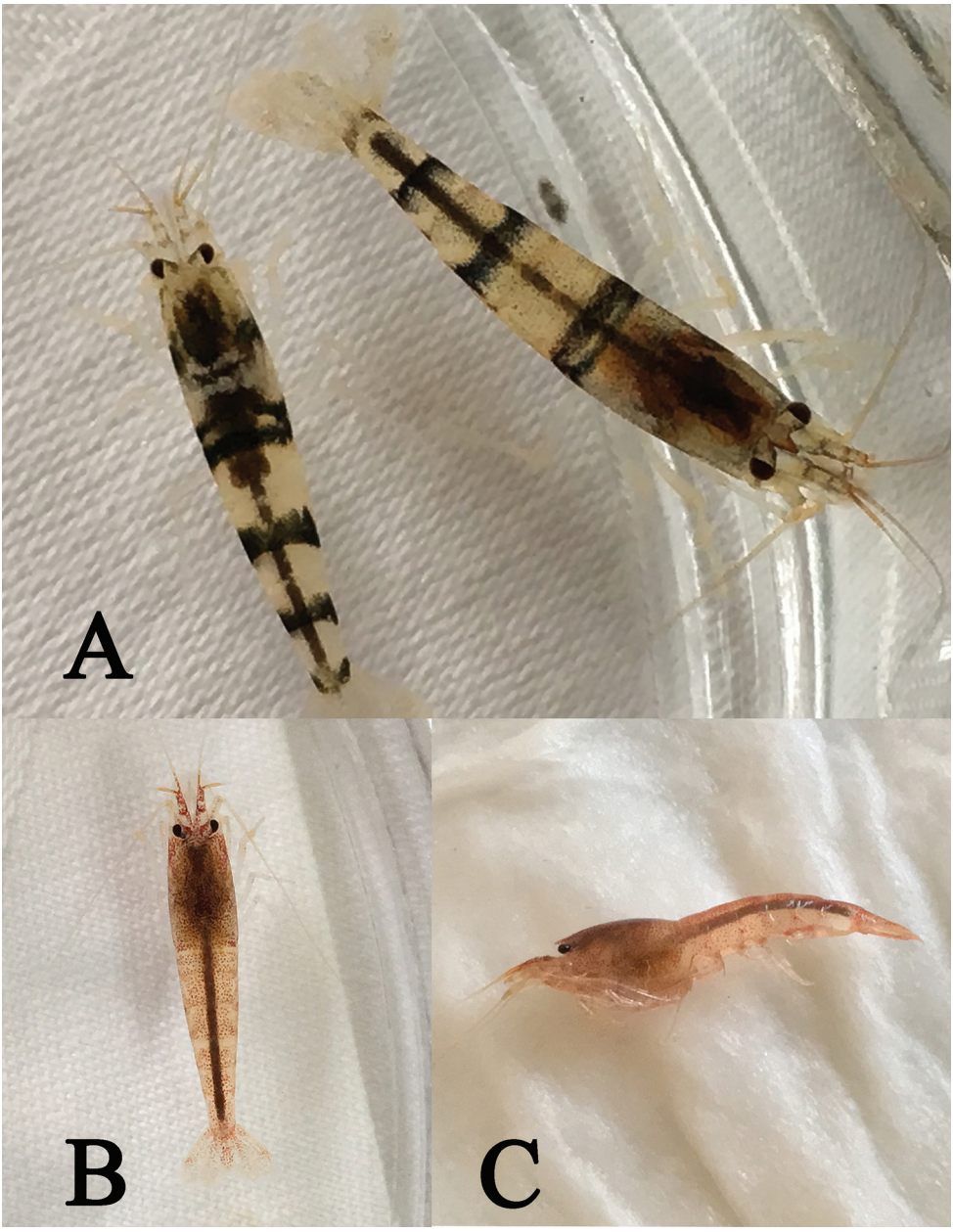

Figure 3. Photos of live specimens of the two species of *Caridina* from Dawanshan Island. **A** *Caridina tetrazona* sp. nov. **B** dorsal view of *C. serrata* **C** lateral view of *C. serrata*.

endopod. Appendix masculina of male 2nd pleopod rod-shaped, reaching to 0.7 length of endopod, appendix interna reaching to 0.7 length of appendix masculina. Uropodal diaeresis with 18–20 movable spinules. Eggs 0.51–0.65 × 0.84–0.97 mm in diameter.

Description. Body: small, slender and sub-cylindrical, males up to 14.8 mm tl, females up to 20.4 mm tl.

Rostrum (Fig. 4A, B): Short, only 0.15–0.32 of cl, straight or slightly sloping downwards; reaching end of basal segment of antennular peduncle, or to just beyond it; armed dorsally with 7–14 teeth, including 3–8 (usually 5–7) on carapace posterior to orbital margin, ventrally with 1–2 teeth; lateral carina dividing rostrum into two unequal parts, continuing posteriorly to orbital margin.

Eyes (Fig. 4A, B): Well developed on short ocular peduncle, cornea globular.

Carapace (Fig. 4A, B): Smooth, glabrous; antennal spine acute, fused with inferior orbital angle; pterygostomian margin broadly rounded or slightly produced forward; no pterygostomian.

Antennule (Fig. 4A–C): Peduncle reaching slightly short of scaphocerite; stylocerite long, reaching 0.3 × of 2nd segment; anterolateral angle reaching 0.2 × of 2nd segment; length of basal segment as long as sum of length of 2nd and 3rd segments, 2nd segment 0.46–0.51 × of basal segment, 1.1–1.3 × of 3rd segment; all segments with sub-marginal plumose setae.

Antenna (Fig. 4D): Peduncle about 0.54 × of scaphocerite; scaphocerite about 3.6 × as long as wide, outer margin straight, ending in strong sub-apical spine, inner and anterior margins with long plumose setae.

Mandible (Fig. 4E): Without palp; left incisor process with 4 sharp teeth; medially 2 groups of setae; molar process ridged.

Maxillula (Fig. 4F): Lower lacinia broadly rounded, with several rows of plumose setae; upper lacinia elongate, medial edge straight, with 29 strong spinules and simple setae; palp simple, slightly expanding distally, with 4 long simple setae.

Maxilla (Fig. 4G): Scaphognathite tapering posteriorly, distally with regular row of long plumose setae and short marginal plumose setae continuing down proximal triangular process, furnished with numerous long plumose setae; upper and middle endite with marginal simple, denticulate and sub-marginal simple setae, distally with plumose setae; lower endite with long simple marginal setae; palp distinctly shorter than cleft of upper endite, wider proximally than distally.

First maxilliped (Fig. 4H): Palp broadly triangular ending in fringe-like tip and with terminal plumose setae; caridean lobe broad, with marginal plumose setae; exopodal flagellum well developed, with distally marginal plumose setae; ultimate and penultimate segments of endopod indistinctly divided; medial and distal margins of ultimate segment with marginal and sub-marginal rows of simple, denticulate and plumose setae; penultimate segments with marginal long plumose setae.

Second maxilliped (Fig. 4I): Ultimate and penultimate segments of endopod indistinctly divided, reflexed against basal segment; inner margin of ultimate, penultimate and basal segments with long setae of various types; exopod flagellum long, slender with marginal plumose setae distally.

Branchial formula typical for genus. Epipod on first four pereiopods.

Third maxilliped (Fig. 5A): Reaches to end of 2nd antennular peduncle segment, endopod three-segmented, penultimate segment as long as basal segment; distal seg-

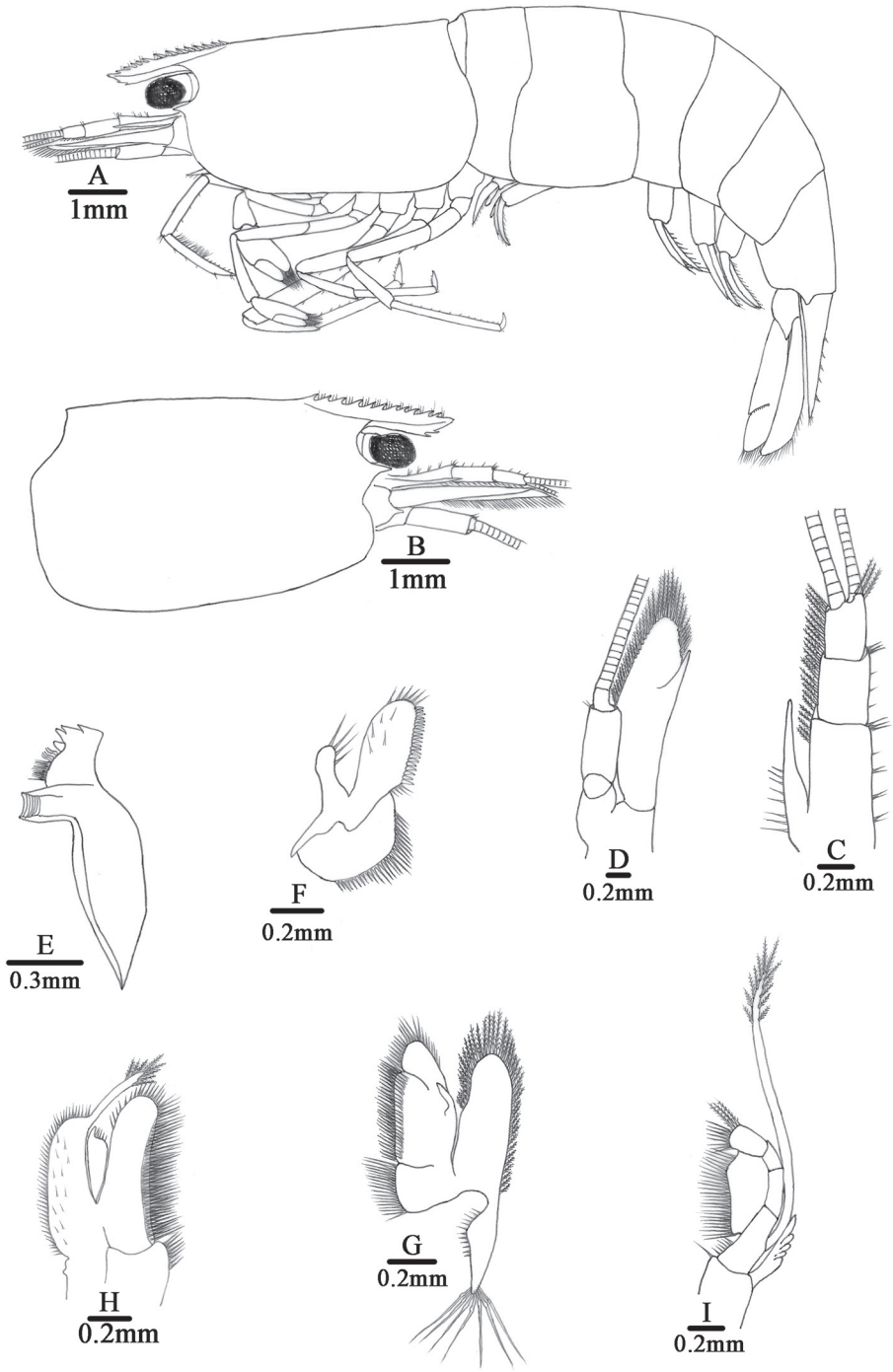

Figure 4. *Caridina tetrazona* sp. nov. **A** Entire animal, lateral view, holotype (FU, 2017-06-27-01) **B–I** paratype (FU, 2017-06-27-02) **B** carapace and cephalic appendages, lateral view **C** antennule **D** antenna **E** mandible **F** maxillula **G** maxilla **H** first maxilliped **I** second maxilliped.

ment 0.87–0.90 × as long as penultimate segment, ending in a large claw-like spine surrounded by simple setae, preceded by about 5–8 spines on distal third of posterior margin, proximally a clump of long and short simple, serrate setae; exopod reaches to end of basal segment of endopod, distal margin with long plumose setae.

First pereiopod (Fig. 5B): Reaches end of eyes; chela 1.8–2.2 × as long as wide; 1.4–1.6 × as long as carpus; movable finger 2.8–3.2 × as long as wide, 0.92–1.1× as long as palm, setal brushes well developed; carpus excavated anterior-dorsally, 1.5–1.8 × as long as high, 0.90–1.0 × as long as merus.

Second pereiopod (Fig. 5C): Reaches about end of 3rd antennular peduncle segment, more slender and longer than first pereiopod; chela 2.6–3.2 × as long as wide; 0.78–0.87 × as long as carpus; movable finger 4.0–4.6 × as long as wide and 1.5–1.7 × as long as palm, setal brushes well developed; carpus 4.9–5.9 × as long as high, slightly excavated anterior, as long as merus.

Third pereiopod (Fig. 5D): Reaches beyond end of scaphocerite; dactylus 2.9–3.5 × as long as wide, ending in prominent claw-like spine surrounded by simple setae, flexor margin bearing 4–5 spines; propodus 4.5–4.9 × as long as dactylus, bearing 8–12 spinules on posterior and lateral margin, 8.4–9.7 × as long as wide; carpus 0.67–0.82 × as long as propodus; merus 1.7–2.0× as long as carpus, with about 3–4 strong spines on the posterior margin.

Fourth pereiopod: Reaches middle of 2nd segment of antennular peduncle; dactylus 3.0–4.2 × as long as wide, ending in prominent claw-like spine surrounded by simple setae, flexor margin bearing 4–6 spines; propodus 4.2–5.1 × as long as dactylus, bearing 9–13 spinules on posterior and lateral margin, 8.5–10.5 × as long as wide; carpus 0.66–0.81 × as long as propodus; merus 1.6–1.8× as long as carpus, with about 3–4 strong spines on the posterior margin.

Fifth pereiopod (Fig. 5E): Reaches middle of 1st segment of antennular peduncle; dactylus 2.8–3.6 × as long as wide, ending in prominent claw-like spine surrounded by simple setae, flexor margin bearing with a row of 27–31 comb-like spinules; propodus 4.7–5.1 × as long as dactylus, bearing 8–11 spinules on posterior and lateral margin, 8.9–11.9 × as long as wide; carpus 0.52–0.62 × as long as propodus; merus 1.3–1.5 × as long as carpus, with about 3–4 strong spines on the posterior margin.

First pleopod (Fig. 5F): Endopod of male subrectangular, wider proximally, 0.56 × as long as exopod, 2.5–2.6 × as long as proximal wide, ending broadly rounded; inner margin slightly concave, bearing short spine-like setae, outer margin slightly convex, bearing long spine-like setae, distinctly longer and stout on distal 1/3, distal end tip bearing nearly equal length shorter spine-like setae; appendix interna well developed, arising from distal 1/3 of endopod, reaching beyond end of endopod, distally with numerous cincinulli.

Second pleopod (Fig. 5G): Appendix masculina rod-shaped, reaching about 0.7 × length of exopod, inner margin and tip bearing numerous spine setae; appendix interna slender, reaching about 0.73 × length of appendix masculina, distally with many cincinulli.

Telson (Fig. 5H): 0.56–0.75 × as long as cl, tapering posterior, dorsal surface with 6 pairs of stout movable spine-like setae including the pair at poster lateral angles;

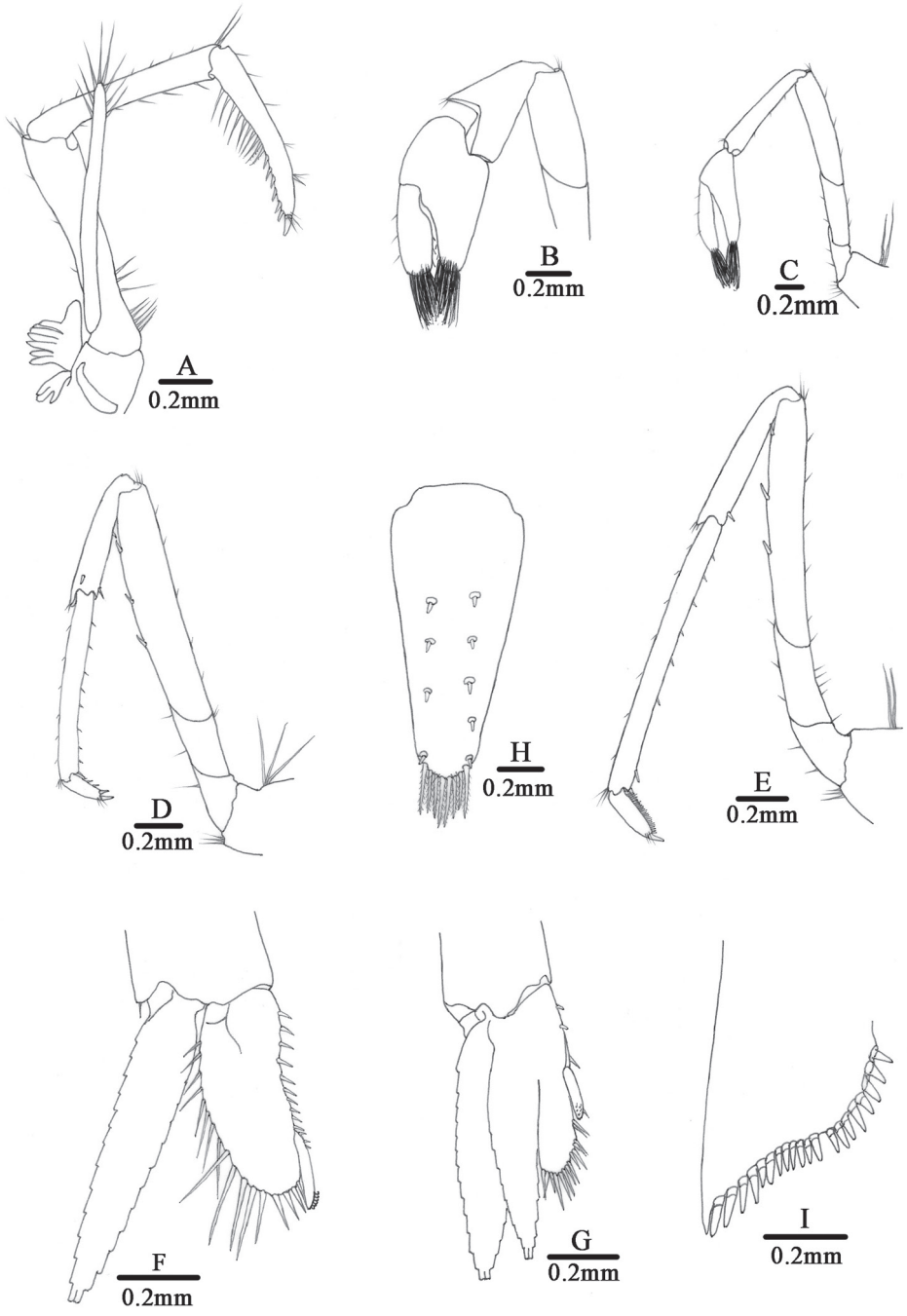

Figure 5. *Caridina tetrazona* sp. nov. paratype (FU, 2017-06-27-02). **A** Third maxilliped **B** first pereiopod **C** second pereiopod **D** third pereiopod **E** fifth pereiopod **F** first pleopod **G** second pleopod **H** telson **I** diaeresis of uropodal exopod.

posterior margin with 4–5 pairs of intermediate plumose setae, the outer one usually strongest and longest, no median projection on posterior margin. Exopodite of uropod bearing a series of 18–20 movable spinules on the diaeresis.

Eggs 0.51–0.65 × 0.84–0.97 mm in diameter.

Coloration: Body semi-translucent, four dark blue bands transverse on the tergum of the 1st, 3rd, 5th, and 6th abdominal segments, appendages mostly translucent (Fig. 3A).

Etymology. *Caridina tetrazona* is a combination of two Latin words, *tetra*, four, and *zona*, band, alluding to its four-banded color pattern.

Remarks. *Caridina tetrazona* sp. nov. is most similar to *C. serrata* Stimpson, 1860 (which also occurs on the same island) in the short rostrum, the shape of the endopod of the male first pleopod, and the similar-sized eggs. It can be easily distinguished from *C. serrata* by the length of the basal segment of the antennular peduncle which is as long as the combined length of 2nd and 3rd segments (versus length of basal segment distinctly longer than the combined length of 2nd and 3rd segments in *C. serrata*); length of penultimate segment of 3rd maxilliped as long as basal segment; the distal segment is distinctly shorter than the penultimate segment (versus penultimate segment distinct shorter than basal segment and distal segment as long as penultimate segment in *C. serrata*); the absence of a projection on the posterior margin of telson (versus with a projection in *C. serrata*), and the slender scaphocerite (3.6–3.7 times as long as wide versus 3.0–3.2 times in *C. serrata*). In addition, the four dark blue bands on the body of live shrimps allow an easy identification in the field. *Caridina tetrazona* sp. nov. also shows close similarity with *C. cantonensis* Yu, 1938 regarding the ratios of various segments of the 1st and 2nd pereiopods. Beside its peculiar coloration, *C. tetrazona* sp. nov. differs from *C. cantonensis* in the short rostrum, which only reaches the end of 1st segment of the antennular peduncle (versus distinctly reaches beyond the end of the 2nd segment in *C. cantonensis*); the endopod of the male first pleopod slender (2.6–2.7 times as long as wide versus 2.1–2.4 times in *C. cantonensis*) and distal part not dilated (versus distally distinctively dilated in *C. cantonensis*); palp of 1st maxilliped ending in a finger-like tip (versus broadly rounded in *C. cantonensis*); and absence of a projection on the posterior telsonic margin (versus with a projection in *C. cantonensis*). *Caridina tetrazona* sp. nov. closely resembles *C. trifasciata* Yam & Cai, 2003, in having similar dark blue bands on their abdomen, and in having the shape of the endopod of the male 1st pleopod and appendix masculina of the male 2nd pleopod similar. *Caridina tetrazona* sp. nov. differs from *C. trifasciata* in its proportionately shorter rostrum (only reaches the end of the 1st segment of the antennular peduncle versus reaches beyond the end of the 2nd segment in *C. trifasciata*); palp of the 1st maxilliped ending in a finger-like tip (versus broadly rounded in *C. trifasciata*); and the slender scaphocerite (3.6–3.7 times as long as wide versus 2.8 times in *C. trifasciata*).

Ecological notes. The type specimens were collected from a small stream at an elevation of 8 m, stn 1, near Longtangzui, Dawanshan Island, Zhuhai City, Guangdong, China (21°56'59.2"N, 113°43'00"E) (Fig. 1). The stream is 2–3 m in width and 0.3–0.5 m in depth. The stream bed consists of rocks interspersed with gravel and

sands patches. The bank was covered with aquatic vegetation. The shrimps live among rocks and marginal vegetation. The stream water was fast flowing and the temperature was 26 °C, pH was 6.4, and dissolved oxygen concentrations was 7.8 mg/1.

Distribution. only known from Guangdong Province, southern China.

Molecular phylogenetic results

The primers used in this study are located at the 5' end of the COI gene, and the new sequencing results are corrected for 624~bp for subsequent analysis. As can be seen from Table 2, pairwise genetic distances between *Caridina tetrazona* sp. nov. and *C. serrata* and *C. cantonensis* are 0.067 and 0.128, respectively. The topology of the Bayesian (BI) trees and the ML tree are basically similar. Phylogenetic trees revealed the relationship between *Caridina tetrazona* sp. nov. and nine other species of Atyidae, with the posterior probability and bootstrap values from the BI and ML analyses shown in Figures 6 and 7.

Discussion

The faunistic and ecological results of the present survey illustrate that the freshwater atyid shrimps are not very diverse along the habitats of the coastline of Dawansha Island; only two species of *Caridina* occur on this island. *Caridina tetrazona* is a new species, while *Caridina serrata* Stimpson, 1860 is known from a wide area and can be commonly found in streams from this island. In addition, it also occurs on neighboring islands, i.e., Hong Kong, Dong'ao Island, Wailingding Island, and Guishan Island (Cai and Ng 1999; Chen et al. 2018). The Wanshan Islands together have the same geological origin, and therefore a close biogeographical connection of their atyid faunas is evident.

Table 2. Pairwise genetic distance among eight *Caridina* species (Atyidae) based on the COI gene. The range of genetic distances between different species is in parentheses.

Species	1	2	3	4	5	6	7
1. *C. cantonensis*							
2. *C. huananensis*	0.189 (0.171–0.207)						
3. *C. lanceifrons*	0.234 (0.221–0.246)	0.246 (0.245–0.246)					
4. *C. mariae*	0.110 (0.100–0.119)	0.216 (0.215–0.216)	0.277 (0.277–0.277)				
5. *C. serrata*	0.149 (0.139–0.159)	0.240 (0.224–0.255)	0.260 (0.252–0.268)	0.144 (0.137–0.150)			
6. *C. tetrazona* sp. nov.	0.128 (0.118–0.138)	0.203 (0.199–0.206)	0.227 (0.227–0.227)	0.137 (0.137–0.137)	0.067 (0.033–0.101)		
7. *C. trifasciata*	0.112 (0.105–0.118)	0.214 (0.206–0.221)	0.256 (0.252–0.260)	0.147 (0.144–0.150)	0.117 (0.100–0.134)	0.091 (0.088–0.094)	
8. *C. zhujiangensis*	0.237 (0.229–0.244)	0.325 (0.321–0.329)	0.265 (0.265–0.265)	0.281 (0.281–0.281)	0.291 (0.279–0.303)	0.263 (0.263–0.263)	0.241 (0.237–0.245)

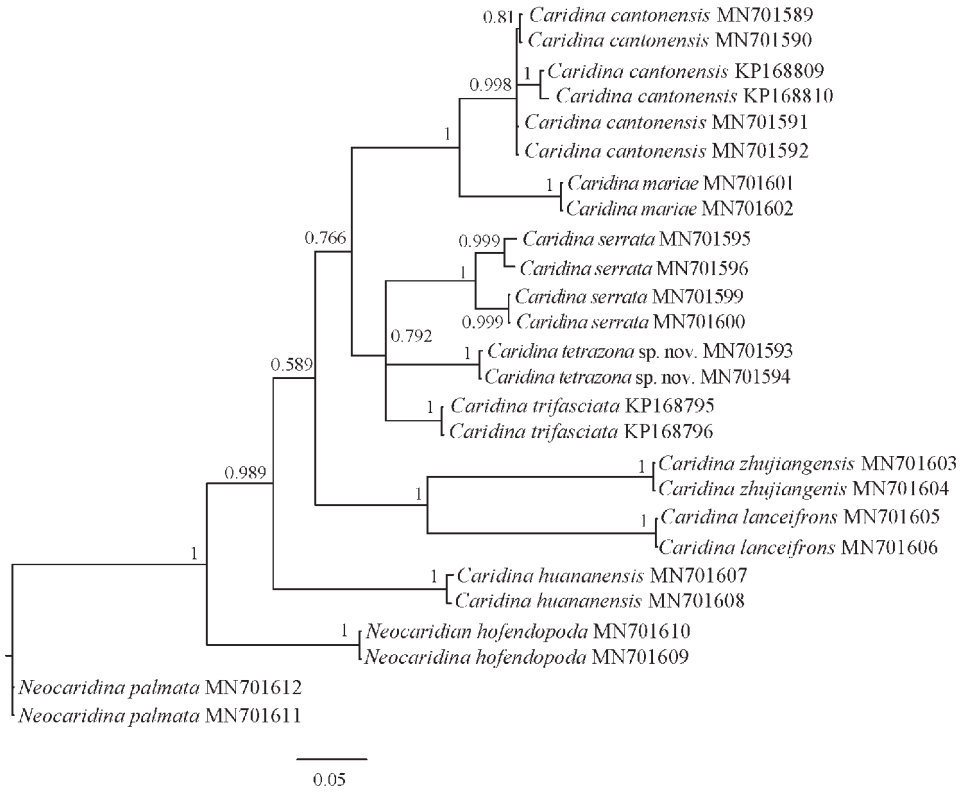

Figure 6. Bayesian inference tree of species of *Caridina* and outgroups (*Neocaridina*) based on COI gene. Support values at the nodes represent posterior probability.

According to the COI sequence, the range of interspecific genetic divergence (K2P) between *Caridina tetrazona* sp. nov. and the other seven species of *Caridina* was 6.7–32.5%. This result is in accordance with the minimum interspecific genetic distance of 2% recommended by Hebert et al. (2003). The new species is most similar in morphology to *C. serrata* and *C. cantonensis*. According to molecular analyses, the distance between the new species and these two is 0.067 and 0.128, respectively. In the phylogenetic tree, the new species (*C. tetrazona* sp. nov.) can also be separated from *C. cantonensis* and *C. serrata*. Therefore, molecular analyses and morphological analysis are congruent, and together provide sufficient evidence to suggest that the rice shrimp in this study is a new taxon.

As these isolated and vicariant atyid shrimps occur in tightly constrained coastal locations, they may be particularly vulnerable to anthropogenic changes. The island has high potential for ecotourism due to its unspoilt natural landscape and ideal climate. The increase in tourism poses a threat to the survival of this species. Moreover, *Caridina tetrazona* sp. nov. displays a striking coloration pattern, which will certainly receive particular attention among aquarists, so the possible threat by over-harvesting is also present. A program should be developed to guide and control

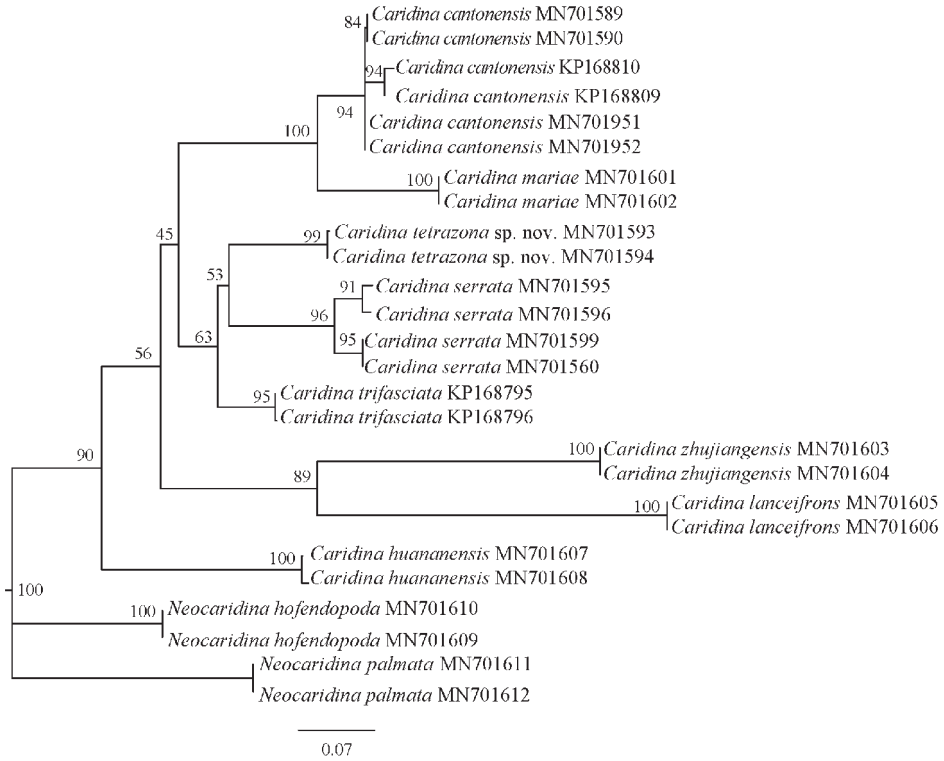

Figure 7. Phylogenetic tree (ML) based on COI gene fragments of 10 shrimp species of *Caridina* and *Neocaridina* (outgroups). Support values at the nodes represent bootstrap values for ML.

ecological tourism on the island. Monitoring changes in wild populations according to local legislation should also be intensified, and campaigns that promote environmental education and raising tourists' awareness of the importance of biodiversity should be encouraged.

Acknowledgements

This study was supported by the Special Fund for Central Public Welfare Research Institutes (Grant No. PM-zx097-201904-134), the Running Cost for Key Laboratory of Utilization and Breeding of Aquatic Resources in Tropical and Subtropical Areas, Ministry of Agriculture and Rural Affairs (Grant No. 9020190008) and the Investigation on Crustaceans in Priority Area of Mangrove Diversity Protection in Guangxi Zhuang Autonomous Region (Grant No. kh19051). We thank Dr. Chao Huang (University of New South Wales) for modifying the manuscript. Thanks are also due to subject editor Ingo Wehrtmann, copy editor Christopher Glasby and two reviewers (Yixiong Cai and Charles Fransen) for providing their valuable suggestions, which greatly improved the manuscript.

References

Bouvier LB (1905) Observations nouvelles sur les crevettes de la famille des Atyides. Bulletin Scientifique de la France et de la Belgique 39: 57–134.

Bouvier LB (1925) Recherches sur la morphologie, les variations et la distribution systématique des crevettes d'eau douce de la famille des Atyidés. Encyclopédie Entomologique 4: 1–370.

Cai YX, Ng NK (1999) A revision of the *Caridina serrata* species group, with descriptions of five new species (Crustacea: Decapoda: Caridea: Atyidae). Journal of Natural History 33: 1603–1638. https://doi.org/10.1080/002229399299789

Chen QH, Chen WJ, Guo ZL (2018) Caridean prawn (Crustacea, Decapoda) from Dong'ao Island, Guangdong, China. Zootaxa 4399(3): 315–328. https://doi.org/10.11646/zootaxa.4399.3.2

De Grave S, Smith KG, Adeler NA, Allen DJ, Alvarez F, Anker A, Cai YX, Carrizo SF, Klotz W, Mantelatto FL, Page TJ, Shy J-Y, Villalobos JL, Wowor D (2015) Dead Shrimp Blues: A global assessment of extinction risk in freshwater shrimps (Crustacea: Decapoda: Caridea). PloS One 10(3): e0120198. https://doi.org/10.1371/journal.pone.0120198

De Mazancourt V, Klotz W, Marquet G, Keith P (2018) Integrative taxonomy helps separate four species of freshwater shrimps commonly overlooked as *Caridina longirostris* (Crustacea: Decapoda: Atyidae) on Indo-West Pacific islands. Invertebrate Systematics 32: 1422–1447. https://doi.org/10.1071/IS18034

Folmer O, Black M, Hoeh W, Lutz R, Vrijenhoek R (1994) DNA primers for amplification of mitochondrial cytochrome c oxidase subunit I from diverse metazoan invertebrates. Molecular Marine Biology and Biotechnology 3(5): 294–299.

He ZJ, Feng ZJ, Li ZK (2004) Plant resources on Wanshan Islands in Zhuhai City, Guangdong Province. Subtropical Plant Science 33(2): 55–59.

Hebert PDN, Ratnasingham S, de Waard JR (2003) Barcoding animal life: cytochrome c oxidase subunit 1 divergences among closely related species. Proceedings of the Royal Society B: Biological Sciences 270 (suppl_1): s96–s99. https://doi.org/10.1098/rsbl.2003.0025

Huang H, You F, Lian JS, Zhang CL, Yang JH, Li XB, Yuan T, Zhang YY, Zhou GW (2012) Status and conservation strategies of the scleractinian coral community in the Wanshan Island at Pearl River Estuary. Marine Science Bulletin 31(2): 189–197.

Huang SH, Wang WC (2000) A conception of constructing the marine ecological park in Wanshan Islands, Zhuhai. Tropical Geography 20(3): 228–232.

Kalyaanamoorthy S, Minh BQ, Wong TKF, Haeseler AV, Jermiin LS (2017) ModelFinder: fast model selection for accurate phylogenetic estimates. Nature Methods 14(6): 587–591. https://doi.org/10.1038/nmeth.4285

Katoh K, Standley DM (2013) MAFFT multiple sequence alignment software version 7: improvements in performance and usability. Molecular Biology and Evolution 30(4): 772–780. https://doi.org/10.1093/molbev/mst010

Kemp S (1918) Zoological results of a tour in the Far East. Crustacea Decapoda and Stomatopoda. Memoirs of the Asiatic Society of Bengal 6: 218–297.

Kumar S, Stecher G, Tamura K (2016) MEGA7: molecular evolutionary genetics analysis version 7.0 for bigger datasets. Molecular Biology and Evolution 33(7): 1870–1874. https://doi.org/10.1093/molbev/msw054

Liang XQ (2004) Crustacea, Decapoda, Atyidae. Fauna Sinica. Invertebrata 36: 1–375. [In Chinese with English abstract]

Liao WQ, Zhang JG, Huang HP (2000) Development of the tourism resources of the Wanshan Islands. Tropical Geography 20(2): 134–138.

Nguyen LT, Schmidt HA, von Haeseler A, Minh BQ (2015) IQ-TREE a fast and effective stochastic algorithm for estimating maximum-likelihood phylogenies. Molecular Biology and Evolution 32(1): 268–274. https://doi.org/10.1093/molbev/msu300

Ortmann AE (1894) A study of the systematic and geographical distribution of the decapod family Atyidae Kingsley. Proceedings of the Academy of Natural Sciences of Philadelphia 46: 397–416.

Ronquist F, Teslenko M, van der Mark P, Ayres DL, Darling A, Höhna S, Larget B, Liu L, Suchard A, Huelsenbeck JP (2012) MrBayes 3.2: efficient Bayesian phylogenetic inference and model choice across a large model space. Systematic Biology 61(3): 539–542. https://doi.org/10.1093/sysbio/sys029

Stimpson W (1860) Prodromus descriptionis animalium evertebratorum, quae in Expeditione ad Oceanum Pacificum Septentrionalem, a Republica Federata missa, Cadwaladaro Ringgold et Johanne Rodgers Ducibus, observavit et descripsit. Pars VIII. Crustacea Macrura. Proceedings of the Academy of Natural Sciences of Philadelphia 12: 22–47.

Yam RSM, Cai YX (2003) *Caridina trifasciata*, a new species of freshwater shrimp (Decapoda: Atyidae) from Hong Kong. Raffles Bulletin of Zoology 5(2): 277–282.

ZooKeys 923: 33–50 (2020)
doi: 10.3897/zookeys.923.47322
http://zookeys.pensoft.net

RESEARCH ARTICLE

A peer-reviewed open-access journal
ZooKeys
Launched to accelerate biodiversity research

New cavernicolous ground beetles from Anhui Province, China (Coleoptera, Carabidae, Trechini, Platynini)

Jie Fang[1], Wenbo Li[1], Xinhui Wang[2], Mingyi Tian[3]

1 *School of Life Science, Anhui University, Hefei, 230601, China* **2** *Wuhua Branch, Guangdong Tobacco, Shuizhai, 514400, Guangdong, China* **3** *Department of Entomology, College of Agriculture, South China Agricultural University, 483 Wushan Road, Guangzhou, 510642, China*

Corresponding author: *Mingyi Tian* (mytian@scau.edu.cn)

Academic editor: *A. Casale* | Received 15 October 2019 | Accepted 29 November 2019 | Published 1 April 2020

http://zoobank.org/B986E66B-0ACD-4AEF-A2F7-65F76F493C53

Citation: Fang J, Li W, Wang X, Tian M (2020) New cavernicolous ground beetles from Anhui Province, China (Coleoptera, Carabidae, Trechini, Platynini). ZooKeys 923: 33–50. https://doi.org/10.3897/zookeys.923.47322

Abstract

A new genus and three new species of cave-adapted ground beetles are reported from the limestone cave Shenxian Dong in Huangshan Shi, southeastern Anhui Province, China. *Shenoblemus* **gen. nov.** is proposed to place the anophthalmic trechine species *S. minusculus* **sp. nov**. This genus is characterized by the tiny but stout body, sub-moniliform antennae, serrated elytral margins near the base, and a wide distance between the fifth and sixth pores of the marginal umbilicate series on the elytra. In addition, two new species, *Wanoblemus huangshanicus* **sp. nov**. (an anophthalmic trechine) and *Jujiroa inexpectata* **sp. nov**. (a microphthalmic platynine), are also described and illustrated from the same cave.

Keywords

carabids, hypogean, new genus, new species, subterranean

Introduction

The first report of the subterranean ground beetles from Anhui Province, eastern China, was published a few years ago (Fang et al. 2016). In that paper one new genus and two new species of anophthalmic trechines were described: *Wanoblemus wui* Tian & Fang, 2016 from the cave Baiyun Dong in Xuancheng Shi and *Cimmeritodes* (*Zhecimmerites*) *parvus* Tian & Li, 2016 from several caves in Chaohu Shi.

In April 2016, one of us (LWB) conducted cave biodiversity investigations in Tongling, Chizhou, Xuancheng, and Huangshan prefectures of Anhui. His efforts were in vain in four of the five explored caves except Shenxian Dong in Huangshan Shi where he achieved success in collecting seven cave-adapted trechine beetles. Further studies in the laboratory confirmed that six of these beetles belonged to a new species of the genus *Wanoblemus* Tian & Fang, 2016. However, the most interesting discovery was the other single male specimen. It is a representative of a new genus of the *Trechoblemus* phyletic series judging from its small and stout body, together with several other peculiar characteristics.

In order to collect more material, we re-visited the cave Shenxian Dong in late 2018 and April 2019 respectively. Unfortunately, we did not find any more specimen of the latter species. However, we collected some more individuals of the *Wanoblemus* species, and, unexpectedly, we discovered a new hypogean Platynini of the genus *Jujiroa* Uéno, 1952.

We herein provide the description of the new genus and describe the aforementioned three new cave-adapted ground beetles.

Material and methods

The material was collected by using an aspirator inside the cave Shenxian Dong, and kept in 55% ethanol before study, except one of each species was kept in 95% ethanol for molecular analysis if two or more specimens were available. Dissections and observations were made under a Leica S8AP0 microscope. Dissected male genital pieces, including the median lobe and parameres of the aedeagus, were preserved in Euparal Mounting Medium (BioQuip Products, Inc., CA, USA) onto small transparent plastic plates and pinned under the specimen. Habitus pictures were taken by means of a Keyence VHX-5000 digital microscope. Genital pictures were taken using a Canon EOS 40D camera connected to a Zeiss AX10 microscope. Female genitalia were dissected before the entire abdomen was removed and placed in cold 10% KOH for one day, then cleaned in lactic acid for one day, and stained in Chlorazol Black which was dissolved in 70% ethanol for thirty seconds. All pictures were processed using Adobe Photoshop CS5 computer software.

Measurements and terminology follow Tian et al. (2016). Terminology for female reproductive tract follows Deuve (1993, 2018) and Liebherr and Will (1998).

Taxonomy

***Shenoblemus* Tian & Fang, gen. nov.**
http://zoobank.org/338E5C04-310D-4737-84D5-8697E6899BCB

Type species. *Shenoblemus minusculus* Tian & Fang, sp. nov. (the cave Shenxian Dong, Huangshan Qu, Huangshan Shi, Anhui).

Generic characteristics. Small-sized beetles for the phyletic series of *Trechoblemus* (Casale and Laneyrie 1982; Jeannel 1928; Casale et al. 1998), or *Trechoblemus* complex (Uéno and Pawlowski 1981), anophthalmic; body short and stout, appendages short; dorsal surface more or less pubescent; head subquadrate, wider than long excluding mandibles, and shorter than pronotum; frontal furrows entire, two pairs of supraorbital and pair of suborbital pores present; right mandible bidentate; labial suture absent, making mentum and submentum completely fused; mentum bisetose, base largely concave, median tooth simple, short and blunt at apex; submentum quadrisetose; antennae short, extending only to about 1/3 of elytra from base, the 7th to 11th antennomeres sub-moniliform; pronotum quadrate, transverse, evidently wider than long, widest near front, at about 1/4 apically, two pairs of lateromarginal setae present, posterior ones located before hind angles, fore angles markedly protruding and sharp, hind ones nearly rectangular and pointed, base nearly straight; elytra stout though distinctly longer than fore body including mandibles, nearly parallel-sided, widest at about middle, surface moderately convex, shoulders distinct, angularly rounded, lateral margins strongly serrated at base, then more or less ciliated throughout; striae obliterated though partly traceable; two dorsal pores present on the 3rd stria, and the preapical present; apical striole weakly defined, connected to the 5th stria; humeral group (the 1st to 4th pores) of marginal umbilicate series equidistantly spaced, median group (the 5th and 6th pores) widely separated each other, the 5th pore forwardly shifted and closer to the 4th than to 6th; protibia without longitudinal groove externally; the 1st and 2nd protarsomeres modified in male, distinctly denticulate inwards at each apex; the 1st protarsomere shorter than 2nd to 4th ones combined in all legs; ventrite VII with one pairs of apical setae in male; male genitalia thin and slender, slightly arcuate.

Remarks. The main characteristics (such as the small and pubescent body, two frontal pores present on the head, fused mentum and submentum, location of dorsal pores on the 3rd stria and an equidistantly spaced humeral group of the marginal umbilicate series) indicate that *Shenoblemus* is a lineage of the *Trechoblemus* phyletic series. It is probably close to the Zhejiangese genus *Microblemus* Uéno, 2007, whose members are also small-sized, with similar head, bidentate right mandible, and have similar chaetotaxy on the elytra (Uéno 2007a). However, *Shenoblemus* can be easily distinguished from *Microblemus* by: (1) antennae sub-moniliform, whereas they are filiform in *Microblemus*; (2) mentum and submentum completely fused, versus only partly fused with labial suture traceable in *Microblemus*; (3) pronotum quadrate and transverse, with fore angles evidently protruding, but cordate and narrow, with fore angles not protruding in *Microblemus*; and (4) elytral base and shoulders simple or moderately serrate in *Shenoblemus*, whereas they are strongly dentate in *Microblemus*.

Shenoblemus may be also related to the sympatric *Wanoblemus* as both genera share some important characteristics: (1) similar chaetotaxy on head and pronotum; (2) 1st and 2nd protarsomeres modified in the male; (3) labial suture missing; and (4) bidentate right mandible (though tricuspid in three individuals of *Wanoblemus huangshanicus* sp. nov.). However, they are evidently different in the following aspects: (1) body much smaller and stouter in *Shenoblemus*; (2) 7th to 11th antennomeres are sub-moniliform in *Shenoblemus*, but filiform in *Wanoblemus*; (3) pronotum strongly transverse, with

fore angles protruding and sharp in *Shenoblemus*, versus narrower, with fore angles not protruding in *Wanoblemus*; (4) lateral margin of elytra strongly serrate near base in *Shenoblemus*, whereas it is weakly subserrate or ciliate in *Wanoblemus*; (5) 5th and 6th pores of the marginal umbilicate series of the elytra widely spaced, making the 5th pore closer to the 4th than to the 6th in *Shenoblemus*, instead of much closer to the 6th than to the 4th in *Wanoblemus*; (6) protibiae without a longitudinal sulcus in *Shenoblemus*, versus a distinct longitudinal sulcus present in *Wanoblemus*; and (7) male genitalia thin and elongate in *Shenoblemus*, versus short and strongly arcuate in *Wanoblemus*.

The following features may separate *Shenoblemus* from another Zhejiangese genus, *Wulongoblemus* Uéno, 2007 whose members have also the 1st and 2nd protarsomeres modified in the male: (1) right mandible bidentate in *Shenoblemus*, but tridentate in *Wulongoblemus*; (2) body small, short, and stout in *Shenoblemus*, whereas it is large and slender in *Wulongoblemus*; (3) pronotum transverse, with fore angles protruding in *Shenoblemus*, versus pronotum longer than wide, with obtuse fore angles in *Wulongoblemus*; (4) antennae sub-moniliform in *Shenoblemus*, instead of filiform in *Wulongoblemus*.

Etymology. "Shen (= "Shenxian", meaning immortal in Chinese) + blemus", referring to the locality of the type species. Gender masculine.

Generic range. China (Anhui).

***Shenoblemus minusculus* Tian & Fang, sp. nov.**
http://zoobank.org/2888D9C3-1870-4244-B846-8EBBB711BC0F
Figs 1–3A, 4A, B

Material. ***Holotype*** male, cave Shenxian Dong, Qiaoshan, Xinming, Huangshan, Anhui, 30°23'9.55"N, 118°14'7.66"E, 366 m in altitude, 2016-IV-22, leg. Wenbo Li, deposited in the insect collections of South China Agricultural University, Guangzhou, China (SCAU).

Diagnosis. Small-sized, eyeless and yellowish-brown beetle, with stout body and short appendages; covered with pubescence which are sparser on head, prothorax and elytra, and denser on abdominal ventrites.

Description. ***Length*****:** 2.45 mm; width: 0.84 mm. Habitus as in Fig. 1. ***Fore body*** (head plus pronotum including mandibles) much shorter than elytra. Microsculpture made of isodiametric meshes irregularly distributed on head, pronotum and elytra.

Head large and widened, a little narrower than head including mandibles, HW/HLm = 0.90, or wider excluding mandibles, HW/HLl = 1.17; widest at about 1/4 of head from base excluding mandibles; front and vertex convex; frontal furrows well-defined and complete, strongly divergent at both anteriorly and posteriorly; genae markedly expanded laterally; anterior and posterior supra-orbital pores close, both at widest area of genae; clypeus quadrisetose, labrum transverse, almost straight in the front margin, 6-setose; mandibles widened and moderately curved at apices; ligula thin and short, adnated with paraglossae; palps short, penultimate joints much stouter than apical ones; the 2nd labial palpomere slightly longer than the 3rd, bisetose on inner margin, with two or three additional setae at subapex on outer margin; the 3rd

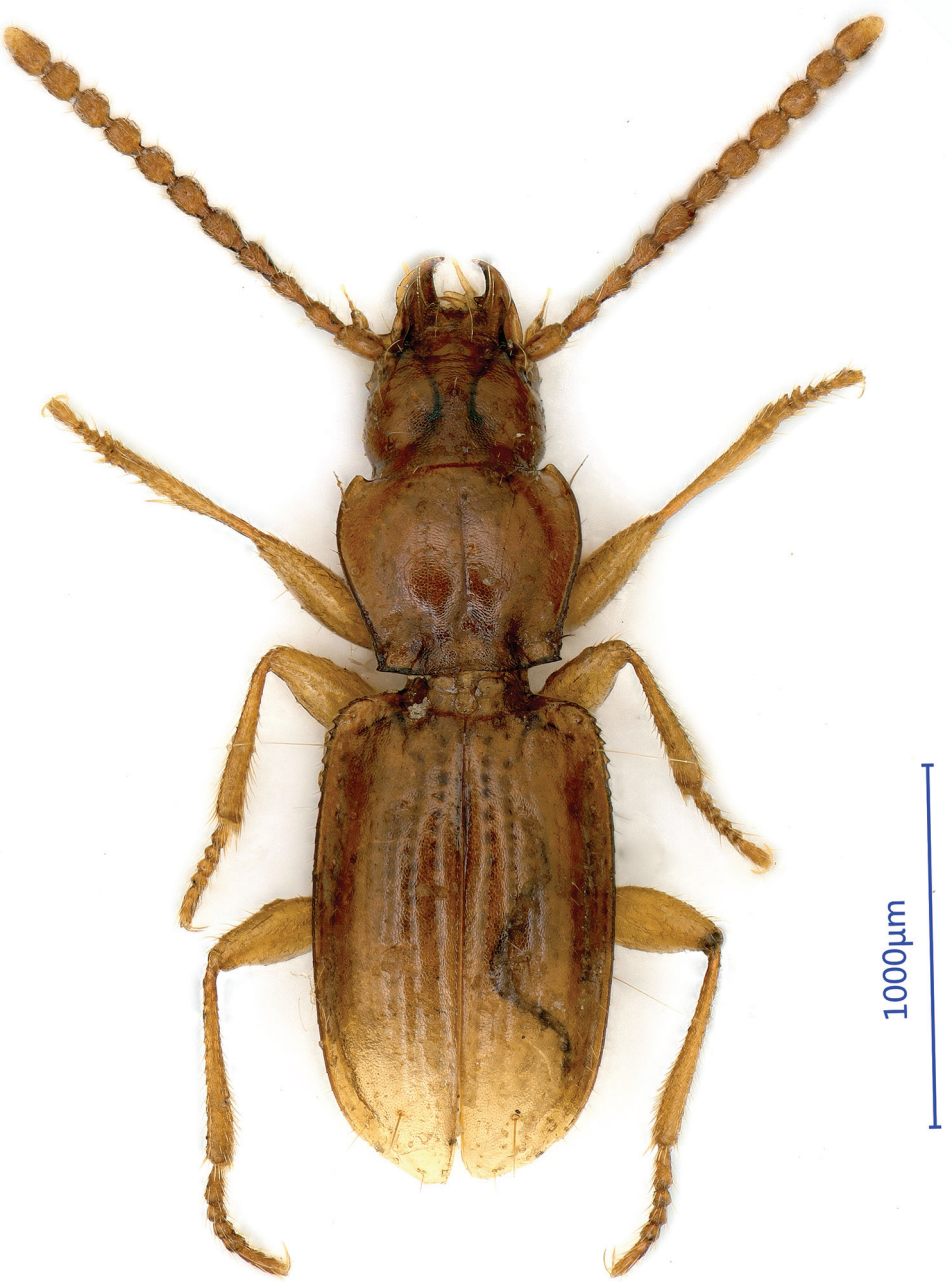

Figure 1. Habitus of *Shenoblemus minusculus*, sp. et gen. nov., male, holotype.

maxillary palpomere as long as the 4th; the 1st–6th antennomeres filiform, while the 7th–11th semi-moniliform; relative length of each antennomere as: the 1st (1.13), 2nd (1.00), 3rd (1.08), 4th (1.04), 5th (1.13), 6th (1.00), 7th (1.04), 8th (1.04), 9th (1.04), 10th (1.00) and 11th (1.42).

Figure 2. Head of *Shenoblemus minusculus*, sp. et gen. nov., male, holotype.

Pronotum moderately transverse, PnW/PnL = 1.21, as long as head (including mandibles), much wider than head, PnW/HW = 1.32; lateral margins finely bordered, anterior lateromarginal pores located at about apical sixth, posterior ones at a little before hind angles; base slightly narrower than front, PbW/PfW = 0.97, both nearly straight and unbordered; hind angles denticulate at tips; both frontal and basal impression faint, basal foveae large and deep; disc moderately convex. Scutellum small and almost rounded.

Elytra much longer than wide, EL/EW = 1.56, wider than pronotum, EW/PnW =1.24; unbordered at base; strial punctures large and widely isolated; basal pores distant from scutellum, anterior and posterior dorsal pores on the 3rd striae at about 1/4 and 4/7 of the elytra from the base respectively; preapical pores at about apical 1/7 of elytra, subequal to suture and apical margin; humeral group of marginal umbilicate

series regular though the 2nd closer to marginal gutter than other; the 5th widely separated from the 6th, apical pores close to elytral margin (Fig. 3A).

Legs short and stout, densely pubescent; protarsi short, the 1st tarsomere much shorter than the 2nd–4th combined in fore and middle legs, whereas slightly shorter in hind legs; abdominal ventrites IV - VI each with a pair of paramedical setae in male.

Male genitalia (Fig. 4A, B): The median lobe of aedeagus moderately sclerotized, rather long and thin, weakly arcuate at median portion, rounded at apex; dorsal margin suddenly folded at about basal quarter; base small, sagittal aileron quite large and hyaline, inner sac provided with a triangular and small copulatory piece, which is about 1/5 as long as aedeagus; in dorsal view, apical lobe widened at subapex, nearly triangular form, longer than wide, with a broadly rounded apex; parameres moderately elongated, right one as long as the left, each armed with two long setae at apex.

Female: Unknown.

Etymology. To refer to the small body size.

Distribution. China (Anhui). Known only from a limestone cave called Shenxian Dong in Huangshan Shi.

The Shenxian Dong limestone cave is more than 3000 m long. It is divided in three parts (front, middle, and back) for touristic purpose. There is an underground stream along the main passage. The single beetle specimen was collected in a dark area approximately 50 m from the entrance.

Wanoblemus huangshanicus **Tian & Li, sp. nov.**
http://zoobank.org/2BD1BC1D-89D0-4C8B-94C3-12F0EB77F55F
Figs 3B, 4C, D, 5B, 6

Material. ***Holotype*****:** male, cave Shenxian Dong, Qiaoshan, Xinming, Huangshan, Anhui, 30°23'9.55"N, 118°14'7.66"E, 366 m in altitude, 2016-IV-22, leg. Wenbo Li, in SCAU; ***Paratypes*****:** 3 males and 2 females, idem; 12 males and 15 females, same cave, 2018-XII-24, leg. Weibo Li, Mengzhen Chen, Zhuanghui Qin, Jingli Cheng & Mingyi Tian, in SCAU and in the animal collections of Anhui University, Hefei, China (AHU) respectively.

Diagnosis. A rather small eyeless trechine beetle, yellowish brown, body thin and elongate, sparsely pubescent.

Description. ***Length*****:** 3.2–3.5 mm (including mandibles); width: 0.9–1.0 mm. Habitus as in Fig. 6.

Head longer than wide, HLm/HW = 1.38–1.42, HLl/HW = 1.08–1.2; right mandible bidentate (but tricuspid in three individuals); antennae extending beyond basal 2/5 of elytra.

Pronotum slightly wider than longer, PnL/PnW = 0.90–0.93, shorter than head, PnL/HLm = 0.72–0.75, wider than head, PnW/HW = 1.20–1.24, base narrower than front, PbW/PfW = 0.83–0.87, lateral margins more contracted behind the widest portion than in *Wanoblemus wui* Tian & Fang, 2016.

Figure 3. Left elytra of two cave trechines to show chaetotaxy **A** *Shenoblemus minusculus*, sp. et gen. nov., male, holotype **B** *Wanoblemus huangshanicus*, sp. nov., male, holotype.

Elytra slightly thinner than those in *W. wui*, longer than fore body, EL/(HLm+PnL) = 1.28–1.31, EL/(HLl+PnL) = 1.50–1.62, much longer than wide, EL/EW = 1.77–1.81; much wider than pronotum, EW/PnW = 1.51–1.53; chaetotaxy similar in *W. wui* (Fig. 3B).

VII ventrite bisetose in male, while quadrisetose in female.

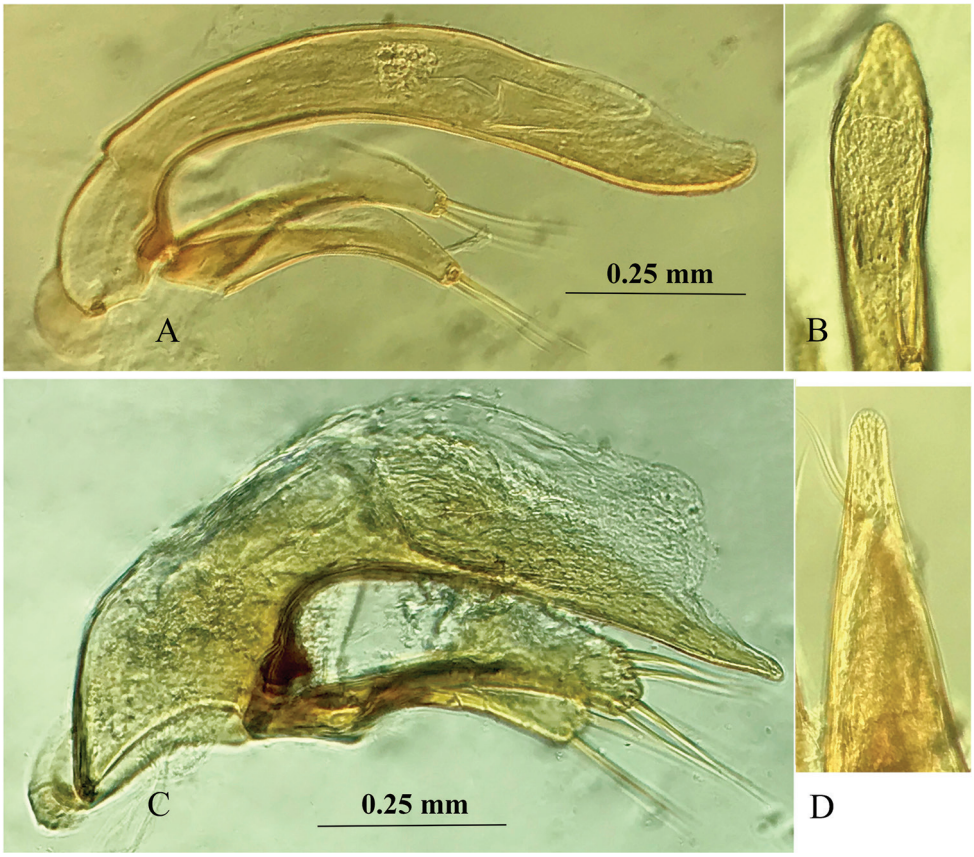

Figure 4. Male genitalia of *Shenoblemus minusculus*, sp. et gen. nov. (**A, B**) and *Wanoblemus huangshanicus*, sp. nov. (**C, D**) **A, C** median lobe and parameres, lateral view **B, D** apical lobe, dorsal view.

Male genitalia (Fig. 4C, D): The median lobe of aedeagus well-sclerotized, small but more elongate than the one of *W. wui*, and less curved ventrally in middle part; membranous opening large, rather sharp at apex, base larger, with a small sagittal aileron; in dorsal view, apical lobe much longer than wide, gently contracted towards apex which is broad; parameres shorter than median lobe, both widened at apices, each armed with four long apical setae.

Remarks. This new species is very similar to the type species *W. wui* which occurs in the cave Baiyun Dong, Xuancheng Shi, approximately 46 km in a straight-line distance from the cave Shenxian Dong. However, the new species is smaller and slenderer than the type species, and with a longer and more elongated aedeagus.

Etymology. To refer to the type locality.

Distribution. China (Anhui). Known only from the cave Shenxian Dong in Huangshan Shi.

The specimens collected in 2016 were found in a small wet area about 300 m from the cave entrance. The specimens collected in 2018 were found in dark areas 200–300 m from the entrance.

Jujiroa inexpectata **Tian & Wang, sp. nov.**
http://zoobank.org/6D0B38E5-FF5F-4F31-87D5-2DA3CEBC58C6
Figs 5C, 7–10

Material. ***Holotype*****:** male, cave Shenxian Dong, Qiaoshan, Xinming, Huangshan, Anhui, 30°23'9.55"N, 118°14'7.66"E, 366 m in altitude, 2018-XII-24, leg. Jingli Cheng, in SCAU; ***Paratypes*****:** 3 males and 2 females, idem, in SCAU; 2 males, same cave, 2019-IV-12, leg. Ye Liu and Wenbo Li, in National Museum of Zoology, Institute of Zoology, Chinese Academy of Sciences, Beijing (IOZ).

Diagnosis. A medium-sized *Jujiroa* species, body de-pigmented, microphthalmic, pronotum widely reflexed along lateral margins, with strongly protruding fore angles and acute hind angles, elytra with three dorsal setiferous pores on the 3rd intervals and mucronate at apices.

Description. ***Length*****:** 12.5–15.0 mm; width: 4.0–5.0 mm. Habitus as in Fig. 7.

Body concolorous, light reddish brown, smooth and glabrous (though sparsely punctate on the reflexed lateral margins of pronotum), strongly shiny. Microsculpture made of nearly isodiametric meshes on front of head, while striate on pronotum and moderately transverse on elytra.

Head ovate (Figs 7, 8), much longer than wide, HLm/HW = 1.8–2.0, HLl/HW = 1.4–1.5; widest at middle of head from base to labrum; genae convex, expanded at sides, frontal furrows short and foveate; two pairs of supra-orbital pores present and nearly on parallel lines; eyes very small, slight convex; clypeus bisetose, labrum emarginate at front; mandibles elongate, teeth evidently reduced; labial suture complete; mentum with two setae on each side just in front of basal pit which was not well-defined; median tooth short, sharply bifid at tip; submentum with two setae on each side, inner ones longer than the outer; ligula short, widened and bisetose at apex; palpomeres slender, the 2nd labial palpomere 1.3 times as long as 3rd, the 3rd maxillary palpomere slightly shorter than 4th; suborbital setae absent; antennae filiform, extending to about apical 1/4 of elytra, the 1st to 3rd antennomeres glabrous, the 2nd shortest, relative length of each antennomere as: the 1st (2.61), 2nd (1.00), 3rd (2.12), 4th (1.90), 5th (2.00), 6th (1.82), 7th (1.83), 8th (1.61), 9th (1.66), 10th (1.34) and 11th (1.48).

Pronotum transverse, PW/PL = 1.20–1.25; slightly shorter than head excluding mandibles; widest at about 1/3 from front, lateral margins including fore and hind angles widely reflexed throughout, distinctly sinuate before hind angles, only basal lateromarginal setae present at hind angles; fore angles extraordinarily protruding, nearly triangular and bluntly sharpened; hind angles nearly rectangular and pointed; whole margins including base and front without borders, base slightly wider than front including fore angles; both base and front truncate. Scutellum small, inverted triangular.

Elytra elongate, much longer than wide, EL/EW = 1.61–1.83; longer than fore body including mandibles, much wider than pronotum; base well-bordered, shoulders nearly rectangular though rounded; widest at about apical 4/7 of elytra, apex protruding backwardly, mucronate, each elytron with an acute spine, both inner angles

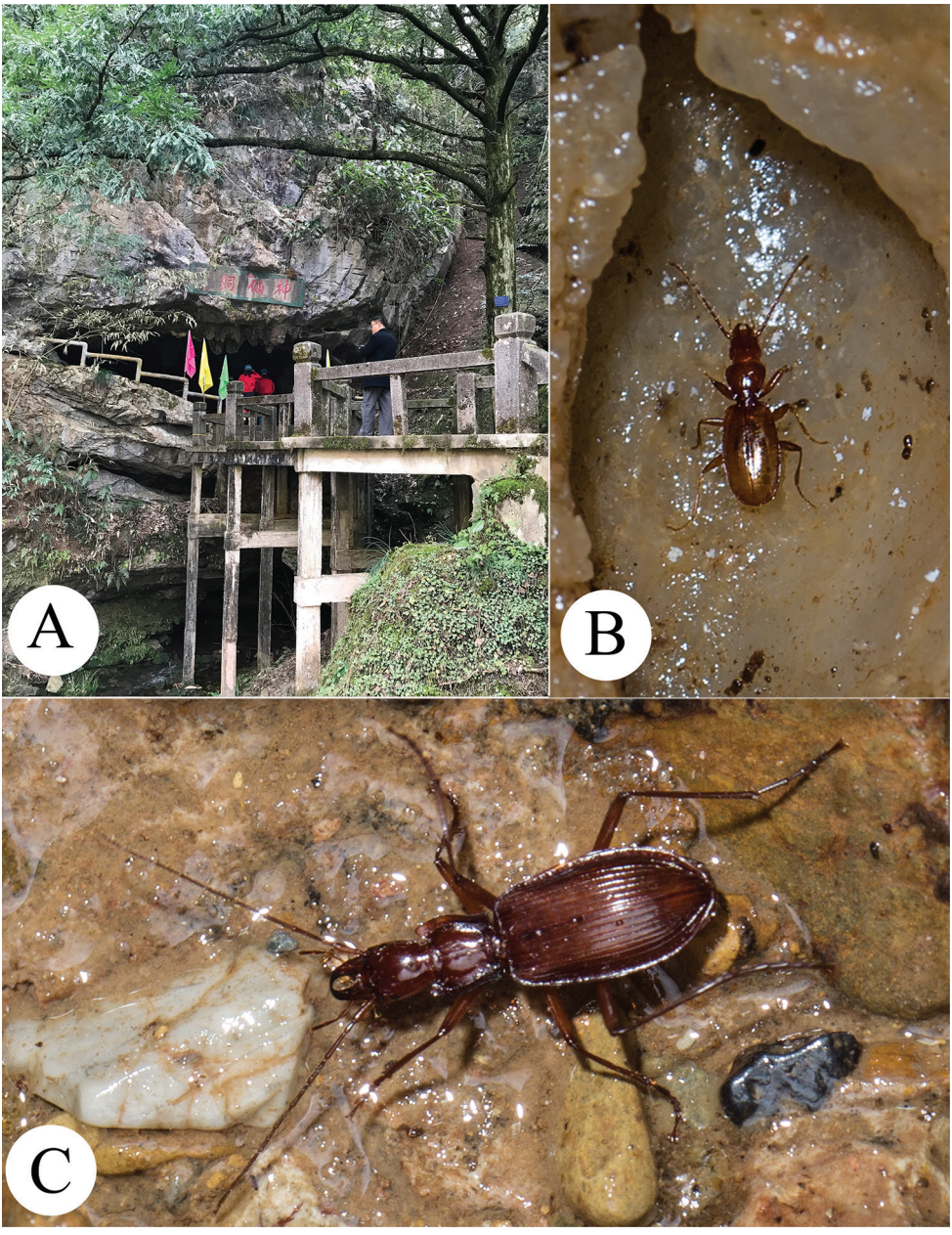

Figure 5. Cave Shenxian Dong, the type locality of three new species **A** entrance **B** a running individual of *Wanoblemus huangshanicus*, sp. nov. **C** a running individual of *Jujiroa inexpectata*, sp. nov.

evidently divergent; disc slightly convex though largely depressed, striae entire, moderately impressed and punctate; scutellar striole short; basal pores present; interval 3 with three dorsal setiferous pores, at about 1/4, 1/2 and 3/4 of elytra from base, respectively, the anterior close to the 3rd stria, the other two close to the 2nd stria; preapical pore

Figure 6. Habitus of *Wanoblemus huangshanicus*, sp. nov., male, holotype.

Figure 7. Habitus of *Jujiroa inexpectata*, sp. nov., male, holotype.

Figure 8. Ventral head of *Jujiroa inexpectata*, sp. nov., male, paratype.

present, at about apical 1/7 of elytra, closer to elytral margin than to suture; two apical pores present; 18 marginal umbilicate pores present throughout.

Ventral surface smooth and glabrous. Legs slender and elongate, procoxa asetose, mesocoxa unisetose, metacoxa bisetose, without inner seta; pro-, and mesotrochanters unisetose, metatrochanters asetose; metafemur bisetose posteriorly in male, trisetose in female; tibiae and tarsi smooth, without longitudinal sulci or striae externally; the 4th tarsomere bilobed in fore and middle legs, whereas deeply emarginated in hind ones.

Figure 9. Male genitalia of *Jujiroa inexpectata*, sp. nov., male, holotype.

Each abdominal ventrite IV-VI bisetose, ventrite VII bisetose in male, but quadrisetose in female.

Male genitalia (Fig. 9): Similar in *Jujiroa satoi* Uéno, 2007, but slenderer and more elongate, with smaller sagittal aileron, wider basal opening and broader parameres. Median lobe thin and narrow, slightly arcuate in middle portion, then gently curved towards apex with a long and blunt apical lobe. In lateral view, apical lobe thin, much longer than wide.

Female reproductive tract (Fig. 10): Abdominal ventrite X sparsely setose; gonocoxites 1 and 2 similar in other *Jujiroa* species, the former bearing eight fringe setae along apical margin, the latter triangular, slightly curved outwardly, blunt at apex, without lateral or dorsal ensiform setae, but with a tiny seta on outer margin and subapical setose organ; bursa copulatrix wide, simply saccate, with middle part evidently folded, narrowed at base; oviduct situated in middle position, both spermathecal gland and spermatheca twisted, connected each other by a short spermathecal gland duct, spermathecal duct fairly long.

Remarks. The genus *Jujiroa* Uéno, 1952 is known from Japan (Habu 1978, 1981; Takakura 1987; Sasakawa 2006), Vietnam, and from Taiwan Province and mainland China (Jedlička 1961; Casale 1988; Uéno and Saito 1991; Vigna Taglianti 1995, Uéno and Kishimoto 2001; Deuve 2004; Uéno 2007b; Deuve and Pütz 2013). All of the five presently known species from mainland China are cave-adapted beetles: *J. rufescens* (Jedlička, 1961) from Jiangxi; *J. iolandae* Vigna Taglianti, 1995, *J. satoi* Uéno, 2007, *J. deliciola* Uéno & Kishimoto, 2001 and *J. lingguanensis* Deuve et Pütz, 2013 from Sichuan; and *J. clarkei* Deuve, 2004 from Guangxi. These species are usually very rare as all are monotypic species (except *J. satoi*, which was described

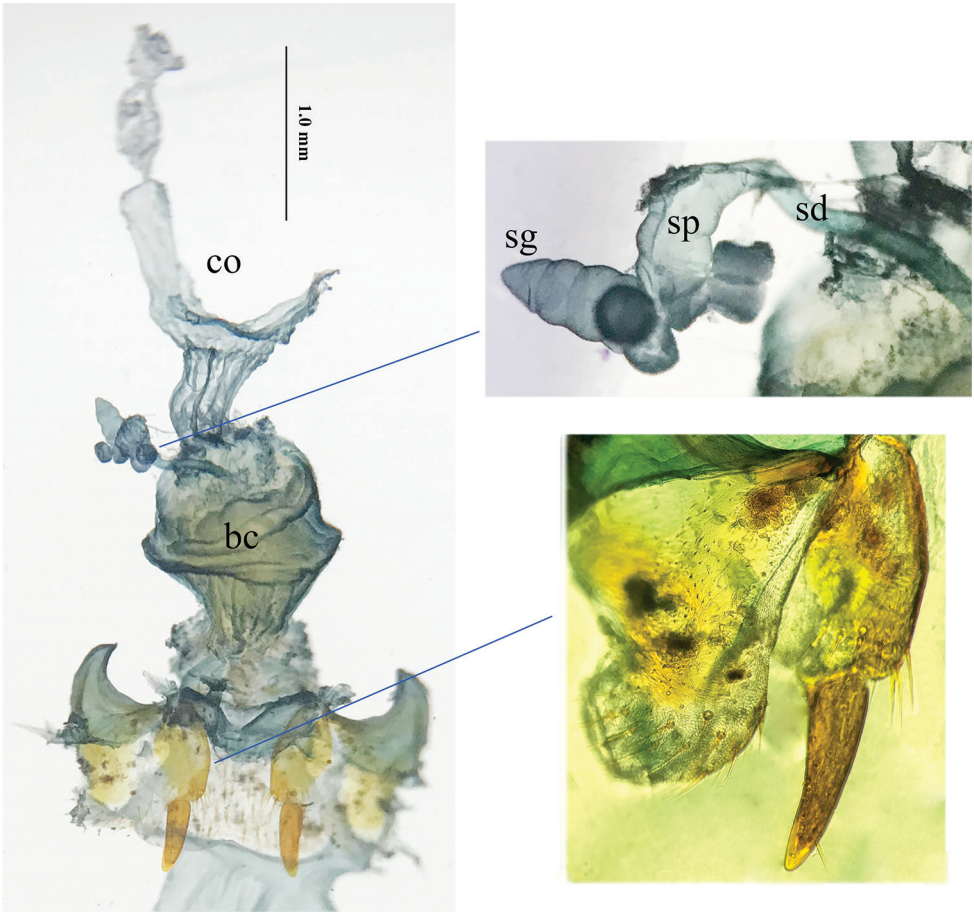

Figure 10. Female reproductive tract of *Jujiroa inexpectata* sp. nov., bc., bursa copulatrix; co., common oviduct; sd., spermathecal duct; sg., spermathecal gland; sp., spermatheca.

based on three type specimens) and are known only by the type material. Therefore, we were quite surprised when we collected several individuals together in the cave during a two-hour survey.

Regarding the hypogean *Jujiroa* species from mainland China, this new species is easily separated from *J. clarkei* by the presence of a spinous elytral apex (apical margin of elytra is rounded in *J. clarkei*), from *J. lingguanensis* by its broader body and sharpened hind angles of pronotum, and from the other three species by its smooth tarsomeres which are without longitudinal sulci.

However, *J. inexpectata* sp. nov. is closely similar to *J. iolandae* Vigna Taglianti, 1995, which occurs in Huaying, Sichuan, but it differs by fore angles of pronotum which is more protruding than in *J. iolandae*, by its elytron which is presence of three dorsal setiferous pores, versus anterior pores absent in *J. iolandae*, and by its tarsi which are smooth, whereas longitudinally striated in *J. iolandae*.

Etymology. To indicate that it was a surprise to find this interesting species.

Distribution. China (Anhui). Known only from the cave Shenxian Dong in Huangshan Shi.

Acknowledgements

We would like to express our appreciation to the owner of the cave Shenxian Dong for allowing us to visit the cave. We thank other members of SCAU cave team for their effort during the survey. We are grateful to Dr. Thierry Deuve (Muséum national d'Histoire naturelle, Paris) and Dr. Arnaud Faille (State Museum of Natural History, Stuttgart) for their constructive suggestions to improve the manuscript. This study was sponsored by a project of Natural Science Foundation of Anhui (Grant no. 1608085MC76), the Specialized Research Fund of Higher Education of Anhui (Grant no. KJ2015A017) and National Foundation of Natural Science of China (NSFC, Grant no. 41871039).

References

Casale A (1988) Revisione Degli Sphodrina (Coleoptera, Carabidae, Sphodrini). Museo Regionale di Scienze Naturali, Torino, Monografie 5, 1024 pp.

Casale A, Laneyrie R (1982) Trechodinae et Trechinae du Monde. Memoires de Biospeologie 9: 1–226.

Casale A, Vigna Taglianti A, Juberthie C (1998) Coleoptera: Carabidae. In: Juberthie C, Decu V (Eds) Encyclopedia Biospeologica II. Société Internationale Biospéologie, Moulis, Bucarest, 1047–1081 pp.

Deuve T (1993) L'abdomen et les genitalia des femelles de Coléoptères Adephaga. Mémoires du Muséum national d'Histoire naturelle, Zoologie 155: 1–184.

Deuve T (2004) Deux nouvelles *Jujiroa* cavernicoles du sud de la Chine et du nord du Vietnam (Coleoptera, Caraboidea). Bulletin de la Société entomologique de France 109(4): 361–366.

Deuve T (2018) What is the epipleurite? A contribution to the subcoxal theory as applied to the insect abdomen. Annales de la Société entomologique de France (N.S.) 54: 1–26. https://doi.org/10.1080/00379271.2018.1431568

Deuve T, Pütz A (2013) Description d'une nouvelle *Jujiroa* cavernicole du Sichuan (Coleoptera, Caraboidea). Bulletin de la Société entomologique de France 118(3): 341–342.

Fang J, Li WB, Tian MY (2016) Occurrence of cavernicolous ground beetles in Anhui Province, eastern China (Coleoptera, Carabidae, Trechinae). ZooKeys 625: 99–110. https://doi.org/10.3897/zookeys.625.9846

Habu A (1978) Carabidae Platynini (Insecta: Coleoptera). Japanese Faunica. Keigaku-Sha, Ltd., Tokyo, 447 pp.

Habu A (1981) A new species of *Ja* found in Shizuoka Prefecture, Japan (Coleoptera, Carabidae). The Entomological Review of Japan 35: 1–5.

Jeannel R (1928) Monographie des Trechinae (Troisième livraison). L'Abeille 35: 1–808.
Jedlička A (1961) Monographie der Paläarktischen *Taphoxenus*-Arten (Coleoptera, Carabidae). Acta entomologica Musei nationalis Pragae 34: 167–219.
Liebherr JK, Will KW (1998) Inferring phylogenetic relationships within Carabidae (Insect: Coleoptera) from characters of the female reproductive tract. In: Ball GE, Casale A, Vigna Taglianti A (Eds) Phylogeny and Classification of Caraboidea (Coleoptera: Adephaga). Museo Regionale di Scienze Naturali, Torino, 107–170 pp.
Sasakawa K (2006) Speciation and dispersal process of *Jujiroa* Uéno, 1952 (Coleoptera, Carabidae) in the Japanese Archipelago, with description of five new species. Biogeography 8: 45–53.
Takakura Y (1987) Description of a new species of the genus *Jujiroa* from Kyushu, Japan (Coleoptera, Harpalidae). Kita-Kyûshû No Konshû 34: 177–178.
Tian MY, Huang SB, Wang XH, Tang MR (2016) Contributions to the knowledge of subterranean trechine beetles in southern China's karsts: five new genera (Insecta: Coleoptera: Carabidae: Trechinae). ZooKeys 564: 121–156. https://doi.org/10.3897/zookeys.564.6819
Uéno SI (2007a) Two new cave trechines (Coleoptera: Trechinae) from Western Zhejiang, East China. Journal of the speleological Society of Japan 32: 9–22.
Uéno SI (2007b) Occurrence of a new cave species of *Jujiroa* (Coleoptera: Carabidae: Platyninae) from Central Sichuan, Southwest China. Elytra 35(1): 21–26.
Uéno SI, Kishimoto T (2001) A new cave species of the genus *Jujiroa* (Coleoptera: Carabidae: Platyninae) from southern Sichuan, Southwest China. Journal of Speleological Society of Japan 16: 1–28.
Uéno SI, Pawlowski J (1981) A new microphthalmic trechine beetle of the *Trechoblemus* Complex from Tian Shan. Annotationes zoologicae japonenses 54: 147–155.
Uéno SI, Saito A (1991) Occurrence of *Jujiroa* (Coleoptera, Carabidae) on the high mountains of Taiwan. Journal of the Speleological Society of Japan 16: 1–28.
Vigna Taglianti A (1995) A new *Jujiroa* from Sichuan, China (Coleoptera, Carabidae). International Journal of Biospeleology 23: 179–190.

ZooKeys 923: 51–63 (2020)
doi: 10.3897/zookeys.923.48337
http://zookeys.pensoft.net

RESEARCH ARTICLE

A peer-reviewed open-access journal
ZooKeys
Launched to accelerate biodiversity research

Two new species of *Agaporomorphus* Guignot from Suriname (Coleoptera, Adephaga, Dytiscidae, Copelatinae)

Kelly B. Miller[1]

1 *Department of Biology and Museum of Southwestern Biology, University of New Mexico, Albuquerque, NM 87131-0001, USA*

Corresponding author: *Kelly B Miller* (kbmiller@unm.edu)

Academic editor: *M. Michat* | Received 10 November 2019 | Accepted 4 January 2020 | Published 1 April 2020

http://zoobank.org/8DB62739-6222-4331-AF37-9DC676B12FC6

Citation: Miller KB (2020) Two new species of *Agaporomorphus* Guignot from Suriname (Coleoptera, Adephaga, Dytiscidae, Copelatinae). ZooKeys 923: 51–63. https://doi.org/10.3897/zookeys.923.48337

Abstract

Two new species are described in the Neotropical genus *Agaporomorphus* Guignot from Suriname: *A. hamatocoles* **sp. nov.** and *A. tortus* **sp. nov**. The species are included in a phylogenetic parsimony analysis of 13 morphological characters and all 12 known species. Two equally parsimonious arrangements are found with the only difference a rearrangement among the *A. knischi* clade. *Agaporomorphus tortus* belongs to the *A. dolichodactylus* group based on presence of an elongate, club-like lobe on the dorsal, basal surface of the male median lobe and long, subsinuate male mesotarsal claws and a small lobe at the apex of male mesotarsomere V. *Agaporomorphus hamatocoles* does not belong to a known species group and is phylogenetically isolated lacking synapomorphies characterizing the other groups, so the species is placed in its own species group. Male genitalia are illustrated for the new species and redrawn for all the species of the *A. dolichodactylus* group, and male mesotarsal claws are illustrated for *A. tortus* and redrawn for other members of the *A. dolichodactylus* group. New distribution records are reported for Suriname for the species *A. colberti* Miller and Wheeler and *A. pereirai* Guignot.

Resumen

Se describen dos nuevas especies en el género neotrópico *Agaporomorphus* Guignot de Surinam: *A. hamatocoles* **sp. nov.** y *A. tortus* **sp. nov**. Las especies se incluyen en un análisis de parsimonia filogenética de 13 carácteres morfológicos y las 12 especies conocidas. Se encuentran dos arreglos igualmente parsimoniosos, con la única diferencia de un reordenamiento entre el clado de *A. knischi*. *Agaporomorphus tortus* pertenece al grupo *A. dolichodactylus* basado en la presencia en el macho de un lóbulo alargado, que parece un palo en la superficie dorsal, al base del lóbulo mediano ; las largas garras mesotarsales subsinuosas; y un lóbulo pequeño en el ápice del mesotarsómero V. *Agaporomorphus hamatocoles* no pertenece a ningún grupo de es-

pecies conocidas, está aislada filogenéticamente y carece de sinapormorfias que caracterizan los otros grupos, así que la especie se coloca en su propio grupo . Los genitales de los machos se ilustran para las nuevas especies y también para todas las especies del grupo *A. dolichodactylus*. Las garras mesotarsales de los machosse ilustran para *A. tortus* y también para los otros miembros del grupo *A. dolichodactylus*. Se informan nuevos registros de distribución para Surinam para las especies *A. colberti* Miller y Wheeler y *A. pereirai* Guignot.

Keywords
Agaporomorphus, diving beetle, South America, taxonomy, water beetle

Introduction

New species of *Agaporomorphus* Guingot have been discovered regularly as collecting has continued in new areas of South America (Miller 2001; 2005; Miller and Wheeler 2008; Miller 2014; Hendrich et al. 2015). Most recently, Hendrich et al. (2015) described a new species and its habitat as well the habitats of several other species in the genus in Peru. This was useful since the habitats for most species of this rare taxon are not known or well-known because specimens are often collected at lights at night. They appear to be generally associated with shaded forest pools in primary forest (Hendrich et al. 2015) or (*A. sharynae* Miller) in leaf-choked backwaters of shaded sandy streams (Miller 2014).

Species of *Agaporomorphus* are known only from lowland tropical South America (Miller 2001; 2005; Miller and Wheeler 2008; Libonatti et al. 2011; Torres et al. 2012; Miller 2014; Hendrich et al. 2015). The new species from Suriname described here bring the number in the genus to 12. *Agaporomorphus pereirai* Guignot was previously the only species known from Suriname. *Agaporomorphus* came out resolved as sister to *Madaglymbus* Shaverdo and Balke, a Malagasy genus, in the analysis by Shaverdo et al. (2008), but relationships among Copelatinae genera remain ambiguous. Members of *Agaporomorphus* have dramatic and unusually complex, asymmetrical male median lobes, and these two new species are no exception exhibiting some morphological structures unique among diving beetles. New records of other described species are also provided.

Materials and methods

Material

The new species are based on specimens from the Snow Entomological Collection, University of Kansas, Lawrence, Kansas, USA (**SEMC**, A.E.Z. Short, curator). The holotypes are deposited in the National Zoological Collection of Suriname, Paramaribo, Suriname (**NZCS**, P. Ouboter, curator). Paratypes are deposited in NZCS, SEMC, and the Museum of Southwestern Biology, Division of Arthropods, University of New Mexico, Albuquerque, New Mexico, USA (**MSBA**, K.B. Miller, curator). In addition, specimens of all other species in the genus, including the holotypes, were examined by the author except *A. julianeae* Hendrich, Apenborn, Burmeister, and Balke.

Measurements

Measurements were acquired using an ocular scale on a Zeiss Discovery V8 dissecting microscope at 50× magnification. Measurements include:

TL total length;
GW greatest width across elytra;
PW greatest pronotal width;
HW greatest width of the head;
EW distance between the eyes;
FL greatest length of the metafemur;
FW greatest width of the metafemur.

The ratios TL/GW, HW/EW, and FL/FW were also calculated to provide an indication of overall shape, eye size, and leg segment size.

Phylogeny

The new species were coded for the 12 characters described by Miller (2001; 2005; 2014) and Miller and Wheeler (2008). A new 13th character was added (see below). Parsimony analysis was done using WinClada to organize character data (Nixon 2002) and Nona for analysis (Goloboff 1995). Phylogenetic methods are the same as in Miller (2001; 2005) and Miller and Wheeler (2008). The two new species described here are included in the analysis along with *A. julianeae* with its characters scored based on the published account (Hendrich et al. 2015). The character matrix is presented in Table 1.

Table 1. Data matrix of assigned states of characters for 12 species of *Agaporomorphus* and generalized outgroup based on numerous examined taxa (e.g., *Copelatus* Erichson, *Madaglymbus* Shaverdo and Balke, *Lacconectus* Motschulsky, and *Exocelina* Broun species). Character 01 coded as additive (others binary). Characters match numbered characters from Miller (2001; 2005; 2014) and Miller and Wheeler (2008).

Species	0000000001111 1234567890123
Outgroup	0000000000000
A. hamatocoles	0000000000000
A. pereirai	0000010000000
A. knischi	0000011111110
A. tambopatensis	0000001111010
A. colberti	0000001111110
A. julianeae	0000001101110
A. silvaticus	0000001000010
A. sharynae	0000011000010
A. grandisinuatus	1010000000001
A. mecolobus	2111100000001
A. dolichodactylus	2111100000001
A. tortus	2111100000001

Character 13. *Apical lobe on male lateral lobe*; (0) not extremely long and slender (Fig. 3), (1) extremely long and slender (Fig. 6). Specimens of *A. dolichodactylus*, *A. grandisinuatus*, *A. mecolobus* and *A. tortus* have the apical lobe on the male lateral lobe long and slender (e.g., Fig. 3). Other *Agaporomorphus*, including *A. hamatocoles*, have this lobe distinctly shorter (e.g., Fig. 6).

Taxonomy

***Agaporomorphus hamatocoles* sp. nov.**
http://zoobank.org/13D50A02-DB96-4BDF-B783-10546861859A
Figures 1–3, 24, 26

Type locality. Suriname, Sipaliwini District, Sipaliwini Savannah Nature Reserve, Four Brothers Mountains, 2.005700N, 55.969151W, 337 m.

Diagnosis. This species does not share many features with other members of the genus and does not have modified antennomeres, modified male mesotarsal claws or a lobe on the apex of mesotarsomere V, it lacks a stridulatory apparatus on the abdomen and metaleg, and lacks a triangular process at the apical margin of visible sternite V of the abdomen. Unique features of *A. hamatocoles* are the strongly hooked male median lobe (Fig. 1) and the elongate curved flagellum on the ventral surface of the male median lobe (Figs 1, 2). These features are diagnostic within *Agaporomorphus*.

Description. ***Measurements*** (*N* = 3). TL = 2.8–3.2 mm, GW = 1.4–1.6 mm, PW = 1.2–1.3 mm, HW = 0.8 mm, EW = 0.5–0.6 mm, FL = 0.7–0.8 mm, FW = 0.2–0.3 mm, TL/GW = 1.9–2.0, HW/EW = 1.5–1.6, FL/FW = 2.9–3.4. Body shape elongate oval, evenly and shallowly curved along lateral margins, curvature continuous between pronotum and elytron.

Coloration. Head and pronotum dark orange. Elytron dark orange throughout except transverse basal band light orange. Ventral surface orange, similar in coloration throughout but legs distinctly lighter in color.

Sculpture and structure. Head shiny, very finely microreticulate comprised of small isodiametric cells; eyes small (HW/EW = 1.5–1.6). Pronotum shiny, similar microreticulation to head; lateral margin slightly curved, extremely finely beaded, bead absent at anterior angle. Elytron with lateral margin shallowly curved; surface shiny, microreticulation extremely fine, apical half with numerous extremely fine punctures. Prosternum elongate, carinate, prosternal process short, strongly carinate medially. Metaventer and metaventral wings smooth and shiny, with very dense, extremely fine microreticulation. Metacoxa smooth and shiny, similar in microsculpture to metaventer; metacoxal lines distinct, region between metacoxal lines narrow medially; metafemur not unusually broadened (FL/FW = 2.9–3.4).

Male genitalia. Median lobe exceptionally complex in shape, strongly asymmetrical; in lateral aspect broad basally, irregularly shaped, apically narrowed with apex dramatically hooked, curved anteriorly on dorsal surface with elongate apex directed

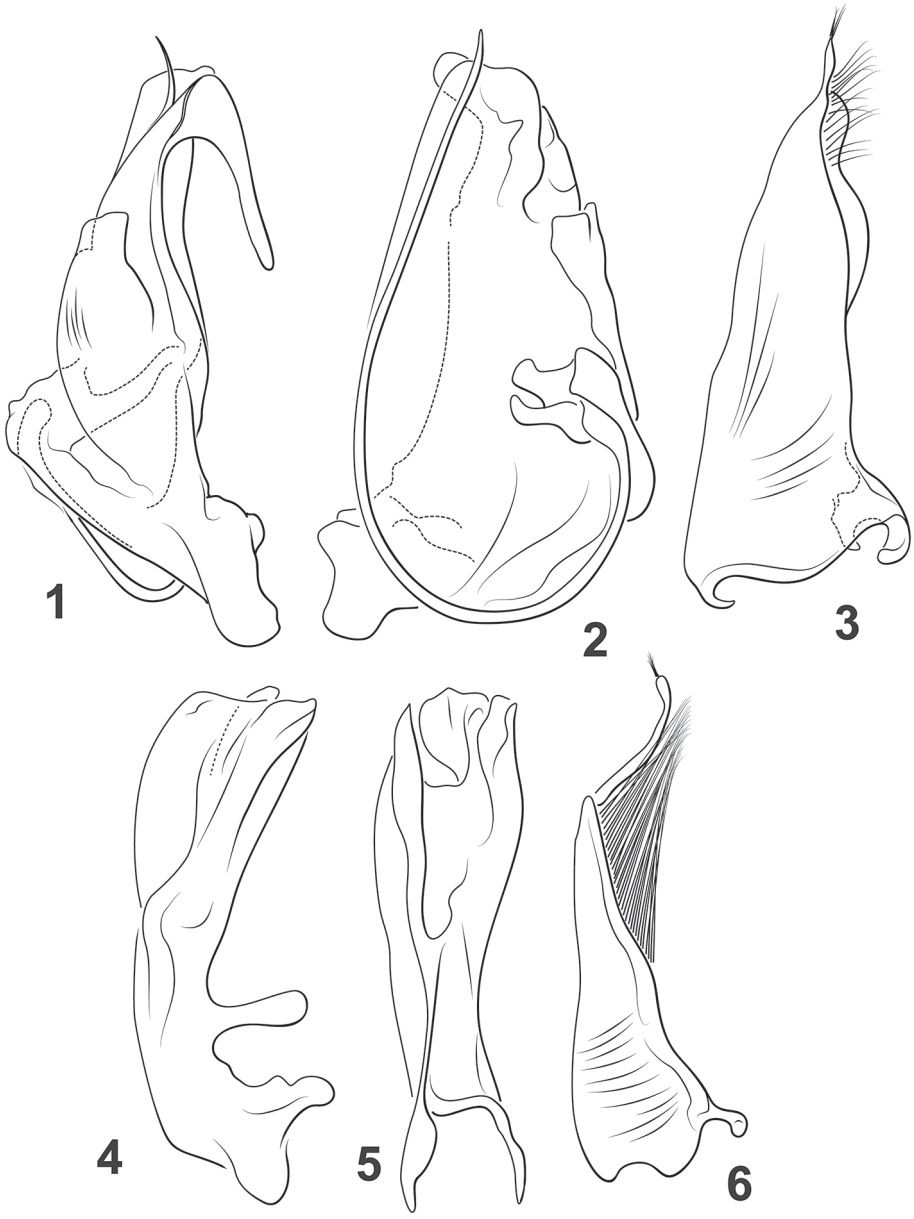

Figures 1–6. *Agaporomorphus* species, male genitalia. **1–3** *A. hamatocoles* **1** male median lobe, right lateral aspect **2** male median lobe, ventral aspect **3** male right lateral lobe, right lateral aspect **4–6** *A. tortus* **4** male median lobe, right lateral aspect **5** male median lobe, ventral aspect **6** male right lateral lobe, right lateral aspect.

posteriorly, curved portion elongate, slender and apically narrowly rounded (Fig. 1); in ventral aspect very broad, lateral margins broadly curved, with slender, long curved "flagellum" extending from left anteroventral region in broad curve along antero-ventral surface along left side to apex, apically sharply pointed (Fig. 2); lateral lobe in lat-

eral aspect robust, apically narrowed, with slender apical lobe, with series of fine setae along apicodorsal margin (Fig. 3).

Sexual dimorphism. Males have the pro-mesotarsomeres I-III distinctly broader than in females with enlarged ventral adhesive setae.

Variation. The few specimens are quite similar to each other in coloration and other features.

Distribution. This species is known only from southern Suriname (Fig. 24).

Habitat. The type series was collected from "detrital pools."

Discussion. This species is quite unlike other species in the genus. The *A. knischi* group is characterized by somewhat similarly shaped male median lobes with a fringe of setae along the dorsal margin of each side and many of them have expanded male antennomeres and/or stridulatory devices on the abdomen and metalegs (Miller 2005; Miller and Wheeler 2008; Hendrich et al. 2015). The *A. dolichodactylus* group has an elongate process on the dorsal surface of the male median lobe and elongate, sinuate mesotarsal claws (Miller 2005). The *A. pereirai* group has none of these features, but the male median lobe has prominent angulate flanges on the ventral side apically and other autapomorphies (Miller 2005). The new species described here does not share any of these characteristic features and is phylogenetically isolated (Fig. 26, see below), so it is placed in its own group, the *A. hamatocoles* species group.

Etymology. This species is named *hamatocoles*, from Latin *hamatus* for hooked and *coles* for penis for the unique shape of the hooked male median lobe in this species (Fig. 2).

Type material. Holotype in NZCS, male labeled, "SURINAME: Sipaliwini District 2.005700N, 55.969151W, 337m Sipaliwini Savannah Nature Res. Four Brothers Mts, detrital pools, 31.iii.2017 leg. Short. SR17-0331-01D/ Holotype *Agaporomorphus hamatocoles* Miller, 2020 [red label with double black line border]." 3 paratypes labeled same as holotype except with "…/Paratype *Agaporomorphus hamatocoles* Miller, 2020 [blue label with black line border]."

Agaporomorphus tortus sp. nov.

http://zoobank.org/8FA75E35-E24C-47D5-9E82-939597462D54
Figures 4–6,16, 17, 24, 26

Type locality. Suriname, Sipaliwini District, Sipaliwini Savannah Nature Reserve, Four Brothers Mountains, 2°00.656'N, 55°59.070'W, 275 m.

Diagnosis. This species is in the *A. dolichodactylus* species group which lacks characteristics of other species groups such as expanded male antennomeres, setae on the dorsal surface of the male median lobe, or stridulatory structures or triangular processes on the abdomen (Miller 2005). Like certain other members of the *A. dolichodactylus* species group, *A. tortus* has similar male genitalia (Figs 4–15) including an elongate process on the basal, dorsal surface of the male median lobe (Fig. 4), a lobe at the end of male mesotarsomere V (Figs 16, 17), and elongate and somewhat sinuate male

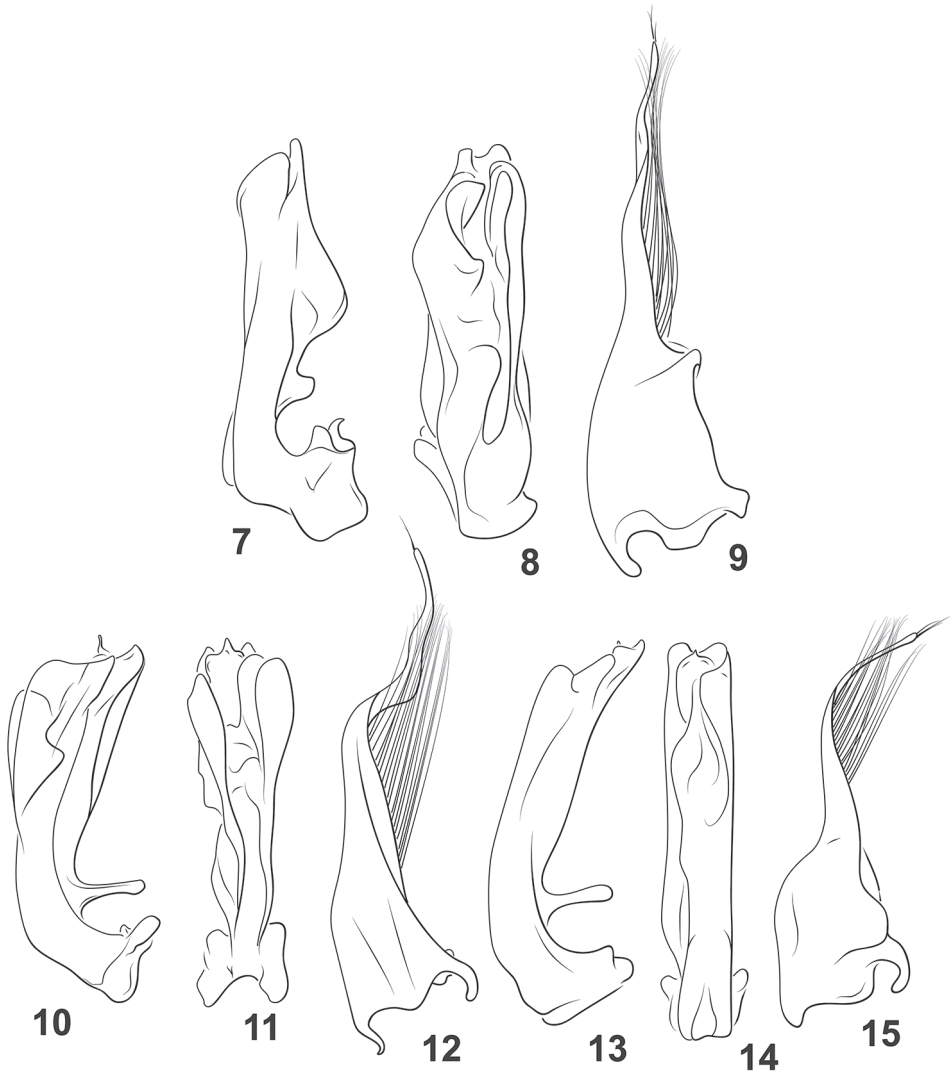

Figures 7–15. *Agaporomorphus* species, male genitalia. **7–9** *A. grandisinuatus* **7** male median lobe, right lateral aspect **8** male median lobe, ventral aspect **9** male right lateral lobe, right lateral aspect **10–12** *A. mecolobus* **10** male median lobe, right lateral aspect **11** male median lobe, ventral aspect **12** male right lateral lobe, right lateral aspect **13–15** *A. dolichodactylus* **13** male median lobe, right lateral aspect **14** male median lobe, ventral aspect **15** male right lateral lobe, right lateral aspect.

mesotarsal claws (Figs 16, 17). From other species in the group this species differs in the shape of the male median lobe which is deeply asymmetrically emarginate apically in ventral aspect (Fig. 5) and with other distinctive shapes (Figs 4, 5).

Description. ***Measurements*** (*N* = 3). TL = 3.0–3.2 mm, GW = 1.5 mm, PW = 1.2–1.3 mm, HW = 0.8–0.9 mm, EW = 0.5 mm, FL = 0.7–0.8 mm, FW = 0.2–

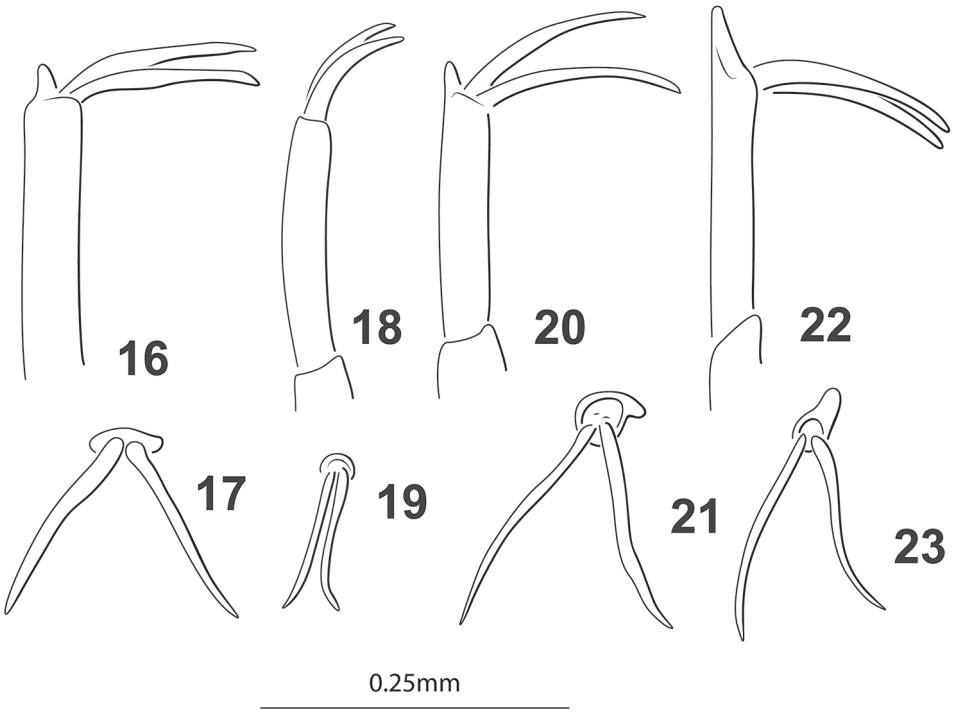

Figures 16–23. *Agaporomorphus* species, male mesotarsomere V and mesotarsal claws. **16, 17** *A. tortus* **16** anterior aspect **17** oblique lateral aspect **18, 19** *A. grandisinuatus* **18** anterior aspect **19** oblique lateral aspect **20, 21** *A. mecolobus* **20** anterior aspect **21** oblique lateral aspect **22, 23** *A. dolichodactylus* **22** anterior aspect **23** oblique lateral aspect.

0.3 mm, TL/GW = 2.0–2.2, HW/EW = 1.6–1.7, FL/FW = 2.9–3.6. Body shape elongate oval, evenly and shallowly curved along lateral margins, curvature continuous between pronotum and elytron.

Coloration. Head, pronotum and elytron orange, similar in coloration throughout dorsal surface. Ventral surface orange, similar in coloration throughout but legs slightly lighter in color.

Sculpture and structure. Head shiny, very finely microreticulate comprised of small isodiametric cells; eyes moderately large (HW/EW = 1.6–1.7). Pronotum shiny, similar microreticulation to head; lateral margin slightly curved, extremely finely beaded, bead absent at anterior angle. Elytron with lateral margin shallowly curved; surface shiny, microreticulation extremely fine, apical half with numerous extremely fine punctures. Prosternum elongate, carinate, prosternal process short, strongly carinate medially. Metaventer and metaventral wings smooth and shiny, with very dense, fine microreticulation. Metacoxa smooth and shiny, similar in microsculpture to metaventer; metacoxal lines distinct, region between metacoxal lines narrow medially; metafemur not unusually broadened (FL/FW = 2.9–3.6).

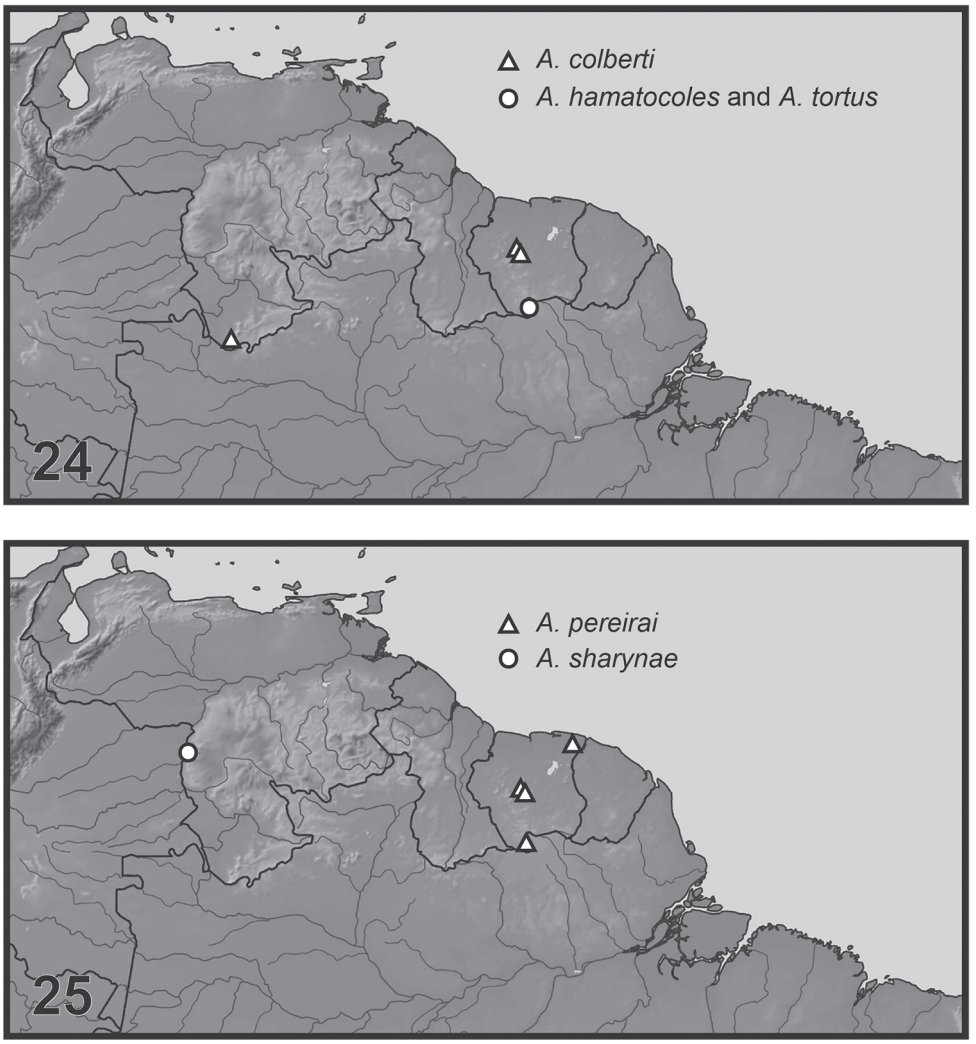

Figures 24, 25. Known distributions of *Agaporomorphus* species of northern South America (*A. pereirai* also known from Brazil, not shown on map).

Male genitalia. Median lobe complex in shape, asymmetrical; in lateral aspect narrow basally, broadened apically, apically broadly truncate with medial small lobe extending beyond truncation (Fig. 4); in ventral aspect broad apically, with complex arrangement of lobes and flanges, apicomedially with large, asymmetrical excavation between surfaces and distinctive deep apical emargination on left side of middle (Fig. 5); lateral lobe in lateral aspect robust basally, apically slender, with long, slender apical lobe, with long series of setae along dorsal margin (Fig. 6).

Sexual dimorphism. Males protarsomeres I–III distinctly broader than in females with four large adhesive setae; females without expansion or adhesive setae. Male mes-

otarsomeres I–III broader than in females, not as strongly expanded as male protarsomeres I–III, male mesotarsomeres with four large ventral adhesives setae; apex of mesotarsomere V extended into small lobe on posterior margin of apex (Figs 16, 17), mesotarsal claws of male elongate, slightly sinuate (Figs 16, 17); females without these mesoleg modifications.

Variation. There is some minor variation in intensity of coloration of the dorsal surface between specimens but this may be because some specimens are more teneral than others.

Distribution. This species is only known from southern Suriname (Fig. 24).

Habitat. The type series was collected from "vegetated pools in savanna."

Discussion. This species belongs to the *A. dolichodactylus* group of *Agaporomorphus* of Miller (2005), and specifically close to *A. dolichodactylus* and *A. mecolobus* (Fig. 26, see below) based on the presence of a long lobe basally on the dorsal margin of the male median lobe (Fig. 4), a distinctive lobe on the apex of the male mesotarsomere V (Figs 16, 17), and male mesotarsal claws long and sinuate (Figs 16, 17). This is the first of the group known from northern South America (Fig. 24) with the other species in Brazil and Peru.

Etymology. This species is named *tortus*, Latin for "twisted" for the complex shape of the male median lobe in this species (Figs 4, 5).

Type material. Holotype in NZCS, male labeled, "Suriname: Sipaliwini District Sipaliwini Savanna Nature Res. 2°00.656'N, 55°59.070'W, 275 m vegetated pools in savanna 1.iv.2017; leg. A.E.Z. Short SR17-0401-01A/ SEMC1542796 KUNHM-ENT [barcode label]/ Holotype *Agaporomorphus tortus* Miller, 2020 [red label with double black line border]." 2 paratypes labeled same as holotype except […SEMC1542807…] and […SEMC1516119…] and paratype label, "…Paratype *Agaporomorphus tortus* Miller, 2020 [blue label with black line border]."

Phylogenetic results. The parsimony analysis resulted in two equally parsimonious trees (L = 17, CI = 82, RI = 92) (Fig. 26). The trees comport well with previous results (Miller 2001; 2005; Miller and Wheeler 2008; Miller 2014) with three main clades characterized by specific distinctive synapomorphies. These correspond to the *A. dolichodactylus*-, *A. knischi*-, and *A. pereirai* groups of Miller (2001) with the exception of the new species *A. hamatocoles* (described above) which has an unresolved position in the tree because of absence of the synapomorphies shared among the other clades in the phylogeny (Fig. 26). The only difference between the trees is a rearrangement within the *A. knischi* clade (Fig. 26). The other new species, *A. tortus*, is resolved with the *A. dolichodactylus* clade based on presence of an elongate lobe on the dorsal base of the male median lobe (Figs 4, 19, 13, shorter and broadly rounded in *A. grandisinuatus*, Fig. 7). Specimens also have long, somewhat sinuate mesotarsal claws with a distinct lobe at the apex of mesotarsomere V (Figs 16, 17) (synapomorphy with *A. dolichodactylus* (Figs 20, 21) and *A. mecolobus* (Figs 22, 23) and a very long apical lobe on the male lateral lobe (Fig. 6), shared with other members of the *A. dolichodactylus* clade (Figs 9, 12, 15).

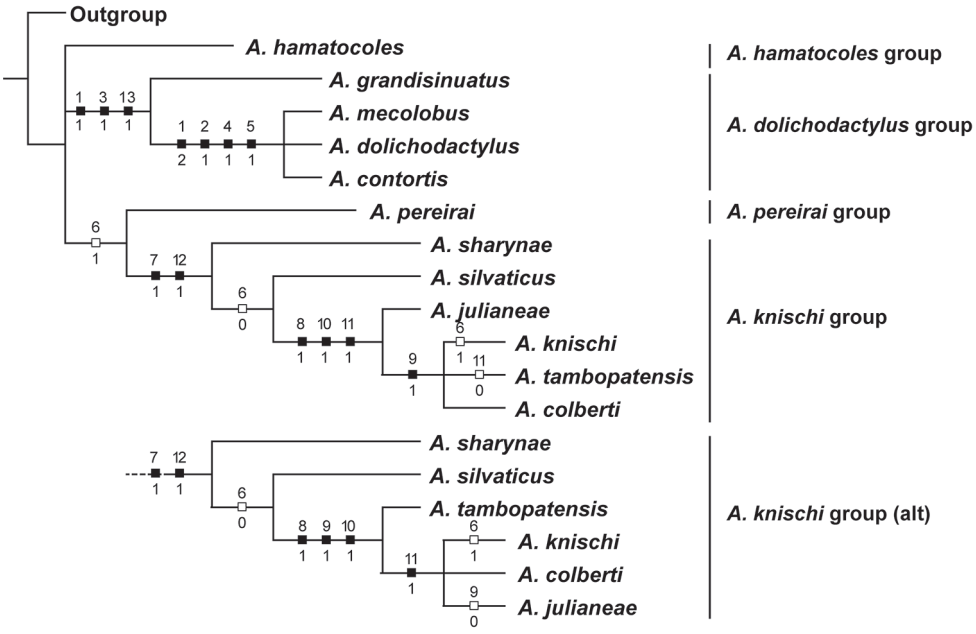

Figure 26. Two equally most parsimonious cladograms of *Agaporomorphus* species derived from parsimony analysis (L = 17, CI = 82, RI = 92): "alt" = alternative equally parsimonious configuration for *A. knischi* clade. Numbers above hatch marks refer to characters. Numbers below hatch marks refer to character state transformations. Characters mapped using "fast" or "acctran" optimization in WinClada (Nixon 2002).

New records of other species of *Agaporomorphus*

***A. colberti* Miller and Wheeler** (Fig. 24). **Suriname**, Sipaliwini District, 3°47.479'N, 56°08.968'W, 320m, CSNR, nr Kappel airstrip, forest pools near Petromia Falls, 13 Aug 2013, Short, Bloom and Kadosoe, legs, SR13-0813-03A (3, KUNHM; SEMC1235490, SEMC1234094, SEMC1234095); Sipaliwini District, 3°47.479'N, 56°08.968'W, 320m, CSNR, nr Kappel airstrip, forested stream and stream pools, 24 Aug 2013, Short and Bloom, legs, SR13-0824-03A (2, KUNHM; SEMC1234951, SEMC0966126); Sipaliwini Dist, 3°55.600'N, 56°11.300'W, 600m, CSNR, Tafelberg Summit, nr Augustus Cr. Camp, pond on trail into Arrowhead basin, 16 Aug 2013, Short and Bloom, legs, SR13-0816-02A (A1, KUNHM: SEMC0930616).

These are the first records of *A. colberti* from Suriname with previous records from Venezuela (Miller and Wheeler 2008: fig. 24).

***A. pereirai* Guignot** (Fig. 25). **Suriname**, Sipaliwini Dist, 3°55.600'N, 56°11.300'W, 600m, CSNR, Tafelberg Summit, nr Augustus Cr. Camp, pond on trail into Arrowhead basin, 17 Aug 2013, Short and Bloom, legs, SR13-0817-01A (1, KUNHM: SEMC0965435, SEMC0965426, SEMC0965425, SEMC0965396,

SEMC0965397); Sipaliwini Dist., 2°00.526'N, 55°58.572'W, 292m, Sipaliwini Savanna Nature Res, side pools of small clearwater stream in savannah, 20 Mar 2017, Short and Baca, legs, SR17-0330-02B (2, KUNHM; SEMC1541937, SEMC1541940); Sipaliwini Dist, 3°53.942'N, 56°10.849'W, 733m, SCNR, Tafelberg Summit, nr Caiman Cr camp, forest detrital pools, 19 Aug 2013, Short and Bloom, legs, SR13-0819-02A (1, KUNHM; SEMC0966170).

Previous records of this species are from Suriname (Cottica River, Moengo, Boven: fig. 25), and Matto-Grosso and Para, Brazil (Guignot 1957; Miller 2001).

Species list of the genus *Agaporomorphus*

***Agaporomorphus knischi* species group**
A. colberti Miller & Wheeler, 2008. Venezuela, Suriname
A. julianeae Hendrich, Apenborn, Burmeister, & Balke, 2013. Peru
A. knischi Zimmermann, 1921. Brazil, Peru, Bolivia
A. sharynae Miller, 2014. Venezuela
A. silvaticus Miller, 2005. Peru
A. tambopatensis Miller, 2005. Peru

***Agaporomorphus dolichodactylus* species group**
A. dolichodactylus Miller, 2001. Brazil, Bolivia
A. grandisinuatus Miller, 2001. Brazil, Peru
A. mecolobus Miller, 2001. Brazil
A. tortus sp. nov. Suriname

***Agaporomorphus hamatocoles* species group**
A. hamatocoles sp. nov. Suriname

***Agaporomorphus pereirai* species group**
A. pereirai Guignot, 1957. Brazil, Suriname

Acknowledgements

Thanks to Andrew E.Z. Short for collecting and providing access to specimens. Paul Ouboter and Vanessa Kadosoe provided invaluable assistance in Suriname to Short. Portions of this work were funded by NSF grants #DEB–0845984 and #DEB-1353426 (K.B. Miller, PI) and #DEB–0816904 (A.E.Z. Short, PI; K.B. Miller, co–PI). Fieldwork in Suriname was funded by National Geographic Grant #9286-13 (A.E.Z. Short, PI). Finally, thank you to Sandra Brantley for helping with Spanish translation.

References

Goloboff P (1995) NONA. 1.5 (32 bit) ed.

Guignot F (1957) Contribution à la connaissance des dytiscidés Sud-Américaines [Coleopt.]. Revue Française d'Entomologie 24: 33–45.

Hendrich L, Apenborn R, Burmeister EG, Balke M (2015) A new species of *Agaporomorphus* Zimmermann, 1921 from Peru (Coleoptera, Dytiscidae, Copelatinae). ZooKeys 512: 63–76. https://doi.org/10.3897/zookeys.512.9505

Libonatti ML, Michat MC, Torres PLM (2011) Key to the subfamilies, tribes and genera of adult Dytiscidae of Argentina (Coleoptera: Adephaga). Revista de la Sociedad Entomológica Argentina 70: 317–336.

Miller KB (2001) On the genus *Agaporomorphus* Zimmermann, 1921 (Coleoptera: Dytiscidae: Copelatinae). Annals of the Entomological Society of America 94: 520–529. https://doi.org/10.1603/0013-8746(2001)094[0520:ROTGAZ]2.0.CO;2

Miller KB (2005) Two New Species of *Agaporomorphus* Zimmermann (Coleoptera: Dytiscidae) from Peru. Zootaxa 1059: 49–59. https://doi.org/10.11646/zootaxa.1059.1.4

Miller KB (2014) *Agaporomorphus sharynae*, a new species of diving beetle (Coleoptera: Dytiscidae: Copelatinae) from Venezuela. Zootaxa 3790: 177–184. https://doi.org/10.11646/zootaxa.3790.1.8

Miller KB, Wheeler QD (2008) A new species of *Agaporomorphus* Zimmermann from Venezuela, and a review of the *A. knischi* species group (Coleoptera: Dytiscidae: Copelatinae). Zootaxa 1859: 63–68. https://doi.org/10.11646/zootaxa.1859.1.4

Nixon KC (2002) WinClada. 1.00.08 ed. Published by the author, Ithaca, NY.

Shaverdo HV, Monaghan MT, Lees DC, Ranaivosolo R, Balke M (2008) *Madaglymbus*, a new genus of Malagasy endemic diving beetles and description of a highly unusual species based on morphology and DNA sequence data (Dytiscidae: Copelatinae). Systematics and Biodiversity 6: 43–51. https://doi.org/10.1017/S1477200007002599

Torres PLM, Michat MC, Libonatti ML, Fernandez LA, Oliva A, Bachmann AO (2012) Aquatic Coleoptera from Mburucuya National Park (Corrientes Province, Argentina). Revista de la Sociedad Entomológica Argentina 71: 57–71.

ZooKeys 923: 65–77 (2020)
doi: 10.3897/zookeys.923.47104
http://zookeys.pensoft.net

RESEARCH ARTICLE

A peer-reviewed open-access journal
ZooKeys
Launched to accelerate biodiversity research

Two new species of *Desmopachria* Babington, 1841 in the *D. convexa* species group (Coleoptera, Adephaga, Dytiscidae, Hydroporinae, Hyphydrini)

Kelly B. Miller[1]

1 *Department of Biology and Museum of Southwestern Biology, University of New Mexico, Albuquerque, NM 87131-0001 USA*

Corresponding author: Kelly B. Miller (kbmiller@unm.edu)

Academic editor: M. Michat | Received 7 October 2019 | Accepted 15 February 2020 | Published 1 April 2020

http://zoobank.org/B10E9E71-8A43-4560-BBAC-47F52E401045

Citation: Miller KB (2020) Two new species of *Desmopachria* Babington, 1841 in the *D. convexa* species group (Coleoptera, Adephaga, Dytiscidae, Hydroporinae, Hyphydrini). ZooKeys 923: 65–77. https://doi.org/10.3897/zookeys.923.47104

Abstract

Two new species are described in the *Desmopachria convexa* species group in the Neotropical genus *Desmopachria* Babington: *D. manco* **sp. nov.** (Guyana), and *D. mortimer* **sp. nov.** (Costa Rica). Two subgroups, the *D. convexa-convexa* and the *D. convexa-signata* groups are defined. *Desmopachria convexa-convexa* species are from North and Central America and have a subapical articulable lobe on the male lateral lobe that is large and elongate and extends well beyond the slender, oblique apex of the lateral lobe. *Desmopachria convexa-signata* species are from South America and have a subapical articulable lobe on the male lateral lobe that is small and discrete and does not extend beyond the truncate apex of the lateral lobe. The male genitalia of all recognized species in the *D. convexa* group are redrawn from the literature. New species are illustrated from specimens and described species have morphological features redrawn from published illustrations.

Resumen

Se describen dos especies nuevas en el grupo de especies *Desmopachria convexa* del género neoprópical *Desmopachria* Babington: *D. manco* **sp. nov.** (Guyana) y *D. mortimer* **sp. nov.** (Costa Rica). Se definen dos subgrupos, el *D. convexa-convexa* y *D. convexa-signata*. Las especies de *D. conveza-convexa* son de Centro y Norte América, y tienen un lóbulo subapical articulado en el lóbulo lateral del macho que es grande y alargado y se extiende mucho más allá del ápice delgado y oblicuo del lóbulo lateral. Las especies

de *D. convexa-signata* son de América del Sur y tienen un lóbulo subapical articulado en el lóbulo lateral del macho que es pequeño y discreto y no se extiende más allá del ápice del lóbulo lateral. Los genitales masculinos de todas las especies reconocidas en el grupo *D. convexa* se vuelven a dibujar a partir de la literatura. Las especies nuevas se ilustran a partir de los ejemplares examinados y las especies descritas tienen características morfológicas redibujadas a partir de ilustraciones publicadas.

Keywords
Taxonomy, New World, diving beetles, systematics

Introduction

The taxonomic situation concerning *Desmopachria* Babington was briefly reviewed most recently by Miller and Wolfe (2018; 2019) and Braga & Ferreira Jr. (2018). *Desmopachria* is a species-rich genus of diving beetles restricted to the New World with numerous species described recently (Braga and Ferreira-Jr. 2010; 2011; 2014; Gustafson and Miller 2012; Makhan 2012; 2015; Megna and Sanchez-Fernandez 2014; Miller 1999; 2001; 2005; Miller and Wolfe 2018; 2019). Currently the genus includes approximately 130 described species, and many more undescribed ones known to exist making it one of the larger genera of diving beetles in the New World.

Two new species are described here from the *D. convexa* species group which are characterized by an articulable appendage on the anterolateral surface of the male lateral lobe (Young 1980; 1981). This group was reviewed by Young (1981) with a number of species described subsequently (Braga and Ferreira-Jr. 2010; Miller 2001; 2005; Young 1990). The group is among the most widespread in *Desmopachria*, occurring throughout eastern North America south into southern South America.

Dichotomous keys are not particularly useful within *Desmopachria*, including the *D. convexa* group. The best strategy for identification of these extremely similar species is comparison of visual diagnostic combinations especially comparison of male genitalia with others in the group (Figs 2–5, 7–8, 11–36, 39–41, 44–46, 49–57).

Material and methods

Measurements

Measurements were made with an ocular scale on a Zeiss Discovery V8 dissecting microscope to 0.1 mm. The diagnostic range of measurements of structures was emphasized, so the largest and smallest specimens were preferentially measured to the extent possible. Measurements include: 1) total length (TL), 2) greatest width across elytra (GW), 3) greatest width of head (HW), and 4) distance between eyes (EW). The ratios TL/GW and HW/EW were also calculated.

Images

Illustrations were made using a drawing tube on a Zeiss Discovery V8 dissecting scope. Sketches were first done in pencil then scanned, placed into an Adobe Illustrator artboard and "inked" digitally using vector lines and modified with brushes.

Material

Specimens of *Desmopachria* were examined representing many species from all species groups including many from the following collections:

CSBD Center for Biological Diversity, University of Guyana (type specimens currently reposed with KUNHM, see below)

KBMC Kelly B. Miller Collection, Museum of Southwestern Biology, University of New Mexico, Albuquerque, NM, USA.

KUNHM University of Kansas Natural History Museum, University of Kansas, Lawrence, Kansas, USA (A.E.Z. Short, curator)

MIZA Museo del Instituto de Zoología Agrícola Francisco Fernández Yépez, Universidad Central de Venezuela, Maracay, Venezuela (L. Joly, curator)

MSBA Museum of Southwestern Biology Division of Arthropods, University of New Mexico, Albuquerque, NM, USA (K.B. Miller, curator)

NZCS National Zoological Collection of Suriname, Paramaribo, Suriname (P. Ouboter, curator)

USNM United States National Collection of Insects, Smithsonian Institution, Washington, DC, USA (T. Erwin, curator)

Taxonomy

The *Desmopachria convexa* group

Diagnosis. The *Desmopachria convexa* group is characterized in the genus by an articulable subapical process on the male lateral lobe of the aedeagus and the male median lobe either apically bifid (e.g., Fig. 15) or trifid (e.g., Fig. 11) with the exception of *D. pilosa* Miller (apically simple, Fig. 52) and *D. majuscula* Young (seemingly absent, Fig. 34). The species are extremely similar to each other in external appearance, though there are some diagnostic variations in size, shape, punctation and coloration. But externally there are often few particularly useful characters for distinguishing closely related species. Males and females are externally extremely similar, as well.

There are two apparent subgroups in the *D. convexa* species group, those with a smaller subapical articulable appendage on the lateral lobe not extending beyond the truncate

apex (e.g., Figs 4, 5) and those with a larger subapical articulable appendage that is leaf-like and extends well beyond the elongate, slender oblique apex of the lateral lobe (e.g., Figs 9, 10). These are referred to here as the *D. convexa-convexa* subgroup (with the larger subapical articulable appendage) and *D. convexa-signata* subgroup (with the smaller subapical articulable lobe). *Desmopachria convexa-convexa* species are found in North and Central America and the Caribbean, and *D. convexa-signata* species are found in South America. It is not clear at this time how these two groups might be related to each other or their monophyletic status, but they seem to be well-characterized by the shared articulable appendage of the male lateral lobes which is unique in *Desmopachria* and Dytiscidae in general.

Comments. This group corresponds to the *Desmopachria convexa-grana* group of Young (1980), which he later revised (Young 1981). Additional new species were described by several investigators (Braga and Ferreira-Jr. 2010; Miller 2001; 2005; Young 1990).

It is possible that several other described species may belong to this species group including *D. attenuata* Régimbart, 1895 (Young 1980), *D. balfourbrownei* Young, 1990, *D. striga* Young, 1990, and *D. subfasciata* Young, 1990 based on illustrations suggesting the presence of a subapical or apical articulable structure on the lateral lobe (Miller 2001). These species have not been well-described making the diagnostic characteristics of the group hard to discern. It does not appear that these species correspond with either of the new species described here, however.

Desmopachria manco sp. nov.

http://zoobank.org/937F3475-5EDC-4269-B1FB-623F3DC78BC9
Figures 1–5, 58

Type locality. Guyana, Region IX, Parabara, trail to mines, 2°05.095'N, 59°14.174'W, 250m.

Type material. Holotype in CSBD (currently in KUNHM, see above), male labeled, "Guyana: Region IX 2°05.095'N, 59°14.174'W, 250 m Parabara, Trail to mines detrital pools in forest leg. Short, Isaacs, Salisbury 2.xi.2013; GY13-1102-01A/ SEMC1271259 KUNHM-ENT/ Holotype *Desmopachria manco* Miller, 2020 [red label with black line border]." Paratypes, 1 labeled, "Guyana: Region IX 2°52.204'N, 59°55.003'W, 124 m nr. Kusad Mts., marshy area leg. Short, Isaacs, Salisbury 27x.2013; GY13-1027-01A/ SEMC1271270 KUNHM-ENT [barcode label]/ Paratype *Desmopachria manco* Miller, 2020 [blue label with black line border]."

The paratype specimen was not dissected but it has the same color pattern, size, and other features as the holotype. It is assigned to this species even though it is from some geographic distance away.

Diagnosis. This is an extremely small species among Dytiscidae and even among *Desmopachria* (Fig. 1; TL = 1.2–1.3 mm). The dorsal diffuse maculae on the elytra are characteristic (Fig. 1). The male genitalia include a dispositively diagnostic set of features (Figs 2–5) and place the species in the *Desmopachria convexa-signata* subgroup (see above). The median lobe is short (Figs 2, 3). In lateral aspect it is irregular in shape,

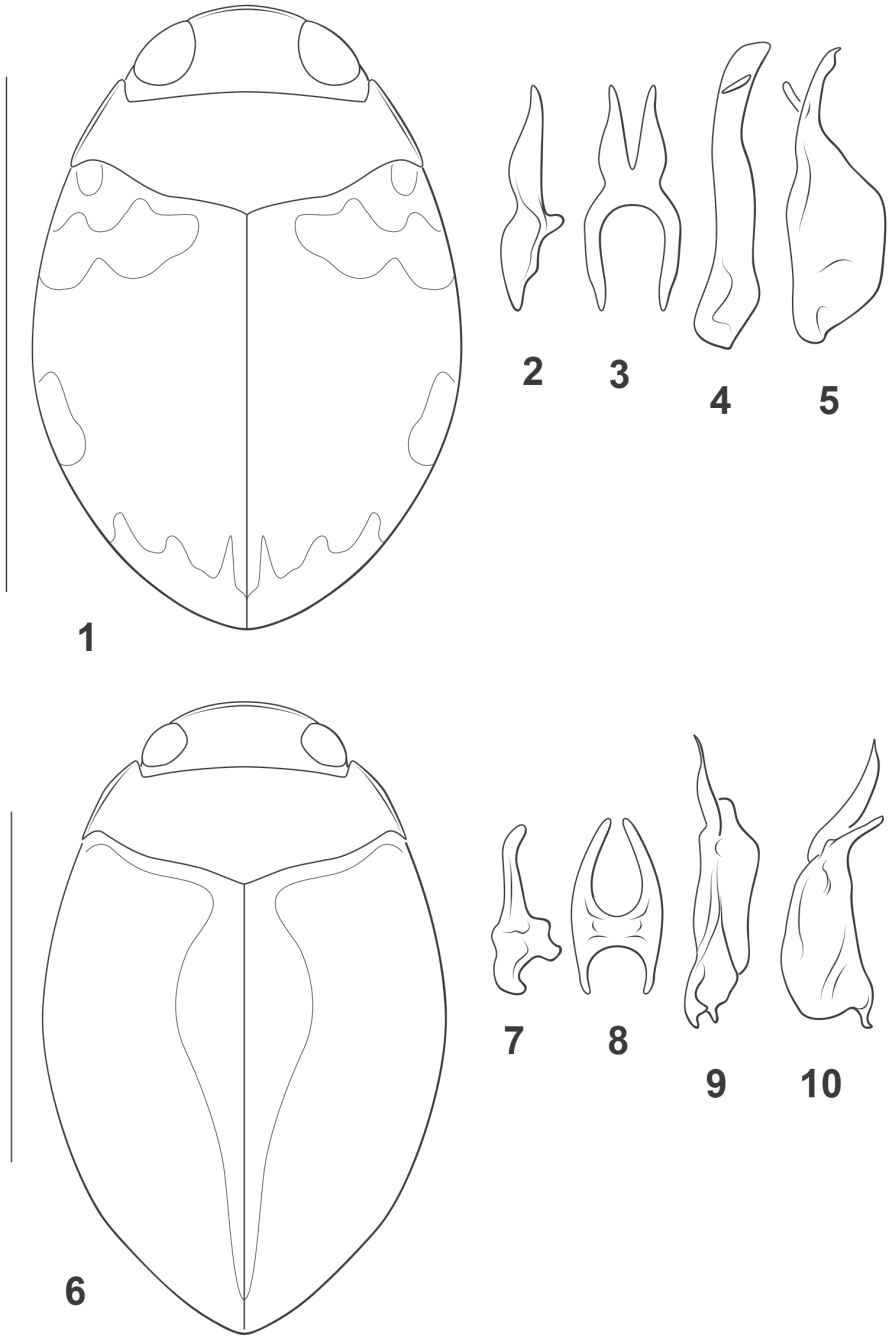

Figures 1–10. *Desmopachria* species. **1–5** *D. manco* **1** habitus **2–5** male genitalia **2** male median lobe, right lateral aspect **3** male median lobe, ventral aspect **4** male left lateral lobe, ventral aspect **5** male left lateral lobe, left lateral aspect **6–10** *D. mortimer* **6** habitus **7–10** male genitalia **7** male median lobe, right lateral aspect **8** male median lobe, ventral aspect **9** male left lateral lobe, ventral aspect **10** male left lateral lobe, left lateral aspect. Scale bars: 1.0 mm (**1, 6**).

medially expanded ventrally and with the apical portion slender, short, slightly curved dorsad and apically narrowly rounded (Fig. 2). In ventral aspect it is very broad, basally deeply U-shaped, apically deeply bifid, each ramus broad basally, apically narrowed and slightly curved laterad (Fig. 3). The lateral lobe in ventral aspect is elongate, broad, of subequal width throughout to a broadly truncate apex, with the subapical articulable lobe small and broad (Fig. 4). The lateral lobe in lateral aspect is very broad basally with the apex slender, subapically slightly expanded on the dorsal margin and apically sharply pointed with the subapical articulable process short and slender (Fig. 5).

Description. ***Measurements.*** TL = 1.2–1.3 mm, GW = 0.8 mm, PW = 0.7 mm, HW = 0.4–0.5 mm, EW = 0.2 mm, TL/GW = 1.9, HW/EW = 2.0. Body round, subspherical, lateral margins continuous between pronotum and elytron (Fig. 1), dorsoventrally broad.

Coloration (Fig. 1). Head and pronotum yellow. Elytron orange, with distinct but weakly margined maculae at humeral angle, anterolaterally extending to near suture, lateromedially and apically; surface not iridescent. Ventral surfaces and appendages yellow.

Sculpture and structure. Head (Fig. 1) broad, anteriorly produced in rounded margin; anterior margin of clypeus margined with conspicuous, continuous, flattened bead; surface of head shiny, very finely and sparsely punctate; eyes large (HW/EW = 1.2–1.4); antennae short, scape and pedicel relatively large and rounded, flagellomere III long and slender, apically expanded, antennomeres IV–X short and broad, lobe at anterodorsal angle, antennomere XI elongate, apically pointed. Pronotum short, lateral margins short, broadly curved with narrow, even bead; surface shiny, nearly impunctate medially, more but sparsely punctate along anterior and posterior margins, punctation variable, fine to course. Elytron moderately broad, laterally broadly curved; surface impunctate. Prosternum extremely short, longitudinally compressed, medially slightly carinate; prosternal process slender anteriorly, with distinctive, small medial tubercle, apically short and broad, concave, apically broadly pointed. Metaventrite broad and evenly smoothly convex medially, surface shiny, impunctate, anteromedially with curved transverse carina between posterior margins of mesocoxal cavities; metaventrite wings extremely slender. Metacoxa with medial portion short, about 1/3 length of metaventrite medially, metacoxal lines distinctly divergent anteriorly; lateral portion of metacoxa extremely large, anteriorly strongly expanded; surface shiny, impunctate, but slightly rugulose medially. Metatrochanter large, longer than ventral margin of metafemur anterior to metatrochanter apex; legs otherwise not noticeably modified. Abdomen with surfaces shiny and smooth, impunctate.

Male genitalia. Male median lobe in lateral aspect short, medially somewhat expanded on ventral margin, apically convergent to sharply angulate apex (Fig. 1). Median lobe in ventral aspect broad, base in broad "U" shape, apically deeply bifid, each ramus elongate, broad basally, and apically pointed (Fig. 2). Lateral lobe in ventral aspect moderately broad, apically gently curved laterad, with apex subtruncate, subapical articulable process oblique and flattened (Fig. 3). Lateral lobe in lateral aspect very broad basally, constricted medially, apically slender, slightly and broadly curved dorsad, apex pointed, subapically articulable lobe slender, directed ventrad (Fig. 4).

Etymology. This species is named *manco*, after Manco, the younger bounty hunter in the Sergio Leone film "For a Few Dollars More".

Distribution. This species is known from two localities in Guyana, Region IX (Fig. 58).

Habitat. The type and paratype were collected in "detrital pools" and a "marshy area."

***Desmopachria mortimer* sp. nov.**
http://zoobank.org/F8656CD2-3D92-4B2B-94DA-5B04F8F029EC
Figures 6–10, 59

Type locality. Costa Rica, Cartago Province, Tapanti National Park, pasture by Rio Orosi, ca. 1200 m.

Type material. Holotype in KUNHM, male labeled, "Costa Rica: Cartago Province Tapanti National Park: 24.v.2006 pasture by Rio Orosi: c. 1200 m leg. A.E.Z. Short, AS-06-043/ SEMC0895195 KUNHM-ENT/ Holotype *Desmopachria mortimer* Miller, 2020 [red label with black line border]." Paratypes, 41, labeled same as holotype except with different specimen barcode labels (Table 1) and each with "Paratype *Desmopachria mortimer* Miller, 2020 [blue label with black line border]."

Diagnosis. This is a moderately sized, somewhat elongate species of *Desmopachria* (Fig. 1; TL = 1.7–1.9 mm). The dorsal coloration is characteristic with diffuse darker regions medially and extending laterally onto the surface of the elytron (Fig. 6). The shape of the male genitalia is diagnostic (Figs 7–10) and place the species in the *Desmopachria convexa-convexa* subgroup (see above). The median lobe is short (Figs 7, 8), and in lateral aspect it is irregularly broad basally with the apical portion slender, short and curved dorsally to a narrowly rounded apex (Fig. 7). In ventral aspect it is very broad, basally broadly U-shaped, apically deeply bifid, with each ramus slender and strongly curved medially (Fig. 8). The lateral lobe in ventral aspect is irregularly shaped, broad, with the apex narrowly truncate and with a subapical articulable lobe that extends well beyond the apex of the lateral lobe and is apically acuminate and sharply pointed (Fig. 9). The lateral lobe in lateral aspect is very broad basally with the apex slender, elongate, directed dorsad, and with the subapical articulable lobe elongate, curved and apically sharply pointed (Fig. 10).

Description. ***Measurements.*** TL = 1.7–1.9 mm, GW = 1.1–1.2 mm, PW = 0.9–1.0 mm, HW = 0.5–0.6 mm, EW = 0.3–0.4 mm, TL/GW = 1.5–1.6, HW/EW = 1.2–1.4. Body broad but slightly elongate posteriorly, lateral margins continuous between pronotum and elytron (Fig. 6), dorsoventrally broad.

Coloration (Fig. 6). Head orange, diffusely darker orange posteriorly. Pronotum orange, with darker orange region along posterior margin. Elytron orange, with diffuse, weakly margined darker regions along anteromedial margin, along elytral suture and expanded somewhat onto disc medially; surface not iridescent. Mesoventrite, metacoxa and abdominal ventrites dark orange, other ventral surfaces and appendages lighter orange.

Sculpture and structure. Head (Fig. 6) broad, anteriorly produced in broadly rounded margin; anterior margin of clypeus margined with conspicuous, continuous narrow bead; surface of head shiny, very finely and sparsely punctate, punctation slightly denser posteriorly; eyes large (HW/EW = 2.0); antennae short, scape and pedicel relatively large and rounded, flagellomere III long and slender, apically ex-

Table 1. SEMC museum numbers for *D. mortimer* paratypes.

SEMC0895144	SEMC0895156	SEMC0895167	SEMC0895182
SEMC0895145	SEMC0895157	SEMC0895168	SEMC0895184
SEMC0895146	SEMC0895158	SEMC0895169	SEMC0895185
SEMC0895147	SEMC0895159	SEMC0895170	SEMC0895190
SEMC0895148	SEMC0895160	SEMC0895171	SEMC0895191
SEMC0895149	SEMC0895161	SEMC0895172	SEMC0895192
SEMC0895150	SEMC0895162	SEMC0895173	SEMC0895193
SEMC0895151	SEMC0895163	SEMC0895175	SEMC0895194
SEMC0895152	SEMC0895165	SEMC0895177	SEMC0895196
SEMC0895153	SEMC0895166	SEMC0895181	SEMC0895197
SEMC0895154			

panded, antennomeres IV–X short and broad, lobe at anterodorsal angle, antennomere XI elongate, apically pointed. Pronotum short, lateral margins short, slightly curved with narrow bead, bead wider medially, slightly angulate medially; surface shiny, nearly impunctate medially, more but sparsely punctate along anterior and posterior margins, punctation variable, fine to course. Elytron moderately broad, laterally broadly curved; surface shiny, more coarsely and evenly punctate than pronotum, punctation shallow and indistinct, of variable sizes. Prosternum extremely short, longitudinally compressed, medially slightly carinate; prosternal process slender anteriorly, with distinctive, small medial tubercle, apically short and broad, concave, apically broadly pointed. Metaventrite broad and evenly smoothly convex medially, surface shiny, with very few indistinct punctures, anteromedially with curved transverse carina between posterior margins of mesocoxal cavities; metaventrite wings extremely slender. Metacoxa with medial portion short, less than 1/2 length of metaventrite medially, metacoxal lines distinctly divergent anteriorly; lateral portion of metacoxa extremely large, anteriorly strongly expanded; surface shiny, evenly but shallowly and indistinctly punctate, punctures evenly distributed. Metatrochanter large, longer than ventral margin of metafemur anterior to metatrochanter apex; legs otherwise not noticeably modified. Abdomen with surfaces shiny and smooth, nearly impunctate.

Male genitalia. Male median lobe in lateral aspect irregularly shaped, apical portion slender, short, slightly curved dorsad, apically narrowly rounded (Fig. 7). Median lobe in ventral aspect very broad, basally U-shaped, apically deeply and broadly bifid, each ramus slender, apically narrowly rounded, gently curved, and convergent medially at apices (Fig. 8). Lateral lobe in ventral aspect irregularly shaped, broad, with subapical articulable lobe slender, undulate, apically sharply pointed and elongate, extending well beyond apex of lateral lobe (Fig. 9). Lateral lobe in lateral aspect broad basally, apex slender, oblique, directed dorsad, subapical articulable process slender, elongate curved and sharply pointed (Fig. 10).

Etymology. This species is named *mortimer*, after Colonel Douglas Mortimer, the older bounty hunter in the film "For a Few Dollars More".

Distribution. This species is known only from one locality in Costa Rica, Prov. Cartago (Fig. 58).

Habitat. The only known habitat information is the type series collected in a “pasture.”

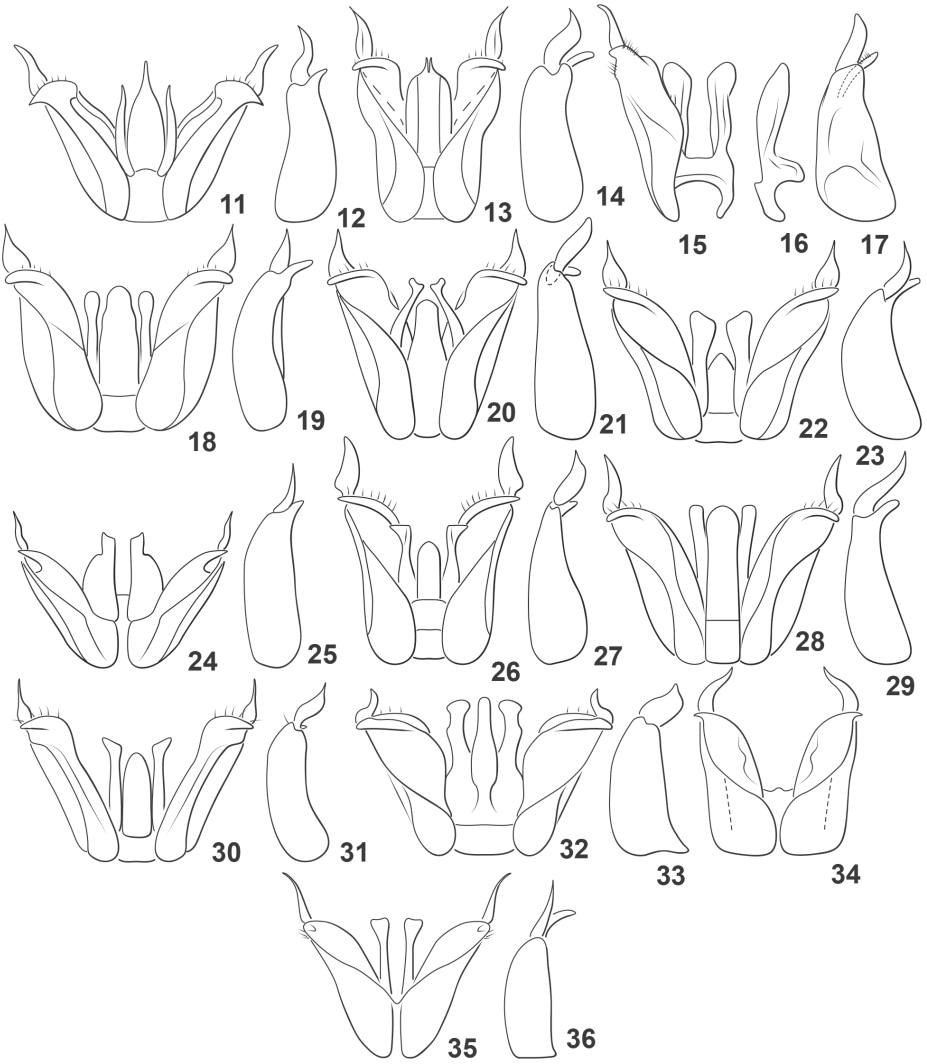

Figures 11–36. *Desmopachria* species, male genitalia. **11, 12** *D. aspera* **11** dorsal aspect **12** right lateral lobe, right lateral aspect **13, 14** *D. cenchramis* **13** dorsal aspect **14** right lateral lobe, right lateral aspect **15–17** *D. challeti* **15** median lobe and right lateral lobe, dorsal aspect **16** median lobe, right lateral aspect **17** right lateral lobe, right lateral aspect **18, 19** *D. ciruclaris* **18** dorsal aspect **19** right lateral lobe, right lateral aspect **20, 21** *D. aspera* **20** dorsal aspect **21** right lateral lobe, right lateral aspect **22, 23** *D. defloccata* **22** dorsal aspect **23** right lateral lobe, right lateral aspect **24, 25** *D. glabella* **24** dorsal aspect **25** right lateral lobe, right lateral aspect **26, 27** *D. grana* **26** dorsal aspect **27** right lateral lobe, right lateral aspect **28, 29** *D. isthmia* **28** dorsal aspect **29** right lateral lobe, right lateral aspect **30, 31** *D. laesslei* **30** dorsal aspect **31** right lateral lobe, right lateral aspect **32, 33** *D. lewisi* **32** dorsal aspect **33** right lateral lobe, right lateral aspect **34** *D. majuscula*, dorsal aspect **35, 36** *D. tarda* **35** dorsal aspect **36** right lateral lobe, right lateral aspect. Redrawn from Young (1981).

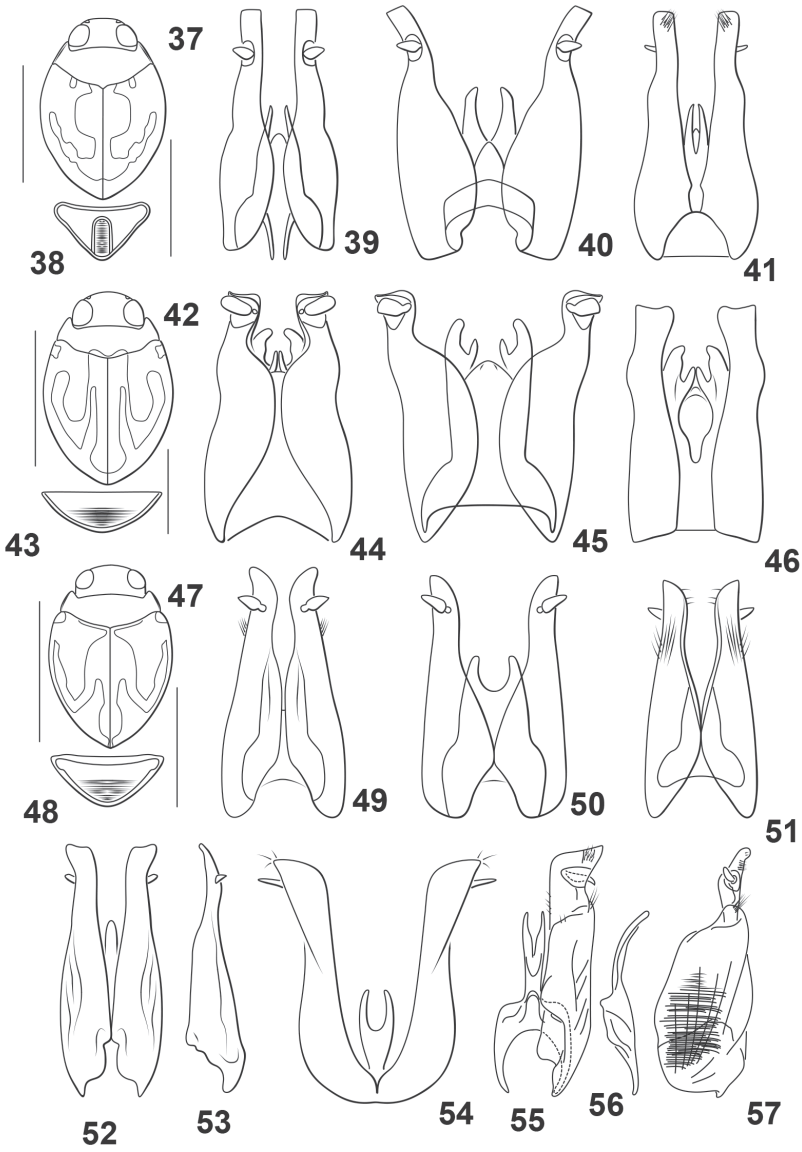

Figures 37–57. *Desmopachria* species. **37–41** *D. cavia* **37** habitus **38** last abdominal ventrite **39–41** male genitalia **39** male genitalia, dorsal aspect **40** male genitalia, ventral aspect **41** male genitalia, dorsal aspect with coverslip **42–46** *D. manus* **42** habitus **43** last abdominal ventrite **44–46** male genitalia **44** male genitalia, dorsal aspect **45** male genitalia, ventral aspect **46** male genitalia, dorsal aspect with coverslip **47–51** *D. varzeana* **47** habitus **48** last abdominal ventrite **49–51** male genitalia **49** male genitalia, dorsal aspect **50** male genitalia, ventral aspect **51** male genitalia, dorsal aspect with coverslip **52, 53** *D. pilosa*, male genitalia **52** dorsal aspect **53** right lateral aspect **54** *D. signata*, male genitalia, dorsal aspect **55–57** *D. signatoides*, male genitalia **55** median lobe and left lateral lobe, dorsal aspect **56** median lobe, right lateral aspect **57** right lateral lobe, right lateral aspect. **37–51** Redrawn from Braga and Ferreira-Jr. (2010) **52, 53** redrawn from Miller (2005) **54** redrawn from Young (1990) **55–57** redrawn from Miller (2001). Scale bars: 1.0 mm (**37, 42, 47**); 0.5 mm for (**38, 43, 48**).

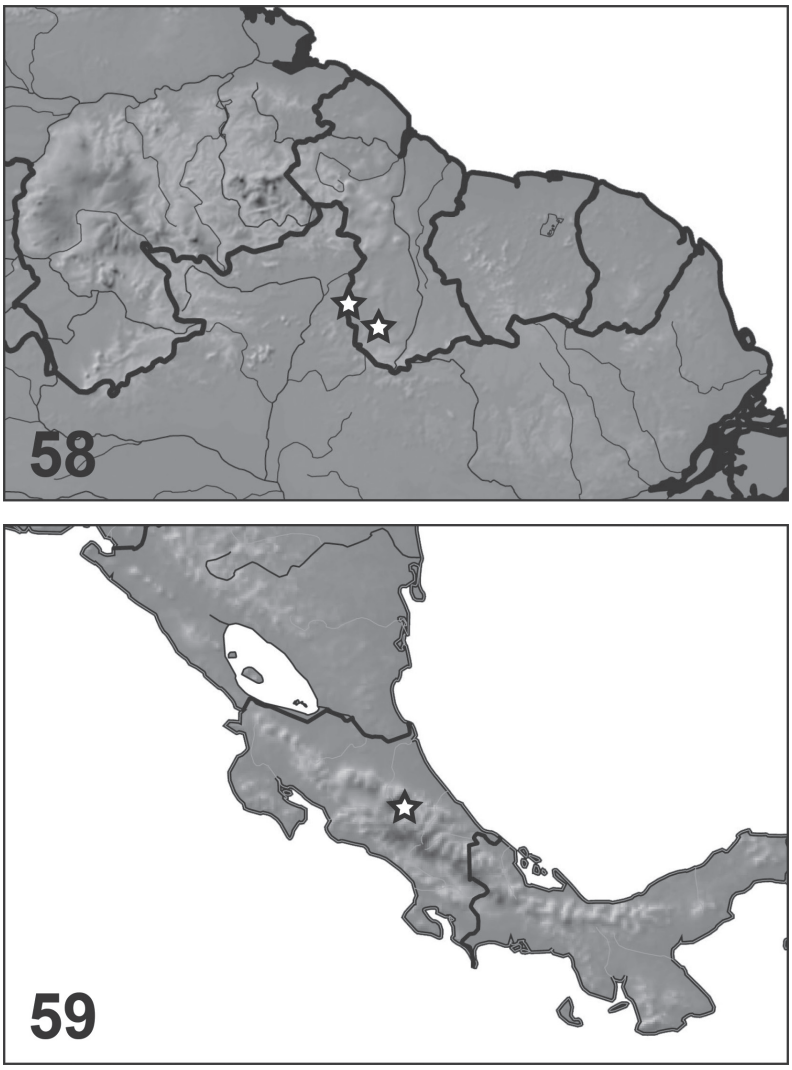

Figures 58, 59. *Desmopachria* new species, distribution. **58** *D. manco* (South America). **59** *D. mortimer* (Central America).

Checklist of *Desmopachria* species in the *D. convexa* group

Desmopachria convexa-convexa species group

D. aspera Young, 1981 (Florida, USA) (Figs 11, 12)
D. cenchramis Young, 1981 (Florida, USA) (Figs 13, 14)
D. challeti Miller, 2001 (Colombia) (Figs 15–17)
D. circularis Sharp, 1882 (Guatemala) (Figs 18,19)
D. convexa (Aubé, 1838) (USA) (Figs 20, 21)

D. defloccata Young, 1981 (Mexico) (Figs 22, 23)
D. glabella Young, 1981 (Cuba) (Figs 24, 25)
D. grana (LeConte, 1855) (USA) (Figs 26, 27)
D. isthmia Young, 1981 (Panama) (Figs 28, 29)
D. laesslei Young, 1981 (Jamaica) (Figs 30, 31)
D. lewisi Young, 1981 (Jamaica) (Figs 32, 33)
D. majuscula Young, 1990 (Guatemala) (Fig. 34)
D. mortimer sp. nov. (Costa Rica) (Figs 6–10)
D. tarda Spangler, 1973 (Cuba) (Figs 35, 36)

***Desmopachria convexa-signata* species group**

D. cavia Braga & Ferreira Jr., 2010 (Brazil) (Figs 37–41)
D. manco sp. nov. (Guyana) (Figs 1–5)
D. manus Braga & Ferreira Jr., 2010 (Brazil) (Figs 42–46)
D. pilosa Miller, 2005 (Peru) (Figs 52, 53)
D. signata Zimmermann, 1921 (Brazil) (Fig. 54)
D. signatoides Miller, 2001 (Bolivia) (Figs 55–57)
D. varzeana Braga & Ferreira Jr., 2010 (Brazil) (Figs 48–51)

Acknowledgements

Thanks to A.E.Z. Short for access to specimens in the University of Kansas Natural History Museum. Portions of this work were funded by the following grants: NSF #DEB–0816904, #DEB–0845984, and #DEB–1353426.

References

Braga RB, Ferreira Jr N (2010) Four new species of *Desmopachria* Babington (Insecta, Coleoptera, Dytiscidae) from the Amazon river floodplain. Zootaxa 2415: 33–42. https://doi.org/10.11646/zootaxa.2415.1.3

Braga RB, Ferreira Jr N (2011) Two new species of *Desmopachria* Babington, 1841 (Coleoptera: Dytiscidae) from Brazil. Aquatic Insects 33: 127–131. https://doi.org/10.1080/01650424.2011.597561

Braga RB, FerreiraJr N (2014) Carnivorous diving beetles of the genus *Desmopachria* (Coleoptera: Dytiscidae) from Brazil: New species, new records, and a checklist. Journal of Insect Science (Tucson) 14: 1–26. https://doi.org/10.1093/jis/14.1.55

Braga RB, Ferreira Jr N (2018) Six new species and new records of the genus *Desmopachria* Babington (Coleoptera: Dytiscidae: Hyphidrini) from Brazil and redescription of *D. varians* Wehncke, 1877. Papéis Avulsos de Zoologia 58: e20185841. https://doi.org/10.11606/1807-0205/2018.58.41

Gustafson G, Miller KB (2012) A new species of *Desmopachria* Babington from Venezuela (Coleoptera: Dytiscidae: Hydroporinae). Koleopterologische Rundschau 82: 71–76.

Makhan D (2012) Four new species of *Desmopachria* (Coleoptera: Dytiscidae) from Suriname. Calodema 235: 1–6.

Makhan D (2015) *Desmopachria barackobamai* sp. nov., a new species of waterbeetle from French Guiana (Coleoptera: Dytiscidae). Calodema 361: 1–2. https://www.researchgate.net/profile/Dewanand_Makhan/publication/312612400_Desmopachria_barackobamai_sp_nov_a_new_species_of_waterbeetle_from_French_Guiana_Coleoptera_Dytiscidae/links/58867681a6fdcc6b791938c2/Desmopachria-barackobamai-sp-nov-a-new-species-of-waterbeetle-from-French-Guiana-Coleoptera-Dytiscidae.pdf

Megna YS, Sanchez-Fernandez D (2014) A new species of *Desmopachria* Babington (Coleoptera: Dytiscidae) from Cuba with a prediction of its geographic distribution and notes on other Cuban species of the genus. Zootaxa 3753: 585–596. https://doi.org/10.11646/zootaxa.3753.6.5

Miller KB (1999) Description of eight new species of *Desmopachria* Babington (Coleoptera: Dytiscidae) from Bolivia. Entomologica Scandinavica 30: 349–359. https://doi.org/10.1163/187631200X00165

Miller KB (2001) Descriptions of new species of *Desmopachria* Babington, 1841 (Coleoptera: Dytiscidae: Hydroporinae: Hyphydrini) with a reassessment of the subgenera and species groups and a synopsis of the species. The Coleopterists Bulletin 55: 219–240. https://doi.org/10.1649/0010-065X(2001)055[0219:DONSOD]2.0.CO;2

Miller KB (2005) Four new species of *Desmopachria* Babington from Peru (Coleoptera: Dytiscidae). Zootaxa 1059: 39–47. https://doi.org/10.11646/zootaxa.1059.1.3

Miller KB, Wolfe GW (2018) Nine New Species in the *Desmopachria nitida* Species-Group of the Neotropical Genus *Desmopachria* Babington, 1841 (Coleoptera: Adephaga: Dytiscidae: Hydroporinae: Hyphydrini). The Coleopterists Bulletin 72: 97–112. https://doi.org/10.1649/0010-065X-72.1.97

Miller KB, Wolfe GW (2019) Three new species in the *Desmopachria striola* species group of *Desmopachria* Babington, 1841 (Coleoptera: Adephaga: Dytiscidae: Hydroporinae: Hyphydrini). The Coleopterists Bulletin 73: 621–628. https://doi.org/10.1649/0010-065X-73.3.621

Young FN (1980) Predaceous water beetles of the genus *Desmopachria* Babington: the subgenera with descriptions of new taxa (Coleoptera: Dytiscidae). Revista de Biologia Tropical 28: 305–321.

Young FN (1981) Predaceous water beetles of the genus *Desmopachria* Babington: the *convexa-grana* group (Coleoptera: Dytiscidae). Occasional Papers of the Florida State Collection of Arthropods 2: 1–9.

Young FN (1990) New Neotropical species of *Desmopachria* (*Desmopachria* s. str.) Babington (Coleoptera: Dytiscidae). Insecta Mundi 4: 1–4.

ZooKeys 923: 79–90 (2020)
doi: 10.3897/zookeys.923.48290
http://zookeys.pensoft.net

RESEARCH ARTICLE

A peer-reviewed open-access journal
ZooKeys
Launched to accelerate biodiversity research

A new *Stamnodes* from the southwestern United States (Lepidoptera, Geometridae, Larentiinae)

Tanner A. Matson[1], David L. Wagner[1]

1 *Department of Ecology and Evolutionary Biology, University of Connecticut, Storrs, Connecticut 06269–3043, USA*

Corresponding author: Tanner Matson (tanner.matson@uconn.edu)

Academic editor: Axel Hausmann | Received 8 November 2019 | Accepted 15 February 2020 | Published 1 April 2020

http://zoobank.org/7242B753-872E-419E-AA90-B5298FA11B94

Citation: Matson TA, Wagner DL (2020) A new *Stamnodes* from the southwestern United States (Lepidoptera, Geometridae, Larentiinae). ZooKeys 923: 79–90. https://doi.org/10.3897/zookeys.923.48290

Abstract

Stamnodes fergusoni **sp. nov.** occurs from extreme southeastern Arizona through southern New Mexico east into western Texas, USA. Identity of the new species can be reliably determined by external features, genitalic characters, and COI haplotypes. Larvae are believed to be specialists on *Salvia pinguifolia* and *S. ballotiflora*. The adult and larval stages and male and female genitalia are illustrated, available DNA barcode data that support the recognition of the new *Stamnodes* are reviewed, and its life history briefly characterized.

Keywords

COI, DNA barcodes, Lamiaceae, *Salvia*, shrubby blue sage, Stamnodini

Introduction

Stamnodes Guenée is one of the most handsome, species-rich, and taxonomically problematic genera of North American Geometridae. Several species remain undescribed and much disagreement surrounds the validity of many recognized species and their current synonymies. The description of *Stamnodes fergusoni* is long overdue; for nearly three decades this species has been known by moth collectors and photographers of west Texas as undescribed (Knudson and Bordelon 2002, Ed Knudson pers. comm. (recently deceased)) and is identified in on-line identification resources (e.g., iNaturalist

and BugGuide) as a new taxon. Douglas Ferguson, the former curator of the Geometridae at the USDA-United States Natural History Museum (USNM), had initiated a manuscript describing the species, but died before he could complete the work.

Here we describe *Stamnodes fergusoni* from southwestern Texas's hill country, westward through New Mexico into extreme southeastern Arizona. The new taxon is believed to be a specialist on woody mints, feeding on *Salvia pinguifolia* (Lamiaceae) in New Mexico and Arizona and presumably on *Salvia ballotiflora* (Lamiaceae) over the core of its range in southwest Texas. We describe and illustrate the larval and adult stages of the new species, illustrate the male and female genitalia, give diagnostic differences that separate this taxon from two phenotypically similar North American congeners: *Stamnodes fervefactaria* (Grote, 1881) and *Stamnodes deceptiva* (Barnes and McDunnough, 1917), and provide a brief account of its biology and distribution.

Materials and methods

Adults were obtained by light trapping with UV and mercury-vapor lights. Larvae were collected from *Salvia pinguifolia* (Lamiaceae) near Carrizozo, New Mexico and Warren, Arizona. The holotype was collected by Jim Vargo in Val Verde Co., TX. The adult description of *S. fergusoni* is based on 74 pinned specimens and 15 additional photographic records; the larval description is based on five larvae (DLW Lot: 2018J32, 2018J35, and 2018J133). 139 genitalic slides of *Stamnodes* were examined: 73 examined from the National Museum of Natural History (USNM), 63 on loan from the Canadian National Collection (CNC), and one slide prepared by TAM for this study. Two slides of *S. fergusoni*, four slides of *S. deceptiva,* and four slides of *S. fervefactaria* were examined. Doug Ferguson's unfinished manuscript describing the new moth was made available by Dr. Alma Solis. In both the *Diagnosis* and *Description,* we sometimes reproduce Doug's original text for genitalic characters; Ferguson's text was both concise and accurate and we could not do better.

Over the course of this study we examined the Nearctic *Stamnodes* holdings (including primary types) of the American Museum of Natural History (**AMNH**) (New York City, NY), Harvard University (**MCZ**) (Cambridge, MA), McGuire Center for Lepidoptera and Biodiversity (**MGCL**) (University of Florida, Gainesville, FL); National Museum of Natural History (**NMNH**) (Washington DC); University of Connecticut (**UCMS**) (Storrs, CT); as well as specimens gifted to us by Edward C. Knudson. We had access to 457 Stamnodini COI barcode submissions: for each of these, we examined the associated voucher specimen or image (when available). 378 of the 457 COI barcodes were used (failed sequences excluded) to generate a neighbor-joining tree, using the default Kimura-2P model in the Barcode of Life Project (BOLD) (http://www.boldsystems.org) (Ratnasingham and Hebert 2007). DNA extraction, PCR amplification, and COI barcode sequencing were performed at the Canadian Centre for DNA Barcoding (Centre for Biodiversity Genomics–University of Guelph)

using their standard Sanger sequencing protocols (Wilson 2012). SimpleMappr (www.simplemappr.net) was used to generate the geographic distribution point map (Shorthouse 2010). Type material has been deposited in the USNM, AMNH, UCMS, TAMUIC, and KSU-MEPAR collections.

Taxonomy

***Stamnodes fergusoni* sp. nov.**
http://zoobank.org/ABACB3A5-E374-4ABE-863F-0C46F73E8A61
Figures 1, 4, 7, 10, 13, 14, 15

Diagnosis. *Stamnodes fergusoni* can be immediately separated from most *Stamnodes* by its orange ground color and pattern of lead-gray patches across the forewing and hindwing. North of Mexico, *Stamnodes fergusoni* may only be confused with *Stamnodes deceptiva* or *Stamnodes fervefactaria*, neither of these species occur in southwest Texas. Although superficially close (and sometimes confused in collections), *S. fergusoni* can be quickly distinguished from the other two species. *Stamnodes fergusoni* can be reliably determined by the bright, white reticulate pattern of the underside of the hindwing and costal area of the forewing (Fig. 1b). In the other two species, the reticulate pattern of fore- and hindwing is cream to dull orange in color (Figs 2b, 3b). The frons of *S. fergusoni* is immediately diagnostic: the dorsal scarlet scales and ventral white scales are separated by a band of black scales (Fig. 4). *Stamnodes fergusoni* also differs from *S. deceptiva* and *S. fervefactaria* by its slightly larger size, lighter orange ground color, brighter scarlet scales at forewing base, and mostly scarlet tegula (Fig. 1).

Male genitalia (Fig. 7) are generally similar to those of *S. deceptiva* except for the following differences: (1) The costal sclerite is fully integrated into the valve and lacks the protruding thumb-like free end of *S. deceptiva*. (2) A prominent hair tuft arising from the low tubercle on the inner face of valve is approximately as long as the uncus or as long as the distance from its place of attachment to the end of the valve in *S. fergusoni*, but only half that length in *S. deceptiva*. (3) The juxta has a posterolateral pair of long, acuminate-conical processes that are lacking in *S. deceptiva*. (4) The vesica has ca. 30 large cornuti and many small cornuti clustered in one large group in *S. fergusoni*; there are two or three large and three or four small cornuti in one group, and many very small ones in another widely separate group in *S. deceptiva*. The male genitalia of *S. fervefactaria* are most similar to those of *S. deceptiva* except that the costal sclerite of the valve does not have a thumb-like free end and is nearly straight, not S-shaped as in *S. deceptiva*; the hair tuft on the valve reaches the end of the costal sclerite (but only half that distance in *S. deceptiva*); and the vesica has only small, poorly developed cornuti (Figs 8, 9). Female genitalia (Fig. 10) are similar to those of *S. deceptiva* and *S. fervefactaria* except for the following differences: (1) The bursa copulatrix has two widely separated signa, the one nearer to the ductus bursae is centered in a large sclerotized area and bears a single thorn-like process inwardly (on interior surface of

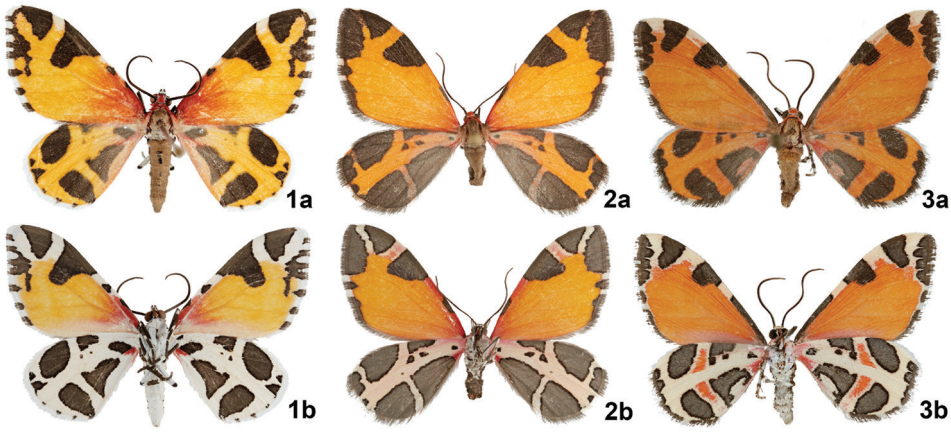

Figures 1–3. Adult *Stamnodes*. **1** *Stamnodes fergusoni* [HOLOTYPE], TX: Val Verde Co., Ranch Road 189 (30.1823°, -100.06°), 19 September 2018, J. Vargo coll., **a** dorsal view, **b** ventral view; **2** *Stamnodes fervefactaria*, Colorado: El Paso Co., ssw of Colorado Springs Hwy. #115 at mkr. #30.2 Los Pinos housing entry [38.5797, -104.9308], 6480ft, 14 August 2004, Chuck Harp coll., BOLD Process ID: LNAUW1876-17, Museum ID: USNM ENT 01343267, **a** dorsal view, **b** ventral view; **3** *Stamnodes deceptiva,* AZ: Cochise Co., Ash Canyon Rd Huachuca Mts., 5100ft, 3 August 1999, Douglas C. Ferguson coll., BOLD Process ID: LNAUS1646-13, Museum ID: USNM ENT 00808502 **a** dorsal view, **b** ventral view.

Figures 4–6. Frontal view of head for *Stamnodes fergusoni* and related species. **4** *Stamnodes fergusoni*; **5** *Stamnodes fervefactaria*; **6** *Stamnodes deceptiva*.

bursa copulatrix); the other signa lacks a process; *Stamnodes deceptiva* has only a single nipple-like signum. (2) The ostium bursae is marked by a relatively large, strongly sclerotized, elongate, subtriangular plate (rounded anteriorly, slightly emarginate posteriorly). (3) Overall, the genitalia are ca. 1.5 × larger than those of *S. deceptiva* and *S. fervefactaria* (Figs 11, 12). The small sclerotized regions forming the bases of the signa of all species are usually depressed externally and convex internally, with or without an inner process. The signa of *S. fervefactaria* are reduced.

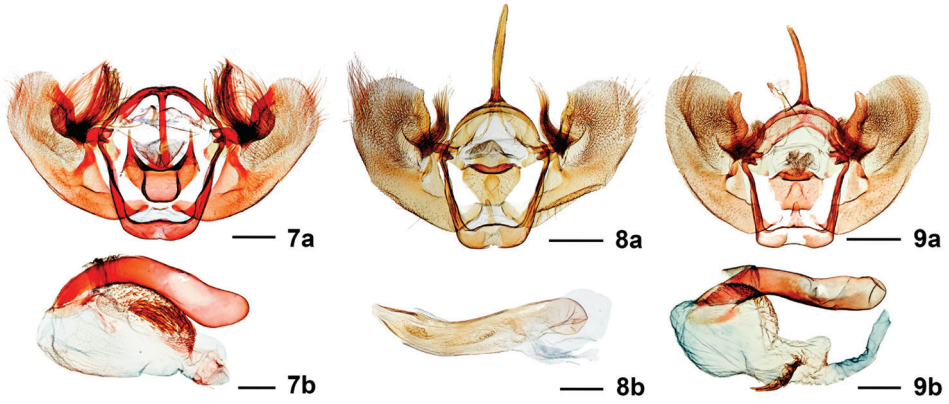

Figures 7–9. Male genitalia. **7** *Stamnodes fergusoni* (USNM58902), **a** genital capsule, **b** aedeagus with everted vesica; **8** *Stamnodes fervefactaria* (USNM55242), **a** genital capsule, **b** aedeagus; **9** *Stamnodes deceptiva* (USNM58903), **a** genital capsule, **b** aedeagus with everted vesica. Scale bars: 0.85 mm (**9a**), 0.25 mm (**9b**).

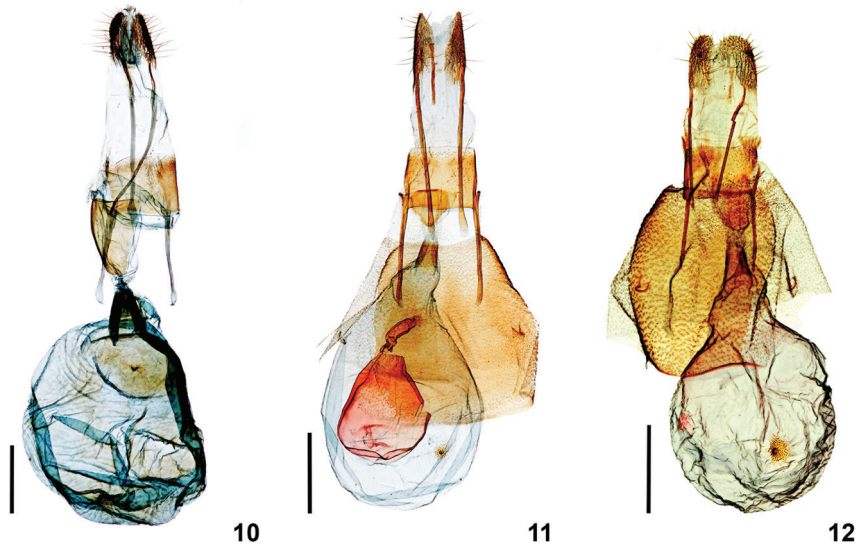

Figures 10–12. Female genitalia. **10** *Stamnodes fergusoni* (TAM-2019-001); **11** *Stamnodes fervefactaria* (USNM55243); **12** *Stamnodes deceptiva* (USNM59079). Scale bar: 1 mm.

Description. ***Adult male.*** Forewing length: 14–16mm (Fig. 1) (N = 74). **Head.** Vertex scarlet, sometimes with scattered snow-white scales near base of antenna and collar; frons with dorsal scarlet and ventral white scales separated by thin transverse band of black scales; laterad black scales continued ventrad into white scaling; white scales along dorsal margin of eye. Labial palpus subequal to diameter of eye, short and slightly porrect, with exceedingly long black scales (especially near base) and sparse white intersegmental scales. Antenna filiform, laterally compressed, 0.5 length of fore-

wing; scape mostly black, typically with small dorsal patch of white scales and several scattered white basal scales; flagellum fuscous with dorsal scales only, lateral and ventral sides bearing abundant microsetae. Collar scarlet with inconspicuous posterior white scales. Lateral patches of gray piliform scales between vertex and collar. **Thorax.** Mesoscutum predominantly light gray dorsally, generally trending from anterior dark gray (except white under patagium) to posterior cream-white, several individuals showing modest pink tone; ventrally bright white. Patagium scarlet; tegula mostly scarlet, basally black, and transitioning to pale, pink piliform scales posteriorly. Legs banded with fuscous and white; tibial spur formula 0–2–4. Coxae snow white. **Forewing.** Scarlet near base, diffusing to light orange near antemedial area (orange ground color paler than that of *S. deceptiva* and *S. fervefactaria*). Costal margin with several lead-gray patches; two small patches near base and antemedial area hugging costal margin (same patches continuous in *S. deceptiva*, and either singular or missing in *S. fervefactaria*); large trigonate to subquadranglar patch near postmedial area terminating near M_3; apical patch more or less trigonate and highly variable, extending along outer margin before terminating prior to tornus, often divided by lobe or ray of orange ground color that extends toward apex. Fringe checkered, alternating white and lead-gray. Underside patterned like upperside. Scarlet base more vibrant on costa; costal and apical areas between lead-gray patches given much more to white than on upperside; checkered fringe pattern often extending into terminal area especially near apex. **Hindwing.** Reticulate light-orange ground color between variable patches and spots of lead-gray (more dissected than *S. fervefactaria*). Inner margin basally scarlet, quickly transitioning to admixture of fuscous, light orange, and scarlet. Approximately five ill-defined lead-gray patches (clockwise from wing base): small, basal oblong patch; small, often broken, costal, triangular antemedial patch; larger, ovate postmedial patch; ovate patch at anal angle, subequal to previous; and large, irregularly triangular patch that runs along inner margin. Often with irregular lead-gray subterminal line that expands into subapical patch, connecting dark areas in fringe. Fringe checkered, lead-gray scaling reduced to almost absent in some specimens. Underside like upperside, except light-orange ground color replaced by bright white, lead-gray patches finely outlined by dark gray, basal lead-gray patch often with small scarlet spot basad. **Abdomen.** Dorsum fuscous, venter pale gray; small black spiracular spots. **Male genitalia** (Fig. 7) ($N = 2$) Uncus long and narrow, tapering slightly at apex. Valva broadly ovate, ca. 2 × longer than wide, outwardly convex at middle of costal margin; broadly rounded at apex; prominent hair tuft arising from low tubercle on inner face of valve approximately as long as uncus or as long as distance from its place of attachment to end of valve. Juxta U-shaped, with posterolateral pair of long, acuminate-conical processes. Aedeagus cylindrical, exceeding length of valva; base broadly rounded; apex with broad concave aperture; vesica with ca. 30 large spinose cornuti surrounded by many smaller spinose cornuti in dense cluster.

Female. Forewing length: 16–17mm ($N = 9$). Outwardly undifferentiated from male. **Female genitalia** (Fig. 10) ($N = 1$). Papillae anales broadly pointed and unfused posteriorly. Posterior apophysis fused with papillae anales anteriorly, long and extend-

ing to intersegment of A9 of A10; anterior apophysis one-half the length of posterior apophysis. Ostium bursae with large, ventral, strongly sclerotized, elongate, subtriangular plate (rounded anteriorly, slightly emarginate posteriorly). Ductus bursae short, sclerotized laterally, subtriangular and opening broadly into corpus bursae. Corpus bursae spheroid with two widely separated signa; signum nearer ductus bursae centered in large sclerotized area and bearing a single thorn-like process directed inward on interior surface; anterior signum without such a process and with rugose areole.

Description of living final instar (Figs 13, 14). Coloration variable, dorsum ranging from green to lavender or mixture of both; venter yellow-green to lime-green, darker than dorsum in green forms. In cross section, venter shallowly hemispherical below white lateral stripe, appearing somewhat flattened. Upper side of white subspiracular stripe diffuse, enveloping spiracles; ventral margin more defined. Primary setae, sharp, relatively long, roughly 2.5-3 × height of spiracle, many borne from black pinaculum positioned atop minute wart. Spiracles tan to pale orange with darker peritreme. Head with circular freckles mostly clustered into tight groups over each lobe and in each corner of frons; primary setae from black pinacula; stemma 3 ca. 1.5 × stemmata 2 and 6.

Description of preserved penultimate instar. Integument roughened and transversely furrowed. Extensively peppered with minute melanized patches which are most visible over each lobe of head and posterior abdominal segments (especially in cleared preparations). Prothoracic spiracle subequal to those on A1-A6 (~0.12 mm high); spiracle on A7 and A8 (~0.16 mm high). Planta of A6 with 20 or 21 secondary setae below level of SV seta, bearing 25 or 26 crochets mostly of two alternating lengths.

Type material examined. ***Holotype male***, TX: Val Verde Co., Ranch Road 189 (30.1823°, -100.06°), Elev. 1676', 19 September 2018, Jim Vargo coll. dry pinned (USNM) (Fig. 1).

Paratype adults. (52♂, 18♀): NM: Lincoln Co., Valley of Fires Recreation Area (33.67977°, -105.92708°), 11 August 2014, Black light trap, Leg. J. Luig & J. Metlevski, Voucher Codes: (363203, 363204), (2♂) (KSU-MEPAR); NM: Lincoln Co., Valley of Fires Recreation Area (33.681795°, -105.923486°), 4–5 September 2015, At light, Leg. J. Metlevski, Voucher Codes: (363197, 363198), (2♂) (KSU-MEPAR); NM: Lincoln Co., Valley of Fires Recreation Area (33.678049°, -105.927135°), 4 September 2015, Mercury vapor light, Leg. J. Metlevski, Voucher Codes: (363193–363196), (4♀) (KSU-MEPAR, TAMUIC); NM: Lincoln Co., Valley of Fires Recreation Area (33.678167°, -105.927492°), 4 September 2015, Black light trap, Leg. J. Metlevski, Voucher Codes: (363199–363202, 367370–367375), (9♂, 1♀) (TAMUIC, USNM, AMNH); TX: Uvalde Co., Concan, 9 November 2015, Ed Knudson coll., (1♂) (UCMS); TX: Uvalde Co., Concan, 28 September 2013 – 1 October 2013, Ed Knudson & Charles Bordelon colls., (1♂, 1♀) (UCMS); TX: Edwards Co., 1.2 km NW Camp Wood [29.6822°, -99.9711°], 13 October 2017, Ann Hendrickson coll., (3♂) (UCMS); TX: Val Verde Co., Seminole Canyon State Park, 20 October 1985, John Rawlins coll., BOLD Process IDs: LNAUV1793-17, LNAUV450-16, Museum IDs: USNM ENT 01276376, 01237649, Genitalic Slide DCF1651, (1♂, 1♀) (USNM); TX: Val Verde Co., Ranch Road 189 (30.1823°, -100.06°), 19 September 2018, Jim

Vargo coll. (1♂, 1♀)(USNM); TX: Val Verde Co., (29.696°, -101.324°), 25 October 2014, Jim Vargo coll. (1♀)(TAMUIC); TX: Val Verde Co., Del Rio, 4 October 1994, Ed Knudson coll., (25♂, 7♀)(MGCL); TX: Uvalde Co., ConCan, 15 October 2001, G. Muise coll., (2♂, 1♀)(MGCL); TX: Uvalde Co., ConCan, 19 October 2000, Ed Knudson coll., (1♂)(MGCL); TX: El Paso Co., Franklin Mts., 17 September 1993, Ed Knudson coll., (3♂)(MGCL); TX: Val Verde Co., Dolan Falls Devil's River, 3–10 October 1994, J. Gillaspy coll., (1♀)(MGCL); TX: Kinney Co., Bracketville, 5 October 1994, Ed Knudson coll., (1♂)(MGCL).

Other material examined. ***Adults.*** TX: (County Unknown), Langley [Langtry], 25 October 1945, (collector unknown), BOLD Process ID: LNAUV1794-17, Museum ID: USNM ENT 01276377, Genitalic Slide USNM58902, (1♂) (USNM); TX: Val Verde Co., Seminole Canyon State Park, 20 October 1985, John Rawlins coll., (damaged by museum pests) (1♂) (USNM); TX: Culberson Co., Guadalupe Mountains National Park north McKittrick Canyon, 28 March 1968, Roy O. Kendall & C. A. Kendall coll., (1♂) (MGCL); NM: Catron Co., Gila National Forest, Forest rd. 94 (33.7181°, -108.4683°), 20 August 2015, Elev. 8200', Ron Parry coll. (from photograph). Additional internet photographic records (mapped in Figure 15) from iNaturalist (https://www.inaturalist.org/observations/): 18390285, 18339093, 9176399, 8832387, 8819801, 8813547, 8801663, 8795069, 8367680, 2360810. BugGuide observations (https://bugguide.net/node/view/): 1322692, 1493681, 1456212, 713503. ***Larvae.*** NM: Lincoln Co., Carrizozo lava flow, 16 September 2018, DLW Lot: 2018J32 & 2018J35, Tanner Matson & David Wagner coll., BOLD Process ID: WAGL1235-18, beaten from *Salvia pinguifolia* (*N* = 5) (UCMS); AZ: Cochise Co., Warren, 23 September 2018, DLW Lot: 2018J133, Tanner Matson, David Wagner, & Mimi Kamp coll., BOLD Process ID: WAGL1401-19, beaten from *Salvia pinguifolia* (*N* = 1) (UCMS).

Distribution. (Fig. 15) Southwest Hill Country (Uvalde, Kinney, Edwards, and Val Verde counties); Franklin Mountains (Franklin County); and Guadalupe Mountains (Culberson County) of Texas (Knudson and Bordelon 2002, and this paper). Carrizozo Malpais lava flow (Lincoln County), New Mexico (where it is abdundant); also Gila National Forest (Catron County), New Mexico (https://southwesternmoths.com). Mule Mountains (Cochise County) of extreme southeastern Arizona. Range into Mexico remains unclarified; we have examined several collections from the north Coahuilan hill country near Ciudad Acuña.

Etymology. The species is named in honor of the late Douglas C. Ferguson, a reigning and much respected authority on the geometrid fauna of North America for more than four decades. Dr. Ferguson's notes, dissections, and collections were valuable assets that guided this effort. Dr. Ferguson was in the process of describing this species before his passing (Knudson and Bordelon 2002) (pers. comm. Charles Covell; Alma Solis).

Biology. The larvae are believed to be specialists on woody *Salvia* (Lamiaceae). *Stamnodes fergusoni* larvae were collected and reared to maturity on *Salvia pinguifolia*

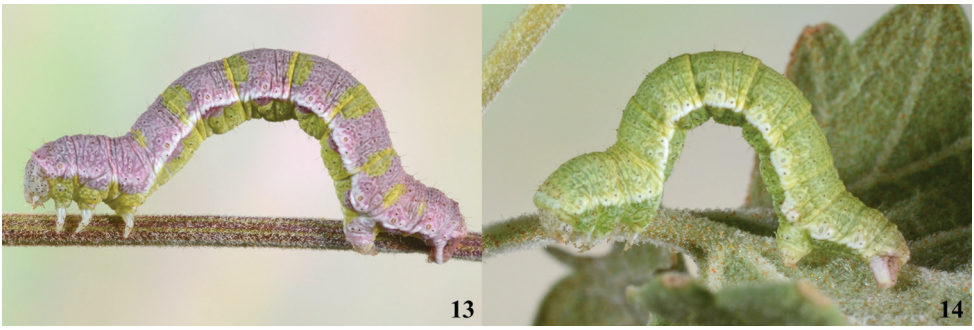

Figure 13–14. Larvae of *Stamnodes fergusoni* on *Salvia pinguifolia*; NM: Lincoln Co., Carrizozo lava flow, DLW Lot: 2018J32, COI Barcode DLW-001425. **13** last instar; **14** penultimate instar.

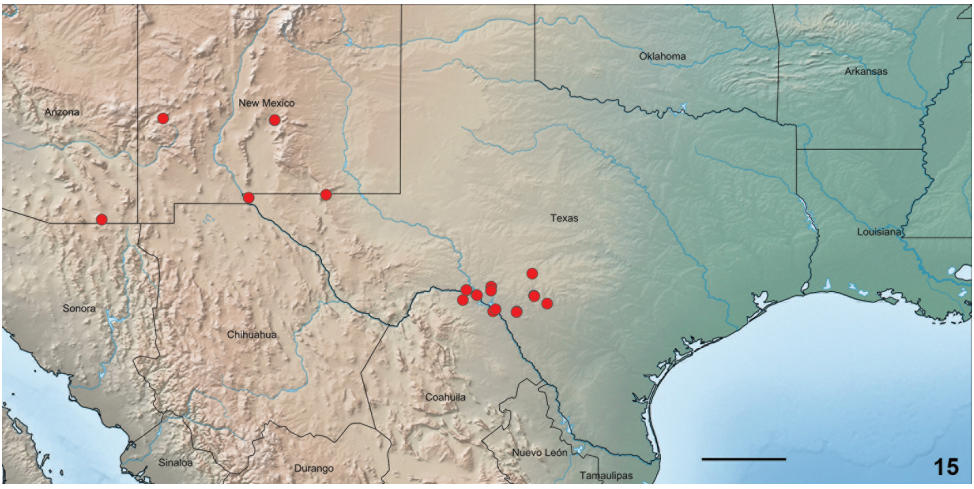

Figure 15. Distribution of *Stamnodes fergusoni* (*N* = 90, red). Single dots may represent > 1 individual. Scale bar: 200 km.

(rock sage) from Carrizozo Malpais, New Mexico (BOLD Process ID: WAGL1235-18, BOLD Sample ID: DLW-001425). A middle instar larva was collected from *Salvia pinguifolia* in Warren, Arizona (BOLD Process ID: WAGL1401-19, BOLD Sample ID: DLW-001401). In the Southwestern Hill Country of Texas, the species is believed to feed on *Salvia ballotiflora* (shrubby blue sage) as this is the only woody *Salvia* at the localities where this species has been taken.

The larvae of *S. fergusoni* were first discovered on *Salvia pinguifolia* plants growing at the bottom of large gas bubbles that formed during the deposition of the Carrizozo Malpais lava field, west of Carrizozo, New Mexico. When the top of a bubble erodes away, the remaining volcanic pit acts as a catch basin for rain and dust, and over time comes to support diverse gardens in an otherwise black ultraxeric landscape. Larvae were found on plants growing within these bubbles, especially where overhanging

lava shelves shield plants from full sun. Smaller, water-stressed plants growing in full sun yielded no *S. fergusoni* larvae. The purple pigments in the caterpillar appear to be derived from the flowers of its host (Fig. 13). In the laboratory, caterpillars were observed with their bodies deeply inserted into the calyx of individual flowers, feeding on reproductive tissues and callow seeds. The caterpillars of *S. deceptiva* and *S. fervefactaria* are so far unknown; we suspect they are using other Lamiaceae.

Stamnodes fergusoni has a single late-summer generation that appears to be tied to the flowering time of its preferred host. The moth is locally common in New Mexico and southwestern Hill Country of Texas with peak adult activity in September and October. Adults fly earlier (first weeks of September) in New Mexico. Several worn individuals were taken in March (2002) from the Guadalupe Mountains, by Roy Kendall. Knudson and Bordelon (2002) believed this collection represented overwintering adults. Mature larvae pupate in leaf litter or over soil. Over most of the species' range, the pupa is believed to overwinter and remain in diapause until the following fall.

Discussion

In June of this year, while working at the USNM, TAM had the pleasure to share desk space with Charles Covell. Charlie informed TAM about a new *Stamnodes* species collected by Ed Knudson in west Texas; the taxon was to be described by Doug Ferguson before his untimely passing. Charlie intended to publish Doug's nearly complete version of this description with the type series Doug had received from Ed Knudson (now at MGCL). Coincidently, our manuscript treating the same moth, spurred by the discovery of the moth's early stages, was nearing completion. With Dr. Covell's and Dr. Alma Solis's blessings, we utilize some of Doug's text in both our diagnosis and genitalic description.

All larval collections are from *Salvia pinguifolia*, a plant that does not occur in southwestern Texas where *Stamnodes fergusoni* is locally common. The woody mint in this region is instead, *Salvia ballotiflora* (shrubby blue sage), which is seemingly the only candidate host for *Stamnodes fergusoni*. In conversations with DLW, Ed Knudson had mentioned that the moth was most commonly encountered in the Tamaulipan scrub associations of Val Verde County, Texas. DLW went to areas described by Knudson in November 2018, and found *S. ballotiflora* to be common through the county, although the third week of November was too late to find larvae and verify that shrubby blue sage is the primary host for this moth in south Texas.

We had access to barcode data for 457 *Stamnodes* and *Stamnoctenis* Warren specimens representing approximately 63 species-level taxa (bins), 378 of the 457 were used (failed sequences excluded). Surprisingly, barcode data placed *S. fergusoni* well outside of a sister relationship with *S. fervefactaria* and *S. deceptiva*, and offered no likely indication of its placement within *Stamnodes*. Uncorrected genetic divergence between the three taxa was greater than six percent for every relationship. Nuclear markers will be required to determine the placement of *S. fergusoni* within *Stamnodes*.

The most recent North American checklist of Lepidoptera (Ferguson, 1983), lists 34 valid species and numerous synonyms for *Stamnodes*. Much disagreement surrounds the validity of the currently recognized species and their synonymies. Online identification sites (e.g., iNaturalist) and genetic databases (e.g., GenBank and Barcodes of Life) are riddled with misapplied names and generic-level (only) identifications. Institutional collections and published literature also reflect considerable taxonomic confusion. Our field collections of larvae for more than a twenty western *Stamnodes* and *Stamnoctenis* species, reveal considerable intraspecific variability in larval phenotypes, a matter further complicated by considerable host overlap across the genus. Such being the case, larvae and associated life history data will be of limited help in sorting out the species-level entities across the genus. Until a modern revisionary treatment employing nuclear markers, genitalic study, and larvae and their attendant life histories can be completed, databases, collections, and on-line resources treating North American Stamnodini will remain plagued with misidentifications and taxonomic uncertainty.

Acknowledgements

We would like to thank the National Museum of Natural History, Smithsonian Institution for their generous contribution of genetic data. In particular, Dr. Scott E. Miller collected much of the DNA barcode data used in this study. We would like to thank Kansas State University's Museum of Entomological and Prairie Arthropod Research, specifically Jan Metlevski for collecting some of the type material, and Gregory Zolnerowich for arranging the loan of this material. Charlie Covell sent material from the McGuire Center for Lepidoptera and Biodiversity, provided Ferguson's unfinished manuscript, and much encouragement. David Wikle alerted us to the abundance of *Stamnodes fergusoni* at Carrizozo, New Mexico, and the likelihood that the hostplant, whatever it is, would be found at the bottom of the gas bubbles that had formed in the lava flow. Jim Vargo donated four type specimens including the holotype. Anne Hendrickson sent photographs, collected type material, and provided lodging for the authors. Dave and Tracy Barker also hosted the authors and sent photographs of adults from their home on the Devil's River in Texas. Mimi Kamp led us to stands of *Salvia pinguifolia* in Warren, AZ that yielded a caterpillar of the new species. A special thank you to the late Ed Knudson and Charles Bordelon (Texas Lepidoptera Survey) for their donation of many specimens and willingness to share their knowledge of Texas *Stamnodes* both with us and others. Jaan Viidalepp, Charlie Covell, and Axel Hausmann provided helpful suggestions that improved earlier versions of this manuscript. DLW is supported by USFS Co-op Agreement 14-CA-11420004-138 and an award from the Richard P. Garmany Fund (Hartford Foundation). TAM was supported by the University of Connecticut's Ecology and Evolutionary Biology Department's EEB Student Award and the Smithsonian Institution's Graduate Student Fellowship.

References

Barnes W, McDunnough JH (1917) Geometridae. Larentiinae. Contributions to the natural history of the Lepidoptera of North America. The Review Press (Decatur, Illinois) 4: 136–137.

Ferguson DC (1983) Geometridae. In: Hodges RW, Dominick T, Davis DR, Ferguson DC, Franclemont JG, Munroe EG, Powell JA (Eds) Check List of the Lepidoptera of America North of Mexico. EW Classey Ltd. & The Wedge Entomological Research Foundation, London, 88–107.

Grote AR (1881) Moths collected by Prof. Snow in New Mexico with list of Eudriini. Papilio 1: 177–178.

Knudson E, Bordelon C (2002) The Stamnodini (Geometridae: Larentiinae) of Texas. News of the Lepidopterists' Society 44: 7–8.

Ratnasingham S, Hebert PD (2007) BOLD: The Barcode of Life Data System (http://www.barcodinglife.org). Molecular Ecology Resources 7: 355–364. https://doi.org/10.1111/j.1471-8286.2007.01678.x

Shorthouse DP (2010) SimpleMappr, an online tool to produce publication-quality point maps. http://www.simplemappr.net [accessed on 29 August 2019]

Wilson JJ (2012) DNA barcodes for insects. In: Kress W, Erickson D (Eds) DNA Barcodes: Methods and Protocols. Totowa, New Jersey, 17–46. https://doi.org/10.1007/978-1-61779-591-6_3

Supplementary material 1

***Stamnodes fergusoni* collection records**

Authors: Tanner A. Matson, David L. Wagner

Data type: species data

Link: https://doi.org/10.3897/zookeys.923.48290.suppl1

ZooKeys 923: 91–113 (2020)
doi: 10.3897/zookeys.923.48420
http://zookeys.pensoft.net

RESEARCH ARTICLE

A peer-reviewed open-access journal
ZooKeys
Launched to accelerate biodiversity research

Diversity of the southern Africa *Lacustricola* Myers, 1924 and redescription of *Lacustricola johnstoni* (Günther, 1894) and *Lacustricola myaposae* (Boulenger, 1908) (Cyprinodontiformes, Procatopodidae)

Pedro H.N. Bragança[1], Ryan M. van Zeeventer[1], Roger Bills[1], Denis Tweddle[1], Albert Chakona[1,2]

1 *South African Institute for Aquatic Biodiversity, Private Bag 1015, Grahamstown, 6140, South Africa*
2 *Department of Ichthyology and Fisheries Science, Rhodes University, Grahamstown, South Africa*

Corresponding author: *Pedro H.N. Bragança* (pedrobra88@gmail.com)

Academic editor: *N. Bogutskaya* | Received 13 November 2019 | Accepted 20 January 2020 | Published 1 April 2020

http://zoobank.org/F138D1ED-8A51-4628-8829-9617AC5D3029

Citation: Bragança PHN, van Zeeventer RM, Bills R, Tweddle D, Chakona A (2020) Diversity of the southern Africa *Lacustricola* Myers, 1924 and redescription of *Lacustricola johnstoni* (Günther, 1894) and *Lacustricola myaposae* (Boulenger, 1908) (Cyprinodontiformes, Procatopodidae). ZooKeys 923: 91–113. https://doi.org/10.3897/zookeys.923.48420

Abstract

Through the analysis of a comprehensive database of COI sequences, with the sequencing of 48 specimens, a first insight into the genetic diversity, distribution and relationships between the southern Africa "*Lacustricola*" species is presented. Species from "*Lacustricola*" occur mainly in freshwater systems within the arid savanna, and are considered to be widely distributed in southern Africa, but most of them are data deficient taxa. Two species are redescribed, "*Lacustricola*" *johnstoni* (Günther, 1894) and "*Lacustricola*" *myaposae* (Boulenger, 1908), based on specimens collected at their respective type localities. Detailed osteological and life colouration information is presented for the first time. "*Lacustricola*" *johnstoni* was described from the Upper Shire River in Mangochi, Lake Malawi but is herein considered as widespread in the Okavango, Zambezi, southern Africa east coastal drainages and the Bangweulu in the Congo System. A sympatric similar species occurring in the Okavango is also identified. "*Lacustricola*" *myaposae* (Boulenger, 1908), was described from the Nseleni River in KwaZulu-Natal Province, South Africa and is herein considered to be endemic to the small coastal river drainages within this region. Lectotypes for both "*L.*" *johnstoni* and "*L.*" *myaposae* are designated. A new species from the Lualaba River in the Congo System, sister to "*L.*" *macrurus* is identified, and the deep bodied "*L.*" *jubbi* is considered sister taxon to a clade including "*L.*" *johnstoni* and "*L.*" *myaposae*.

Keywords
African lampeyes, diversity, DNA barcoding, fish, freshwater, taxonomy, topminnows

Introduction

The Procatopodidae comprises approximately 100 small oviparous killifishes distributed across the major African freshwater systems (Ghedotti 2000; Bragança and Costa 2019). Fishes of this family are popularly known as African lampeyes due to the presence of a characteristic iridescent reflective colouration in the dorsal region of the eye. Historically, a close relationship between the procatopodids, the Amazon miniature oviparous killifish species of *Fluviphylax* Whitley, 1965 and the American live-bearing poeciliids had been suggested based on morphological phylogenies (Parenti 1981; Costa 1996; Ghedotti 2000). Subsequent investigation of molecular data provided better insights into the relationships among the main clades of Cyprinodontiformes (Pollux et al. 2014; Pohl et al. 2015; Helmstetter et al. 2016; Reznick et al. 2017; Bragança et al. 2018; Bragança and Costa 2018). More recently, Bragança et al. (2018) provided a comprehensive molecular phylogeny of the Cyprinodontiformes based on sequences of one mitochondrial and five nuclear genes. Results from this study refuted monophyly of the family Poeciliidae, and the African lampeyes were assigned to the family Procatopodidae which is considered to be sister group of the Old World Aphaniidae and Valenciidae (Bragança et al. 2018). Findings from these aforementioned studies stimulated further interest in establishing the relationships among the African procatopodids.

Bragança and Costa (2019) published a more inclusive molecular time calibrated phylogenetic analysis directed to assess the internal relationships among the little known African lampeye genera, revealing the timing and diversification patterns among procatopodids and evidencing the paraphyly of some of its proposed genera. According to Bragança and Costa (2019), Procatopodidae split from Aphaniidae and Valenciidae as a consequence of the trans-Saharan sea retreat during the Late Eocene-Early Oligocene transition, and most clades diversified during the moist-wet climate stability period from the Late Oligocene/Early Miocene until the Middle Miocene. However, the extreme aridification and climatic instability seen in the Late Miocene and in the Pliocene-Pleistocene respectively, probably promoted diversification of one particular African lampeye clade in savannahs and arid environments. Within this clade there are the widely distributed "*Poropanchax*" *normani* (Ahl, 1928), and species belonging to *Micropanchax* Myers, 1924, *Poropanchax* Clausen, 1967, *Rhexipanchax* Huber, 1999 and the southern Africa "*Lacustricola*" Myers, 1924 species (Bragança and Costa 2019).

The genus *Lacustricola* was found to be polyphyletic, i.e. with two distinct and non-related species groups. The first group comprised all eastern Africa species including the type species of the genus, *L. pumilus* (Boulenger, 1906); and the second group comprises all southern Africa species (Bragança and Costa 2019). The southern Africa *Lacustricola* species were considered to be sister to *Micropanchax* and both these genera contain species that are currently considered to have broad distribution ranges across

the African savannah associated water systems (Bragança and Costa 2019). Ongoing critical evaluation integrating molecular, morphological and osteological data support the proposed split of *Lacustricola* (Bragança unpublished data). This work will result in the establishment of new generic names, but in the present study, *Lacustricola* refers to species belonging to the eastern Africa clade and "*Lacustricola*" to species from the southern Africa clade, following Bragança and Costa (2019).

The southern "*Lacustricola*" clade is much more diverse than the eastern clade. Species in the southern clade have broad distribution ranges across most river systems in southern Africa, from the Nseleni in the south through the Okavango, Cunene, Kwanza, Zambezi, coastal river drainages in Mozambique and tributaries of the Congo (Wildekamp et al. 1986; Skelton 2001). The deep bodied species previously placed in the genus *Hypsopanchax* Myers, 1924, such as *H. jubbi* Poll & Lambert, 1965, *H. jobaerti* Poll & Lamberti, 1965 and *H. stiassnyae* Van der Zee, Sonnenberg & Mbimbi Mayi Munene, 2015 were recently found to belong to the southern *Lacustricola* clade (Bragança and Costa 2019; Bragança unpublished data). There are three main subgroups within the southern clade. These are the "*L.*" *katangae* (Boulenger, 1912) group which is defined by a zigzag black mark along the lower portion of the flank, the "*L.*" *hutereaui* (Boulenger, 1913) group which is defined by the presence of barred dorsal, anal and caudal-fins and a conspicuous reticulate pattern on scale margins, and the "*L.*" *johnstoni* (Günther,1894) group which is defined by a slender body and lack of the aforementioned characters. All three subgroups have broadly similar distribution patterns, with some species occurring sympatrically.

The present study builds and expands on previous efforts by incorporating a comprehensive database of mitochondrial COI sequences ("DNA-barcodes") to examine the diversity and map the distribution of species and lineages in the southern "*Lacustricola*" clade. However, because of considerable sampling gaps there is lack of data for some topotypes of currently recognised species and their synonyms; therefore, the purpose of the present study is to provide a first snapshot of the diversity within the southern "*Lacustricola*" clade and provide a roadmap for future taxonomic revision of this group. The paper also provides updated descriptions and diagnoses for "*L.*" *johnstoni* (Günther, 1894) and "*L.*" *myaposae* (Boulenger, 1908) based on data from comprehensive conspecific topotypic specimens of these species, respectively, in Mangochi, Lake Malawi, Malawi and in the Nseleni River, in KwaZulu Natal, South Africa, as well as examination of the species syntypes. We have also selected and designated the following specimens as lectotypes for "*L.*" *johnstoni* (BMNH 1893.11.15.95) and "*L.*" *myaposae* (BMNH 1907.4.17.88), to contribute to the ongoing effort in studying and describing the southern Africa "*Lacustricola*" diversity.

Materials and methods

Specimens examined, preservation, and fixation

The present study included specimens and tissue samples that were collected from historical surveys and recent expeditions in southern Africa and were deposited into

the National Collection Facility at the NRF-South African Institute for Aquatic Biodiversity (**NRF-SAIAB**), the Federal University of Rio de Janeiro (**UFRJ**) in Rio de Janeiro, Brazil and the Royal Museum for Central Africa (**RMCA**) in Tervuren, Belgium. "*Lacustricola*" *johnstoni* and "*L.*" *myaposae* syntypes from the Natural History Museum (**BMNH**), London, UK were examined from photographs, and lectotypes were designated. Fishes were sampled using various gears including electrofishing, seine nets, traps/fyke nets and dip nets. Captured fishes were anaesthetised with clove oil, digitally photographed and a small piece of muscle tissue was dissected from the right side of each specimen and preserved in 95% ethanol in the field for genetic analysis. Tissue samples were stored at -80 °C at the NRF-SAIAB, Grahamstown. Voucher specimens were fixed in 10% formalin in the field and were then transferred through 10% and 50% to 70% ethanol for long-term storage upon returning from the field. Specimens examined for the redescription of "*L.*" *johnstoni* and "*L.*" *myaposae* are listed in the taxonomic accounts section. A list of samples included in the molecular analysis with their respective localities and GenBank accession numbers are presented in Suppl. material 1.

Morphological study and osteological preparations

Meristics and morphometric data of "*L.*" *johnstoni* and "*L.*" *myaposae* were taken from specimens fixed in formalin and transferred to 70% ethanol (material listed in the taxonomy accounts section). Body measurements are presented as proportions of standard length (SL) and head measurements are expressed as proportions of head length (HL). Measurements were obtained using digital callipers under a dissecting microscope following Costa (1988). Osteological studies were made on cleared and stained specimens prepared according to Taylor and Dyke (1985), and nomenclature for bone structures followed Costa (2006). Most osteological illustrations were made on the left side, unless these were damaged. Nomenclature for frontal squamation follows Hoedeman (1956) and that for head sensory canals follows Gosline (1949), except for the posterior section of supraorbital canal, here called the posterior infraorbital canal.

Taxon sampling

Mitochondrial COI sequences of 48 specimens representing most of the southern Africa "*Lacustricola*" species were included in this study. In addition to the sequences produced in this study, other sequences were selected from GenBank (Suppl. material 1). We generated COI sequences for samples of conspecific specimens (topotypes) collected close to the type localities of "*L.*" *johnstoni*, "*L.*" *myaposae* and "*L.*" *katangae* and these were designated as topogenetypes following Chakrabarty (2010). Information on the locality details of samples used and GenBank accession numbers are presented in Suppl. material 1. The procatopodid species "*Poropanchax*" *normani* which is known as

sister to all other genera and species within the savannah and arid environment clade (Bragança and Costa 2019) was selected as outgroup. Species belonging to the southern Africa *Lacustricola* clade will be referred to as belonging to "*Lacustricola*", following Bragança and Costa (2019), indicating that species from the southern Africa clade are not related to *L. pumilus*, the genus type species.

DNA extraction, PCR, and sequencing

DNA was extracted from preserved tissues using the salting out method (Sunnucks et al. 1996) and by using the GeneJet Genomic DNA Purification kit (Thermo Fisher Scientific) and the NucleoSpin Tissue kit (Machery-Nagel Gmbh & Co. KG) following the manufacturer's standard protocol for animal tissue isolation. A fragment of the mitochondrial cytochrome oxidase subunit I (COI) gene was amplified by polymerase chain reaction (PCR) using the general universal DNA barcoding primer set: LCO1490 and HCO 2198 (Folmer et al. 1994). PCRs were performed with a Veriti 96 well thermal cycler (Applied Biosystems) and each reaction mixture (25 µL) contained 100–200 ng template DNA, 14.4 µL of water, 2.5 µL deoxynucleotide triphosphate (dNTP) (10 mM), 2.5 mM $MgCl_2$, 2.5 µL PCR buffer (10X), 0.5 µL of each primer (20 pmol) and 0.1 µL *Taq* DNA polymerase (Southern Cross Biotechnology, Cape Town). The PCR amplification profile was 95 °C for 5 min, followed by 35 cycles of 95 °C for 1 min, 43–47 °C for 1min and 72 °C for 2 min, and then final extension at 72 °C for 7 min. PCR products were purified with Exosap (Applied Biosystems), cycle-sequenced using BigDye Cycle Sequencing Kit (Applied Biosystems, Foster City, CA, USA) and sequenced at the NRF-SAIAB using an ABI 3730xl DNA Analyzer (Applied Biosystems) or in Macrogen, South Korea.

Alignment, evolution model, and phylogenetic analysis

Sequences were cleaned, aligned and trimmed to equal lengths (676 bp) using the program MEGA 7.0 (Kumar et al. 2016). The sequence evolution model HKY+I+G was selected using the corrected Akaike's Information Criteria (AICc) as implemented in JMODELTEST 2 (Darriba et al. 2012). Phylogenetic analyses were conducted through Bayesian inference (BI), using the program MRBAYES v3.2.5 (Ronquist et al. 2012) and Maximum Likelihood (ML), using the program GARLI 2.0 (Zwickl 2006). When performing MRBAYES v3.2.5, BI was conducted using two Markov chain Monte Carlo (MCMC) runs of four chains each for 3 million generations and a sampling frequency of 1000. The quality of the MCMC chains, stationarity and the respective ESS values of analysis parameters were checked in Tracer 1.6, and the analysis was finished when parameters were above 200. A 25% burn-in was removed in MRBAYES v3.2.5. A Maximum Likelihood stepwise-addition starting tree was performed in GARLI 2.0, with 100 attachment branches for each taxon and ten independent search replicates. The support values of the ML analysis were calculated by 1000 bootstrap replications (Felsenstein 1985).

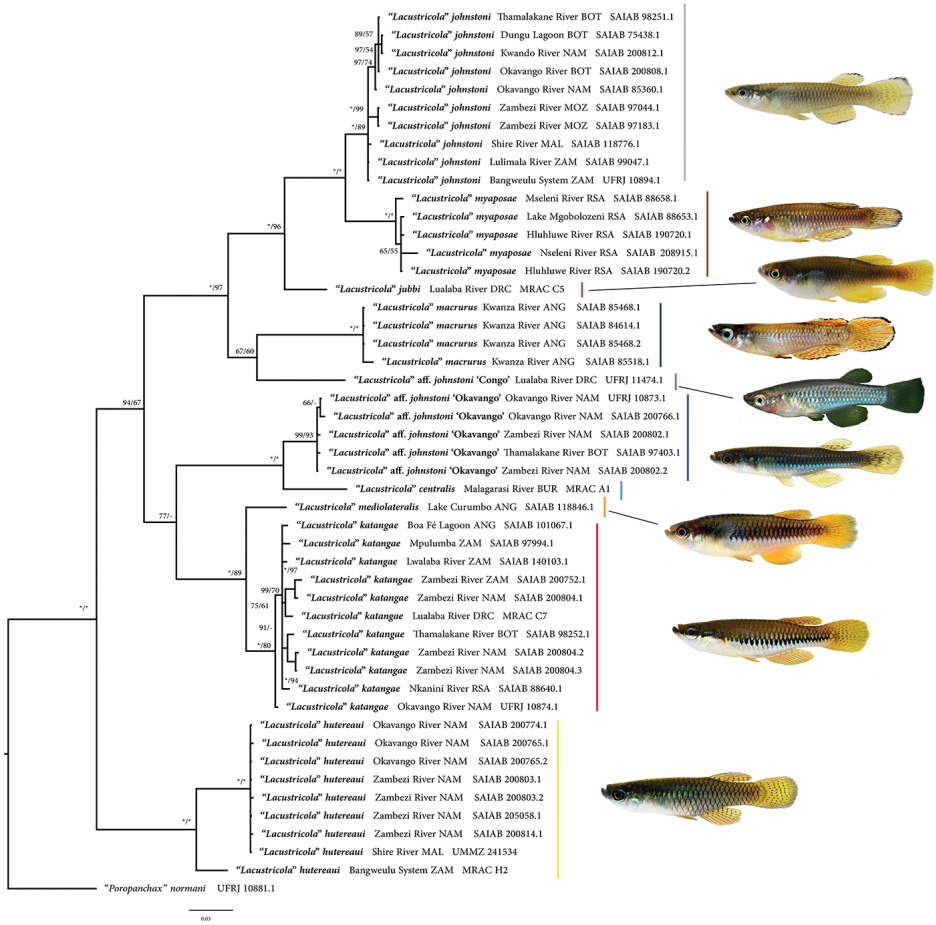

Figure 1. Phylogenetic relationships between southern Africa "*Lacustricola*" haplotypes, based on COI mitochondrial DNA sequences. Numbers left to the bar indicate posterior probability values and on the right are bootstrap support values from the maximum likelihood analysis. Asterisks indicate maximum values. Colours next to each species name correspond to the same colours as depicted in the distribution map (Figure 2). Abbreviations refer to the country where the specimens were collected: ANG = Angola, BOT = Botswana, BUR = Burundi, DRC = Democratic Republic of Congo, NAM = Namibia, MAL = Malawi, MOZ = Mozambique, RSA = Republic of South Africa, ZAM = Zambia.

Results

Molecular phylogenetic analyses

ML and the BI analyses recovered trees with comparable topologies (Fig. 1). Haplotypes belonging to the '"*Lacustricola*" *hutereaui* group were recovered as sister to all the southern African "*Lacustricola*" haplotypes, being supported by maximum support values (Fig. 1). The "*L.*" *hutereaui* group contains two genetic lineages, one comprising haplotypes

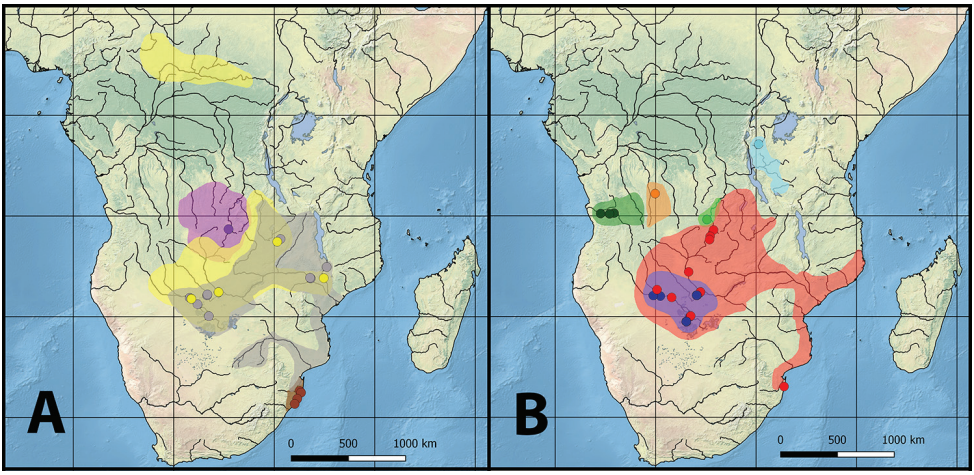

Figure 2. Southern Africa "*Lacustricola*" distribution maps. Spots correspond to the exact localities for the haplotypes included in this study, and the shaded area refers to the inferred distribution for each species. Map **A** yellow – "*Lacustricola*" *hutereaui*; grey – "*L.*" *johnstoni*; brown – "*L.*" *myaposae*; and purple – "*L.*" *jubbi.* Map **B** dark green – "*L.*" *macrurus*; orange – "*L.*" *mediolateralis*; red – "*L.*" *katangae*; light blue – "*L.*" *centralis*; blue – "*L.*" aff. *johnstoni* 'Okavango'; light green – "*L.*" aff. *johnstoni* 'Congo'.

derived from specimens of the Zambezi and Okavango region and the other comprising a haplotype from the Lualaba River, a major tributary of the Congo River basin (Fig. 2). Haplotypes of "*Lacustricola*" *katangae* and "*L.*" *mediolateralis* (Poll, 1967) were recovered as sister groups. "*Lacustricola*" *katangae* haplotypes were found to be broadly distributed, occurring in the Congo, Upper Zambezi and Okavango river systems (Figs 1, 2).

Haplotypes including "*L.*" *centralis* (Seegers, 1996), from the Malagarasi River in eastern Africa, and an undescribed species which occurs in the Okavango drainage, herein named "*Lacustricola*" aff. *johnstoni* "Okavango" were recovered as sister groups (Figs 1, 2). However, the relationship between haplotypes of "*L.*" *centralis*, "*L.*" aff. *johnstoni* "Okavango", "*L.*" *katangae* and "*L.*" *mediolateralis* had low support. The analyses recovered a well-supported clade containing "*L.*" *johnstoni* s.s., "*L.*" *myaposae*, "*L.*" *jubbi*, "*L.*" *macrurus* and an undescribed species, "*L.*" aff. *johnstoni* "Congo" (Fig. 1). Haplotypes of "*Lacustricola*" *jubbi* were recovered as the basally diverging lineage which is sister to a clade containing two sister species, "*L.*" *myap*osae and "*L.*" *johnstoni* s.s.

"*Lacustricola*" *johnstoni* s. s. is widely distributed in southern Africa, with a range extending from the Lower Zambezi system (i.e., the Shire River/Lake Malawi system), through the Middle and Upper Zambezi to the Okavango system and the Bangweulu catchment in the Congo River system (Fig. 2). "*Lacustricola*" *myaposae* is endemic to the eastward draining river systems of the Maputaland region in South Africa and Mozambique (Fig. 2). "*Lacustricola*" *jubbi*, which was previously placed in the deep bodied *Hypsopanchax* genus occurs in the Upper Zambezi from where it was first described, and in the Lualaba River, Upper Congo River system, where it co-occurs with "*L.*" aff. *johnstoni* "Congo" (Fig. 2). "*Lacustricola*" *macrurus* is endemic to the Kwanza River system and the adjacent Lake

Sarmento at Marimba, Angola, that drains into the Congo River system (Fig. 2). Given the existence of several unidentified lineages within the southern "*Lacustricola*" clade, the present study aims to provide comprehensive redescriptions of "*L.*" *johnstoni* s. s. and "*L.*" *myaposae* as part of a long-term effort to revise the taxonomy of this genus.

Taxonomic accounts

"Lacustricola" johnstoni (Günther, 1894)

Figures 3, 4

Haplochilus johnstoni Günther, 1894: 627 [original description: Mangochi (former Fort Johnston), Malawi].

Material examined. BMNH 1893.11.15.95, Lectotype; BMNH 1893.11.15.92-94,96-99, 7 Paralectotypes; Mangochi (former Fort Johnston), Malawi. Examined by photographs and x-rays – SAIAB 35820, 18 (5 C&S), 24.7–35.4 mm SL; Upper Shire River, Mangochi, Malawi, 14°26'60"S, 35°15'60"E; col: D. Tweddle & N. G. Willoughby; 19 Sep. 1971. – SAIAB 8311, 3, 31.3–32.5 mm SL; Shire River, Liwonde, Malawi; col: D. Tweddle & N. G. Willoughby; 20 Oct. 1975. – SAIAB 34384, 1, 29.1 mm SL; Shire River, Liwonde Barrage, Malawi, 15°04'S, 35°13'E; col: D. Tweddle & P. Skelton; 26 Oct. 1989. – SAIAB 34388, 1, 35.7 mm SL; Monkey Bay, Lake Malawi, Malawi, 14°04'S, 34°55'E; 17 Oct. 1989. – SAIAB 40800, 15 (4 C&S), 30.1–33.2 mm SL; Bridge over Dwambadzi River, Malawi, 12°14'S, 33°59'E; col: D. Tweddle & P. Skelton; 06 Sep. 1992. – SAIAB 11237, 7, 26.2–36.2 mm SL; Monkey Bay, Lake Malawi, Malawi, 14°3'00"S, 34°55'00"E; col: D.H. Eccles; 31 Oct. 1974. – SAIAB 11876, 8, 27.2–34.7 mm SL; Shire River, Liwonde Barrage, Malawi, 15°3'37"S, 35°13'7"E; col: D. Tweddle & T. Makinen; 27 May. 2011.

Diagnosis. "*Lacustricola*" *johnstoni* is distinguished from all congeners from the "*L.*" *katangae* clade by the absence of a zigzag black mark along the flank (vs. presence); and from congeners belonging to the "*L.*" *hutereaui* clade by the absence of a barred dorsal, anal and caudal-fins and also by the absence of a conspicuous reticulate pattern on scale margins. It is further distinguished from all congeners except "*L.*" *myaposae* and "*L.*" *moeruensis* by the presence of orange dorsal, anal and caudal-fins in females (vs. hyaline); it is distinguished from "*L.*" *myaposae* by the presence of a bluish colouration in the posterior region of flank (vs. light purple colouration); a slender body profile, male body depth 20.6–24.4% of SL (vs. 26.0–30.9% of SL), female body depth 19.7–22.5% of SL (vs. 22.8–25.1% of SL); a shorter dorsal-fin base length in males 8.7–11.6% of SL (vs. 11.9–13.1% of SL) and in females 7.3–10.1% of SL (vs. 10.8–11.6% SL); a less deep head in males 61.9–67.0% of HL (vs. 70.7–79.8% of HL) and in females 59.4–63.5% of HL (vs. 66.6–69.6% of HL); and a hyaline pectoral-fin in males (vs. orange). Other morphometric characters presenting a slight overlap but useful in distinguishing "*L.*" *johnstoni* from "*L.*" *myaposae* are: a comparatively narrow cau-

dal peduncle, depth of 12.6–14.5% of SL in males and 11.2–12.7% of SL in females (vs. 14.0–17.1% of SL in males and 12.9–13.7% of SL in females); a comparatively elongated caudal-fin, 30.1–33.8% of SL in males and 28.9–31.2% of SL in females (vs. 27.5–30.2% of SL in males and 25.3–28.5% of SL in females); and a comparatively deep, laterally compressed head, 57.1–63.2% of HL in males and 59.0–64.7% of HL in females (vs. 63.1–67.9% of HL in males and 65.3–68.1% of HL in females). "*Lacustricola*" *johnstoni* is distinguished from "*L.*" *moeruensis* by a comparatively slender body and a more backward positioned dorsal-fin, first proximal radial of dorsal-fin between neural spine of vertebrae 16 and 17 (vs. 13 and 14).

Description. Morphometric data are presented in Table 1. Maximum recorded adult size 35.6 mm SL. Dorsal profile of body approximately straight to slightly convex from snout tip to dorsal-fin origin; convex along dorsal-fin base. Ventral profile convex from lower jaw to beginning of anal-fin base; slightly convex along the anal-fin base and nearly straight on caudal peduncle. Anterior portion of body laterally compressed, becoming more compressed behind anal-fin origin.

There is clear sexual dimorphism in fin shape and size (Figs 3, 4). In males, dorsal-fin is rounded and elongated, almost reaching the caudal-fin base; its origin in vertical between 7th and 9th anal-fin rays; anal-fin rounded and elongated, reaching middle of the caudal peduncle. Pelvic-fin length variable, reaching between urogenital papillae aperture and the base of third anal-fin ray. In females, dorsal and anal-fins are not elongated and do not extend posteriorly to caudal-fin base. Caudal-fin slender in both sexes. Pectoral-fin elliptical, in both males and females, its posterior margin reaching vertical just behind pelvic-fin base. In females, pelvic-fin shorter than in males, tip reaching region just before urogenital opening. In both males and females, dorsal-fin rays 7(17), 8(13) and 9(2); anal-fin rays 12(4), 13(12), 14(14) and 15(2); caudal-fin rays 19(2), 20(10), 21(17), 22(2) and 23(1); pectoral-fin rays 12(13), 13(18) and 14(1); pelvic-fin rays 6.

Frontal squamation G-patterned (Fig. 5). Head neuromasts placed in shallow grooves. Cephalic lateral line system: anterior portion of supraorbital sensory canal open, with three neuromasts, anteriormost one anteriorly displaced from the other two; posterior portion open, with three exposed neuromasts; anterior infra-orbital canal partially closed, with two pores and one free neuromast, but in juveniles and subadults all anterior infraorbital canal can be open; median portion of infra-orbital region with series of nine to eleven minute neuromasts; posterior infra-orbital canal closed, with two pores; preopercular canal closed in both dorsal and ventral portions with seven or eight pores; mandibular canal represented by two neuromasts, one in vertical through corner of mouth and the other anteriorly positioned in the lower jaw ventral portion. Longitudinal series of scales 27(3), 28(18), 29(9); transverse series of scales 7; circumpeduncular scales 10; predorsal scales 17(1), 18(18), 19(11).

Osteology. Osteological structures are presented in Fig. 6. Mesethmoid and vomer absent. Frontals, anterior margin, extending anteriorly between nasals. Parasphenoid medial process short, not contacting pterophenoid; anterior margin rounded. Lateral ethmoid overlapping with anterior portion of parasphenoid. Posterior process of supraoccipital long, reaching first vertebra. Lachrymal rectangular. Premaxillary and

Table 1. Morphometric data of "*Lacustricola*" *johnstoni* and "*L.*" *myaposae*.

	"*Lacustricola*" *johnstoni*		"*Lacustricola*" *myaposae*	
	males (*N* = 12)	**females (*N* = 10)**	**males (*N* = 7)**	**females (*N* = 4)**
Standard length (mm)	29.0–34.6	27.7–35.6	31.3–38.1	30.2–39.0
Percent of standard length				
Body depth	20.6–24.4	19.7–22.5	26.0–30.9	22.8–25.1
Caudal peduncle depth	12.6–14.5	11.2–12.7	14.0–17.1	12.9–13.7
Pre-dorsal length	67.6–73.9	71.6–73.9	67.5–72.3	68.5–70.7
Pre-pelvic length	43.0–48.6	44.9–49.7	45.1–49.5	46.4–47.8
Length of dorsal-fin base	8.7–11.6	7.3–10.1	11.9–13.1	10.8–11.6
Length of anal-fin base	16.8–21.1	13.2–16.6	16.0–20.0	15.0–16.2
Caudal-fin length	30.1–33.8	28.9–31.2	27.5–30.2	25.3–28.5
Pectoral-fin length	18.6–22.1	18.8–20.8	18.7–22.4	17.5–19.5
Pelvic-fin length	15.5–22.8	13.2–14.6	14.0–18.0	11.9–12.9
Head length (mm)	6.9–8.4	6.2–7.9	8.2–9.5	7.2–9.8
Percent of head length				
Head depth	61.9–67.9	59.4–63.5	70.7–79.8	66.6–69.6
Head width	57.1–63.2	59.0–64.7	63.1–67.9	65.3–68.1
Snout length	21.0–23.9	19.2–23.4	20.7–22.8	22.2–24.4
Lower jaw length	9.5–12.3	8.7–11.0	9.8–14.3	8.9–11.2
Eye diameter	35.7–39.5	36.2–41.1	35.8–38.5	37.2–39.2

dentary teeth well developed. Retroarticular triangular or subtriangular. Dentary deep. Dorsal process of maxilla broad overlapping the ascending process of premaxilla; ventral process greatly reduced, consisting of a rounded ventromedial bulge. Ventral arm of maxilla broad, laterally expanded. Medial surface of premaxilla ascending process with a straight or slightly concave profile. Entopterygoid posterior portion and sympletic bone keel deep. Opercle triangular, anterodorsal process present. Anterior process of anterior ceratohyal does not extend ventrally to ventral hypohyal. Urohyal ventral margin concave. First and second basibranchials with expanded lateral bone flanges. Cartilaginous portion of basihyal shorter than osseous portion. Fourth ceratobranchial anterior third with teeth. Second pharyngobranchial plate with teeth. First epibranchial base, broad, more than three times anterior portion width. Supracleithrum rounded. Posttemporal rod-like, ventral arm absent. Cleithrum bony flange not covering scapula foramen. Ventral postcleithrum, slender, similar in width to adjacent first pelural rib. Basipterygium, posterior process, shorter or about the same size of medial process. Anal-fin proximal radials about the same length and parallel to each other. Hypurals completely fused. Parahypural proximal end overlapping the preural centrum. Total vertebrae 30(4) and 31(5), precaudal 13(2) and 14(7) and caudal 16(1), 17(4) and 18(4). First proximal radial of dorsal-fin between neural spine of vertebrae 16 and 17. First proximal radial of anal-fin between pleural rib of vertebrae 11 and 13. Gill rakers on first branchial arch 10(1) and 11(3). Branchiostegal rays 5.

Colouration in alcohol. Overall colouration of body pale brown yellow with minute chromatophores sparsely distributed, and some organised chromatophores forming an inconspicuous reticulate pattern along flank scales margin (Fig. 3). Ventral surface scarcely pigmented. Pale brown chromatophores along whole mid-body line of flank. Head overall colouration yellowish brown. Brown chromatophores on dorsum

Figure 3. "*Lacustricola*" *johnstoni* preserved colouration: **A** male SAIAB 118776, 34.7 mm SL **B** female SAIAB 118776, 32.0 mm SL; from Shire River at Liwonde Barrage, Malawi.

Figure 4. "*Lacustricola*" *johnstoni* colouration in life: **A** male SAIAB 118776, 31.0 mm SL **B** female SAIAB 118776, 26 mm SL; from Shire River at Liwonde Barrage, Malawi.

of head. Minute chromatophores concentrated in the lower jaw and pre-orbital region, forming a distinct darker region. Iris silver, darker close to pupil; dark pigment concentrated on dorsal margin of eye. All fins hyaline in females, with melanophores sparsely

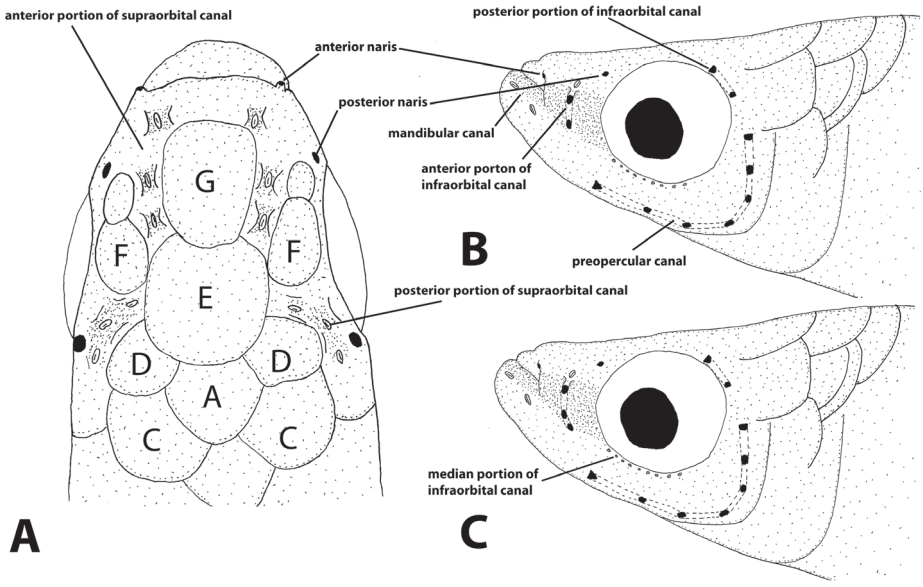

Figure 5. Cephalic pores and head squamation pattern: **A, B** head dorsal and lateral view of "*L.*" *johnstoni* **C** head lateral view of "*L.*" *myaposae.*

concentrated only on fins membranes and along fin rays; melanophores forming small inconspicuous spots on male dorsal-fins, rarely forming two distinct bands; melanophores forming two distinct parallel dark bands in the anal-fin medial portion; region close to anal-fin rays insertion hyaline; caudal-fin with conspicuous dark blotches in the middle rays that could be organised in distinct bands or not; pectoral and pelvic-fin with melanophores sparsely concentrated on fins membranes and along fin rays. Female urogenital opening pocket scales with dark brown chromatophores.

Colouration in life. Males (Fig. 4A). Flanks bright blue, with small scattered bright green dots. Cupric iridescent blotch on region just posterior to pectoral-fin. Dorsum yellow-brown. Ventral surface white between head and region anterior to pelvic-fin origin; bright blue between pelvic-fin and the end of the anal-fin insertion; ventral region of caudal peduncle whitish yellow. Side of head predominantly bluish silver, dorsal portion yellow-brown, post-orbital region with a distinct green bright blotch. Iris dark grey, light yellow close to pupil. Eye bright silver on dorsal portion. Lower jaw and pre-orbital region dark brown-grey, forming a distinct horizontal band. Pectoral-fin hyaline; all other fins yellowish brown with brown dots on fins arranged in distinct rows. Dorsal-fin with two to four rows; anal-fin with two to three rows; and caudal-fin with four to five rows, but in some specimens the brown dots are scattered over the fin and not arranged in distinct rows. Some males may present a distinct black distal margin on anal, dorsal and caudal-fins.

Females (Fig. 4B). Flanks bright blue. Cupric iridescent blotch on region just posterior to pectoral-fin. Dorsum yellow-brown. Venter white between head and region just anterior to urogenital opening; bright blue between region just anterior to urogenital opening and

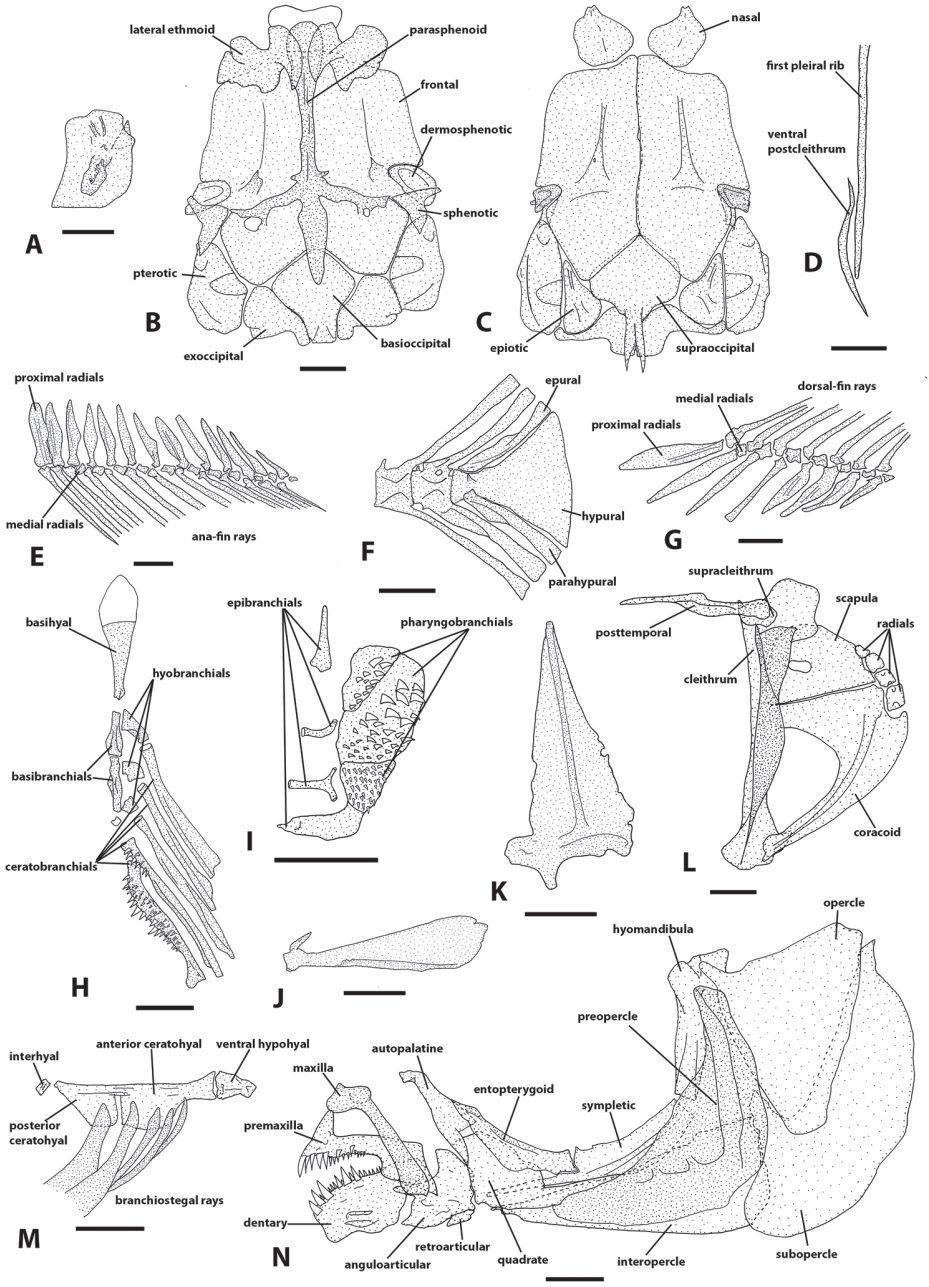

Figure 6. Osteological plate of "*L.*" *johnstoni* (SAIAB 35820) from the Upper Shire River, Mangochi, Malawi. **A** Lachrymal **B** neurocranium, ventral view **C** neurocranium dorsal view **D** ventral post-cleithrum and first pleural rib, lateral view **E** anal-fin radials and proximal radials, left lateral view **F** caudal-fin skeleton, left lateral view **G** dorsal-fin radials and proximal radials, left lateral view **H** left branchial arches ventral portion, ventral view **I** right dorsal portion of branchial arches, ventral view **J** urohyal, left lateral view **K** left basipterygium, dorsal view **L** left shoulder girdle, lateral view **M** right hyoid bar, lateral view **N** left jaws, jaws suspensorium and opercular apparatus, lateral view. Scale bars: 1 mm.

anal-fin insertion; whitish yellow along the anal-fin insertion to caudal peduncle. Scales around urogenital opening covered with dark chromatophores. Side of head predominantly bluish silver, ventral portion white, dorsal portion yellow-brown, post-orbital region with a distinct green bright blotch. Iris dark grey, light yellow close to pupil. Eye bright silver on dorsal portion. Lower jaw and pre-orbital region dark brown-grey, forming a distinct horizontal band. Pectoral and pelvic-fins hyaline; dorsal-fin orange, distal margin hyaline; anal-fin base hyaline, distal portion orange; caudal-fin orange, distal region hyaline.

Distribution and habitat. "*Lacustricola*" *johnstoni* is a widespread species occurring in the Lower, Middle and Upper Zambezi River, including the Shire River and Lake Malawi, the Limpopo River, and is also present in the Okavango system (Fig. 2). The species is usually found associated with marginal vegetation along the banks of small and large rivers, or in swampy areas, as well as along the shores of Lake Malawi and Lake Kariba.

"Lacustricola" myaposae (Boulenger, 1908)

Figures 7, 8

Haplochilus myaposae Boulenger 1908:232 [original description: Myaposa River, Zululand, KwaZulu-Natal, South Africa].

Material examined. BMNH 1907.4.17.88, Lectotype; Myaposa River, Kwazulu-Natal, South Africa. Examined by photographs and x-rays. SAIAB 96619, 10 (2 C&S), 18.1–27.9 mm SL; Mhlathuze, KwaZulu-Natal, South Africa 28°50'18"S, 31°54'41"E; col: B. Ellender, O. Weyl & R. Karsing; 27 May. 2010. – SAIAB 88658, 31 (6 C&S), 21.3–38.0 mm SL; Bridge at Mseleni, KwaZulu-Natal, South Africa, 27°21'49"S, 32°31'33"E; col: B. Kramer, E. Swartz, P.T. Maake; 31 Oct. 2009. – SAIAB 96560, 1, 30.2 mm SL; Nseleni River Nature Reserve, KwaZulu-Natal, South Africa, 28°41'57"S, 32°0'4"E; col: R. Jones, O. Weyl; B. Ellender & R. Karsing; 23 May. 2010. – SAIAB 86637, 1, 34.0 mm SL; St Lucia area 2, KwaZulu-Natal, South Africa, 28°20'44"S, 32°21'14"E; col: R. Karssing, J. Craigie, S. Khubela, R. Ndlhovu, A. Xoswa; 08 Sep. 2009. – SAIAB 47128, 1, 40.5 mm SL; KwaZulu-Natal, South Africa; 31 Jan. 1989. – SAIAB 83143, 2, 38.1–38.2 mm SL; Greater St Lucia Wetland Park, Ozabeni, Ovalweni crossing, KwaZulu-Natal, South Africa, 27°38'59"S, 32°38'9"E; col: J.D. Craigie & R. Karssing; 29 May. 2007. – SAIAB 96591, 9 (2 C&S), 21.1–36.2 mm SL; Upper Nseleni in sugar Estate, Richards Bay, KwaZulu-Natal, South Africa, 28°40'27"S, 31°57'51"E; col: B. Ellender, O. Weyl & R. Karsing; 24 May. 2010. – SAIAB 83149, 3, 34.7–38.1 mm SL; Greater St Lucia Wetland Park, Ozabeni, Samango crossing, KwaZulu-Natal, South Africa, 27°37'3"S, 32°33'2"E; col: N. Rivers-Moore & R. Karssing; 30 May. 2007. – SAIAB 208915, 6; Makat Farm in Jamela, Mposa River, a tributary of the Nseleni River, KwaZulu-Natal, South Africa, 28°39'18"S, 32°01'48"E; col: A. Chakona, N. Mazungula & B. Motshegoa; 4 Sep. 2015.

Diagnosis. "*Lacustricola*" *myaposae* is distinguished from all congeners from the "*L.*" *katangae* clade by the absence of a zigzag black mark along the flank (vs. presence);

and from congeners belonging to the "*L.*" *hutereaui* clade by the absence of barred dorsal, anal and caudal-fins and also by the absence of a conspicuous reticulate pattern on scales margin. It is further distinguished from all congeners except "*L.*" *johnstoni* and "*L.*" *moeruensis* by the presence of an orange dorsal, anal and caudal-fins in females (vs. hyaline); it is distinguished from "*L.*" *johnstoni* and "*L.*" *moeruensis* by the presence of light purple colouration in the posterior region of flank (vs. absence); an orange pectoral-fin in males (vs. hyaline); and by a distinct colouration pattern in both dorsal and anal-fins in which melanophores become continuously more concentrated close to fin margins, forming a grey zone before the margin become entirely dark (vs. absence of this colouration pattern). "*Lacustricola*" *myaposae* is further distinguished from "*L.*" *johnstoni* by a deeper body profile, males body depth 26.0–30.9% of SL (vs. 20.6–24.4%of SL), females body depth 22.8–25.1% of SL (vs. 19.7–22.5% of SL); a longer dorsal-fin base length in males 11.9–13.1%of SL (vs. 8.7–11.6% of SL) and in females 10.8–11.6% SL (vs. 7.3–10.1% SL); and a deeper head in males 70.7–79.8% of HL (vs. 61.9–67.0% of HL) and in females 66.6–69.6% of HL (vs. 59.4–63.5% of HL). Other morphometric characters presenting a slight overlap but useful in distinguishing "*L.*" *myaposae* from "*L.*" *johnstoni* are: a deeper caudal peduncle, 14.0–17.1% of SL in males and 12.9–13.7% of SL in females (vs. 12.6–14.5% of SL in males and 11.2–12.7% of SL in females); a shorter caudal-fin, 27.5–30.2% of SL in males and 25.3–28.5% of SL in females (vs. 30.1–33.8% of SL in males and 28.9–31.2% of SL in females); and a deeper head, 63.1–67.9% of HL in males and 65.3–68.1% of HL in females (vs. 57.1–63.2% of HL in males and 59.0–64.7% of HL in females).

Description. Morphometric data are presented in Table 1. Maximum recorded adult size 39.0 mm SL. Dorsal profile of body approximately straight to slightly convex from snout tip to dorsal-fin origin; convex along dorsal-fin base, and nearly straight on caudal peduncle. Ventral profile convex from lower jaw to beginning of anal-fin base; slightly convex along the anal-fin base and nearly straight on caudal peduncle. Caudal peduncle slightly deeper in males. Anterior portion of body laterally compressed, becoming more compressed behind anal-fin origin.

Dorsal-fin rounded in males not reaching caudal-fin base; its origin in vertical between 6th and 7th anal-fin rays. (Fig. 7) Anal-fin rounded in males, tip not reaching vertical through dorsal-fin tip. Dorsal and anal-fins are not elongated in females. Caudal-fin slender. Pectoral-fin elliptical, its posterior margin reaching vertical just behind pelvic-fin base. Pelvic-fin length in males longer than in females, reaching urogenital papillae aperture; short in females, tip reaching region just before urogenital opening. Pelvic-fin bases medially separated by interspace broader than width of each pelvic-fin base. Dorsal-fin rays 8(7), 9(20), 10(10) and 11(2); anal-fin rays 12(1), 13(9), 14(14) and 15(15); caudal-fin rays 20(3), 21(7), 22(9), 23(6), 24(9), 25(3) and 26(1); pectoral-fin rays 11 (2), 12(18) and 13(19); pelvic-fin rays (6).

Frontal squamation G-patterned (Fig. 5). Head neuromasts placed in shallow grooves. Cephalic lateral line system: anterior portion of supraorbital sensory canal open, with three neuromasts, anteriormost one anteriorly displaced from the other two; posterior portion open, with three exposed neuromasts; anterior infra-orbital ca-

Figure 7. "*Lacustricola*" *myaposae* preserved colouration: **A** male SAIAB 96591, 31.7 mm SL **B** female SAIAB 96591, 35.7 mm SL; from Nseleni River, KwaZulu-Natal, Republic of South Africa.

nal partially closed, with three pores and one free neuromast, but in juveniles and subadults all anterior infraorbital canal can be opened with three exposed neuromasts; median portion of infra-orbital region with series of eight to nine minute neuromasts; posterior infra-orbital canal closed, with two pores; preopercular canal closed in both dorsal and ventral portions with seven pores; mandibular canal represented by two neuromasts, one in vertical through corner of mouth and the other anteriorly positioned in the lower jaw ventral portion. Longitudinal series of scales 26(14), 27(11), 28(8), 29(1); transverse series of scales (7); circumpeduncular scales (10); predorsal scales 16(17), 17(16), 18(3).

Osteology. Osteological structures are presented in Fig. 6. Mesethmoid and vomer absent. Frontals, anterior margin, extending anteriorly between nasals. Parasphenoid medial process short, not contacting pterosphenoid; anterior margin rounded. Lateral ethmoid overlapping with anterior portion of parasphenoid. Posterior process of supraoccipital long, reaching first vertebra. Lachrymal rectangular. Premaxillary and dentary teeth well developed. Retroarticular triangular or subtriangular. Dentary deep. Dorsal process of maxilla broad overlapping the ascending process of premaxilla; ventral process greatly reduced, consisting of a rounded ventromedial bulge. Ventral arm of maxilla broad, laterally expanded. Medial surface of premaxilla ascending process with a straight or slightly concave profile. Entopterygoid posterior portion and sympletic bone keel deep. Opercle triangular, anterodorsal process present. Anterior process of anterior ceratohyal does not extend ventraly to ventral hypohyal. Urohyal ventral margin concave. First and second basibranchials with expanded lateral bone flanges. Cartilaginous portion of basihyal shorter than osseous portion. Fourth ceratobranchial anterior third with teeth. Second pharyngobranchial plate with teeth. First epibranchial base, broad, more than three times anterior portion width. Supracleithrum rounded.

Posttemporal rod-like, ventral arm absent. Cleithrum bony flange not covering scapula foramen. Ventral postcleithrum slender, similar in width to adjacent first pelural rib. Basipterygium, posterior process, shorter or about the same size of medial process. Anal-fin proximal radials about the same length and parallel to each other. Hypurals completely fused. Parahypural proximal end overlapping the preural centrum. Total vertebrae 28(1), 29(8) and 30(1), precaudal 12(9) and 13(1) and caudal 16(2), 17(7) and 18(1). First proximal radial of dorsal-fin between neural spine of vertebrae 13 and 14. First proximal radial of anal-fin between pleural rib of vertebrae 11 and 12. Gill rakers on first branchial arch 9(1), 10(2) and 11(1). Branchiostegal rays 5.

Colouration in alcohol. Overall colouration of body pale brownish yellow with minute chromatophores sparsely distributed, and some organised chromatophores forming an inconspicuous reticulate pattern along margins of flank scales, more conspicuous along the longitudinal series of scales on mid-body line of flank (Fig. 7). Ventral surface scarcely pigmented. Pale brown chromatophores along whole mid-body line of flank. Head overall colouration yellowish brown. Dark brown chromatophores on dorsum of head. Minute chromatophores concentrate in the lower jaw and pre-orbital region, forming a distinct darker region. Iris silver, darker close to pupil; dark pigment concentrated on dorsal margin of eye. All fins hyaline in females, with melanophores sparsely concentrated only on fins membranes and along fin rays; high concentration of melanophores on males dorsal-fin, with small hyaline spots on fin membrane, close to rays insertion; dorsal-fin margin dark; melanophores on anal-fin becoming continuously more concentrated close to fin margin; region close to anal-fin rays insertion hyaline; caudal-fin with conspicuous dark blotches in the middle rays that could be organised in distinct bands or not, melanophores on fin distal portion becoming continuously more concentrate close to fin margin; pelvic-fin dark, with numerous small chromatophores; pectoral-fin with chromatophores sparsely concentrated on fins membranes and along fin rays. Female urogenital opening pocket scales with few sparse dark brown chromatophores.

Colouration in life. Males (Fig. 8A). Flanks yellow brown, scattered with yellow-green metallic dots along the flank; posterior region of flank purple, more conspicuous posteriorly on caudal peduncle. Small cupric iridescent blotch on flank region just posterior to pectoral-fin. Dorsum yellow-brown. Ventral surface white between lower jaw and opercle margin; light yellow between opercle margin and urogenital opening; greyish brown between urogenital opening and caudal peduncle. Side of head predominantly bluish silver, dorsal portion yellow-brown, post-orbital region with a distinct green bright blotch. Iris dark grey, light yellow close to pupil. Eye bright silver on dorsal portion. Lower jaw and pre-orbital region dark brown-grey, forming a distinct horizontal band. Pectoral-fin base hyaline, distal portion orange; pelvic-fin yellow with dark chromatophores on fins tip; anal-fin with two orange-brown rows and melanophores on becoming continuously more concentrate close to fin margin; dorsal-fin orange-yellow with two-three dark bars on its posterior portion, margin black; caudal-fin orange-yellow with three vertical bands that could be organised in distinct bands or not, melanophores on fin distal portion becoming continuously more concentrate close to fin margin.

Figure 8. "*Lacustricola*" *myaposae* colouration in life: **A** male SAIAB 208915, 33.0 mm SL **B** female SAIAB 208915, 35.2 mm SL; from Nseleni River, KwaZulu-Natal, Republic of South Africa.

Females (Fig. 8B). Flanks bright blue, scattered with green metallic dots along the flank; posterior region of flank purple, more conspicuous posteriorly on caudal peduncle. Cupric iridescent blotch on region just posterior to pectoral-fin. Dorsum yellow-brown. Venter white between head and pelvic-fin insertion; bright blue between pelvic-fin and end of caudal-fin; grey on caudal peduncle. Scales around urogenital opening covered with dark chromatophores. Side of head predominantly bluish silver, ventral portion white, dorsal portion yellow-brown, post-orbital region with a distinct green bright blotch. Iris dark grey, light yellow close to pupil. Eye bright silver on dorsal portion. Lower jaw and pre-orbital region dark brown-grey, forming a distinct horizontal band. Pectoral-fin first rays orange-brown; pelvic-fin hyaline, with a faint orange colouration on fin base; dorsal-fin orange, distal margin hyaline; anal-fin base hyaline, distal portion orange; caudal-fin orange, distal region hyaline.

Distribution and habitat. "*Lacustricola*" *myaposae* is only known from the coastal river drainages and lacustrine systems in Kwazulu-Natal Province of South Africa to coastal lagoons south of the Maputo River in Mozambique (Fig. 2). The species is usually found associated with marginal vegetation along the banks of small and large rivers in freshwater. Despite occurring in a coastal area, little is known about the salinity tolerance capacity of "*L.*" *myaposae*.

Remarks. Only one specimen was found among the syntypes (original catalogue number BMNH 1907.4.17.88-89) of "*Lacustricola*" *myaposae*, one specimen is missing (pers. comm. James Maclaine), thus this remaining individual was designated as the Lectotype (BMNH 1907.4.17.88).

Discussion

The present study provided the first insight into the phylogenetic diversity and relationships between the southern Africa "*Lacustricola*" species. Among the major challenges and impediments for taxonomic studies within this genus is the assumption that some species (e.g. "*L.*" *katangae*, "*L.*" *johnstoni*, and "*L.*" *hutereaui*) are broadly distributed over southern Africa and the lack of detailed information about species boundaries. Thus, this paper is a first attempt to approach both impediments, through a combined broad COI mitochondrial gene sampling of most southern Africa "*Lacustricola*" species and the redescriptions of "*L.*" *myaposae* and "*L.*" *johnstoni*, the latter a species that has been considered to be widespread in southern Africa. However, it is worth mentioning that despite no evidence of introgression within the Procatopodidae, considering the presence of sympatric species this is a possibility, and phylogenetic relationships based only on mitochondrial DNA may fail in identifying that, and not necessarily reflect the species phylogeny. In addition, another main concern is that given the limited COI sampling for some regions, the results must be seen as a first effort in investigating the little-known southern Africa "*Lacustricola*".

Both, ML and BI analyses supported "*L.*" *hutereaui* and "*L.*" *katangae* as belonging to distinct groups, each one with clear distinct colouration patterns. The "*Lacustricola*" *katangae* group (including also "*L.*" *mediolateralis*) is easily recognised by the presence of a zigzag pattern black band along the flank, whereas specimens belonging to the "*L.*" *hutereaui* group have barred dorsal, anal and caudal-fins and a conspicuous reticulate pattern on scale margins. Despite generally having broadly similar distribution ranges, the contrasting genetic patterns between the "*L.*" *katangae* and "*L.*" *hutereaui* groups suggest that these groups had different evolutionary histories in response to the paleogeographic and paleoclimatic events in the region. "*Lacustricola*" *katangae* was found to be a single widely distributed species with small genetic divergence among haplotypes and no discernible pattern of geographic structuring across its range which extends from the KwaZulu Natal Province of South Africa in the south to the Congo system. In contrast, the "*L.*" *hutereaui* group contained two distinct lineages, the first comprising samples from the Okavango and Zambezi systems, and another one represented by a single haplotype from the Lualaba River in the Congo system. There are a number of possibilities regarding taxonomic status of the two lineages identified within the "*L.*" *hutereaui* group. Firstly, they could potentially represent two species that are new to science. Secondly, one of them could represent "*L.*" *hutereaui* from the northern savannahs of the Congo in the Democratic Republic of Congo, or they could also potentially represent two known synonyms of "*L.*" *hutereaui*, namely "*L.*" *baudoni* (Myers, 1924b) from northern Congo savannahs in Central African Republic, and "*L.*" *chobensis* (Fowler, 1935) from the Chobe River at Kasane, close to the Zambezi river confluence. Determination of the taxonomic status of these lineages and evaluation of the validity of the two junior synonyms of "*L.*" *hutereaui* will require inclusion of topotypic samples from the type localities of "*L.*" *hutereaui* and "*L.*" *baudoni* which were not available for the present study.

One of the key contributions of this paper was provision of detailed redescriptions of "*L.*" *johnstoni* and "*L.*" *myaposae*. The lack of a clear diagnosis for "*L.*" *johnstoni* in particular, resulted in this species essentially becoming a "waste basket taxon" for all slender-bodied topminnows with bluish colouration. This was demonstrated by the fact that several samples from a number of ichthyological collections that were labelled as "*L.*" *johnstoni* did not form a distinct clade, but instead, some of these samples clustered with other species, for example "*L.*" *macrurus*, "*L.*" *centralis* and "*L.*" *myaposae*. The incorporation of COI sequences from the type locality of "*L.*" *johnstoni* in the Shire River allowed identification of "*L.*" *johnstoni* s. s. and revealed, for the first time, that specimens with a slender body and bluish colouration are not necessarily conspecific with this species nor are they closely related to it. For example, Bragança and Costa (2019) erroneously classified sample (UFRJ 10873) as "*L.*" *johnstoni*, which in this study has been recovered as "*L.*" aff. *johnstoni* 'Okavango', while a juvenile specimen that was tentatively identified as "*L.*" *matthesi* (UFRJ 10894) by the same authors has been found to correspond to "*L.*" *johnstoni* in the present study. Two new candidate species were recognised, "*L.*" aff. *johnstoni* 'Congo' from the upper Lualaba River in the Congo system that is sister to "*L.*" *macrurus*, a species known from the Kwanza River and upper Kasai River, a Congo River tributary, and "*L.*" aff. *johnstoni* 'Okavango' from the Okavango and Upper Zambezi drainages that is sister to "*L.*" *centralis*, the only known southern Africa *Lacustricola* species occurring in the eastern African Malagarasi River. The distinction between "*L.*" *johnstoni* and "*L.*" aff. *johnstoni* 'Okavango' in the field or relying only on morphology could be really challenging because both have the same body profile and occur sympatrically in the Okavango Delta. Thus, we consider the COI barcoding approach a useful tool in distinguishing both species, if their distinctiveness is confirmed with additional data apart from COI-barcoding.

Following an integrative taxonomy perspective, in addition to the COI molecular haplotype analysis, detailed information on the morphology, colouration pattern and osteology were presented for the first time for the until then little known "*L.*" *johnstoni* and "*L.*" *myaposae*. A detailed redescription of "*L.*" *johnstoni*, based on specimens from and close its type locality is herein considered the first step before describing new species and investigating more deeply the genetic and species diversity within the broadly distributed "*L.*" *johnstoni*. Despite the broad sampling, further studies directed to fill important gaps, applying different species delimitation methods and maybe incorporating different markers are needed to better understand the diversity within "*L.*" *johnstoni* and other southern Africa *Lacustricola* groups.

Acknowledgements

We are grateful to James Maclaine and Kevin Webb from the BMNH, London, UK in providing photographs and x-rays from the type series of "*L.*" *johnstoni* and "*L.*" *myaposae* and in providing new catalogue numbers for the lectotypes. We are also, grateful to Nkosinathi Mazungula for the assistance in the field and Tholoana Ntokoane for generating some of the "*Lacustricola*" sequences for this study. This work was support-

ed by the National Research Foundation (NRF) of South Africa under the Foundational Biodiversity Information Programme: Biodiversity surveys in priority inland areas (IBIP) grants (grant reference no. IBIP-BS13100251309). We hereby acknowledge the use of the equipment provided by the NRF-SAIAB Molecular Genetic Laboratory and the NRF-SAIAB Collection Management Centre. The authors acknowledge that opinions, findings, and conclusions or recommendations expressed in this publication generated by the NRF supported research are those of the authors and that the NRF accepts no liability whatsoever in this regard.

References

Ahl E (1928) Beiträge zur Systematik der africanischen Zahnkarpfen. Zoologischer Anzeiger 79: 115–116.

Bragança PHN, Costa WJEM (2018) Time-calibrated molecular phylogeny reveals a Miocene–Pliocene diversification in the Amazon miniature killifish genus *Fluviphylax* (Cyprinodontiformes: Cyprinodontoidei). Organisms, Diversity and Evolution 18: 345–353. https://doi.org/10.1007/s13127-018-0373-7

Bragança PHN, Costa WJEM (2019) Multigene fossil-calibrated analysis of the African lampeyes (Cyprinodontoidei: Procatopodidae) reveals an early Oligocene origin and Neogene diversification driven by palaeogeographic and palaeoclimatic events. Organisms, Diversity and Evolution 19: 1–18. https://doi.org/10.1007/s13127-019-00396-1

Bragança PHN, Amorim PF, Costa WJEM (2018) Pantanodontidae (Teleostei, Cyprinodontiformes), the sister group to all other cyprinodontoid killifishes as inferred by molecular data. Zoosystematics and Evolution 94: 137–145. https://doi.org/10.3897/zse.94.22173

Boulenger GA (1906) Fourth contribution to the ichthyology of Lake Tanganyika. Report on the collection of fishes made by Dr. W. A. Cunnington during the Third Tanganyika Expedition, 1904–1905. Transactions of the Zoological Society of London 17: 537–601. https://doi.org/10.1111/j.1096-3642.1905.tb00037.x

Boulenger GA (1908) On a collection of freshwater fishes, Batrachians and Reptiles from Natal and Zululand, with descriptions of new species. Annals of the Natal government. 1: 219–239.

Boulenger GA (1912) Description d'un poisson nouveau du genre *Haplochilus* provenent du Katanga. Revue de Zoologie Africaine 2: 47–48.

Boulenger GA (1913) Sur une petite collection de poissons récueillis das l'Uelé, par la mission dirigée par M. Hutereau. Revue de Zoologie Africaine 2(2): 155–161.

Chakrabarty P (2010) Genetypes: a concept to help integrate molecular phylogenetics and taxonomy. Zootaxa 2632: 67–68. https://doi.org/10.11646/zootaxa.2632.1.4

Clausen HS (1967) Tropical Old World cyprinodonts. Akademisk Forlag, Copenhagen, 64 pp.

Costa WJEM (1988) Sistemática e distribuição do complexo de espécies *Cynolebias minimus* (Cyprinodontiformes, Rivulidae), com a descrição de duas espécies novas. Revista Brasileira de Zoologia 5: 557–570. https://doi.org/10.1590/S0101-81751988000400004

Costa WJEM (1996) Relationships, monophyly and three new species of the neotropical miniature poeciliid genus *Fluviphylax* (Cyprinodontiformes: Cyprinodontoidei). Ichthyological Exploration of Freshwaters 7: 111–130.

Costa WJEM (2006) Descriptive morphology and phylogenetic relationships among species of the Neotropical annual killifish genera *Nematolebias* and *Simpsonichthys* (Cyprinodontiformes: Aplocheiloidei: Rivulidae). Neotropical Ichthyology 4: 1–26. https://doi.org/10.1590/S1679-62252006000100001

Darriba D, Taboada GL, Doallo R, Posada D (2012) jModelTest 2: more models, new heuristics and parallel computing. Nature Methods 9: 772. https://doi.org/10.1038/nmeth.2109

Felsenstein J (1985) Confidence limits on phylogenies: an approach using the bootstrap. Evolution 39: 783–791. https://doi.org/10.1111/j.1558-5646.1985.tb00420.x

Folmer O, Black M, Hoeh W, Lutz R, Vrijenhoek R (1994) DNA primers for amplification of mitochondrial cytochrome c oxidase subunit I from diverse metazoan invertebrates. Molecular Marine Biology and Biotechnology 3: 294–299.

Fowler HW (1935) Scientific results of the Vernay-Lang Kalahari expedition, March to September 1930. Fresh-water fishes. Annals of the Transvaal Museum 16: 251–293.

Ghedotti MJ (2000) Phylogenetic analysis and taxonomy of the poecilioid fishes (Teleostei: Cyprinodontiformes). Zoological Journal of the Linnean Society 130: 1–53. https://doi.org/10.1111/j.1096-3642.2000.tb02194.x

Gosline WA (1949) The sensory canals of the head in some cyprinodont fishes, with particular reference to the genus *Fundulus*. Occasional Papers of the Museum of Zoology from University of Michigan 519: 1–17.

Günther A (1894) Second report on the reptiles, batrachians and fishes transmitted by Mr. H.H. Johnston C.B. from British Central Africa. Proceedings of the Zoological Society of London 1894: 616–628.

Helmstetter AJ, Papadopulos AST, Igea J, Van Dooren TJM, Leroi AM, Savolainen V (2016) Viviparity stimulates diversification in an order of fish. Nature Communications 7: 11271. https://doi.org/10.1038/ncomms11271

Hoedeman JJ (1956) Die bisher beschriebenen Formen und Arten der Gattung *Rivulus* Poey. Aquarium Terrarium 1956: 199–202.

Huber JH (1999) Updates to the phylogeny and systematics of the African lampeye schooling cyprinodonts (Cyprinodontiformes: Aplocheilichthyinae). Cybium 23: 53–77.

Kumar S, Stecher G, Tamura K (2016) MEGA7: Molecular evolutionary genetics analysis version 7.0 for bigger datasets. Molecular Biology and Evolution 33: 1870–1874. https://doi.org/10.1093/molbev/msw054

Myers GS (1924) New genera of African poeciliid fishes. Copeia 129: 42–43. https://doi.org/10.2307/1436003

Myers GS (1924b) A new Poeciliid fish of the genus *Micropanchax* from Ubangui. American Museum Novitates 122: 1–3.

Parenti LR (1981) A phylogenetic and biogeographic analysis of cyprinodontiform fishes (Teleostei, Atherinomorpha). Bulletin of the American Museum of Natural History 168: 335–357.

Pohl M, Milvertz FC, Meyer A, Vences M (2015) Multigene phylogeny of cyprinodontiform fishes suggests continental radiations and a rogue taxon position of *Pantanodon*. Vertebrate Zoology 65: 37–44.

Poll M (1967) Contribution à la faune ichthyologique de l'Angola. Publicações Culturais, Companhia de Diamantes de Angola (DIAMANG), Lisbon, 381 pp.

Poll M, Lambert JG (1965) Contribution a L'etude systematic et zoogeographique des Procatopodinae de L'Afrique central (Pisces, Cyprinodontidae). Bulletin des Séances. Académie Royale des Sciences d'Outre-Mer 2: 615–631.

Pollux BJA, Meredith RW, Springer MS, Garland T, Reznick DN (2014) The evolution of the placenta drives a shift in sexual selection in live-bearing fish. Nature 513: 233–236. https://doi.org/10.1038/nature13451

Reznick DN, Furness AI, Meredith RW, Springer MS (2017) The origin and biogeographic diversification of fishes in the family Poeciliidae. PLoS One 12: e0172546. https://doi.org/10.1371/journal.pone.0172546

Ronquist F, Teslenko M, Van der Mark P, Ayres D, Darling A, Hohna S et al. (2012) MrBayes 3.2: Efficient Bayesian phylogenetic inference and model choice across a large model space. Systematic Biology 61: 539–542.

Seegers L (1996) The Fishes of the Lake Rukwa Drainage. Annales du Musée Royal de l'Afrique Centrale, Sciences Zoologiques 287: 1–407.

Skelton PH (2001) A Complete Guide to the Freshwater Fishes of Southern Africa. Struik Publishers, Cape Town, 395 pp.

Sunnucks P, England PR, Taylor AC, Hales DF (1996) Microsatellite and chromosome evolution of parthenogenetic Sitobion aphids in Australia. Genetics 144: 747–756.

Taylor WR, Dyke V (1985) Revised procedures for staining and clearing small fishes and other vertebrates for bone and cartilage study. Cybium 9: 107–109.

Van der Zee JR, Sonnnenberg R, Munene JJMM (2015) *Hypsopanchax stiassnyae*, a new poeciliid fish from the Lulua River (Democratic Republic of Congo) (Teleostei: Cyprinodontiformes). Ichthyological Exploration of Freshwaters 26: 87–96.

Wildekamp RH, Romand R, Scheel JJ (1986) Cyprinodontidae. In: Daget J, Gosse JP, Van den Audenaerde, T (Eds) Check–list of the freshwater fishes of Africa 2 (CLOFFA 2). ISNB, MRAC, ORSTOM, Brussels, Tervuren, Paris, 165–276.

Zwickl DJ (2006) Genetic algorithm approaches for the phylogenetic analysis of large biological sequence datasets under the maximum likelihood criterion. PhD thesis, Austin, Texas, United States of America: University of Texas at Austin.

Supplementary material 1

Species localities and Genbank Acession numbers: acession numbers in bold refers to sequences developed in the present study

Authors: Pedro H.N. Bragança, Ryan M. van Zeeventer, Roger Bills, Denis Tweddle, Albert Chakona

Data type: species data

Link: https://doi.org/10.3897/zookeys.923.48420.suppl1

ZooKeys 923: 115–140 (2020)
doi: 10.3897/zookeys.923.47172
http://zookeys.pensoft.net

RESEARCH ARTICLE

A peer-reviewed open-access journal
ZooKeys
Launched to accelerate biodiversity research

A new species of *Leptobrachella* (Anura, Megophryidae) from Guizhou Province, China

Tao Luo[1*], Ning Xiao[2*], Kai Gao[3], Jiang Zhou[1]

1 *State Engineering Tecenology Instiiute For Karst Desertification Control School of Karst Science, Guizhou Normal University, Guiyang 550001, Guizhou, China* **2** *Guiyang Nursing Vocational College, Guiyang, Guizhou, 550003, China* **3** *Ministry of Education Key Laboratory for Biodiversity and Ecological Engineering, College of Life Sciences, Beijing Normal University, Beijing 100875, China*

Corresponding author: Jiang Zhou (zhoujiang@ioz.ac.cn)

Academic editor: Angelica Crottini | Received 9 October 2019 | Accepted 15 February 2020 | Published 1 April 2020

http://zoobank.org/104B0C71-0826-4C50-938B-FD78C4D403A6

Citation: Luo T, Xiao N, Gao K, Zhou J (2020) A new species of *Leptobrachella* (Anura, Megophryidae) from Guizhou Province, China. ZooKeys 923: 115–140. https://doi.org/10.3897/zookeys.923.47172

Abstract

This study describes a new species of the genus *Leptobrachella*, *Leptobrachella suiyangensis* **sp. nov.** from the Huoqiuba Nature Reserve, Suiyang County, Guizhou Province, China, based on morphological data and phylogenetic analyses (16S rRNA mtDNA). The new species can be distinguished from other congeners by the molecular divergence and by a combination of morphological characters, including body size, dorsal and ventral patterns, dorsal skin texture, size of the pectoral and femoral glands, degree of webbing and fringing on the toes and fingers, dorsum coloration, and iris coloration in life. Currently, the genus *Leptobrachella* contains 75 species, 21 of which are found in China, including seven species reported from Guizhou Province. The uncorrected sequence divergence percentage between *Leptobrachella suiyangensis* **sp. nov.** and all homologous DNA sequences available for the 16S rRNA gene was found to be >4.7%. The new record of the species and its relationships with others in the same genus imply that species distribution, habitat variation, environmental adaptation, and diversity of the genus *Leptobrachella* in southwest China need to be further investigated.

* These authors contributed equally to this paper

Keywords
Leptobrachella suiyangensis sp. nov., mitochondrial DNA, morphology, Southwest China

Introduction

The genus *Leptolalax* Dubois, 1983 in the family Megophryidae Bonaparte, 1850 is regarded to be closely associated with the genus *Leptobrachella* Smith, 1925 and has been assigned as a synonym of the genus *Leptobrachella* based on a large-scale molecular analysis (Chen et al. 2018). The genus *Leptobrachella* is now considered to contain 74 species. The genus is widely distributed from southwestern China to northeastern India and Myanmar (Fei et al. 2012; Frost 2019), extending to mainland Indochina, peninsular Malaysia, and the islands of Borneo (Rowley et al. 2016, 2017a; Yang et al. 2016; Yuan et al. 2017; Wang et al. 2018; Nguyen et al. 2018). Currently, 20 species of this genus are known from China. They are: *Leptobrachella alpina* (Fei, Ye & Li, 1990) and *L. bourreti* (Dubois, 1983) from Yunnan and Guangxi; *L. eos* (Ohler, Wollenberg, Grosjean, Hendrix, Vences, Ziegler & Dubois, 2011) and *L. nyx* (Ohler, Wollenberg, Grosjean, Hendrix, Vences, Ziegler & Dubois, 2011) from Yunnan; *L. laui* (Sung, Yang & Wang, 2014) and *L. yunkaiensis* Wang, Li, Lyu & Wang, 2018 from southern Guangdong, including Hong Kong; *L. liui* (Fei & Ye, 1990) from Fujian, Jiangxi, Guangdong, Guangxi, Hunan, and Guizhou; *L. oshanensis* (Liu, 1950) from Gansu, Sichuan, Chongqing, Guizhou, and Hubei; *L. purpuraventra* Wang, Li, Li, Chen & Wang, 2019 and *L. bijie* Wang, Li, Li, Chen & Wang, 2019 from Guizhou; *L. purpurus* (Yang, Zeng & Wang, 2018), *L. pelodytoides* (Boulenger, 1893), *L. tengchongensis* (Yang, Wang, Chen & Rao, 2016) and *L. yingjiangensis* (Yang, Zeng & Wang, 2018) from Yunnan; *L. ventripunctata* (Fei, Ye & Li, 1990) from Guizhou and Yunnan; *L. mangshanensis* (Hou, Zhang, Hu, Li, Shi, Chen, Mo & Wang, 2018) from southern Hunan, and *L. sungi* (Lathrop, Murphy, Orlov & Ho, 1998), *L. maoershanensis* (Yuan, Sun, Chen, Rowley & Che, 2017), *L. shangsiensis* Chen, Liao, Zhou & Mo, 2019, and *L. wuhuangmontis* Wang, Yang & Wang, 2018 from Guangxi (Sung et al. 2014; Yang et al. 2016, 2018; Yuan et al. 2017; Wang et al. 2018, 2019; Hou et al. 2018; Chen et al. 2018, 2019; Wang et al. 2019; AmphibiaChina 2019).

During a field survey in June 2018 in a montane evergreen forest, Suiyang County, Guizhou Province (Fig. 1), we collected three different species of the family Megophryidae co-occurring in this small-fragmented forest. The specimens could be morphologically separated from one another. Subsequent studies based on morphological and molecular data indicated that two of the three could be classified as *Megophrys minor* Stejneger and *M. spinata* Liu and Hu, while the third population, differing significantly from the other two, was further analyzed via morphological characters. Subsequent 16S rRNA sequences from these specimens revealed that the collection represented distinct evolving lineages and belong to the genus *Lepobrachella*. Combining morphological characters, acoustic data, and molecular divergence, we described the specimens as a new species.

Materials and methods

Sampling

Eight specimens collected from the aforementioned area (Fig. 1) were euthanized with chlorobutanol solution and fixed in 10% formalin for 24 h, and then stored in 75% ethanol. Liver and muscular tissues were taken before fixing and preserved in 95% alcohol at -20 °C. All of the specimens are kept at the College of Life Sciences, Guizhou Normal University (GZNU), Guiyang City, Guizhou Province, China.

DNA Extraction, PCR and sequencing

DNA samples were extracted from muscular tissues with a DNA extraction kit (Tiangen Biotech (Beijing) Co. Ltd). The mitochondrial gene and 16S ribosomal RNA gene (16S rRNA) were sequenced (951bp). The fragmented genes were amplified with primer pairs L3975 (5'-CGCCTGTTTACCAAAAACAT-3') and H4551 (5'-CCGGTCTGAACTCAGATCACGT-3') for 16S rRNA (Simon et al. 1994). PCR amplifications were performed in a 20 μl reaction volume with the following cycling conditions: an initial denaturing step at 95 °C for five min; 35 cycles of denaturing at 95 °C for 40 s, annealing at 53 °C for 40 s and extending at 72 °C for 1 min, followed by a final extending

Figure 1. Collection locality (red circle) of *Leptobrachella suiyangensis* sp. nov. from Suiyang County, Guizhou province, China used in this study.

step of 72 °C for 10 min. PCR products were purified with spin columns. The purified products were sequenced with both forward and reverse primers using a BigDye Terminator Cycle Sequencing Kit according to the guidelines of the manufacturer. The products were sequenced on an ABI Prism 3730 automated DNA sequencer at Shanghai Majorbio Bio-pharm Technology Co. Ltd. All sequences have been deposited in GenBank (Table 1). For molecular analyses, a total of 77 sequences (74 sequences downloaded from GenBank and three our new sequences) from 55 species of the genus *Leptobrachella* were used, including one undescribed species from C hina, that is, the populations from Huoqiuba Nature Reserve, Suiyang County, and Guizhou Province. Three species which sequences downloaded from GenBank are used as outgroups (*Leptobrachium huashen* Fei & Ye, 2005, *Leptobrachium* cf. *chapaense* (Bourret, 1937) and *Megophrys major* Boulenger, 1908 (Chen et al. 2018; Wang et al. 2019; Table 1).

Table 1. Localities and voucher data for all specimens used in this study.

ID	Species	Locality	Voucher no.	GenBank no.
1	*Leptobrachella suiyangensis* sp.nov.	Suiyang County, Guizhou, China	GZNU20180606002	MK829648
2	*Leptobrachella suiyangensis* sp.nov.	Suiyang County, Guizhou, China	GZNU20180606005	MK829649
3	*Leptobrachella suiyangensis* sp.nov.	Suiyang County, Guizhou, China	GZNU20180606006	MK829650
4	*Leptobrachella aerea*	Vilabuly, Savannakhet, Laos	NCSM 76038	MH055809
5	*Leptobrachella aerea*	Phong Nha-Ke Bang, Quang Binh, Vietnam	RH60165	JN848437
6	*Leptobrachella alpina*	Huangcaoling, Yunnan, China	KIZ046816	MH055866
7	*Leptobrachella applebyi*	Song Thanh Nature Reserve, Quang Nam, Vietnam	AMS R171704	HM133598
8	*Leptobrachella baluensis*	Tambunan, Sabah, Borneo, Malaysia	SP 21604	LC056792
9	*Leptobrachella bidoupensis*	Bidoup, Lam Dong, Vietnam	NCSM 77321	HQ902883
10	*Leptobrachella bijie*	Zhaozishan Nature Reserve, Bijie City, Guizhou, China	SYS a007313/CIB110002	MK414532
11	*Leptobrachella bijie*	Zhaozishan Nature Reserve, Bijie City, Guizhou, China	SYS a007314	MK414533
12	*Leptobrachella botsfordi*	Fansipan, Lao Cai, Vietnam	AMS R 176540	MH055952
13	*Leptobrachella bourreti*	Sapa, Lao Cai, Vietnam	1999.566	KR827860
14	*Leptobrachella brevicrus*	Gunung Mulu National Park, Sarawak, Malaysia	UNIMAS 8957	KJ831303
15	*Leptobrachella dringi*	Gunung Mulu, Malaysia	KUHE:55610	AB847553
16	*Leptobrachella eos*	Boun Tay, Phongsaly, Laos	NCSM 80551	MH055887
17	*Leptobrachella eos*	Zhushihe, Yunnan, China	SYS a003959	MH055888
18	*Leptobrachella firthi*	Ngoc Linh Nature Reserve, Kon Tum, Vietnam	AMS: R 176506	JQ739207
19	*Leptobrachella fritinniens*	Gunung Mulu, Malaysia	KUHE55371	AB847557
20	*Leptobrachella gracilis*	Gunung Mulu, Malaysia	KUHE55624	AB847560
21	*Leptobrachella hamidi*	Bukit Lanjan, Selangor, Malaysia	KUHE17545	AB969286
22	*Leptobrachella heteropus*	Larut, Perak, Malaysia	KUHE15487	AB530453
23	*Leptobrachella isos*	Gia Lai, Vietnam	AMS R 176469	KT824767
24	*Leptobrachella itiokai*	Mulu NP, Sarawak, Borneo, Malaysia	KUHE 55845	LC137802
25	*Leptobrachella juliandringi*	Mulu NP, Sarawak, Borneo, Malaysia	KUHE 55333	LC056780
26	*Leptobrachella kajangensis*	Tioman, Malaysia	LSUHC 4431	LC202001
27	*Leptobrachella kecil*	Cameron, Malaysia	KUHE 52440	LC202004
28	*Leptobrachella khasiorum*	Khasi Hills, Meghalaya, India	SDBDU 2009.329	KY022303
29	*Leptobrachella liui*	Wuyi Shan, Fujian, China	SYS a001597	KM014547
30	*Leptobrachella liui*	Wuyi Shan, Fujian, China	ZYCA907	MH055908
31	*Leptobrachella laui*	Shenzhen, Guangdong, China	SYS a002450	MH055904
32	*Leptobrachella laui*	Shenzhen, Guangdong, China	SYS a001515	KM014545

ID	Species	Locality	Voucher no.	GenBank no.
33	*Leptobrachella macrops*	Phu Yen, Vietnam	ZMMU-A5823	MG787993
34	*Leptobrachella mangshanensis*	Mangshan, Hunan, China	MSZTC201701	MG132196
35	*Leptobrachella mangshanensis*	Mangshan, Hunan, China	MSZTC201702	MG132197
36	*Leptobrachella maoershanensis*	Mao'er Shan, Guangxi, China	KIZ07614	MH055927
37	*Leptobrachella maoershanensis*	Mao'er Shan, Guangxi, China	KIZ027236	MH055928
38	*Leptobrachella marmorata*	Borneo, Malaysia	KUHE53227	AB969289
39	*Leptobrachella maura*	Borneo, Malaysia	SP21450	AB847559
40	*Leptobrachella melanoleucus*	Surat Thani, Thailand	KUHE:23845	LC201999
41	*Leptobrachella melica*	Cambodia, Ratanakiri	MVZ258198	HM133600
42	*Leptobrachella minimus*	Doi Chiang Dao, Chiangmai, Thailand	THNHM07418	JN848402
43	*Leptobrachella minimus*	Doi Suthep, Thailand	KUHE:19201	LC201981
44	*Leptobrachella mjobergi*	Gading NP, Sarawak, Borneo, Malaysia	KUHE:47872	LC056787
45	*Leptobrachella nahangensis*	Na Hang Nature Reserve, Tuyen Quang, Vietnam	ROM 7035	MH055853
46	*Leptobrachella nahangensis*	Na Hang, Tuyen Quang, Vietnam	ZMMU-NAP-02259	MH055854
47	*Leptobrachella nyx*	Ha Giang, Vietnam	ROM 36692	MH055816
48	*Leptobrachella oshanensis*	Emei Shan, Sichuan, China	KIZ025776	MH055895
49	*Leptobrachella oshanensis*	Emei Shan, Sichuan, China	Tissue ID: YPX37492	MH055896
50	*Leptobrachella pallida*	Vietnam: Lam Dong	UNS00511	KU530190
51	*Leptobrachella parva*	Mulu National Park, Sarawak, Malaysia	KUHE:55308	LC056791
52	*Leptobrachella petrops*	Cham Chu Nature Reserve, Tuyen Quang, Vietnam	VNMN:2016 A.06	KY459998
53	*Leptobrachella picta*	Borneo, Malaysia	UNIMAS 8705	KJ831295
54	*Leptobrachella pluvialis*	Fansipan, Lao Cai, Vietnam	ROM 30685	MH055843
55	*Leptobrachella pluvialis*	Sapa, Lao Cai, Vietnam	ZMMU-A-5222-02262	MH055844
56	*Leptobrachella puhoatensis*	Pu Hu, Thanh Hoa, Vietnam	VNMN:2016 A.23	KY849587
57	*Leptobrachella purpura*	Yingjiang, Yunnan Province, China	SYS a006530	MG520354
58	*Leptobrachella purpura*	Yingjiang, Yunnan Province, China	SYS a006531	MG520355
59	*Leptobrachella purpuraventra*	Wujing Nature Reserve, Bijie City, Guizhou, China	SYS a007081	MK414517
60	*Leptobrachella purpuraventra*	Wujing Nature Reserve, Bijie City, Guizhou, China	SYS a007277/CIB110003	MK414518
61	*Leptobrachella pyrrhops*	Lam Dong, Vietnam	ZMMU A-5208	KP017575
62	*Leptobrachella sabahmontana*	Borneo, Malaysia	BORNEENSIS 12632	AB847551
63	*Leptobrachella shangsiensis*	Guangxi, China	NHMG1401032	MK095460
64	*Leptobrachella shangsiensis*	Guangxi, China	NHMG1401033	MK095461
65	*Leptobrachella solus*	Hala-Bala, Thailand	KUHE:23261	LC202007
66	*Leptobrachella solus*	Tam Dao, Vinh Phuc, Vietnam	ROM 20236	MH055858
67	*Leptobrachella tengchongensis*	Gaoligong Shan, Yunnan, China	SYS a004598	KU589209
68	*Leptobrachella tengchongensis*	Gaoligong Shan, Yunnan, China	SYS a003766	MH055897
69	*Leptobrachella ventripunctatus*	Zhushihe, Yunnan, China	SYS a004536	MH055831
70	*Leptobrachella wuhuangmontis*	Mt. Wuhuang, Pubei County, Guangxi, China	SYS a003485	MH605577
71	*Leptobrachella wuhuangmontis*	Mt. Wuhuang, Pubei County, Guangxi, China	SYS a003486	MH605578
72	*Leptobrachella yingjiangensis*	Yingjiang, Yunnan, China	SYS a006533	MG520350
73	*Leptobrachella yingjiangensis*	Yingjiang, Yunnan, China	SYS a006532	MG520351
74	*Leptobrachella yunkaiensis*	Dawuling Forest Station, Maoming City, Guangdong, China	SYS a004663	MH605584
75	*Leptobrachella yunkaiensis*	Dawuling Forest Station, Maoming City, Guangdong, China	SYS a004664 / CIB107272	MH605585
76	*Leptobrachella zhangyapingi*	Chiang Mai, Thailand	KIZ07258	MH055864
77	*Leptobrachella zhangyapingi*	Pang Num Poo, Chiang Mai Province,Thailand	JK-2013	JX069979
78	*Leptobrachium huashen*	Yunnan, China	KIZ049025	KX811931
79	*Leptobrachium* cf. *chapaense*	Sapa, Lao Cai, Vietnam	AMS R 171623	KR018126
80	*Megophrys major*	Kon Tum, Vietnam	AMS R 173870	KY476333

Phylogenetic analyses

All sequences were aligned by MUSCLE v. 3.6 with the default settings (Edgar 2004). Trimming with the gaps partially deleted was performed in MEGA 7.0 (Kumar et al. 2016), while within high variable regions, all gaps were removed.

Phylogenetic trees were constructed with both Maximum Likelihood (ML) and Bayesian Inference (BI). The ML was conducted in IQ-TREE (Nguyen et al. 2015) with 2000 ultrafast bootstrapping (Hoang et al. 2018) and was performed until a correlation coefficient of at least 0.99 was reached. The BI was performed in MrBayes v. 3.2.1 (Ronquist et al. 2012), and the best-fit model was obtained by the Akaike Information Criterion (AIC) computed with PartitionFinder 2 (Lanfear et al. 2016), resulting in the best-fitting nucleotide substitution models of GTR + I + G with for BI and ML analysis. Two independent processes were conducted for 10 million generations, sampling every 1000, with four independent chains and a burn-in of 25%. Convergence was assessed referring to the criteria of all parameters having reached stationarity and having obtained satisfactory effective sample sizes (>200) using Tracer v. 1.6. (Rambaut et al. 2014). Nodes in the trees were considered well supported when Bayesian posterior probabilities (BPP) were ≥0.95 and ML ultrafast bootstrap values (UFB) was ≥95 % (Chen et al. 2018; Hoang et al. 2018). Uncorrected *p*-distances based on 16S rRNA were calculated in MEGA v. 7.0 (Kumar et al. 2016).

Morphological and morphometric analyses

Morphometric data were taken from eight of most well-preserved adult specimens. Measurements were recorded to the nearest 0.1 mm (Watters et al. 2016) with digital calipers following the methods of Fei et al. (2009) and Rowley et al. (2013). These measurements were as follows:

SVL snout-vent length (from tip of snout to vent)
HDL head length (from tip of snout to rear of jaws)
HDW head width (head width at commissure of jaws)
SNT snout length (from tip of snout to the anterior corner of the eye)
EYE eye diameter (diameter of the exposed portion of the eyeballs)
IOD interorbital distance (minimum distance between upper eyelids)
IND internasal distance (distance between nares)
UEW upper eyelid width (measured as the greatest width of the upper eyelid)
NEL nostril-eyelid length (distance from nostril to eyelid)
NSL nostril-snout length (distance from nostril to snout)
TMP tympanum diameter (horizontal diameter of tympanum)
TEY tympanum-eye distance (distance from anterior edge of tympanum to posterior corner of eye)
TIB tibia length (distance from knee to heel)
ML manus length (distance from tip of third digit to proximal edge of inner palmar tubercle)

LAHL length of the lower arm and hand (distance from tip of the third finger to elbow)
HLL hindlimb length (distance from tip of fourth toe to vent)
FOT foot length (from proximal edge of the inner metatarsal tubercle to the tip of the fourth toe)

Sex was determined by direct observation of calls in life, the presence of internal vocal sac openings, and the presence of eggs in the abdomen through external inspection. Comparative morphological data of *Leptobrachella* species were obtained from the references listed in Table 2. Due to the high likelihood of undiagnosed diversity within the genus (Rowley et al. 2016; Yang et al. 2016), where available, we relied on examination of topotypic material and/or original species descriptions.

Table 2. Obtained references of 74 known congeners of the genus *Leptobrachella*, respectively.

ID	Leptobrachella species	Literature obtained
1	*L. aerea* (Rowley, Stuart, Richards, Phimmachak & Sivongxay, 2010)	Rowley et al. 2010c
2	*L. alpina* (Fei, Ye & Li, 1990)	Fei et al. 2009
3	*L. applebyi* (Rowley & Cao, 2009)	Rowley and Cao 2009
4	*L. arayai* (Matsui, 1997)	Matsui 1997
5	*L. ardens* (Rowley, Tran, Le, Dau, Peloso, Nguyen, Hoang, Nguyen & Ziegler, 2016)	Rowley et al. 2016
6	*L. baluensis* Smith, 1931	Dring 1983; Eto et al. 2016
7	*L. bidoupensis* (Rowley, Le, Tran & Hoang, 2011)	Rowley et al. 2011
8	*L. bijie* Wang, Li, Li, Chen & Wang, 2019	Wang et al. 2019
9	*L. bondangensis* Eto, Matsui, Hamidy, Munir & Iskandar, 2018	Eto et al. 2018
10	*L. botsfordi* (Rowley, Dau & Nguyen, 2013)	Rowley et al. 2013
11	*L. bourreti* (Dubois, 1983)	Ohler et al. 2011
12	*L. brevicrus* Dring, 1983	Dring 1983; Eto et al. 2015
13	*L. crocea* (Rowley, Hoang, Le, Dau & Cao, 2010)	Rowley et al. 2010a
14	*L. dringi* (Dubois, 1987)	Inger et al. 1995; Matsui and Dehling 2012
15	*L. eos* (Ohler, Wollenberg, Grosjean, Hendrix, Vences, Ziegler & Dubois, 2011)	Ohler et al. 2011
16	*L. firthi* (Rowley, Hoang, Dau, Le & Cao, 2012)	Rowley et al. 2012
17	*L. fritinniens* (Dehling & Matsui, 2013)	Dehling and Matsui 2013
18	*L. fuliginosa* (Matsui, 2006)	Matsui 2006
19	*L. fusca* Eto, Matsui, Hamidy, Munir & Iskandar, 2018	Eto et al. 2018
20	*L. gracilis* (Günther, 1872)	Günther 1872; Dehling 2012b
21	*L. hamidi* (Matsui, 1997)	Matsui 1997
22	*L. heteropus* (Boulenger, 1900)	Boulenger 1900
23	*L. isos* (Rowley, Stuart, Neang, Hoang, Dau, Nguyen & Emmett, 2015)	Rowley et al. 2015a
24	*L. itiokai* Eto, Matsui & Nishikawa, 2016	Eto et al. 2016
25	*L. juliandringi* Eto, Matsui & Nishikawa, 2015	Eto et al. 2015
26	*L. kajangensis* (Grismer, Grismer & Youmans, 2004)	Grismer et al. 2004
27	*L. kalonensis* (Rowley, Tran, Le, Dau, Peloso, Nguyen, Hoang, Nguyen & Ziegler, 2016)	Rowley et al. 2016
28	*L. kecil* (Matsui, Belabut, Ahmad & Yong, 2009)	Matsui et al. 2009
29	*L. khasiorum* (Das, Tron, Rangad & Hooroo, 2010)	Das et al. 2010
30	*L. lateralis* (Anderson, 1871)	Anderson 1871; Humtsoe et al. 2008
31	*L. laui* (Sung, Yang & Wang, 2014)	Sung et al. 2014
32	*L. liui* (Fei & Ye, 1990)	Fei et al. 2009; Sung et al. 2014
33	*L. macrops* (Duong, Do, Ngo, Nguyen & Poyarkov, 2018)	Duong et al. 2018
34	*L. maculosa* (Rowley, Tran, Le, Dau, Peloso, Nguyen, Hoang, Nguyen & Ziegler, 2016)	Rowley et al. 2016
35	*L. mangshanensis* (Hou, Zhang, Hu, Li, Shi, Chen, Mo & Wang, 2018)	Hou et al. 2018
36	*L. maoershanensis* (Yuan, Sun, Chen, Rowley & Che, 2017)	Yuan et al. 2017
37	*L. marmorata* (Matsui, Zainudin & Nishikawa, 2014)	Matsui et al. 2014b

ID	Leptobrachella species	Literature obtained
38	*L. maura* (Inger, Lakim, Biun & Yambun, 1997)	Inger et al. 1997
39	*L. melanoleuca* (Matsui, 2006)	Matsui 2006
40	*L. melica* (Rowley, Stuart, Neang & Emmett, 2010)	Rowley et al. 2010b
41	*L. minima* (Taylor, 1962)	Taylor 1962; Ohler et al. 2011
42	*L. mjobergi* Smith, 1925	Eto et al. 2015
43	*L. nahangensis* (Lathrop, Murphy, Orlov & Ho, 1998)	Lathrop et al. 1998
44	*L. natunae* (Günther, 1895)	Günther 1895
45	*L. nokrekensis* (Mathew & Sen, 2010)	Mathew and Sen 2010
46	*L. nyx* (Ohler, Wollenberg, Grosjean, Hendrix, Vences, Ziegler & Dubois, 2011)	Ohler et al. 2011
47	*L. oshanensis* (Liu, 1950)	Fei et al. 2009
48	*L. pallida* (Rowley, Tran, Le, Dau, Peloso, Nguyen, Hoang, Nguyen & Ziegler, 2016)	Rowley et al. 2016
49	*L. palmata* Inger & Stuebing, 1992	Inger and Stuebing 1992
50	*L. parva* Dring, 1983	Dring 1983
51	*L. pelodytoides* (Boulenger, 1893)	Boulenger 1893; Ohler et al. 2011
52	*L. petrops* (Rowley, Dau, Hoang, Le, Cutajar & Nguyen, 2017)	Rowley et al. 2017a
53	*L. picta* (Malkmus, 1992)	Malkmus 1992
54	*L. platycephala* (Dehling, 2012)	Dehling 2012a
55	*L. pluvialis* (Ohler, Marquis, Swan & Grosjean, 2000)	Ohler et al. 2000, 2011
56	*L. puhoatensis* (Rowley, Dau & Cao, 2017)	Rowley et al. 2017b
57	*L. purpuraventra* Wang, Li, Li, Chen & Wang, 2019	Wang et al. 2019
58	*L. purpurus* (Yang, Zeng & Wang, 2018)	Yang et al. 2018
59	*L. pyrrhops* (Poyarkov, Rowley, Gogoleva, Vassilieva, Galoyan & Orlov, 2015)	Poyarkov et al. 2015
60	*L. rowleyae* (Nguyen, Poyarkov, Le, Vo, Ninh, Duong, Murphy & Sang, 2018)	Nguyen et al. 2018
61	*L. sabahmontana* (Matsui, Nishikawa & Yambun, 2014)	Matsui et al. 2014a
62	*L. serasanae* Dring, 1983	Dring 1983
63	*L. shangsiensis* Chen, Liao, Zhou & Mo, 2019	Chen et al. 2019
64	*L. sola* (Matsui, 2006)	Matsui 2006
65	*L. sungi* (Lathrop, Murphy, Orlov & Ho, 1998)	Lathrop et al. 1998
66	*L. tadungensis* (Rowley, Tran, Le, Dau, Peloso, Nguyen, Hoang, Nguyen & Ziegler, 2016)	Rowley et al. 2016
67	*L. tamdil* (Sengupta, Sailo, Lalremsanga, Das & Das, 2010)	Sengupta et al. 2010
68	*L. tengchongensis* (Yang, Wang, Chen & Rao, 2016)	Yang et al. 2016
69	*L. tuberosa* (Inger, Orlov & Darevsky, 1999)	Inger et al.1999
70	*L. ventripunctata* (Fei, Ye & Li, 1990)	Fei et al. 2009
71	*L. wuhuangmontis* Wang, Yang & Wang, 2018	Wang et al. 2018
72	*L. yingjiangensis* (Yang, Zeng & Wang, 2018)	Yang et al. 2018
73	*L. yunkaiensis* Wang, Li, Lyu & Wang, 2018	Wang et al. 2018
74	*L. zhangyapingi* (Jiang, Yan, Suwannapoom, Chomdej & Che, 2013)	Jiang et al. 2013

Results

Phylogenetic trees from Maximum likelihood (ML) and Bayesian inference (BI) were constructed based on DNA sequences of the mitochondrial 16S rRNA gene with a length of 500 bp. The trees present identical topologies (Fig. 2) with the clustered population of *Leptobrachella* from Huoqiuba Nature Reserve, in which *L. alpina* + *L. purpurus* and the population of *Leptobrachella* from Huoqiuba Nature Reserve show relatively high node supporting values (0.68 in BI and 71% in ML) and exhibit a separate evolving lineage. The smallest pairwise genetic divergence between the population from Suiyang County and all other species of the genus *Leptobrachella* is 4.71%. This indicates that there is substantial genetic divergence between the species in *Leptobrachella* and the specimens from Suiyang County, indicating that this new population can be regarded to be a separate lineage and is valid to be described as a new species as below.

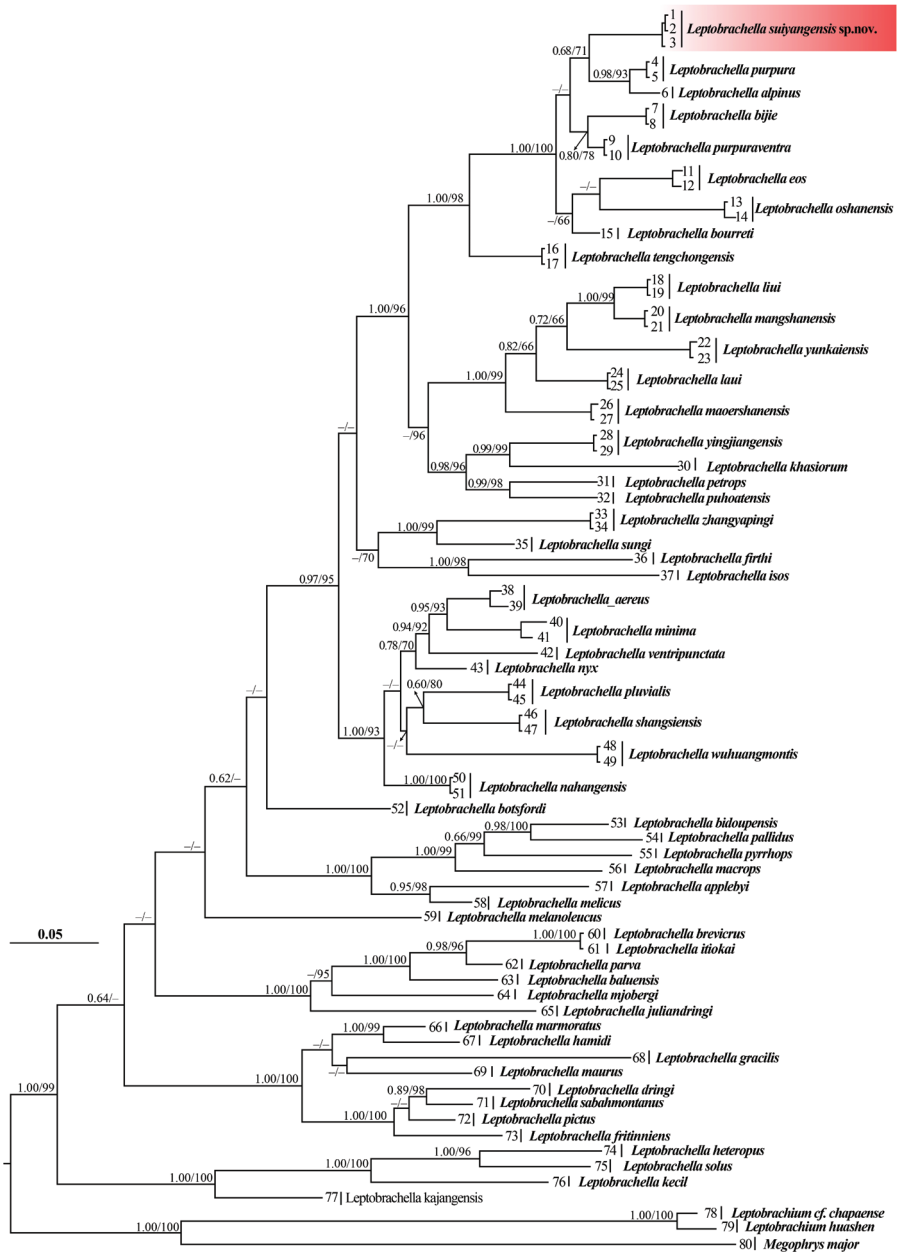

Figure 2. Bayesian inference tree derived from partial DNA sequences of the mitochondrial 16S r RNA gene. Numbers before slashes indicate Bayesian posterior probabilities (displayed >0.60 values), and numbers after slashes are ultrafast bootstrap support for maximum likelihood (2000 replicates) analyses (>60 retained). The symbol "–" represents value below 0.60/60. The scale bar represents 0.05 nucleotide substitutions per site.

Taxonomic account

***Leptobrachella suiyangensis* sp. nov.**
http://zoobank.org/75EDCF88-0293-40E9-83FE-47785145864C
Table 3, Figs 3, 4

Type material. ***Holotype.*** GZNU20180606007, adult male, collected by Tao Luo (TL hereafter) on 7 June 2018 from the Huoqiuba Nature Reserve (28.4805°N, 107.0764°E, 1501 m. a.s.l.; Fig. 1), Suiyang County, Guizhou Province, China.

Paratypes. Five adult males (GZNU20180606002, GZNU20180606005, GZNU20180606006, GZNU20180606008), and three adult females (GZNU20180606001, GZNU20180606003, GZNU20180606004). They were collected from the holotype locality on 6 June 2018.

Etymology. The specific epithet "suiyangensis" refers to the name of the holotype locality, Taibai Town in Suiyang County of Guizohu Province, China. We suggest as its English name "Suiyang Leaf-litter Toad," and its Chinese name as "Sui Yang Zhang Tu Chan (绥阳掌突蟾)".

Diagnosis. The specimens were assigned to the genus *Leptobrachella* on the basis of the following characters: (1) small body size; (2) having an elevated inner metacarpal tubercle; (3) having macro-glands on body (including supra-axillary, femoral and ventrolateral glands); (4) lacking vomerine teeth; (5) having small tubercles on eyelids; (6) anterior tip of snout with whitish vertical bar (Dubois 1983; Matsui 1997, 2006; Lathrop et al. 1998; Delorme et al. 2006; Das et al. 2010). *Leptobrachella suiyangensis* sp. nov. can be distinguished from its congeners by referring to the following characters: (1) small body size (SVL 28.7–29.7 mm in males, 30.5–33.5 mm in females); (2) dorsal skin shagreened, with some of the granules forming longitudinal short skin ridges; (3) tympanum distinctly discernible, slightly concave, with a deep, black, supratympanic line; (4) ventrolateral glands are distinct, forming a dotted line; (5) dorsal surface shagreened and granular, lacking enlarged tubercles or warts, with some of the granules forming short longitudinal folds; (6) flanks with several distinct and large dark blotches; (7) ventral surface of throat grey-white, and surface of chest and belly yellowish creamy-white with marbled texture or with irregular light brown speckling; (8) supra-axillary, femoral, pectoral and ventrolateral glands are distinctly visible; (9) absence of webbing and lateral fringes on fingers, and toes feature rudimentary webbing and a weak lateral fringes; (10) relatively short hindlimbs (TIB/SVL ratio in males 0.46–0.47); (11) longitudinal ridges under the toes are interrupted at the articulations; (12) relative finger lengths I <II < IV < III, relative toe lengths I < II < V < III < IV; (13) dorsum greyish-brown, with small light-orange granules and distinct darker brown markings scattered with irregular light-orange pigmentation, and bicolored iris, coppery orange on the upper half and silver grey on the lower half.

Description of the holotype. GZNU20180606007 (adult male), small body size (SVL 28.7 mm); the head length is slightly larger than the head width (HDL/HDW ratio 1.06); the snout is slightly protruding, projecting beyond the margin of the lower

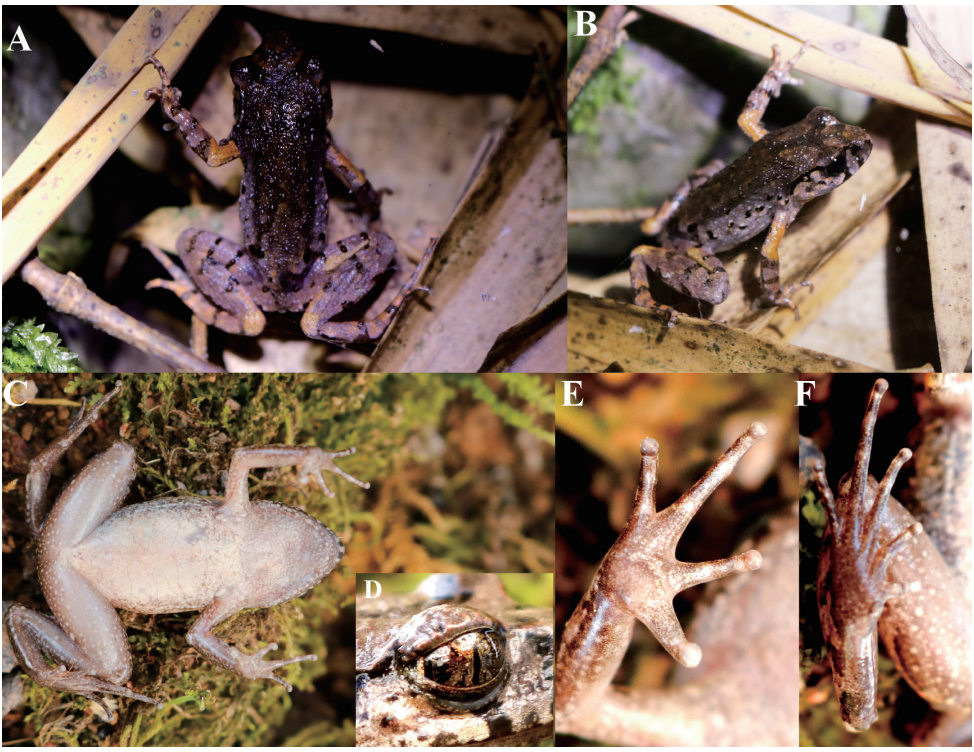

Figure 3. Holotype of *Leptobrachella suiyangensis* sp. nov. (GZNU20180606007) in life. **A** Dorsal view **B** Dorsolateral view **C** Ventral view **D** Right eye shown iris coloration **E** Volar view of the left hand **F** Plantar view of the left foot.

jaw; the nostril is between the snout and the eye (NSL/NEL ratio 0.39); the canthus rostralis is gently rounded; the loreal region is slightly concave; the interorbital space is flat; larger (IOD 2.9 mm) than the upper eyelid (1.6 mm in width), and the internarial distance is 2.8 mm; with vertical pupil; snout length is slightly larger than eye diameter (SNT/EYE ratio 1.71); tympanum is distinct and rounded, its diameter (TMP 2.1 mm) is smaller than that of the eye diameter (EYE 2.4 mm) and longer than the tympanum-eye distance (TMP/TEY ratio 1.91); deep black supratympanic line is present; weakly black supratympanic line exists (Fig. 3C); tympanic rim is distinctly elevated relative to the skin of the temporal region; supratympanic ridge is distinct, extending from the eye to the supra-axillary gland; a few indistinct tubercles present on supratympanic ridge; absent vomerine teeth; vocal sac openings is slit-like, located posterior-laterally on the floor of the mouth close to the margins of the mandible; long and wide tongue, with a small shallow notch at the posterior tip.

The tips of the fingers are rounded, slightly swollen; relative finger lengths are presented as: I <II < IV < III; nuptial pad is absent; absent subarticular tubercles (Fig. 3F); a large, round inner palmar tubercle is distinctly separated from a small, round outer palmar tubercle; finger webbing and dermal fringes absent. Toe tips are similar to those

of the fingers; the relative toe length is presented as: I <II <V<III <IV; absent subarticular tubercles; distinct dermal ridges present under the 3rd to 5th toes; pronounced larger, oval inner metatarsal tubercle, outer metatarsal tubercle is absent; rudimentary toe webbing; weak lateral fringes present on all toes. Tibia is slightly shorter than half of the snout-vent length (TIB/SVL ratio 0.46); tibiotarsal articulation reaches to the anterior eye; heels meet each other when thighs are appressed at right angles referring to the body.

Dorsal skin is shagreened and scattered with fine and rounded granules, some of the granules forming short longitudinal folds; ventral skin smooth; large pectoral gland, elongated oval, 1.5 mm in length; small femoral gland, rounded, 0.7 mm in diameter, situated on the posteroventral surface of the thigh, closer to tibiotarsal articulation than to the vent; risen supra-axillary gland, 1.3 mm in diameter; ventrolateral gland is distinct as small white dots forming an incomplete line (Fig. 3D).

Measurements of holotype (in mm). Holotype: SVL 28.7, HDL 9.9, HDW 9.3, SNT 4.1, EYE 2.4, IOD 2.9, INT 2.8, UEW 1.6, NEL 2.8, NSL 1.1, TMP 2.1, TEY 1.1, TIB 13.1, HND 7.2, LAHL 13.4, HLL 43.3, FOT 12.5.

Coloration of holotype in life. Dorsal skin purple-brown; brown-purplish with dark-brown marks between the eyes and the scapular region, which are scattered with some deep yellow-orange granules more concentrated on the upper eyelid (Fig. 3C). A dark brown Y-pattern exists between eyes, linked with dark brown W-shaped marks between axillae. Tympanum is light brown-grey; black-brown tubercles present on dorsum of the body and the limb; those on dorsal side are much more distinct and dense; anterior upper lip features distinct blackish-brown patches; transverse dark-brown bars exist on dorsal surface of the limbs two or three (elbow and upper arms are an exception); indistinct black or brown blotches present on the flanks from groin to axilla; elbow and upper arms have no dark bars but with distinct dark-orange coloration; fingers and toes show indistinct brown blotches; a black spot is present on the loreal region; lower edge of the upper drum ridge is prominently black; ventral surface of the throat is grey-white, and surface of chest and belly is yellowish creamy-white, ventral part with distinct or indistinct light brown speckling mixed with marble texture; ventral surface of the thighs is dark grey and scattered with small light white spots. Supra-axillary gland milky yellow; iris is bicolored, coppery orange on the upper half and silver grey on the lower half.

Coloration of holotype in preservative. In preservation, there are dark brown marks on the dorsum and flanks; dorsum of the body and hindlimbs are dark brown, while dorsum of the forelimbs is yellowish brown; transverse bars on the limbs become more distinct, and dark-brown patterns, marks and spots on the back are indistinct; ventral surface of the body is yellowish brown with brown marbling on the sides and chest; orange supra-axillary, femoral, pectoral and ventrolateral glands fade to greyish white.

Variations. Measurements of the type series are shown in Table 4. Females (mean of SVL (32.0 ± 1.5 mm, n = 3) have larger body size than males (mean of SVL 29.2 ± 0.4 mm, n = 5) (Table 4). In life (Fig. 5), all paratypes match overall characters of the holotype, except the surface of the belly that is scattered with brown speckling

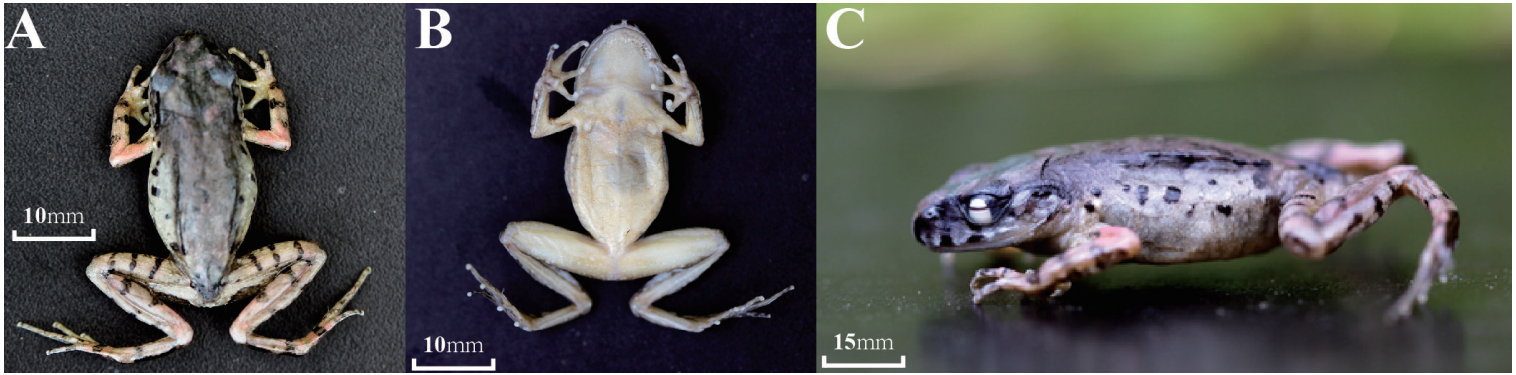

Figure 4. Holotype of *Leptobrachella suiyangensis* sp. nov. (GZNU20180606007) in preservative. **A** Dorsal view **B** Ventral views **C** Lateral views.

Table 3. Measurements (in mm) of the type series of *Leptobrachella suiyangensis* **sp.nov.** (H = holotype, P = paratype,M= male, F= female, another abbreviations defined in text).

Specimen	Type status	Sex	SVL	HDL	HDW	SNT	EYE	IOD	IND	UEW	NEL	NSL	TMP	TEY	TIB	HND	LAHL	HLL	FOT
GZNU20180606007	H	M	28.7	9.9	9.3	4.1	2.4	2.9	2.8	1.6	2.8	1.1	2.1	1.1	13.1	7.2	13.4	43.3	12.5
GZNU20180606008	P	M	29.2	10.5	9.8	4.6	2.8	2.8	2.9	2.1	2.3	1.7	1.2	1.9	13.4	7.0	13.2	43.4	12.9
GZNU20180606002	P	M	29.7	12.1	10.1	5.0	3.9	3.2	3.7	3.1	2.3	1.3	2.3	1.4	13.8	7.1	13.3	44.4	12.3
GZNU20180606005	P	M	29.0	11.8	10.3	4.5	3.3	3.4	3.1	2.0	2.7	1.1	1.9	1.6	13.5	6.5	13.4	41.8	12.9
GZNU20180606006	P	M	29.2	11.4	10.4	4.0	3.8	3.2	3.2	2.6	2.6	2.2	1.8	1.3	13.6	7.4	13.3	42.8	12.6
GZNU20180606001	P	F	32.0	12.6	10.7	4.7	3.7	3.5	3.5	3.0	2.4	1.3	2.6	1.7	15.2	7.1	13.4	44.7	13.9
GZNU20180606003	P	F	30.5	10.3	10.9	4.7	3.7	3.1	3.1	2.2	2.3	1.5	3.5	1.4	15.2	7.4	13.8	45.3	16.6
GZNU20180606004	P	F	33.5	13.1	12.1	4.9	3.6	3.1	3.6	2.8	3.1	1.8	3.8	1.7	17.4	8.1	16.7	53.8	14.4

Figure 5. Paratypes of *Leptobrachella suiyangensis* sp. nov. in life. **A** GZNU20180606005, adult male (**A**), (**B**) GZNU20180606002, adult male **C** GZNU20180606003, adult female.

Table 4. Measurements (in mm), and body proportions of *Leptobrachella suiyangensis* **sp.nov.** from Suiyang County, Guizhou Province, China.

Measurements	Males Range (mean ± SD), n = 5	Females Range (mean ± SD), n = 3
SVL	28.7–29.7 (29.2 ± 0.4)	30.5–33.5 (32.0 ± 1.5)
HDL	9.9–12.1 (11.1 ± 0.9)	10.3–13.1 (12.0 ± 1.5)
HDW	9.3–10.4 (10.0 ± 0.4)	10.7–12.1 (11.2 ± 0.8)
SNT	4.0–5.0 (4.4 ± 0.4)	4.7–4.9 (4.8 ± 0.1)
EYE	2.4–3.9 (3.2 ± 0.6)	3.6–3.7 (3.7 ± 0.1)
IOD	2.8–3.4 (3.1 ± 0.2)	3.1–3.5 (3.2 ± 0.2)
INT	2.8–3.7 (3.1 ± 0.4)	3.1–3.6 (3.4 ± 0.3)
UEW	1.6–3.1 (2.3 ± 0.6)	2.2–3.0 (2.7 ± 0.4)
NEL	2.3–2.8 (2.5 ± 0.2)	2.3–3.1 (2.6 ± 0.4)
NSL	1.1–2.2 (1.5 ± 0.5)	1.3–1.8(1.5 ± 0.3)
TMP	1.2–2.3 (1.9 ± 0.4)	2.6–3.8 (3.3 ± 0.6)
TEY	1.1–1.9 (1.5 ± 0.3)	1.4–1.7 (1.6 ± 0.2)
TIB	13.1–13.8 (13.5 ± 0.3)	15.2–17.4 (15.9 ± 1.3)
HND	6.5–7.4 (7.0 ± 0.3)	7.1–8.1 (7.5 ± 0.5)
LAHL	13.2–13.4 (13.3 ± 0.1)	13.4–16.7 (14.6 ± 1.8)
HLL	41.8–44.4 (43.1 ± 0.9)	44.7–53.8 (47.9 ± 5.1)
FOT	12.3–12.9 (12.6 ± 0.3)	13.9–16.6 (15.0 ± 1.4)
HDL/HDW	1.06–1.20 (1.12 ± 0.06)	0.90–1.20 (1.07 ± 0.15)
HDL/SVL	0.34–0.41 (0.38 ± 0.03)	0.30–0.40 (0.37 ± 0.06)
SNT/HDL	0.35–0.44 (0.40 ± 0.03)	0.40–0.50 (0.43 ± 0.06)
SNT/EYE	1.05–1.71 (1.41 ± 0.27)	1.30–1.40 (1.33 ± 0.06)
EYE/TMP	1.14–2.33 (1.80 ± 0.45)	1.00–1.40 (1.17 ± 0.21)
EYE/SNT	0.59–0.95 (0.73 ± 0.15)	0.70–0.80 (0.77 ± 0.06)
TMP/EYE	0.43–0.88 (0.59 ± 0.18)	0.70–1.10 (0.93 ± 0.21)
TIB/SVL	0.46–0.47 (0.46 ± 0.01)	0.50
LAHL/SVL	0.45–0.47 (0.46 ± 0.01)	0.40–0.50 (0.47 ± 0.06)
HLL/SVL	1.44–1.51 (1.48 ± 0.03)	1.40–1.60 (1.50 ± 0.10)
TIB/HLL	0.30–0.32 (0.31 ± 0.01)	0.30

in the holotype (that for females is more distinct; GZNU20180606001). Under the condition of preservation, however, some specimens become slightly darker brown compared to the holotype.

Distribution and habitats. Currently, *Leptobrachella suiyangensis* sp. nov. is known only from its holotype locality, Huoqiuba Nature Reserve, Suiyang County, Guizhou Province, China (Fig. 1). The specimens were collected in a stream (ca 1.5 m in width and ca 10 cm in depth) and from nearby well-preserved bamboo forests (1501 m a.s.l.). During June, males were calling from under bamboo leaves; others perch on or under rocks by the side of the stream.

Comparisons

Leptobrachella suiyangensis sp. nov. differs from all other species of *Leptobrachella* based on morphological and molecular evidence. Phylogenetically, *L. suiyangensis* sp. nov., *L. alpina* and *L. purpurus* form a clade. Genetically, among this clade, the smallest genetic distance, at 5.49%, is between *L. suiyangensis* sp. nov. and *L. alpina*, and the largest genetic distance is 6.27% (*L. suiyangensis* sp. nov. and *L. purpurus*). Morphologically, the new species can be distinguished from *L. alpina* by having a larger body size of males (28.7–29.7 mm vs 24.0–26.4 mm); having narrower lateral fringes on the toes of the male (vs wide in males); dorsum purple-brown to dark purple-brown or grey-purple ground colour; ventral yellowish creamy-white with marbled texture on the chest and belly or with irregular light-brown speckling (vs almost uniformly gray-brown on dorsal part, ventral nearly immaculately creamy white, brown specking on margins); ventrolateral glands are characterized by small white dots forming an incomplete line (vs small white dots forming a complete line longitudinally); shoulder-gland is orange-yellow (vs white, around gland); head length greater than head width, HDL/HDW ratio 1.12 (vs head length equal to head width, HDL/HDW ratio 1.00). The new species can be distinguished from *L. purpurus* by body size of males (28.7–29.7 mm vs 25.0–27.5 mm); having narrow lateral fringes on the toes of males (vs wide in males); dorsum purple-brown to dark purple-brown or grey-purple ground color, ventral yellowish creamy-white with marbled texture on the chest and belly or with irregular light-brown speckling (vs dorsum coloration purplish brown, ventral side dull white with an indistinct grey dusting); throat immaculate gray (vs throat immaculate pinkish; almost dark orange-yellow on the upper arm (vs upper arms with distinct coppery orange coloration); dark bars on dorsal surface of tibia and tarsus very narrow, especially those on dorsal skin of tarsus (vs relatively broader dark bars on dorsal surface of tibia and tarsus); tibiotarsal articulation reaches to the anterior eye (vs tibiotarsal articulation reaches to posterior corner of the eye); relative length of fingers I <II < IV < III (vs I = II = IV < III).

Compared with the 26 known congeners in the genus *Leptobrachella* found south of the Isthmus of Kra, referring to the presence or absence of supra-axillary and ventrolateral glands, *L. suiyangensis* sp. nov. can be easily distinguished from *L. arayai*, *L. dringi*, *L. fritinniens*, *L. gracilis*, *L. hamidi*, *L. heteropus*, *L. kajangensis*, *L. kecil*, *L. marmorata*, *L. maura*, *L. melanoleuca*, *L. picta*, *L. platycephala*, *L. sabahmontana* and *L. sola*, all of which are lack of supra-axillary and ventrolateral glands (Dubois et al. 2010;

Dehling and Matsui 2013; Matsui et al. 2014). As for the comparison referring to the body size, the new species shows a significantly larger body size (SVL, 28.7–29.7 mm in males) than *L. baluensis* (14.9–15.9 mm in males), *L. brevicrus* (17.1–17.8 mm in males), *L. itiokai* (15.2–16.7 mm In males), *L. juliandringi* (17.0–17.2 mm in males), *L. mjobergi* (15.7–19.0 mm in males), *L. natunae* (17.6 mm in one adult male), *L. parva* (15.0–16.9 mm in males), *L. palmata* (14.4–16.8 mm in males), *L. serasanae* (16.9 mm in one adult male), and *Leptobrachella* sp. 3 "baluensis" (15.0–16.0 mm in males).

From the remaining 48 known congeners in the genus *Leptobrachella* found north of the Isthmus of Kra (Table 5) with SVL 28.7–29.7 mm in males and SVL 30.5–33.5 mm in females, *L. suiyangensis* sp. nov. can be distinguished from the larger *L. bourreti* (42.0–45.0 mm in females), *L. eos* (33.1–34.7 mm in males and 40.7 in one female), *L. lateralis* (36.6 mm in females), *L. nahangensis* (40.8 mm in one male), *L. nyx* (37.0–41.0 mm in females), *L. pyrrhops* (30.8–34.3 mm in males), *L. sungi* (48.3–52.7 mm in males and 56.7–58.9 mm in females), *L. tamdil* (32.3 mm in males) and *L. zhangyapingi* (45.8–52.5 mm in males), and from the smaller *L. alpina* (24.0–26.4 mm in males), *L. applebyi* (19.6–22.3 mm in males and 21.7–26.4 mm in females), *L. ardens* (21.3–24.7 mm in males and 24.5 mm in female), *L. bidoupensis* (18.5–25.4 mm in males and 29.2–29.4 mm in females), *L. khasiorum* (24.5–27.3 mm in males), *L. laui* (24.8–26.7 mm in males), *L. maculosa* (24.2–26.6 in males and 27.0 mm in one female), *L. melica* (19.5–22.7 mm in males), *L. maoershanensis* (29.1 mm in one female), *L. petrops* (23.6–27.6 mm in males), *L. pluvialis* (21.3–22.3 mm in males), *L. purpurus* (25.0–27.5 mm in males), *L. rowleyae* (23.1–28.1 mm in males and 27.0–27.8 mm in females), *L. ventripunctata* (25.5–28.0 mm in males), *L. tengchongensis* (23.9–26.0 mm in males and 28.8–28.9 mm in females) and *L. yingjiangensis* (25.7–27.6 mm in males).

In having irregular, light-brown speckling on the flanks, the new species differs from *L. aerea*, *L. botsfordi*, *L. crocea*, *L. firthi*, *L. isos*, *L. pallida*, *L. petrops* and *L. tuberosa*, all of which lack distinct irregular, light-brown speckling on the flanks. By having rudimentary webbing on the toes, the new species differs from *L. kalonensis*, *L. oshanensis*, *L. pallida*, *L. petrops*, and *L. tadungensis*, all of which lack webbing on the toes; and from *L. pelodytoides*, which has wide webbing on the toes. By having narrow lateral fringes on toes, the new species differs from *L. ardens*, *L. eos*, *L. firthi*, *L. isos*, *L. khasiorum*, *L. laui*, *L. liui*, *L. purpurus*, *L. tamdil*, *L. yingjiangensis* and *L. yunkaiensis*, all of which have wide lateral fringes on the toes; from *L. bidoupensis*, *L. bourreti*, *L. fuliginosa* and *L. mangshanensis*, all of which have weak lateral fringes on the toes; and from *L. crocea*, *L. kalonensis*, *L. lateralis*, *L. macrops*, *L. minima*, *L. nyx*, *L. oshanensis*, *L. pallida*, *L. pyrrhops*, *L. tadungensis*, *L. tuberosa*, and *L. ventripunctata,* all of which lack lateral fringes on the toes. By having dorsal surface shagreened with small granules, and in lacking enlarge tubercles or warts, the new species differs from *L. applebyi*, *L. bidoupensis, L. kalonensis*, *L. melica, L. minima*, *L. nahangensis*, *L. shangsiensis* and *L. tadungensis*, all of which have the dorsum smooth, and *L. alpina* (dorsum smooth, some with small warts), *L. fuliginosa* (dorsum smooth with fine tubercles), *L. laui* (dorsum with round granular tubercle, lacking skin ridges), *L. liui* (dorsum with round tubercles), *L. macrops* (dorsum roughly granular with large tubercles), *L. maoershanensis*

Table 5. Selected diagnostic characters for species described herein and species in the genus *Leptobrachella* occurring north of the Isthmus of Kra (modified from Rowley et al. 2017; Yuan et al. 2017; Hou et al. 2018; Wang et al. 2018).

ID	Species	Males SVL (mm)	Black spots on flanks	Toes webbing	Fringes on toes	Ventral coloration	Dorsal skin texture
1	*L. suiyangensis* sp. nov.	28.7–29.7	Yes	Rudimentary	Narrow	Yellowish creamy-white with marble texture chest and belly or with irregular light brown speckling	Shagreen with small granules
2	*L. aerea*	25.1–28.9	No	Rudimentary	Wide	Near immaculate creamy white, brown specking on margins	Finely tuberculate
3	*L. alpinus*	24.0–26.4	Yes	Rudimentary	Wide in males	Creamy-white with dark spots	Relatively smooth, some with small warts
4	*L. applebyi*	19.6–22.3	Yes	Rudimentary	No	Reddish brown with white speckling	Smooth
5	*L. ardens*	21.3–24.7	Yes	No	No	Reddish brown with white speckling	Smooth- finely shagreened
6	*L. bidoupensis*	18.5–25.4	Yes	Rudimentary	Weak	Reddish brown with white speckling	Smooth
7	*L. botsfordi*	29.1–32.6	No	Rudimentary	Narrow	Reddish brown with white speckling	Shagreened
8	*L. bourreti*	28.0–36.2	Yes	Rudimentary	Weak	Creamy white	Relatively smooth, some with small warts
9	*L. crocea*	22.2–27.3	No	Rudimentary	No	Bright orange	Highly tuberculate
10	*L. eos*	33.1–34.7	No	Rudimentary	Wide	Creamy white	Shagreened
11	*L. firthi*	26.4–29.2	No	Rudimentary	Wide in males	Creamy white	Shagreened with fine tubercles
12	*L. fuliginosa*	28.2–30.0	Yes	Rudimentary	Weak	White with brown dusting	Nearly smooth, few tubercles
13	*L. isos*	23.7–27.9	No	Rudimentary	Wide in males	Creamy white with white dusting on margins	Mostly smooth, females more tuberculate
14	*L. kalonensis*	25.8–30.6	Yes	No	No	Pale, speckled brown	Smooth
15	*L. khasiorum*	24.5–27.3	Yes	Rudimentary	Wide	Creamy white	Isolated, scattered tubercles
16	*L. lateralis*	26.9–28.3	Yes	Rudimentary	No	Creamy white	Roughly granular
17	*L. laui*	24.8–26.7	Yes	Rudimentary	Wide	Creamy white with dark brown dusting on margins	Round granular tubercles
18	*L. liui*	23.0–28.7	Yes	Rudimentary	Wide	Creamy white with dark brown spots on chest and margins	Round granular tubercles with glandular folds
19	*L. macrops*	28.0–29.3	Yes	Rudimentary	No	Greyish-violet with white speckling	Roughly granular with larger tubercles
20	*L. maculosa*	24.2–26.6	Yes	No	No	Brown, less white speckling	Dorsum mostly smooth with numerous tiny tubercles
21	*L. mangshanensis*	22.2–27.8	Yes	Rudimentary	Weak	White speckles on throat and belly	Nearly smooth
22	*L. maoershanensis*	25.2–30.4	Yes	Rudimentary	Narrow	Creamy white chest and belly with irregular black spots	Longitudinal folds
23	*L. melica*	19.5–22.7	Yes	Rudimentary	No	Reddish brown with white speckling	Smooth
24	*L. minima*	25.7–31.4	Yes	Rudimentary	No	Creamy white	Smooth
25	*L. nahangensis*	40.8	Yes	Rudimentary	No	Creamy white with light specking on throat and chest	Smooth

26	*L. nokrekensis*	26.0–33.0	Yes	Rudimentary	unknown	Creamy white	Tubercles and longitudinal folds
27	*L. nyx*	26.7–32.6	Yes	Rudimentary	No	Creamy white with white with brown margins	Rounded tubercles
28	*L. oshanensis*	26.6–30.7	Yes	No	No	Whitish with no markings or only small, light grey spots	Smooth with few glandular ridges
29	*L. pallida*	24.5–27.7	No	No	No	Reddish brown with white speckling	Tuberculate
30	*L. pelodytoides*	27.5–32.3	Yes	Wide	Narrow	Whitish	Small, smooth warts
31	*L. petrops*	23.6–27.6	No	No	Narrow	Immaculate creamy white	Highly tuberculate
32	*L. pluvialis*	21.3–22.3	Yes	Rudimentary	No	Dirty white with dark brown marbling	Smooth, flattened tubercles on flanks
33	*L. puhoatensis*	24.2–28.1	Yes	Rudimentary	Narrow	Reddish brown with white dusting	Longitudinal skin ridges
34	*L. purpurus*	25.0–27.5	Yes	Rudimentary	Wide	Dull white with indistinct grey dusting	Shagreen with small tubercles
35	*L. pyrrhops*	30.8–34.3	Yes	Rudimentary	No	Reddish brown with white speckling	Slightly shagreened
36	*L. rowleyae*	23.4–25.4	Yes	No	No	Pinkish milk-white to light brown chest and belly with numerous white speckles	Smooth with numerous tiny tubercles
37	*L. sungi*	48.3–52.7	No or small	Wide	Weak	White	Granular
38	*L. shangsiensis*	24.9–29.4	Yes	Narrow	Narrow	Yellowish creamy-white with marble texture	Smooth
39	*L. tadungensis*	23.3–28.2	Yes	No	No	Reddish brown with white speckling	Smooth
40	*L. tamdil*	32.3	Yes	Wide	Wide	White	Weakly tuberculate
41	*L. tengchongensis*	23.9–26.0	Yes	Rudimentary	Narrow	White with dark brown blotches	Shagreened with small tubercles
42	*L. tuberosa*	24.4–29.5	No	Rudimentary	No	White with small grey spots/streaks	Highly tuberculate
43	*L. ventripunctata*	25.5–28.0	Yes	Rudimentary	No	Chest and belly with dark brown spots	Longitudinal skin ridges
44	*L. wuhuangmontis*	25.6–30.0	Yes	Rudimentary	Narrow	Greyish white mixed by tiny white and black dots	Rough, scattered with dense conical tubercles
45	*L. yingjiangensis*	25.7–27.6	Yes	Rudimentary	Wide	Creamy white with dark brown flecks on chest and margins	Shagreened with small tubercles
46	*L. yunkaiensis*	25.9–29.3	Yes	Rudimentary	Wide	Belly pink with distinct or indistinct speckling	Shagreened with short skin ridges and raised warts
47	*L. zhangyapingi*	45.8–52.5	No	Rudimentary	Wide	Creamy-white with white with brown margins	Mostly smooth with distinct tubercles
48	*L. bijie*	29.0–30.4	Yes	Rudimentary	Narrow	White with distinct nebulous greyish speckling on chest and ventrolateral flanks	Shagreened and granular
49	*L. purpuraventra*	27.3–29.8	Yes	Rudimentary	Narrow	Grey purple with distinct nebulous greyish speckling on chest and ventrolateral flanks	Shagreened and granular

(dorsum smooth with small warts), *L. nokrekensis* (dorsum tubercles and longitudinal folds), *L. pelodytoides* (dorsum with small, smooth warts), *L. puhoatensis* (dorsum longitudinal skin ridges), *L. tuberosa* (dorsum highly tuberculate), *L. yunkaiensis* (dorsum with raised warts), *L. wuhuangmontis* (dorsum rough with conical tubercles), and *L. bijie* and *L. purpuraventra* (dorsum shagreened and granular). By the yellowish creamy-white with marbled chest and belly or with irregular light-brown speckling, the new species differs from *L. alpinus*, *L. applebyi*, *L. ardens*, *L. bidoupensis*, *L. botsfordi* and *L. pyrrhops* (ventral reddish brown with white speckling), *L. aerea* (ventral nearly immaculate creamy-white with brown specking on margins), *L. bijie* (ventral white with distinct nebulous greyish speckling on chest and ventrolateral flanks), *L. crocea* (ventral bright orange), *L. khasiorum, L. nokrekensis* and *L. yingjiangensis* (ventral creamy white), *L. macrops* (ventral greyish-violet with white speckling), *L. puhoatensis* (ventral reddish-brown with white dusting), *L. purpurus* (ventral dull white with indistinct grey dusting), *L. purpuraventra* (ventral grey-purple with distinct nebulous greyish speckling on the chest and ventrolateral flanks), *L. tuberosa* (ventral white with small grey spots and streaks), *L. ventripunctata* (chest and belly with large dark brown spots), *L. wuhuangmontis* (ventral greyish white), and *L. yunkaiensis* (belly pink with speckling). A comparative morphological data (selection) of *Leptobrachella suiyangensis* sp. nov. and 48 recognized *Leptobrachella* species occurring north of the Isthmus of Kra are listed in Table 5.

Discussion

Phylogenetic analyses based on mitochondrial DNA and nuclear DNA all suggested that the new species belongs to *Leptobrachella* but is separate from its congeners. Genetic distance of the 16S rRNA gene between the new species and its closely related species (*L. bijie*, *L. purpuraventra*, *L. alpina* and *L. purpurus*) was 4.71–6.27%, within the expected range of interspecific divergences in amphibians (Fouquet et al. 2007), and this genetic distance is much higher than between many sister species, of which, most species have been completely recognized as valid species. For example, in *Leptobrachella*, the *p*-distance = 2.35% between *L. purpurus* and *L. alpina*. Finally, a series of morphological characters were found to be different between the new species and its congenerson. All in all, multiple pieces of evidence support the validity of the new species.

The new species described in this study increases the number of species of *Leptobrachella* to 75, with 21 recorded from China (Fei et al. 2012; Sung et al. 2014; Yang et al. 2016, 2018; Yuan et al. 2017; Hou et al. 2018; Wang et al. 2018, 2019; Chen et al. 2018, 2019; Frost 2019). Before the description of the new species herein, only 12 species were recorded from southwest China. This highlights the underestimation of the species diversity of the genus *Leptobrachella*. Additional field surveys are required to understand the true diversity of amphibians in this genus, which will be useful for conservation strategies.

Studies on the taxonomy and phylogeny of the genus *Leptobrachella* were difficult to perform because of the morphological conservativeness of the species; in the field, many species appear to be very similar morphologically, and there exist sympatric species. This likely hinders our understanding of these cryptic species (Ohler et al. 2010; Sung et al. 2014; Yang et al. 2016, 2018; Yuan et al. 2017; Hou et al. 2018; Wang et al. 2018, 2019; Chen et al. 2019). The high species diversity and the degree of endemism indicated that the speciation pattern and sympatry mechanism of species in the genus *Leptobrachella* also need additional investigation.

Currently, to our knowledge, *L. suiyangensis* sp. nov. is restricted to rocky streams in bamboo forests. However, the type locality of *L. suiyangensis* sp. nov. has faced habitat loss and human disturbance, such as artificial grazing and herb collection, which could possibly threaten this species. *Leptobrachella suiyangensis* sp. nov. is range-restricted to Kuankuoshui National Nature Reserve, which borders the nearby Huoqiuba Nature Reserve and is in the eastern Ta-lou Mountains. These areas feature subtropical evergreen broad-leaved forest and evergreen deciduous broad-leaved mixed forest. Thus, it is likely that other populations of *L. suiyangensis* sp. nov. may be discovered in the Kuankuoshui Nature Reserve in the near future.

Acknowledgements

This project was supported by the key project of science-technology of basic condition platform granted by The Ministry of Science and Technology of the People's Republic of China (Grant No. 2005DKA21402); The National Top Discipline Construction Project of Guizhou Province; Geography in Guizhou Normal University (85 2017 Qianjiao Keyan Fa); and The Project of Science and Technology Program of Guizhou Province, "Study of biological and ecological vales for Fanjingshan World Natural Heritage Nomination of Tongren City (3052 2015 Qiankehe SY)". We thank Bo Song and Hongtao Cui for their help in sample collection. We thank Professor Ruliang Pan and LetPub (http://www.letpub.com) for its linguistic assistance during the preparation of this manuscript.

References

Anderson J (1871) A list of the reptilian accession to the Indian Museum, Calcutta from 1865 to 1870, with a description of some new species. Journal of the Asiatic Society of Bengal 40: 12–39.

Boulenger GA (1893) Concluding report on the reptiles and batrachians obtained in Burma by Signor L. Fea dealing with the collection made in Pegu and the Karin Hills in 1887–88. Annali del Museo Civico di Storia Naturale di Genova 13: 304–347.

Boulenger GA (1900) Descriptions of new batrachians and reptiles from the Larut Hills, Perak. Annals and Magazine of Natural History (Series 7) 6: 186–194. https://doi.org/10.1080/00222930008678356

Boulenger GA (1908) A revision of the Oriental pelobatid batrachians (genus *Megalophrys*). Proceedings of the Zoological Society of London 1908: 407–430. https://doi.org/10.1111/j.1096-3642.1908.tb01852.x

Bourret R (1937) Notes herpétologiques sur l'Indochine française. XIV. Les batraciens de la collection du Laboratoire des Sciences Naturelles de l'Université. Descriptions de quinze especes ou variétés nouvelles. Annexe au Bulletin Général de l'Instruction Publique, Hanoi 1937: 5–56.

Chen JM, Poyarkov NJ, Suwannapoom C, Lathrop A, Wu YH, Zhou WW, Yuan ZY, Jin JQ, Chen HM, Liu HQ, Nguyen TQ, Nguyen SN, Duong TV, Eto K, Nishikawa K, Matsui M, Orlov NL, Stuart BL, Brown RM, Rowley J, Murphy RW, Wang YY, Che J (2018) Large-scale phylogenetic analyses provide insights into unrecognized diversity and historical biogeography of Asian leaf-litter frogs, genus *Leptolalax*, (Anura: Megophryidae). Molecular Phylogenetics and Evolution 124: 162–171. https://doi.org/10.1016/j.ympev.2018.02.020

Chen, W, Liao XW, Zhou SC, Mo YM (2019) A new species of *Leptobrachella* (Anura: Megophryidae) from southern Guangxi, China. Zootaxa 4563(1): 67–82. https://doi.org/10.11646/zootaxa.4563.1.3

Dring J (1983) Frogs of the genus *Leptobrachella* (Pelobatidae). Amphibia–Reptilia 4(2): 89–102. https://doi.org/10.1163/156853883X00012

Dubois A (1983) Note préliminaire sur le genre *Leptolalax* Dubois, 1980 (Amphibiens, Anoures), avec diagnose d'une espèce novelle du Vietnam. Alytes 2: 147–153.

Dubois A (1987) Miscellanea taxinomica batrachologica (I). Alytes. Paris 5[1986]: 7–95.

Delorme M, Dubois A, Grosjean S, Ohler A (2006) Une nouvelle ergotaxinomie des Megophryidae (Amphibia, Anura). Alytes 24(1–4): 6–21.

Das I, Tron RKL, Rangad D, Hooroo RN (2010) A new species of *Leptolalax* (Anura: Megophryidae) from the sacred groves of Mawphlang, Meghalaya, north-eastern India. Zootaxa 2339: 44–56. https://doi.org/10.11646/zootaxa.2339.1.2

Dehling JM (2012a) Eine neue Art der Gattung *Leptolalax* (Anura: Megophryidae) vom Gunung Benom, Westmalaysia/A new species of the genus *Leptolalax* (Anura: Megophryidae) from Gunung Benom, Peninsular Malaysia. Sauria 34: 9–21.

Dehling JM (2012b) Redescription of *Leptolalax gracilis* (Günther, 1872) from Borneo and taxonomic status of two populations of *Leptolalax* (Anura: Megophryidae) from Peninsular Malaysia. Zootaxa 3328: 20–34. https://doi.org/10.11646/zootaxa.3328.1.2

Dubois A, Grosjean S, Ohler A, Adler K, Zhao EM (2010) The nomenclatural status of some generic nomina of Megophryidae (Amphibia, Anura). Zootaxa 2493: 66–68. https://doi.org/10.11646/zootaxa.2493.1.6

Dehling JM, Matsui M (2013) A new species of *Leptolalax* (Anura: Megophryidae) from Gunung Mulu National Park, Sarawak, East Malaysia (Borneo). Zootaxa 3670(1): 33–44.

Duong VT, Do DT, Ngo CD, Nguyen TQ, Poyarkov Jr, NA (2018) A new species of the genus *Leptolalax* (Anura: Megophryidae) from southern Vietnam. Zoological Research 39(3): 181–196. https://doi.org/10.24272/j.issn.2095-8137.2018.009

Edgar RC (2004) MUSCLE: multiple sequence alignment with high accuracy and high throughput. Nucleic Acids Research 32(5): 1792–1797. https://doi.org/10.1093/nar/gkh340

Eto K, Matsui M, Nishikawa K (2015) Description of a new species of the genus *Leptobrachella* (Amphibia, Anura, Megophryidae) from Borneo. Current Herpetology 34(2): 128–139. https://doi.org/10.5358/hsj.34.128

Eto K, Matsui M, Nishikawa K (2016) A new highland species of dwarf litter frog genus *Leptobrachella* (Amphibia: Anura: Megophryidae) from Sarawak. Raffles Bulletin of Zoology 64: 194–203.

Eto K, Matsui M, Hamidy A, Munir M, Iskandar D (2018) Two New Species of the Genus Leptobrachella (Amphibia: Anura: Megophryidae) from Kalimantan, Indonesia. Current Herpetology 37(2): 95–105. https://doi.org/10.5358/hsj.37.95

Fei L, Ye CY, HuangYZ (1990) Key to Chinese Amphibians. Publishing House for Scientific and Technological Literature, Chongqing, 364 pp. [in Chinese]

Fei L, Ye CY (1992) The classification of Pelobatidae (*Leptolalax*) and a new species in China. Acta Zoologica Sinica 38(3): 245–253. [in Chinese]

Fei L, Ye CY (2005) An Illustrated Key to Chinese Amphibians. Sichuan Publishing House of Science and Technology, Chongqing, 340 pp. [in Chinese]

Fouquet A, Gilles A, Vences M, Marty C, Blanc M, Gemmell1 NJ (2007) Underestimation of species richness in Neotropical frogs revealed by mtDNA analyses. PLoS ONE 2(10): e1109. https://doi.org/10.1371/journal.pone.0001109

Fei L, Hu SQ, Ye CY, Huang YZ (2009) Fauna Sinica. Amphibia, Vol. 2, Anura. Science Press, Beijing, 957 pp. [in Chinese]

Fei L, Ye CY, Jiang JP (2012) Colored Atlas of Chinese Amphibians and yheir Distributions. Sichuan Science and Technology Press, Sichuan, 619 pp. [in Chinese]

Frost DR (2019) Amphibian Species of the World: an Online Reference. Version 6.0. Electronic Database. American Museum of Natural History, New York. http://research.amnh.org/herpetology/amphibia/index.html [Accessed on: 2019-8-13]

Günther A (1872) On the reptiles and amphibians of Borneo. Proceedings of the Zoological Society of London 1872: 586–600.

Günther A (1895) The reptiles and batrachians of the Natuna Islands. Novitates Zoologicae 2(4): 499–502.

Grismer LL, Grismer JL, Youmans TM (2004) A new species of *Leptolalax* (Anura: Megophryidae) from Pulau Tioman, West Malaysia. Asiatic Herpetological Research 10: 8–11.

Hu SQ, Zhao EM, Liu CC (1973) A survey of amphibians and reptiles in Kweichow province, including a herpetofaunal analysis. Acta Zoologica Sinica 19: 149–181.

Humtsoe LN, Bordoloi S, Ohler A, Dubois A (2008) Rediscovery of a long known species, *Ixalus lateralis* Anderson, 1871. Zootaxa 1921: 24–34. https://doi.org/10.11646/zootaxa.1921.1.2

Hoang DT, Chernomor O, von Haeseler A, Minh BQ, Vinh L (2018) UFBoot2: improving the ultrafast bootstrap approximation. Molecular Biology and Evolution 35(2): 518–522. https://doi.org/10.1093/molbev/msx281

Hou Y, Zhang MF, Hu F, Li SY, Shi SC, Chen J, Mo XY, Wang B (2018) A new species of the genus *Leptolalax* (Anura, Megophryidae) from Hunan, China. Zootaxa 4444(3): 247–266. https://doi.org/10.11646/zootaxa.4444.3.2

Inger RF, Stuebing RB (1992) A new species of frog of the genus *Leptobrachella* Smith (Anura: Pelobatidae), with a key to the species from Borneo. Raffles Bulletin of Zoology 39(1): 99–103.

Inger RF, Stuebing RB, Tan F (1995) New species and new records of anurans from Borneo. Raffles Bulletin of Zoology 43: 115–132.

Inger RF (1997) A new species of *Leptolalax* (Anura: Megophryidae) from Borneo. Asiatic Herpetological Research 7: 48–50. https://doi.org/10.5962/bhl.part.18855

Inger RF, Orlov N, Darevsky I (1999) Frogs of Vietnam: a report on new collections. Fieldiana, Zoology 92: 1–46. https://doi.org/10.5962/bhl.title.3478

Jiang K, Yan F, Suwannapoom C, Chomdej S, Che J (2013) A new species of the genus *Leptolalax* (Anura: Megophryidae) from northern Thailand. Asian Herpetological Research 4(2): 100–108. https://doi.org/10.3724/SP.J.1245.2013.00100

Kumar S, Stecher G, Tamura K (2016) MEGA7: Molecular Evolutionary Genetics Analysis Version 7.0 for Bigger Datasets. Molecular Biology and Evolution 33(7): 1870–1874. https://doi.org/10.1093/molbev/msw054

Liu CC (1950) Amphibians of Western China. Fieldiana, America Zoology Memoires 2: 1–400. https://doi.org/10.5962/bhl.title.2977

Lathrop A, Murphy RW, Orlov N, Ho CT (1998) Two new species of *Leptolalax* (Anura: Megophryidae) from northern Vietnam. Amphibia-Reptilia 19: 253–267. https://doi.org/10.1163/156853898X00160

Lanfear R, Frandsen PB, Wright AM, Senfeld T, Calcott B (2016) PartitionFinder 2: new methods for selecting partitioned models of evolution for molecular and morphological phylogenetic analyses. Molecular Biology and Evolution 34(3): 772–773. https://doi.org/10.1093/molbev/msw260

Malkmus R (1992) *Leptolalax pictus* sp. n. (Anura: Pelobatidae) vom Mount Kinabalu/Nord-Borneo. Sauria 14: 3–6.

Matsui M (1997) Call characteristics of Malaysian *Leptolalax* with a description of two new species (Anura: Pelobatidae) Copeia 1997: 158–165. https://doi.org/10.2307/1447851

Matsui M (2006) Three new species of *Leptolalax* from Thailand (Amphibia, Anura, Megophryidae). Zoological Science 23(9): 821–830. https://doi.org/10.2108/zsj.23.821

Matsui M, Belabut DM, Ahmad N, Yong HS (2009) A new species of *Leptolalax* (Amphibia, Anura, Megophryidae) from peninsular Malaysia. Zoological Science 26(3): 243–247. https://doi.org/10.2108/zsj.26.243

Mathew R, Sen N (2010) Description of a new species of *Leptobrachium* Tschudi, 1838 (Amphibia: Anura: Megophryidae) from Meghalaya, India. Records of the Zoological Survey of India 109: 91–108.

Matsui M, Dehling J M (2012) Notes on an enigmatic Bornean megophryid, *Leptolalax dringi* Dubois, 1987 (Amphibia: Anura). Zootaxa 3317(1): 49–58. https://doi.org/10.11646/zootaxa.3317.1.4

Matsui M, Zainudin R, Nishikawa K (2014a) A new species of *Leptolalax* from Sarawak, western Borneo (Anura: Megophryidae). Zoological Science 31(11): 773–779. https://doi.org/10.2108/zs140137

Matsui M, Nishikawa K, Yambun P (2014b) A new *Leptolalax* from the mountains of Sabah, Borneo (Amphibia, Anura, Megophryidae). Zootaxa 3753(3): 440–452. https://doi.org/10.11646/zootaxa.3753.5.3

Mahony S, Foley NM, Bijumn SD, Teeling EC (2017) Evolutionary history of the Asian horned frogs (Megophryinae): integrative approaches to timetree dating in the absence of a

fossil record. Molecular Biology and Evolution 34(3): 744–771. https://doi.org/10.1093/molbev/msw267

Matsui M, Eto K, Nishikawa K, Hamidy A, Belabut D, Ahmad N, Panha S, Khonsue W, Grismer LL (2017) Mitochondrial phylogeny of *Leptolalax* from Malay Peninsula and *Leptobrachella* (Anura, Megophryidae). Current Herpetology 36(1): 11–21. https://doi.org/10.5358/hsj.36.11

Murphy RW, Lathrop A, Ho CT, Orlov N (1998) Two new species of *Leptolalax* (Anura: Megophryidae) from northern Vietnam. Amphibia-Reptilia 19(3): 253–267. https://doi.org/10.1163/156853898X00160

Nguyen LT, Schmidt HA, Haeseler, A von, Minh BQ (2015) IQ-TREE: a fast and effective stochastic algorithm for estimating maximum-likelihood phylogenies. Molecular Biology and Evolution 32(1): 268–274. https://doi.org/10.1093/molbev/msu300

Nguyen LT, Poyarkov Jr NA, Le DT, Vo BD, Phan HT, Van DT, Murphy WR, Nguyen SN (2018) A new species of *Leptolalax* (Anura: Megophryidae) from Son Tra Peninsula, central Vietnam. Zootaxa 4388(1): 1–21. https://doi.org/10.11646/zootaxa.4388.1.1

Ohler A, Marquis O, Swan S, Grosjean S (2000) Amphibian biodiversity of Hoang Lien Nature Reserve (Lao Cai Province, northern Vietnam) with description of two new species. Herpetozoa 13 (1/2): 71–87.

Ohler A, Wollenberg KC, Grosjean S, Hendrix R, Vences M, Ziegler T, Dubois A (2011) Sorting out *Lalos*: description of new species and additional taxonomic data on megophryid frogs from northern Indochina (genus *Leptolalax*, Megophryidae, Anura). Zootaxa 3147: 1–83. https://doi.org/10.11646/zootaxa.3147.1.1

Oberhummer E, Barten C, Schweizer IN, Das I, Haas AL, Hertwig ST (2014) Description of the tadpoles of three rare species of megophryid frogs (Amphibia: Anura: Megophryidae) from Gunung Mulu, Sarawak, Malaysia. Zootaxa 3835: 59–79. https://doi.org/10.11646/zootaxa.3835.1.3

Poyarkov NA, Rowley JJ, Gogoleva SI, Vassilieva AB, Galoyan EA, Orlov N L (2015) A new species of *Leptolalax* (Anura: Megophryidae) from the western Langbian Plateau, southern Vietnam. Zootaxa 3931: 221–252. https://doi.org/10.11646/zootaxa.3931.2.3

Rowley JJ, Cao TT (2009) A new species of *Leptolalax* (Anura: Megophryidae) from central Vietnam. Zootaxa 2198 (5): 51–60. https://doi.org/10.11646/zootaxa.2198.1.5

Rowley JJ, Hoang DH, Le TTD, Dau QV, Cao TT (2010a) A new species of *Leptolalax* (Anura: Megophryidae) from Vietnam and further information on *Leptolalax tuberosus.* Zootaxa 2660: 33–45.

Rowley JJ, Stuart BL, Neang T, Emmett DA (2010b) A new species of *Leptolalax* (Anura: Megophryidae) from northeastern Cambodia. Zootaxa 2567: 57–68. https://doi.org/10.11646/zootaxa.2567.1.3

Rowley JJ, Stuart BL, Richards SJ, Phimmachak S, Sivongxay N (2010c) A new species of *Leptolalax* (Anura: Megophryidae) from Laos. Zootaxa 2681: 35–46. https://doi.org/10.11646/zootaxa.2681.1.3

Rowley JJ, Le DTT, Tran DTA, Hoang DH (2011) A new species of *Leptobrachella* (Anura: Megophryidae) from southern Vietnam. Zootaxa 2796: 15–28. https://doi.org/10.11646/zootaxa.2796.1.2

Rowley JJ, Hoang HD, Dau VQ, Le TTD, Cao TT (2012) A new species of *Leptolalax* (Anura: Megophryidae) from central Vietnam. Zootaxa 3321: 56–68. https://doi.org/10.11646/zootaxa.3321.1.4

Ronquist F, Teslenko M, Van Der Mark P, Ayres DL, Darling A, Höhna S, Larget B, Liu L,Suchard MA, Huelsenbeck JP (2012) MrBayes 3.2: efficient Bayesian phylogenetic inference and model choicem across a large model space. Systematic Biology 61: 539–542. https://doi.org/10.1093/sysbio/sys029

Rowley JJ, Dau VQ, Nguyen TT (2013) A new species of *Leptolalax* (Anura: Megophryidae) from the highest mountain in Indochina. Zootaxa 3737 (4): 415–428. https://doi.org/10.11646/zootaxa.3737.4.5

Rambaut A, Suchard MA, Xie D, Drummond AJ (2014) Tracer v1. 6. http://beast.bio.ed.ac.uk/Tracer [Accessed on: 2019-3-7]

Rowley JJ, Stuart BL, Neang T, Hoang HD, Dau VQ, Nguyen TT, Emmett DA (2015a) A new species of *Leptolalax* (Anura: Megophryidae) from Vietnam and Cambodia. Zootaxa 4039: 401–417. https://doi.org/10.11646/zootaxa.4039.3.1

Rowley JJL, Tran DTA, Frankham GJ, Dekker AH, Le DTT, Nguyen TQ, Dau VQ, Hoang HD (2015b) Undiagnosed Cryptic Diversity in Small, Microendemic Frogs (*Leptolalax*) from the Central Highlands of Vietnam. PLoS ONE 10 (5): e0128382. https://doi.org/10.1371/journal.pone.0128382

Rowley JJ, Tran DTA, Le DTT, Dau VQ, Peloso PLV, Nguyen TQ, Hoang HD, Nguyen TT, Ziegler T (2016) Five new, microendemic Asian Leaf-litter Frogs (*Leptolalax*) from the southern Annamite mountains, Vietnam. Zootaxa 4085: 63–102. https://doi.org/10.11646/zootaxa.4085.1.3

Rowley JJ, Dau VQ, Hoang HD, Le DTT, Cutajar TP, Nguyen TT (2017a) A new species of *Leptolalax* (Anura: Megophryidae) from northern Vietnam. Zootaxa 4243: 544–564. https://doi.org/10.11646/zootaxa.4243.3.7

Rowley J J, Dau V Q, Cao T T (2017b) A new species of *Leptolalax* (Anura: Megophryidae) from Vietnam. Zootaxa 4273(1): 61–79. https://doi.org/10.11646/zootaxa.4273.1.5

Smith MA (1925) Contributions to the herpetology of Borneo. Sarawak Museum Journal 3: 15–34.

Stejneger L(1926) Two new tailless amphibians from western China. Proceedings of the Biological Society of Washington 39: 53–54.

Smith MA (1931) The herpetology of Mt. Kinabalu, North Borneo, 13,455 ft. Bulletin of the Raffles Museum. Singapore 5: 3–32.

Simon C, Frati F, Beckenbach A, Crespi B, Liu H, Flook P (1994) Evolution, weighting, and phylogenetic utility of mitochondrial gene sequences and a compilation of conserved polymerase chain reaction primers. Annals of the Entomological Society of America 87: 651–701. https://doi.org/10.1093/aesa/87.6.651

Sengupta S, Sailo S, Lalremsanga HT, Das A, Das I (2010) A new species of *Leptolalax* (Anura: Megophryidae) from Mizoram, north-eastern India. Zootaxa 2406: 56–68. https://doi.org/10.11646/zootaxa.2406.1.3

Sung YH, Yang JH, Wang YY (2014) A new species of *Leptolalax* (Anura: Megophryidae) from southern China. Asian Herpetological Research 5(2): 80–90. https://doi.org/10.3724/SP.J.1245.2014.00080

Taylor EH (1962) The amphibian fauna of Thailand. University of Kansas Science Bulletin 43: 265–599. https://doi.org/10.5962/bhl.part.13347

Watters JL, Cummings ST, Flanagan RL, Siler CD (2016) Review of morphometric measurements used in anuran species descriptions and recommendations for a standardized approach. Zootaxa 4072(4): 477–495. https://doi.org/10.11646/zootaxa.4072.4.6

Wang J, Yang JH, Li, Y, Lyu ZT, Zeng ZC, Liu ZY, Ye YH, Wang YY (2018) Morphology and molecular genetics reveal two new *Leptobrachella* species in southern China (Anura, Megophryidae). ZooKeys 776: 105–106. https://doi.org/10.3897/zookeys.776.22925

Wang J, Li YL, Li Y, Chen HH, Zeng YJ, Shen JM, Wang YY (2019) Morphology, molecular genetics, and acoustics reveal two new species of the genus *Leptobrachella* from northwestern Guizhou Province, China (Anura, Megophryidae). ZooKeys 848: 119–154. https://doi.org/10.3897/zookeys.848.29181

Yang JH, Wang YY, Chen GL, Rao DQ (2016) A new species of the genus *Leptolalax* (Anura: Megophryidae) from Mt. Gaoligongshan of western Yunnan Province, China. Zootaxa 4088: 379–394. https://doi.org/10.11646/zootaxa.4088.3.4

Yuan ZY, Sun RD, Chen J, Rowley JJ, Wu ZJ, Hou SB, Wang SN, Che J (2017) A new species of the genus *Leptolalax* (Anura: Megophryidae) from Guangxi, China. Zootaxa 4300(4): 551–570. https://doi.org/10.11646/zootaxa.4300.4.5

Yang JH, Zeng ZC, Wang YY (2018) Description of two new sympatric species of the genus *Leptolalax* (Anura: Megophryidae) from western Yunnan of China. PeerJ 6: e4586. https://doi.org/10.7717/PeerJ.458

ZooKeys 923: 141–156 (2020)
doi: 10.3897/zookeys.923.39665
http://zookeys.pensoft.net

RESEARCH ARTICLE

A peer-reviewed open-access journal
ZooKeys
Launched to accelerate biodiversity research

Comparative genomics reveals bamboo feeding adaptability in the giant panda (*Ailuropoda melanoleuca*)

Xin He[1,2,3*], Walter H. Hsu[4*], Rong Hou[1,2,3], Ying Yao[1,2,3], Qin Xu[1,2,3], Dandan Jiang[1,2,3], Longqiong Wang[1,2,3], Hairui Wang[1,2,3]

1 *Chengdu Research Base of Giant Panda Breeding, Chengdu, 610081, China* **2** *Sichuan Key Laboratory of Conservation Biology for Endangered Wildlife, Chengdu, 610081, China* **3** *Sichuan Academy of Giant Panda, Chengdu, 610081, China* **4** *Department of Biomedical Sciences, Iowa State University, Ames 50011, IA, USA*

Corresponding author: *Hairui Wang* (wang200108143@aliyun.com)

Academic editor: *J. Maldonado* | Received 3 September 2019 | Accepted 18 December 2019 | Published 1 April 2020

http://zoobank.org/5DA8E748-9506-408E-BC8B-33B723AD46FA

Citation: He X, Hsu WH, Hou R, Yao Y, Xu Q, Jiang D, Wang L, Wang H (2020) Comparative genomics reveals bamboo feeding adaptability in the giant panda (*Ailuropoda melanoleuca*). ZooKeys 923: 141–156. https://doi.org/10.3897/zookeys.923.39665

Abstract

The giant panda (*Ailuropoda melanoleuca*) is one of the world's most endangered mammals and remains threatened as a result of intense environmental and anthropogenic pressure. The transformation and specialization of the giant panda's diet into a herbivorous diet have resulted in unique adaptabilities in many aspects of their biology, physiology and behavior. However, little is known about their adaptability at the molecular level. Through comparative analysis of the giant panda's genome with those of nine other mammalian species, we found some genetic characteristics of the giant panda that can be associated with adaptive changes for effective digestion of plant material. We also found that giant pandas have similar genetic characteristics to carnivores in terms of olfactory perception but have similar genetic characteristics to herbivores in terms of immunity and hydrolytic enzyme activity. Through the analysis of gene family expansion, 3752 gene families were found, which were enriched in functions such as digestion. A total of 93 genes under positive selection were screened out and gene enrichment identified these genes for the following processes: negative regulation of cellular metabolic process, negative regulation of nitrogen compound metabolic process, negative regulation of macromolecule metabolic process and negative regulation of metabolic process. Combined with the KEGG pathway, it was found that genes such as CREB3L1, CYP450 2S1, HSD11B2, LRPAP1 play a key role in digestion. These genes may have played a key role in the pandas' adaptation to its bamboo diet.

* Contributed equally as the first authors

Keywords
adaptation, bamboo diet, dietary transition, digestion, feeding habits

Introduction

Diet may be the most important selective force in animal evolution (Kim et al. 2016). In this regard, the giant panda (*Ailuropoda melanoleuca*) is interesting because it has not only undergone a dietary transition but has also developed an obligate bamboo diet (O'Brien 1987; Wei et al. 2015a). The fossil record suggests that giant pandas started to consume bamboo in the late Pliocene or early Pleistocene (Jin et al. 2007). Giant pandas belong to the order Carnivora and have a digestive tract typical of the carnivorous members of the group, but feed exclusively on low nutritious and low-calorific content bamboo (Wei et al. 2012). Although giant pandas have been found to retain the ability to eat meat both in the wild and in captivity, 99% of their diet consists of bamboo (Wei et al. 2015a).

Bamboo is a low nutrition/energy food comprising of 70–80% cellulose, hemicellulose, and lignin and 20–30% protein, soluble carbohydrate, and fat (Wu et al. 2017). Meanwhile, giant pandas have a very low digestive capacity for bamboo: 75–90% of the protein, only 27% of the hemicellulose, and 8% of the cellulose is utilized (Zhang et al. 2014). Despite this, they have survived on a bamboo diet probably for more than 2 million years (Myr). The monotonous diet has probably resulted in a number of morphological, ecological and genetic adaptations (Wei et al. 2015b). Giant pandas have a pseudothumb on the forepaw, and have evolved a strong mandible and flattened teeth to help them chew and eat bamboo (Endo et al. 1999; Zhao et al. 2010). Giant pandas have acquired a suite of optimal foraging, habitat use, and activity rhythm strategies in adapting to their low energy diet (O'Brien 1987; Zhang et al. 2014; Nie et al. 2015b). The study of the giant panda genome reveals that the umami receptor TAS1R1 gene has become a pseudogene due to a 2 bp insertion in exon 3 and a 6 bp deletion in exon 6 (Li et al. 2010). The umami receptor senses components of meat and other protein-rich foods. Therefore, the loss of function of the TAS1R1 gene may have contributed to the panda's dietary switch (Zhao et al. 2010). In addition, little is known about the molecular mechanisms by which giant pandas adapt to bamboo diets. Some studies have shown that giant panda's digestion of bamboo mainly depends on its gut microbiota (Li et al. 2010; Wei et al. 2015b; Guo et al. 2018; Zhang et al. 2018). It is unknown as to what caused the adaptive changes in giant pandas.

The genome sequences of wild animal species are rapidly being accumulated, providing rich resources for the study of adaptation, trait evolution, species divergence, and population structure analyses (Li et al. 2010; Kim et al. 2016). Here, we investigated the giant panda's adaptation to a bamboo diet using comparative genomics among mammalian species with different feeding habits. In the present study, we detected putative molecular adaptation mechanisms of giant pandas to the bamboo diet, providing new insights into the research and protection of giant pandas.

Materials and methods

Abbreviations

Myr: million years; **BLAST**: basic local alignment search tool; **GO**: gene ontology; **KEGG**: Kyoto Encyclopedia of Genes and Genomes; **NCBI**: National Center for Biotechnology Information; **dN/dS**: non-synonymous/synonymous rate ratio; **ML**: maximum likelihood; **CREB3L1**: cAMP-responsive element binding protein 3 like 1; **CYP450 2S1**: cytochrome P450, family 2, subfamily s, polypeptide 1; **HSD11B2**: corticosteroid 11-beta-dehydrogenase isozyme 2; **LRPAP1**: low density lipoprotein receptor related protein associated protein 1

Genome data query

We performed comparative genomic analysis of 10 mammalian species with different diets including the giant panda (*Ailuropoda melanoleuca*); four species of mammals with carnivorous diets: wolf (*Canis lupus familiaris*), tiger (*Panthera tiger*) polar bear (*Ursus maritimus*) and sperm whale (*Physeter catodon*)); two species with herbivorous diets: white rhinoceros (*Ceratotherium simum simum*) and gorilla (*Gorilla gorilla*); and three species of omnivores: macaque (*Macaca mulatta*), human (*Homo sapiens*) and mouse (*Mus musculus*). For the present study, we downloaded the genome sequences, protein sequences and annotation files of the 10 species from the NCBI website (2018/3/7) (Table 1).

Gene family analysis

OrthoFinder (OrthoFinder-2.2.7) software was used for the gene orthology analysis (Emms and Kelly 2015). We first performed all-blast-all alignment of the protein sequences of all species, and then clustered these proteins according to the alignment results; each of which is a gene family. Based on the results of the gene family analysis, the common and unique gene families shared between the giant panda and the carnivore and herbivore groups were analyzed. A Venn diagram was used to depict the common and unique gene families. These genes were enriched and annotated by Go-TermFinder (Boyle et al. 2004) and KEGG pathways (Kanehisa 2002; Kanehisa et al. 2004) to analyze the differences in gene function.

Comparative evolution analysis

The single-copy gene protein sequences were compared using the MAFFT (v7.158b (2014/06/27)) software (Katoh et al. 2005); the regions with poor comparison quality were removed using the trimAl (v1.4.rev22) software (Capella-Gutiérrez et al. 2009), and the parameter was set to automated1. Subsequently, 1000 times of the bootstrap test were performed using the PROTGAMMAJTT model, RAxML (v8.2.12) software (Stamata-

Table 1. Data sources of comparative genomics of the giant panda.

Species	Download Website
Ailuropoda melanoleuca	ftp://ftp.ncbi.nlm.nih.gov/genomes/all/GCF/000/004/335/GCF_000004335.2_AilMel_1.0/GCF_000004335.2_AilMel_1.0_genomic.fna.gz
	ftp://ftp.ncbi.nlm.nih.gov/genomes/all/GCF/000/004/335/GCF_000004335.2_AilMel_1.0/GCF_000004335.2_AilMel_1.0_protein.faa.gz
	ftp://ftp.ncbi.nlm.nih.gov/genomes/all/GCF/000/004/335/GCF_000004335.2_AilMel_1.0/GCF_000004335.2_AilMel_1.0_genomic.gff.gz
Canis lupus familiaris	ftp://ftp.ncbi.nlm.nih.gov/genomes/all/GCF/000/002/285/GCF_000002285.3_CanFam3.1/GCF_000002285.3_CanFam3.1_genomic.fna.gz
	ftp://ftp.ncbi.nlm.nih.gov/genomes/all/GCF/000/002/285/GCF_000002285.3_CanFam3.1/GCF_000002285.3_CanFam3.1_protein.faa.gz
	ftp://ftp.ncbi.nlm.nih.gov/genomes/all/GCF/000/002/285/GCF_000002285.3_CanFam3.1/GCF_000002285.3_CanFam3.1_genomic.gff.gz
Ceratotherium simum simum	ftp://ftp.ncbi.nlm.nih.gov/genomes/all/GCF/000/283/155/GCF_000283155.1_CerSimSim1.0/GCF_000283155.1_CerSimSim1.0_genomic.fna.gz
	ftp://ftp.ncbi.nlm.nih.gov/genomes/all/GCF/000/283/155/GCF_000283155.1_CerSimSim1.0/GCF_000283155.1_CerSimSim1.0_protein.faa.gz
	ftp://ftp.ncbi.nlm.nih.gov/genomes/all/GCF/000/283/155/GCF_000283155.1_CerSimSim1.0/GCF_000283155.1_CerSimSim1.0_genomic.gff.gz
Gorilla gorilla	ftp://ftp.ncbi.nlm.nih.gov/genomes/all/GCF/000/151/905/GCF_000151905.2_gorGor4/GCF_000151905.2_gorGor4_genomic.fna.gz
	ftp://ftp.ncbi.nlm.nih.gov/genomes/all/GCF/000/151/905/GCF_000151905.2_gorGor4/GCF_000151905.2_gorGor4_protein.faa.gz
	ftp://ftp.ncbi.nlm.nih.gov/genomes/all/GCF/000/151/905/GCF_000151905.2_gorGor4/GCF_000151905.2_gorGor4_genomic.gff.gz
Homo sapiens	ftp://ftp.ncbi.nlm.nih.gov/genomes/all/GCF/000/001/405/GCF_000001405.38_GRCh38.p12/GCF_000001405.38_GRCh38.p12_genomic.fna.gz
	ftp://ftp.ncbi.nlm.nih.gov/genomes/all/GCF/000/001/405/GCF_000001405.38_GRCh38.p12/GCF_000001405.38_GRCh38.p12_protein.faa.gz
	ftp://ftp.ncbi.nlm.nih.gov/genomes/all/GCF/000/001/405/GCF_000001405.38_GRCh38.p12/GCF_000001405.38_GRCh38.p12_genomic.gff.gz
Macaca mulatta	ftp://ftp.ncbi.nlm.nih.gov/genomes/all/GCF/000/772/875/GCF_000772875.2_Mmul_8.0.1/GCF_000772875.2_Mmul_8.0.1_genomic.fna.gz
	ftp://ftp.ncbi.nlm.nih.gov/genomes/all/GCF/000/772/875/GCF_000772875.2_Mmul_8.0.1/GCF_000772875.2_Mmul_8.0.1_protein.faa.gz
	ftp://ftp.ncbi.nlm.nih.gov/genomes/all/GCF/000/772/875/GCF_000772875.2_Mmul_8.0.1/GCF_000772875.2_Mmul_8.0.1_genomic.gff.gz
Mus musculus	ftp://ftp.ncbi.nlm.nih.gov/genomes/all/GCF/000/001/635/GCF_000001635.26_GRCm38.p6/GCF_000001635.26_GRCm38.p6_genomic.fna.gz
	ftp://ftp.ncbi.nlm.nih.gov/genomes/all/GCF/000/001/635/GCF_000001635.26_GRCm38.p6/GCF_000001635.26_GRCm38.p6_protein.faa.gz
	ftp://ftp.ncbi.nlm.nih.gov/genomes/all/GCF/000/001/635/GCF_000001635.26_GRCm38.p6/GCF_000001635.26_GRCm38.p6_genomic.gff.gz
Panthera tiger	ftp://ftp.ncbi.nlm.nih.gov/genomes/all/GCF/000/464/555/GCF_000464555.1_PanTig1.0/GCF_000464555.1_PanTig1.0_genomic.fna.gz
	ftp://ftp.ncbi.nlm.nih.gov/genomes/all/GCF/000/464/555/GCF_000464555.1_PanTig1.0/GCF_000464555.1_PanTig1.0_protein.faa.gz
	ftp://ftp.ncbi.nlm.nih.gov/genomes/all/GCF/000/464/555/GCF_000464555.1_PanTig1.0/GCF_000464555.1_PanTig1.0_genomic.gff.gz
Physeter catodon	ftp://ftp.ncbi.nlm.nih.gov/genomes/all/GCF/002/837/175/GCF_002837175.1_ASM283717v1/GCF_002837175.1_ASM283717v1_genomic.fna.gz
	ftp://ftp.ncbi.nlm.nih.gov/genomes/all/GCF/002/837/175/GCF_002837175.1_ASM283717v1/GCF_002837175.1_ASM283717v1_protein.faa.gz
	ftp://ftp.ncbi.nlm.nih.gov/genomes/all/GCF/002/837/175/GCF_002837175.1_ASM283717v1/GCF_002837175.1_ASM283717v1_genomic.gff.gz

Species	Download Website
Ursus maritimus	ftp://ftp.ncbi.nlm.nih.gov/genomes/all/GCF/000/687/225/GCF_000687225.1_UrsMar_1.0/GCF_000687225.1_UrsMar_1.0_genomic.fna.gz
	ftp://ftp.ncbi.nlm.nih.gov/genomes/all/GCF/000/687/225/GCF_000687225.1_UrsMar_1.0/GCF_000687225.1_UrsMar_1.0_protein.faa.gz
	ftp://ftp.ncbi.nlm.nih.gov/genomes/all/GCF/000/687/225/GCF_000687225.1_UrsMar_1.0/GCF_000687225.1_UrsMar_1.0_genomic.gff.gz

kis 2014) to construct a ML evolutionary tree. Based on the results of the single-copy gene alignment, the MCMCtree program with the Paml software (Yang 1997) was used to estimate the divergence time between species. The fossil time was calibrated as follows: a) divergence time between dogs and cats was > 43 Myr and < 65 Myr (Wesley-Hunt and Flynn 2005; Eizirik et al. 2010; Meredith et al. 2011); b) primates and rodents diverged > 65 Myr (Wesley-Hunt and Flynn 2005); c) Canidae and Ursidae diverged >37 Myr (Wesley-Hunt and Flynn 2005). By using different random numbers and running the program twice, we found that the correlation between the two estimates was 0.999, indicating that the time accuracy of this estimation was very high. The Cafe software (De Bie et al. 2006) was used to estimate the expansion and contraction of gene families, and the Go-TermFinder (Boyle et al. 2004) was used to analyze the GO enrichment annotation of these genes and the KEGG pathway (Kanehisa et al. 2004) enrichment.

Positive selection gene

The giant panda gene was chosen as the foreground and the genes of the remaining species as the background. The positive selection analysis was used to determine whether there was a significant difference between the non-synonymous replacement rate and the proportion of synonymous replacement rates (dN/dS) between foreground and background branches. The null hypothesis parameters were: model = 2, NSsites = 2, fix_omega = 1, omega = 1. Alternative hypothesis parameters were: model = 2, NSsites = 2, fix_omega = 0. Chi programs using Paml software (Yang 1997) were utilized to compare LRT differences between the two models. The QVALUE of R package (Halekoh et al. 2006) was used for multiple inspections and corrections. Identification of genes that were under positive selection in the giant panda branch ensued. The GO enrichment annotation analysis was performed on these genes using Go-TermFinder (Boyle et al. 2004), and the KEGG pathway (Kanehisa et al. 2004) enrichment analysis was also performed.

Results

Gene family

A total of 517,058 protein-coding genes from 10 species were used for the gene family analysis; 481,081 genes were identified in 24,788 gene families, including 911 single-

Table 2. Statistical results of gene families.

Property	Value
Number of genes	517,058
Number of genes in orthogroups	481,081
Number of unassigned genes	35,977
Percentage of genes in orthogroups	93.00%
Percentage of unassigned genes	7.00%
Number of orthogroups	24,788
Number of species-specific orthogroups	169
Number of genes in species-specific orthogroups	1108
Percentage of genes in species-specific orthogroups	0.20%
Mean orthogroup size	19.4
Median orthogroup size	15
Number of orthogroups with all species present	14,680
Number of single-copy orthogroups	911

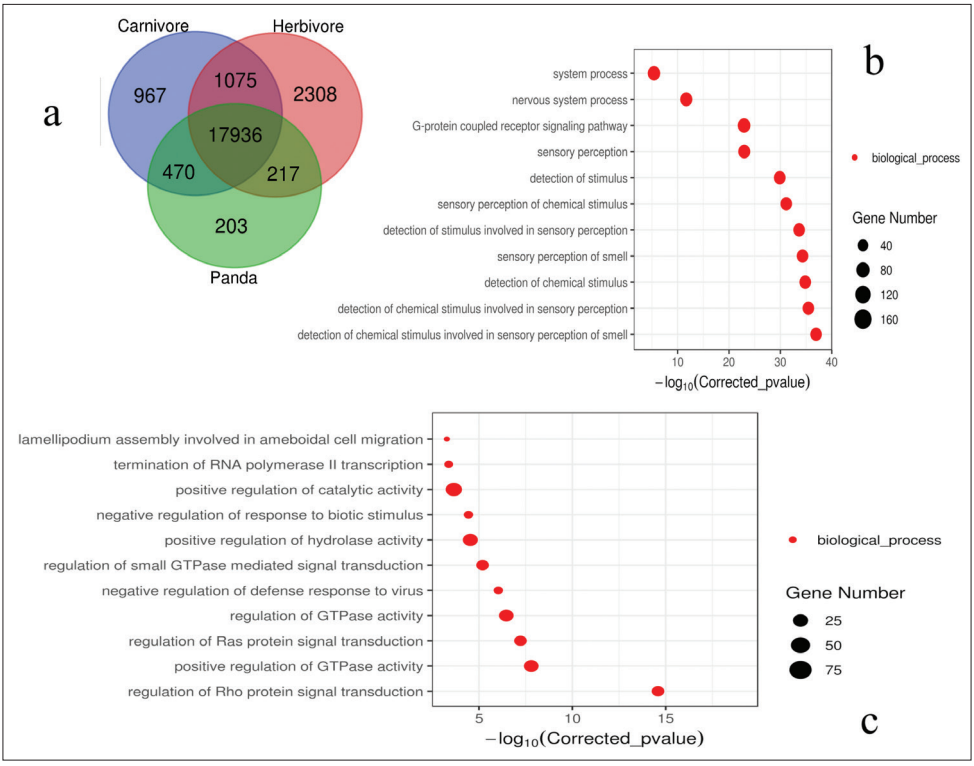

Figure 1. The enrichment analysis of shared genes between the giant panda and mammalian species with different feeding habits. Giant pandas have the characteristics of both carnivores and herbivores. Studies show that it is close to carnivores in perception and close to herbivores in physiological functions. The abscissa is the pair value of the corrected p value, and the corrected $p < 0.05$ is taken as the threshold value. **a** shared genes between the giant panda and other mammalian species with different feeding habits **b** gene enrichment analysis of the giant panda and carnivores **c** gene enrichment analysis of the giant panda and herbivores.

copy true orthologous genes across all 10 species (Table 2). There were 470 shared gene families in giant pandas and carnivores, and these gene families are enriched in the sense of smell and chemical stimulus detection awareness, etc. At the same time, there were 217 gene families shared with herbivores, which are enriched in virus defense mechanisms, positive regulation of hydrolase activity, negative regulation of biological stimulation and positive regulation of catalytic activity (Fig. 1).

Phylogenetic analysis

The phylogenetic tree constructed using all 10 mammalian species based on single-copy gene family data estimated the time of divergence between giant panda and polar bear to be 21 Myr (Fig. 2). The giant panda had a 3752-gene family expansion and a 1966-xcgene family contraction (Fig. 2). The KEGG enrichment analysis of the expansion gene families showed an enrichment in digestion-related pathways such as salivary secretion, pancreatic secretion, insulin secretion and parathyroid hormone synthesis, secretion and action (Fig. 3). The KEGG enrichment of the contractile gene was not significant, but the cytochrome CYP450 gene family, which normally shrinks in carnivores, was not found in the giant panda's contractile gene family.

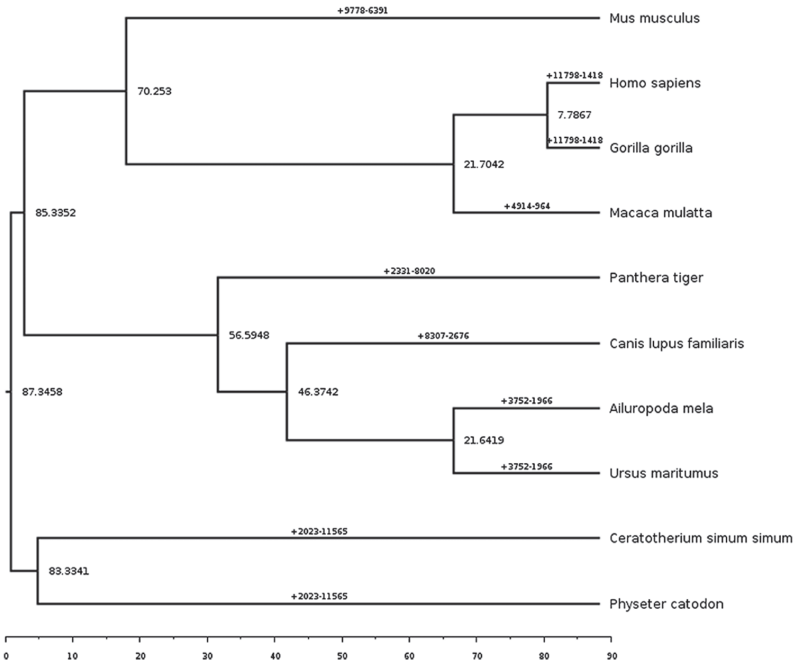

Figure 2. Analysis of the evolution of giant panda gene family. The number of points represent the time of divergence, in millions of years (Myr). The numbers on the branches represent the number of genes, - for contraction, + for expansion.

Figure 3. The KEGG enrichment analysis of the giant panda expansion gene family. The abscissa is the pair value of the corrected p value, and the corrected $p < 0.05$ is taken as the threshold value.

Positive selection gene

A total of 93 genes were identified to be under positive selection in the giant panda branch. In the GO enrichment analysis, it was found that the positive gene enrichment was selected for the negative regulation of the cellular metabolic process, negative regulation of the nitrogen compound metabolic process, negative regulation of the macromolecule metabolic process and negative regulation of the metabolic process (Fig. 4). The biological function of all genes was analyzed by the KEGG pathway. The following genes were detected in giant pandas: cAMP-responsive element binding protein 3-like 1(CREB3L1), cytochrome P450 family 2, subfamily S, polypeptide 1(CYP450 2S1) and other metabolism-related genes. CREB3L1 regulates glucose metabolism, while CYP450 2S1 is a key gene involved in vitamin A metabolism. These may have played a key role in the giant pandas' adaptation to the bamboo diet.

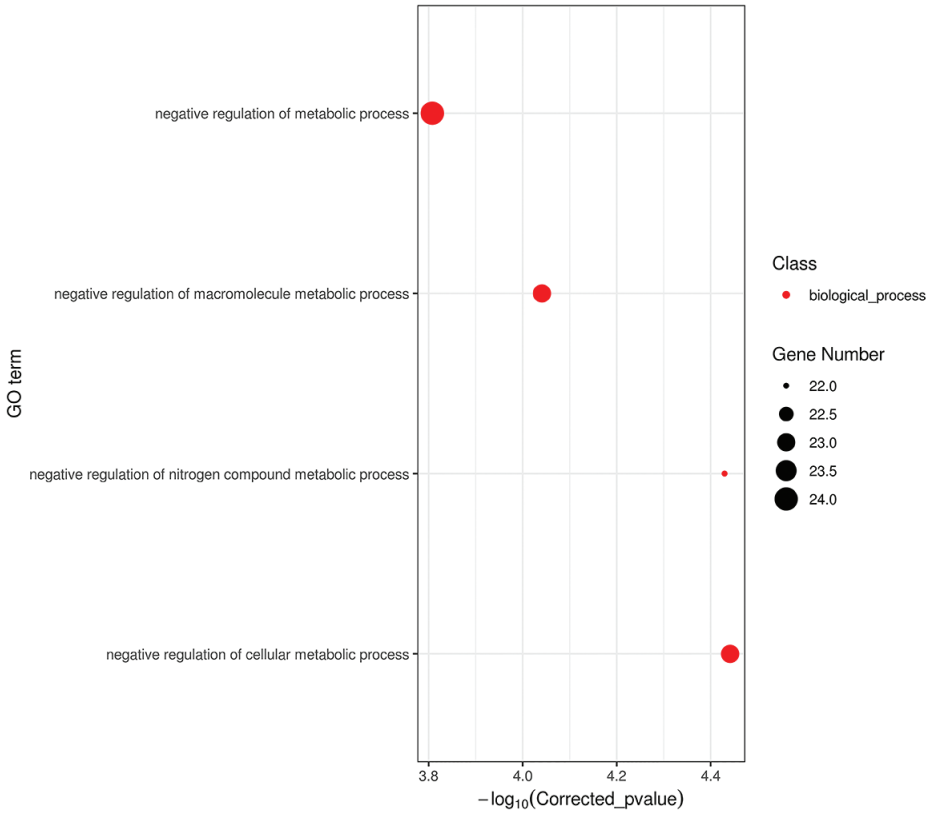

Figure 4. The GO enrichment analysis of giant panda positive selection gene. The abscissa is the pair value of the corrected p value, and the corrected $p < 0.05$ is taken as the threshold value.

Discussion

The carnivorous diet of the ancestors of the giant panda has gradually evolved into a strict bamboo diet since the late Pliocene or early Pleistocene. In order to adapt to this change in diet, giant pandas developed adaptive evolution genetically, physiologically and morphologically. By comparing the genes that the giant panda shares with several carnivorous and herbivorous species, we found that they share genes with similar smell and perception functions (Charlton et al. 2009). This is consistent with previous findings that giant pandas have an acute sense of smell (Reik and Walter 1998; Zhu et al. 2017). Giant pandas are active at night and during the day, and their keen sense of smell enables them to move around better in dark conditions at night (Reik and Walter 1998). Giant pandas also use olfactory cues to respond to mating signals and to determine the different kinds of food (Zhu et al. 2017). However, in terms of the microbial defense mechanisms (Lecellier et al. 2005), giant pandas tend to act like a herbivore. Giant pandas show a positive regulation of hydrolase activity (Rammler et al. 1973), a negative regulation of biological stimulation, and a positive regulation of catalytic activity (Antonov et al. 1988). These functions might help giant pandas defend against vegetative toxins in bamboo, and at the same time effectively digest and absorb the nutrients in bamboo. Studies have shown that bamboo contains cyanide, but pandas can break cyanide down in their digestive system (Huang et al. 2016).

Giant pandas have several families of amplified genes, among which salivary secretion, pancreatic secretion, insulin secretion and parathyroid hormone synthesis, secretion and function pathways may be important for the digestion and adaptation of giant pandas to bamboo. The sialaden and pancreas are important glands for the digestive system; the increased saliva secretion can help giant pandas lubricate the gut for digesting the starch in bamboo (Maynard and Loosli 1969). The amylase gene copy number of the giant panda is higher than that of the genomes of carnivores that we queried, which is consistent with the fact that the giant panda eats mainly hemicellulose and starchy materials (Zhang et al. 2018). Bamboo is mostly indigestible, and its content of starch and other carbohydrates could be the giant panda's main source of energy. The pancreas secretes a variety of digestive enzymes which can help giant pandas digest better the macromolecules in bamboo and facilitate the absorption of nutrients (Eckert et al. 1988; Wu et al. 2017). The increase in the salivary and pancreatic secretions may be a key digestive strategy for giant pandas in response to the dietary change to bamboo. Insulin is one of the hormones secreted by the pancreas, which promotes the muscle and liver to absorb, store and utilize glucose; in addition, insulin promotes the synthesis and storage of fat and protein, and inhibits the decomposition and utilization of fat and protein (Schmidt-Nielsen 1997; Hill et al. 2004). Bamboo has few nutrients and is difficult to digest. Insulin secretion could help giant pandas transfer and store digested nutrients with maximum efficiency. Parathyroid hormone mainly increases serum calcium and decreases serum phosphorus. The giant panda may benefit from parathyroid hormone in promoting the renal distal tubule and collecting duct to reabsorb calcium ions, helping the body to reduce calcium loss and increase the use of

calcium (Maynard and Loosli 1969; Eckert et al. 1988; Schmidt-Nielsen 1997; Hill et al. 2004). Further studies to determine whether there are changes in the expression of the aforementioned gene products are warranted. These studies will help to verify the adaptability of giant pandas in changing feeding habits from meat to plants.

In the present study, 93 genes were found under positive selection in the genome of the giant panda. The GO enrichment analysis detected that these genes were concentrated in the negative regulation mechanism of metabolism. Activation of this mechanism could reduce their own metabolism and energy needed for adaptation to ecological changes. The results of the present study are consistent with the report showing that in order to cope with the low energy and nutrition content of the bamboo diet, giant pandas reduce their own metabolism, reduce behavioral activities, and eat voraciously to meet their own energy demand (Nie et al. 2015a). At the same time, through the KEGG pathway of the positive selection gene (Zhang et al. 2014; Fuhrmeister et al. 2016), CREB3L1 could suppress the glucose metabolism-related gene expression; and down-regulation of CREB3L1 could weaken the effect of sugar dysplasia and control of glucose levels in the body (Greenwood et al. 2015). This gene is also involved in the pancreatic function, which helps pandas digest bamboo (KEGG reference pathway: ko04152). Bamboo is the sole source of vitamins for pandas. To meet this nutritional challenge, pandas need to be more efficient at absorbing and using nutrients. Pandas can synthesize retinoids from beta-carotene in bamboo, which can be converted to vitamin A, which is metabolized to retinoic acid. Through the study of convergent evolution of giant panda and red panda, it was found that the CYP450 gene family of the giant panda plays an important role in the metabolism of vitamin A (Hu et al. 2017). We also found a CYP450 2S1 gene in our study. CYP450 2S1 is a member of the CYP450 gene family, which is involved in the nutritional metabolism of arachidonic acid and vitamin A in giant pandas (Molotkov et al. 2004). The excessive accumulation of retinoic acid causes harm to physical development (KEGG reference pathway: ko00830).

Other genes hint at adaptations in other directions. For example, the HSD11B2 gene can encode type 2 11β-hydroxysteroid dehydrogenase and participate in intracellular homeostasis, and convert cortisol to cortisone. It is an inactive corticosteroid that can prevent obesity and high blood pressure (Mune et al. 2013). In the present study, we found that LRPAP1, a gene related to myopia, was elevated in giant pandas, which provided a new clue for the giant pandas' poor eyesight (Aldahmesh et al. 2013). The protein/enzyme expression from these genes need to be investigated in future studies to verify the results of the present study.

Conclusion

Changes in diet composition during animal evolution likely created strong selective pressures in multiple biological processes. The giant pandas' dietary habits have shifted dramatically from a carnivorous diet to a strict bamboo diet. The reasons for the changes in the diet of giant pandas are still largely unknown. With the development of high

throughput, next generation sequencing technology and the open availability of genome-wide data, we explored the adaptability of giant pandas from a genomic perspective.

In this study, the comparative genomics of species with different feeding habits was used to elucidate the genes responsible for the adaptation of giant pandas to herbivory. The giant panda retains the characteristics of a carnivore in its sensory abilities, but is similar to a herbivore in terms of physiology, such as digestion. These adaptations also help the panda digest bamboo and metabolize nutrients by regulating its digestive and endocrine secretions. Here, we elucidated the molecular/genomic mechanism of giant pandas' adaptation to dietary changes and the adoption of dietary specializations in the digestive system. However, the function of these genes in giant pandas need to be further verified. In response to changes in diet, the giant panda's genome has undergone important evolutionary adaptations that help it better digest bamboo and metabolize nutrients.

This study also provides new perspectives and insights for the adaptive evolution of giant pandas. In addition, these findings also provide the molecular theoretical basis for the adaptation mechanism of giant panda's dietary changes, and present additional information that can be used for the management and protection of this endangered species.

Acknowledgments

The authors wish to thank the Shanghai Personal Biotechnology Co., Ltd for the bioinformatics analysis support provided.

This work was supported by Sichuan Science and Technology Program (2018JY0349) and the Program of the Giant Panda Breeding Research Foundation (CPF2017-10).

References

Aldahmesh MA, Khan AO, Alkuraya H, Adly N, Anazi S, Al-Saleh AA, Mohamed JY, Hijazi H, Prabakaran S, Tacke M (2013) Mutations in LRPAP1 are associated with severe myopia in humans. The American Journal of Human Genetics 93: 313–320. https://doi.org/10.1016/j.ajhg.2013.06.002

Antonov VK, Dyakov VL, Mishin AA, Rotanova TV (1988) Catalytic activity and association of pancreatic lipase. Biochimie 70: 1235–1244. https://doi.org/10.1016/0300-9084(88)90190-3

Boyle EI, Weng S, Gollub J, Jin H, Botstein D, Cherry JM, Sherlock G (2004) GO: TermFinder – open source software for accessing Gene Ontology information and finding significantly enriched Gene Ontology terms associated with a list of genes. Bioinformatics 20: 3710–3715. https://doi.org/10.1093/bioinformatics/bth456

Capella-Gutiérrez S, Silla-Martínez JM, Gabaldón T (2009) trimAl: a tool for automated alignment trimming in large-scale phylogenetic analyses. Bioinformatics 25: 1972–1973. https://doi.org/10.1093/bioinformatics/btp348

Charlton BD, Huang Y, Swaisgood RR (2009) Vocal discrimination of potential mates by female giant pandas (*Ailuropoda melanoleuca*). Biology Letters 5: 597–599. https://doi.org/10.1098/rsbl.2009.0331

De Bie T, Cristianini N, Demuth JP, Hahn MW (2006) CAFE: a computational tool for the study of gene family evolution. Bioinformatics 22: 1269–1271. https://doi.org/10.1093/bioinformatics/btl097

Eckert R, Randall R, Augustine G (1988) Animal physiology: mechanisms and adaptations. WH Freeman & Co, 127–130.

Eizirik E, Murphy WJ, Koepfli K-P, Johnson WE, Dragoo JW, Wayne RK, O'Brien SJ (2010) Pattern and timing of diversification of the mammalian order Carnivora inferred from multiple nuclear gene sequences. Molecular Phylogenetics and Evolution 56: 49–63. https://doi.org/10.1016/j.ympev.2010.01.033

Emms DM, Kelly S (2015) OrthoFinder: solving fundamental biases in whole genome comparisons dramatically improves orthogroup inference accuracy. Genome Biology 16: 157. https://doi.org/10.1186/s13059-015-0721-2

Endo H, Yamagiwa D, Hayashi Y, Koie H, Yamaya Y, Kimura J (1999) Role of the giant panda's 'pseudo-thumb'. Nature 397: 309–310. https://doi.org/10.1038/16830

Fuhrmeister J, Zota A, Sijmonsma TP, Seibert O, Cıngır Ş, Schmidt K, Vallon N, de Guia RM, Niopek K, Diaz MB (2016) Fasting-induced liver GADD45β restrains hepatic fatty acid uptake and improves metabolic health. EMBO Molecular Medicine 8: 654–669. https://doi.org/10.15252/emmm.201505801

Greenwood M, Greenwood MP, Mecawi AS, Loh SY, Rodrigues JA, Paton JFR, Murphy D (2015) Transcription factor CREB3L1 mediates cAMP and glucocorticoid regulation of arginine vasopressin gene transcription in the rat hypothalamus. Molecular Brain 8: 68. https://doi.org/10.1186/s13041-015-0159-1

Guo W, Mishra S, Zhao J, Tang J, Zeng B, Kong F, Ning R, Li M, Zhang H, Zeng Y (2018) Metagenomic study suggests that the gut microbiota of the giant panda (*Ailuropoda melanoleuca*) may not be specialized for fiber fermentation. Frontiers in Microbiology 9: 229. https://doi.org/10.3389/fmicb.2018.00229

Halekoh U, Højsgaard S, Yan J (2006) The R package geepack for generalized estimating equations. Journal of Statistical Software 15: 1–11. https://doi.org/10.18637/jss.v015.i02

Hill RW, Wyse GA, Anderson M, Anderson M (2004) Animal physiology. Sinauer Associates Sunderland, MA, 147–149.

Hu Y, Wu Q, Ma S, Ma T, Shan L, Wang X, Nie Y, Ning Z, Yan L, Xiu Y, Wei F (2017) Comparative genomics reveals convergent evolution between the bamboo-eating giant and red pandas. Proceedings of the National Academy of Sciences USA 114: 1081–1086. https://doi.org/10.1073/pnas.1613870114

Huang H, Yie S, Liu Y, Wang C, Cai Z, Zhang W, Lan J, Huang X, Luo L, Cai K, Hou R, Zhang Z (2016) Dietary resources shape the adaptive changes of cyanide detoxification function in giant panda (*Ailuropoda melanoleuca*). Scientific Reports 6: 34700–34700. https://doi.org/10.1038/srep34700

Jin C, Ciochon RL, Dong W, Hunt RM Jr., Liu J, Jaeger M, Zhu Q (2007) The first skull of the earliest giant panda. Proceedings of the National Academy of Sciences USA 104: 10932–10937. https://doi.org/10.1073/pnas.0704198104

Kanehisa M (2002) The KEGG database. silico simulation of biological processes. Novartis Foundation Symposium 247: 91–103. https://doi.org/10.1002/0470857897.ch8

Kanehisa M, Goto S, Kawashima S, Okuno Y, Hattori M (2004) The KEGG resource for deciphering the genome. Nucleic Acids Research 32: D277–D280. https://doi.org/10.1093/nar/gkh063

Katoh K, Kuma K-i, Toh H, Miyata T (2005) MAFFT version 5: improvement in accuracy of multiple sequence alignment. Nucleic Acids Research 33: 511–518. https://doi.org/10.1093/nar/gki198

Kim S, Cho YS, Kim HM, Chung O, Kim H, Jho S, Seomun H, Kim J, Bang WY, Kim C, An J, Bae CH, Bhak Y, Jeon S, Yoon H, Kim Y, Jun J, Lee H, Cho S, Uphyrkina O, Kostyria A, Goodrich J, Miquelle D, Roelke M, Lewis J, Yurchenko A, Bankevich A, Cho J, Lee S, Edwards JS, Weber JA, Cook J, Kim S, Lee H, Manica A, Lee I, O'Brien SJ, Bhak J, Yeo JH (2016) Comparison of carnivore, omnivore, and herbivore mammalian genomes with a new leopard assembly. Genome Biology 17: 211. https://doi.org/10.1186/s13059-016-1071-4

Lecellier C-H, Dunoyer P, Arar K, Lehmann-Che J, Eyquem S, Himber C, Saïb A, Voinnet O (2005) A cellular microRNA mediates antiviral defense in human cells. Science 308: 557–560. https://doi.org/10.1126/science.1108784

Li R, Fan W, Tian G, Zhu H, He L, Cai J, Huang Q, Cai Q, Li B, Bai Y, Zhang Z, Zhang Y, Wang W, Li J, Wei F, Li H, Jian M, Li J, Zhang Z, Nielsen R, Li D, Gu W, Yang Z, Xuan Z, Ryder OA, Leung FC, Zhou Y, Cao J, Sun X, Fu Y, Fang X, Guo X, Wang B, Hou R, Shen F, Mu B, Ni P, Lin R, Qian W, Wang G, Yu C, Nie W, Wang J, Wu Z, Liang H, Min J, Wu Q, Cheng S, Ruan J, Wang M, Shi Z, Wen M, Liu B, Ren X, Zheng H, Dong D, Cook K, Shan G, Zhang H, Kosiol C, Xie X, Lu Z, Zheng H, Li Y, Steiner CC, Lam TT, Lin S, Zhang Q, Li G, Tian J, Gong T, Liu H, Zhang D, Fang L, Ye C, Zhang J, Hu W, Xu A, Ren Y, Zhang G, Bruford MW, Li Q, Ma L, Guo Y, An N, Hu Y, Zheng Y, Shi Y, Li Z, Liu Q, Chen Y, Zhao J, Qu N, Zhao S, Tian F, Wang X, Wang H, Xu L, Liu X, Vinar T, Wang Y, Lam TW, Yiu SM, Liu S, Zhang H, Li D, Huang Y, Wang X, Yang G, Jiang Z, Wang J, Qin N, Li L, Li J, Bolund L, Kristiansen K, Wong GK, Olson M, Zhang X, Li S, Yang H, Wang J, Wang J (2010) The sequence and de novo assembly of the giant panda genome. Nature 463: 311–317. https://doi.org/10.1038/nature08696

Maynard LA, Loosli JK (1969) Animal nutrition. Animal nutrition. 6th edn.

Meredith RW, Janečka JE, Gatesy J, Ryder OA, Fisher CA, Teeling EC, Goodbla A, Eizirik E, Simão TLL, Stadler T (2011) Impacts of the Cretaceous Terrestrial Revolution and KPg extinction on mammal diversification. Science 334: 521–524. https://doi.org/10.1126/science.1211028

Molotkov A, Ghyselinck NB, Chambon P, Duester G (2004) Opposing actions of cellular retinol-binding protein and alcohol dehydrogenase control the balance between retinol storage and degradation. Biochemical Journal 383: 295–302. https://doi.org/10.1042/BJ20040621

Mune T, Suwa T, Morita H, Isomura Y, Takada N, Yamamoto Y, Hayashi M, Yamakita N, Sasaki A, Takeda N (2013) Longer HSD11B2 CA-repeat in impaired glucose tolerance and type 2 diabetes. Endocrine Journal: EJ12-0108. https://doi.org/10.1507/endocrj.EJ12-0108

Nie Y, Speakman JR, Wu Q, Zhang C, Hu Y, Xia M, Yan L, Hambly C, Wang L, Wei W (2015a) Exceptionally low daily energy expenditure in the bamboo-eating giant panda. Science 349: 171–174. https://doi.org/10.1126/science.aab2413

Nie Y, Zhang Z, Raubenheimer D, Elser JJ, Wei W, Wei F (2015b) Obligate herbivory in an ancestrally carnivorous lineage: the giant panda and bamboo from the perspective of nutritional geometry. Functional Ecology 29: 26–34. https://doi.org/10.1111/1365-2435.12302

O'Brien SJ (1987) The ancestry of the giant panda. Scientific American 257: 102–107. https://doi.org/10.1038/scientificamerican1187-102

Rammler DH, Haugland R, Shavitz R (1973) Hydrolytic enzyme substrates I: Chemical synthesis and characterization. Analytical Biochemistry 52: 180–197. https://doi.org/10.1016/0003-2697(73)90343-6

Reik W, Walter J (1998) Imprinting mechanisms in mammals. Current Opinion in Genetics & Development 8: 154–164. https://doi.org/10.1016/S0959-437X(98)80136-6

Schmidt-Nielsen K (1997) Animal physiology: adaptation and environment. Cambridge University Press, 6–8.

Stamatakis A (2014) RAxML version 8: a tool for phylogenetic analysis and post-analysis of large phylogenies. Bioinformatics 30: 1312–1313. https://doi.org/10.1093/bioinformatics/btu033

Wei F, Hu Y, Yan L, Nie Y, Wu Q, Zhang Z (2015a) Giant pandas are not an evolutionary cul-de-sac: evidence from multidisciplinary research. Molecular Biology and Evolution 32: 4–12. https://doi.org/10.1093/molbev/msu278

Wei F, Hu Y, Zhu L, Bruford MW, Zhan X, Zhang L (2012) Black and white and read all over: the past, present and future of giant panda genetics. Molecular Ecology 21: 5660–5674. https://doi.org/10.1111/mec.12096

Wei F, Wang X, Wu Q (2015b) The giant panda gut microbiome. Trends in Microbiology 23: 450–452. https://doi.org/10.1016/j.tim.2015.06.004

Wesley-Hunt GD, Flynn JJ (2005) Phylogeny of the Carnivora: basal relationships among the carnivoramorphans, and assessment of the position of 'Miacoidea' relative to Carnivora. Journal of Systematic Palaeontology 3: 1–28. https://doi.org/10.1017/S1477201904001518

Wu Q, Wang X, Ding Y, Hu Y, Nie Y, Wei W, Ma S, Yan L, Zhu L, Wei F (2017) Seasonal variation in nutrient utilization shapes gut microbiome structure and function in wild giant pandas. Proceedings of the Royal Society B: Biological Sciences 284. https://doi.org/10.1098/rspb.2017.0955

Yang Z (1997) PAML: a program package for phylogenetic analysis by maximum likelihood. Bioinformatics 13: 555–556. https://doi.org/10.1093/bioinformatics/13.5.555

Zhang W, Liu W, Hou R, Zhang L, Schmitz-Esser S, Sun H, Xie J, Zhang Y, Wang C, Li L (2018) Age-associated microbiome shows the giant panda lives on hemicelluloses, not on cellulose. The International Society for Microbial Ecology Journal 12, 1319–1328. https://doi.org/10.1038/s41396-018-0051-y

Zhang Z, Sheppard JK, Swaisgood RR, Wang G, Nie Y, Wei W, Zhao N, Wei F (2014) Ecological scale and sea sonal heterogeneity in the spatial behaviors of giant pandas. Integrative Zoology 9: 46–60. https://doi.org/10.1111/1749-4877.12030

Zhao H, Yang JR, Xu H, Zhang J (2010) Pseudogenization of the umami taste receptor gene Tas1r1 in the giant panda coincided with its dietary switch to bamboo. Molecular Biology and Evolution 27: 2669–2673. https://doi.org/10.1093/molbev/msq153

Zhu J, Arena S, Spinelli S, Liu D, Zhang G, Wei R, Cambillau C, Scaloni A, Wang G, Pelosi P (2017) Reverse chemical ecology: Olfactory proteins from the giant panda and their interactions with putative pheromones and bamboo volatiles. Proceedings of the National Academy of Sciences 114: E9802–E9810 https://doi.org/10.1073/pnas.1711437114